

---

**ADVANCED EVOKED POTENTIALS**

---

## **TOPICS IN NEUROSURGERY**

Lunsford, L. Dade (ed.) *Modern Stereotactic Neurosurgery*, 1988, ISBN: 0-89838-950-X.

---

# **ADVANCED EVOKED POTENTIALS**

edited by

**HANS LÜDERS**

Cleveland Clinic Foundation



**KLUWER ACADEMIC PUBLISHERS**  
**BOSTON/DORDRECHT/LONDON**

---

Distributors

for the United States and Canada: Kluwer Academic Publishers, 101 Philip Drive, Assinippi Park, Norwell, MA, 02061, USA

for the UK and Ireland: Kluwer Academic Publishers, Falcon House, Queen's Square, Lancaster LA1 1RN, UK

for all other countries: Kluwer Academic Publishers Group, Distribution Centre, P.O. Box 322, 3300 AH Dordrecht, The Netherlands

---

**Library of Congress Cataloging-in-Publication Data**

Advanced evoked potentials.

(Topics in neurosurgery)

Includes index.

1. Evoked potentials (Electrophysiology) 2. Brain—Diseases—Diagnosis.

I. Lüders, Hans. II. Series. [DNLM: 1. Evoked Potentials. WL 102 A244]  
RC386.6.E86A34 1987 616.8'07547 87-22139 ISBN 0-89838-963-1

---

ISBN 978-1-4684-9009-1 ISBN 978-1-4684-9007-7 (eBook)

DOI 10.1007/978-1-4684-9007-7

© 1989 by Kluwer Academic Publishers, Boston  
Softcover reprint of the hardcover 1st edition 1989

All rights reserved. No part of this publication may be reproduced, stored in a retrieval system, or transmitted in any form or by any means, mechanical, photocopying, recording, or otherwise, without the prior written permission of the publishers, Kluwer Academic Publishers, 101 Philip Drive, Assinippi Park, Norwell, MA 02061, USA

---

## CONTENTS

Contributing Authors	vii
Preface	ix
1. Theory of Near-Field and Far-Field Evoked Potentials	1
JUN KIMURA, THORU YAMADA, D. DAVID WALKER	
2. Critical Analysis of the Methods Used to Identify Generator Sources of Evoked Potential (EP) Peaks	29
HANS LÜDERS, RONALD P. LESSER, DUDLEY S. DINNER, HAROLD H. MORRIS, III, ELAINE WYLLIE	
3. Critical Analysis of Somatosensory Evoked Potential Recording Techniques	65
JOHN E. DESMEDT	
4. Critical Analysis of Pattern Evoked Potential Recording Techniques	87
IVAN BODIS-WOLLNER	
5. Critical Analysis of Short-Latency Auditory Evoked Potential Recording Techniques	105
ISAO HASHIMOTO	
6. Clinical Use of Evoked Potentials: A Review	143
HAROLD H. MORRIS, III, HANS LÜDERS, DUDLEY S. DINNER, RONALD P. LESSER, ELAINE WYLLIE	
7. Evoked Potentials in Multiple Sclerosis and Optic Neuritis	161
KEITH H. CHIAPPA	
8. Evoked Potentials in Non-Demyelinating Diseases	181
FRANÇOIS MAUGUIÈRE	

vi Contents

9. Sensory Evoked Potentials in Coma and Brain Death CARL ROSENBERG, ARNOLD STARR	223
10. Electrophysiologic Monitoring of Neural Function during Surgery JASPER R. DAUBE	241
Index	271

---

## CONTRIBUTING AUTHORS

Ivan Bodis-Wollner

Professor of Neurology and Ophthalmology  
Mt. Sinai School of Medicine  
1200 5th Avenue  
New York, NY 10029

Keith H. Chiappa

Director of the EEG and Evoked Potentials Unit  
Clinical Neurophysiology Laboratory  
Bigelow Building 11  
Massachusetts General Hospital  
Boston, MA 02114

Jasper R. Daube

Director, EMG Laboratory  
Mayo Clinic  
200 First Street, SW  
Rochester, MN 55905

John E. Desmedt

Director of the Brain Research Unit  
University of Brussels

Boulevard de Waterloo 115  
1000 Brussels, Belgium

Isao Hashimoto  
Chief, Department of Neurosurgery  
Tokyo-toritsu-fuchu-byoin  
Fuchu-city  
Musashidai 2-9-2  
Tokyo, Japan

Jun Kimura  
Department of Neurology  
0181 RCP  
University of Iowa Hospitals and Clinics  
Iowa City, Iowa 52240

Hans Lüders  
Head, Section of Epilepsy and  
Clinical Neurophysiology  
Department of Neurology/S-53  
Cleveland Clinic Foundation  
9500 Euclid Avenue  
Cleveland, OH 44106

François Mauguière  
Director, Laboratoire de Neurophysiologie Sensorielle  
Service EEG Hôpital Neurologique  
50 Boulevard Pinel 69003  
Lyon, France

Harold H. Morris, III  
Section of Epilepsy and Clinical Neurophysiology  
Department of Neurology/S-53  
Cleveland Clinic Foundation  
9500 Euclid Avenue  
Cleveland, OH 44106

Carl Rosenberg  
Department of Neurology  
California College of Medicine  
University of California at Irvine  
Irvine, CA 92717



---

## PREFACE

Over the last twenty to thirty years the progressively increasing availability of averaging machines has made evoked potential testing available not only in the major neurological diagnostic centers but also in the office of many neurologists in private practice. This rapid development was closely paralleled by clinical research in evoked potentials and the publishing of books covering in detail the basic techniques necessary to obtain evoked potentials and the main clinical applications of evoked potentials. Less work was done, however, to define some of the general principles underlying the recording of evoked potentials or to analyze critically the recording techniques or the actual practical value of the information provided by evoked potential testing.

In this book an attempt has been made to cover this gap. It is assumed that the reader has a good understanding of basic recording techniques and is familiar with the main applications of clinical evoked potentials. The main emphasis of the first two chapters is to define with more precision some of the physical principles that influence the voltage distribution and are used for defining the generator sources of evoked potentials. This is followed by a critical analysis of recording techniques and of its main clinical applications. Finally there is one chapter that gives an overview on application of evoked potentials for surgical monitoring. This is a rapidly growing field that also has been covered only incompletely in previous publications.

I hope that some of the material presented in this book will provide a more solid scientific basis to the study of evoked potentials and this in turn will strengthen the clinical value of evoked potential testing.

---

## 1. THEORY OF NEAR-FIELD AND FAR-FIELD EVOKED POTENTIALS

JUN KIMURA  
THORU YAMADA  
D. DAVID WALKER

The theory of far-field recording originally developed in the studies of brain-stem auditory evoked potentials [1–3]. More recently, investigators have applied this concept to the analysis of short latency somatosensory evoked potentials (SEPs) recorded over the scalp after stimulation of the median or tibial nerve [4–17].

Stationary far-field peaks may originate from fixed neural generators such as those which occur at synapses in relay nuclei. However, based on the latency of simultaneously recorded near-field potentials, along the course of the somatosensory pathway, the initial positive peaks of the scalp recorded median, or tibial SEPs, occur before the nerve action potentials reach the second order neurons in the dorsal column [9, 11, 12, 16, 18]. These peaks, therefore, must result from axonal volleys of the first order afferents [15, 16]. The relationship between the near-field and far-field potentials largely remains to be elucidated. Particularly puzzling is the appearance of stationary peaks from a traveling source at certain fixed points in time.

If the current from a deep generator spreads through the volume conductor, a referential recording fails to localize the source of the signal detected by the recording electrodes because it represents a distant potential [19–23]. Thus, to determine the origin of far-field activity, one must trace the moving potential along its path with bipolar recording. Comparison between bipolar and referential recording may then provide a temporal relationship between near-field and far-field potentials. The median and radial nerves are directly

accessible to surface recording over the hand and along the digits for a detailed analysis of field distribution. Recent studies using such simple models have elucidated possible physiologic mechanisms for the generation of stationary peaks from a moving source at certain points in time [24–27].

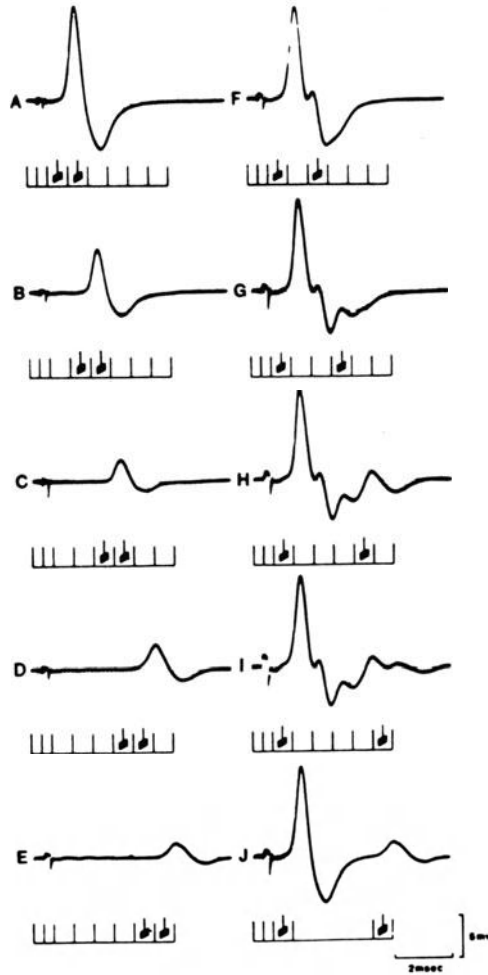
### ANIMAL STUDIES

In a series of important contributions, Nakanishi [28] reported interesting observations on the bull frogs' action potentials recorded by fluid electrodes, i.e., two pools of Ringer's solution containing a nerve immersed through a slot of the partition. He used a plastic box with eight compartments, dividing the first two chambers for stimulating electrodes at intervals of 1.5 cm and the remaining six chambers for recording electrodes at intervals of 2.0 cm. A systematic removal of several silk threads embedded in Vaseline around the nerve at each slot regulated the impedance between the adjacent fluid electrodes.

Stimulation of the nerve at the initial chambers gave rise to a biphasic action potentials recorded by adjacent fluid electrodes in the subsequent chambers. Two electrodes placed in one chamber detected no potential difference during traveling of the impulse through the Ringer solution [29]. With wider separation between the two recording electrodes, the number of peaks in the action potential increased to equal the number of partitions between the electrodes. The peaks became greater in amplitude in direct proportion to the impedance between the adjacent fluid electrodes at a given slot in question (figure 1-1).

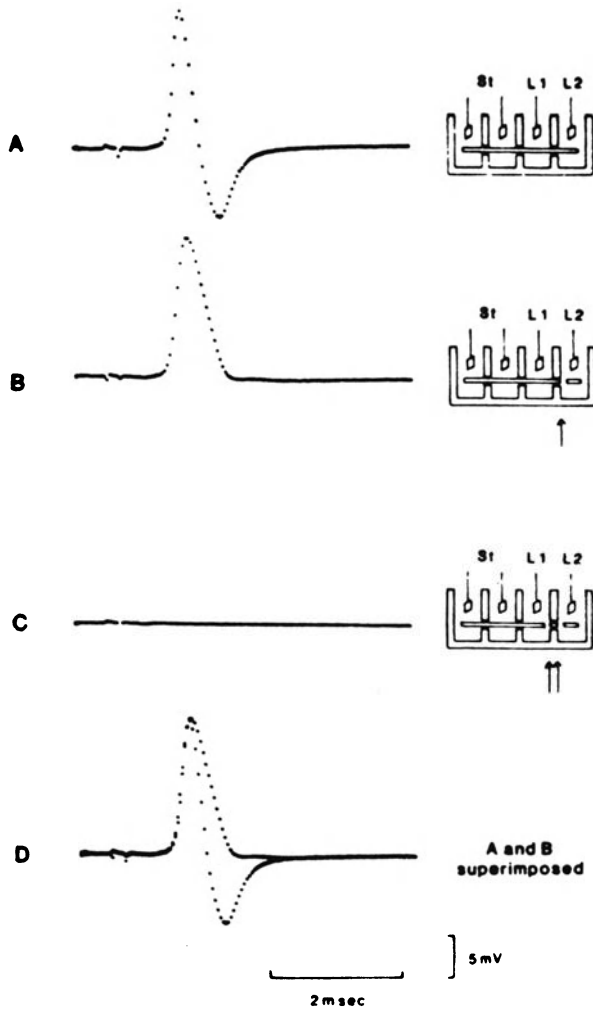
These findings led Nakanishi to conclude that a stationary potential results from the traveling impulse whenever the impedance of the conducting medium changes suddenly. The traditional dipole concept assumes that the nerve impulse travels through an infinite, electrically homogeneous conducting medium [19]. In reality, however, the peripheral nerve impulse must traverse various regions with differing impedance. Interpretation of the action potential in this clinical domain, therefore, must take into account the effect of the inhomogeneity of the surrounding tissues.

In a subsequent experiment, Nakanishi [30] verified the generation of action potential at the slot of the partition, and documented a proportional relationship between the impedance across the chambers and the amplitude of the recorded potential. In this study, he further demonstrated that the biphasic action potential recorded between the adjacent fluid electrodes became monophasic following section of the nerve at the point of exit from the slot to the next compartment. Cutting the nerve at the point of its entrance to the slot totally abolished the evoked potential. In support of his original hypothesis, the action potentials recorded by the fluid electrodes with two partitions between them equaled the algebraic sum of two individual potentials recorded by the adjacent electrode across each partition (figure 1-2).



**Figure 1-1.** Action potentials recorded by fluid electrodes placed at various positions. The inset just below each action potential indicates the position of the recording electrodes (closed rhombus). The two chambers with shorter length on the left side are those for stimulating electrodes. Note that the number of peaks of the action potential is equal to that of the partition between the recording electrodes. From Nakanishi [28].

Physiologic characteristics of the action potentials recorded by fluid electrodes resemble those of the far-field potentials registered over the scalp following stimulation of the median nerve. Thus, Nakanishi postulated that some of the short latency positive far-field peaks of the median SEP might result from the change of impedance along the course of the pathway. He concluded that far-field potentials could occur as if generated at fixed sites, such as just beneath the clavicle and foramen magnum as the impulse initiated



**Figure 1-2.** Action potentials recorded by the adjacent fluid electrodes before and after cutting off the nerve at the point of the entrance and the exit of the partition. A: before cutting off the nerve. B: after cutting off the nerve at the point of the exit of the partition. C: after cutting of the nerve at the point of both the entrance and the exit of the partition. D: both action potentials A and B were superimposed. The inset indicates stimulating and recording techniques. St, stimulation; L1, L2 recording electrodes. Arrows indicate the point where the nerve was cut off. From Nakanishi [30].

in the median nerve travels through various regions where the volume resistance might change abruptly [31].

The initial positivity,  $P_9$  or  $P_1$  of Nakanishi, however, more precisely coincides with the propagating impulse crossing the shoulder joint, as postulated earlier [15] and subsequently confirmed by a number of studies [32–34]. Thus,

P<sub>9</sub> appears slightly before and not concomitant with the arrival of the axonal volley at the clavicular site. In cats, a reversal of the polarity of P<sub>9</sub> occurs with abduction of the upper arm to a high position on the side stimulated [35]. Further, a change in direction and position of the traveling nerve impulse causes a reversal of action potential polarity when tested *in vitro* using the bull frog sciatic nerve [35]. These observations demonstrate the dependency of the far-field potential on the direction of the propagating source at the volume conductor junctions. Additionally, and perhaps more importantly, an effect induced by a dimensional change of the volume conductor at the shoulder plays a major role as described below.

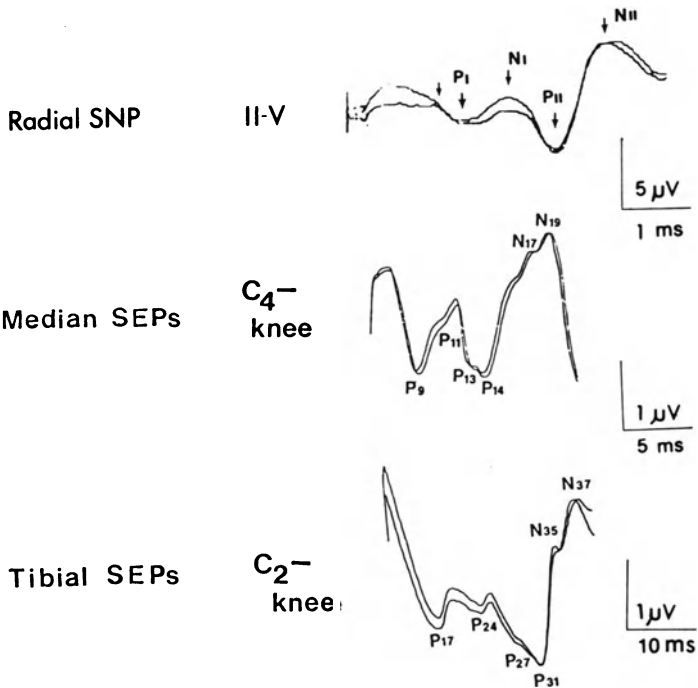
#### **SHORT LATENCY PEAKS OF MEDIAN AND TIBIAL SEPS**

The available data suggest that the four scalp-recorded positive peaks, P<sub>17</sub>, P<sub>24</sub>, P<sub>27</sub>, and P<sub>31</sub> of the tibial SEPs are analogous to P<sub>9</sub>, P<sub>11</sub>, P<sub>13</sub> and P<sub>14</sub> of the median SEPs (figures 1-3 & 1-4). Like P<sub>9</sub>, which originates near the shoulder joint [5, 8, 11, 12, 36-38], P<sub>17</sub> is a far-field potential generated near the hip joint. Like P<sub>11</sub>, thought to arise near the entry into the spinal cord [11, 12, 39, 40, 41], P<sub>24</sub> corresponds to the entry of the sensory impulse to the conus medullaris. Like P<sub>13</sub>, P<sub>27</sub> represents a rostral spinal cord potential. The last positive potential, P<sub>31</sub>, arises from the brainstem analogous to P<sub>14</sub>, which also occurs concomitant with the arrival of the impulse at the medial lemniscus of the medulla. This is in contrast to the first negative peaks, N<sub>17</sub> or N<sub>18</sub>, and N<sub>19</sub> of median SEPs, and N<sub>35</sub> and N<sub>37</sub> of tibial SEPs, which probably represent thalamic and cortical discharges.

In the analysis of scalp-recorded SEPs, one tends to attribute the far-field peaks to specific neural structures along the somatosensory pathways. It is not known, however, why the impulse traveling along the first order afferents gives rise to standing potentials at certain points in time in the absence of fixed neural discharges. Such stationary peaks may occur with a sudden change in direction of the propagating impulse, at branching points of the nerve or as the result of altered conduction properties of the nerve of the surrounding tissue. A postural change altering the angle between the arm and the shoulder can influence the latency value of P<sub>9</sub> of median SEPs in humans [18] or in cats [31]. An abrupt change in resistance of the conducting medium can lead to the generation of an action potential [28, 30]. Detailed observation in humans supports the contention that a major change in physical characteristics of the conducting medium may give rise to some of the subcortical SEP peaks [42, 43].

#### **JUNCTIONAL POTENTIALS GENERATED BY PERIPHERAL NERVE VOLLEYS**

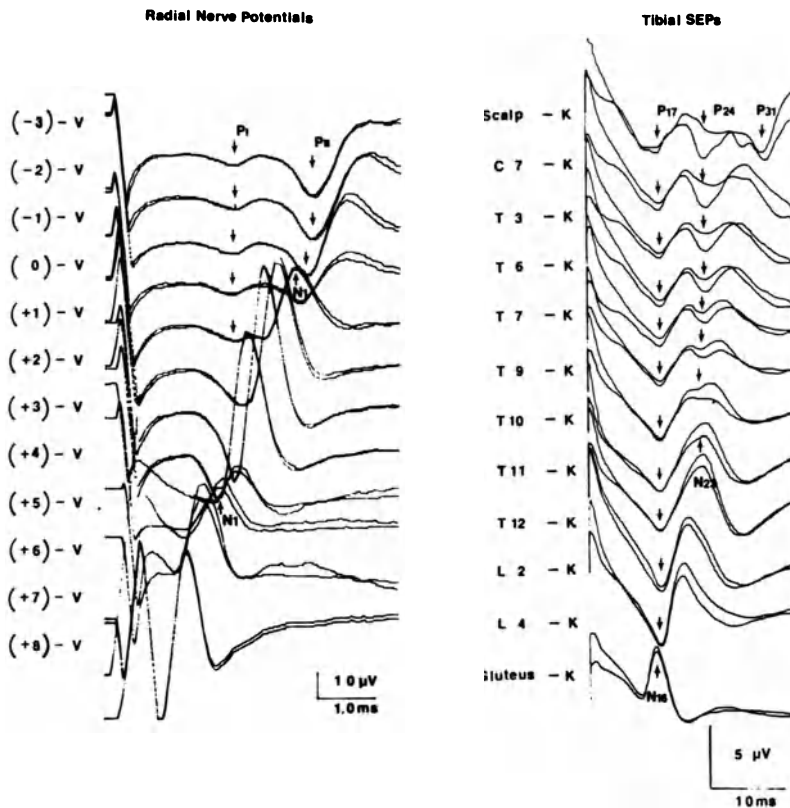
In a series of studies, we have explored the relationship between a change of volume conductor geometry and the occurrence of stationary peaks from a traveling source [15, 17]. The technique consisted of supramaximal stimula-



**Figure 1-3.** Scalp recorded SEPs using a non-cephalic reference after stimulation of the median nerve at the wrist (middle) and tibial nerve at the ankle (bottom). Both median and tibial SEPs consist of four positive peaks initially and two negative peaks thereafter, all within the first 20 and 40 msec following the stimulus, respectively. For comparison, the top tracing shows far-field potentials, PI-NI and PII-NII, recorded from digit II referenced to digit V, after stimulation of the radial sensory fibers at the forearm.

tion of a nerve with surface electrodes, and bipolar and referential recording of the compound sensory action potentials from multiple points along the course of the nerve. An eight channel averager simultaneously displayed near-field and far-field potentials in 1.5 cm increments from the distal forearm to the tip of a digit across the palm or dorsum of the hand. The zero (0) level represented the base of the digit with the other recording sites indicated by a number from the zero level, assigning a negative (-) sign distally. We used rectangular electrodes, firmly attached to the skin with collodion, over the hand and distal forearm, and ring electrodes along the digit.

A fast recovery amplifier [44], with a frequency response of 10 Hz to 3 KHz (3 dB down), allowed accurate analysis of short latency responses within the first few milliseconds. Single stimuli usually elicited discrete compound sensory nerve potentials. To improve the resolution, however, each test set consisted of an average of 50 summated responses. Two sets of averaging confirmed consistency of the recorded response for each electrode derivation.

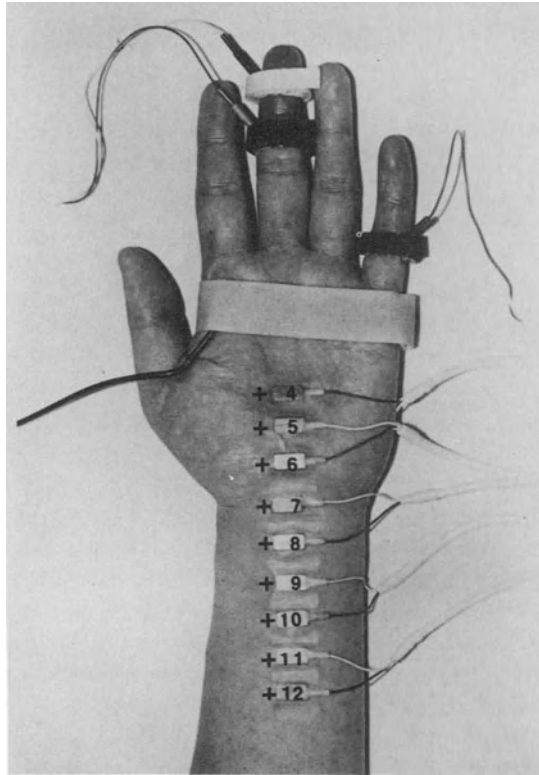


**Figure 1-4.** Antidromic radial nerve potentials (left) recorded referentially with  $G_1$  over the dorsum of the hand and along the second digit, and  $G_2$ , around the fifth digit (V) versus tibial SEPs (right) recorded referentially with  $G_1$  over the scalp, along the spine and near the gluteal fold, and  $G_2$ , at the knee (K), after stimulation of the tibial nerve at the ankle. The far-field peaks of the radial nerve potentials, P<sub>I</sub> and P<sub>II</sub> (arrows pointing down), appeared coincident with the entry of the propagating impulse, N<sub>I</sub> (arrows pointing up), into the wrist and the base of the second digit, respectively. Similarly, P<sub>17</sub> and P<sub>24</sub> of the tibial SEPs signaled the arrival of the traveling volleys at the pelvic girdle and conus medullaris as indicated by the near-field potentials, N<sub>16</sub> and N<sub>23</sub>, respectively.

According to convention, an upward deflection resulted when  $G_1$  became negative relative to  $G_2$ . We designated the propagating near-field potentials by polarity and Arabic numerals, e.g., P<sub>1</sub> and N<sub>1</sub>, and the stationary far-field peaks using Roman subscripts, e.g., P<sub>I</sub> and N<sub>I</sub>. However, the distinction between the near-field and far-field components was not always absolute. In referential recording of a traveling source, a stationary far-field activity often merged into propagating near-field potentials as described below.

Studies included recording of the orthodromic and antidromic median sensory potentials, and antidromic radial sensory potentials. A total of 20



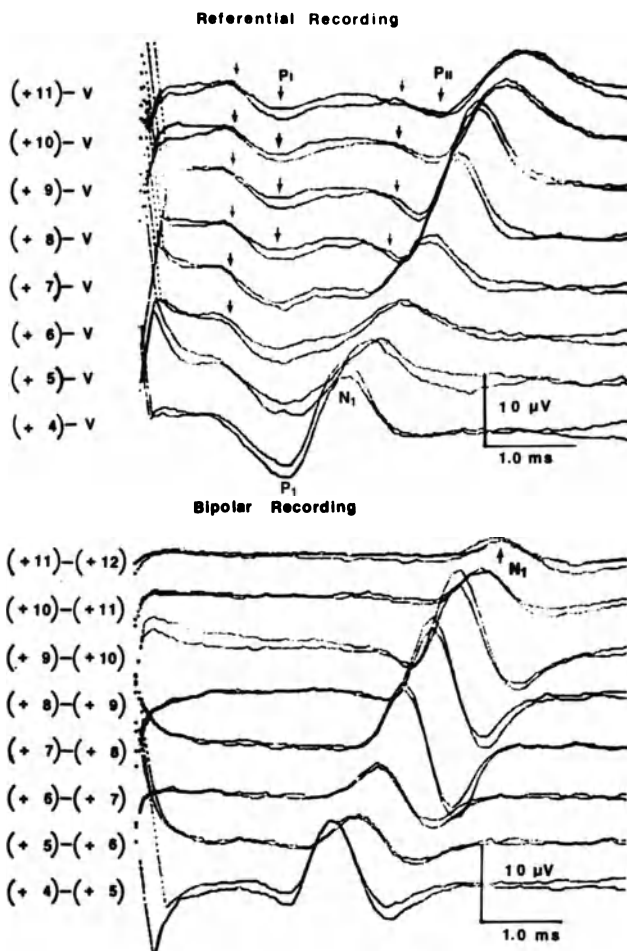


**Figure 1-5.** Serial recording sites in 1.5 cm increments along the course of the median nerve. The 0 level was at the base of the third digit. The ring electrode around the fifth digit is an indifferent lead for referential recording. Sensory nerve action potentials were recorded orthodromically following stimulation of the digital nerve with a pair of ring electrodes near the tip of the third digit.

subjects participated in three sets of experiments in various combination. To consolidate the presentation, we will describe experimental design, electrode placement and test results altogether, for each of the three categories of investigation, under separate headings.

### **Median nerve—orthodromic potential**

For orthodromic study of the median nerve, we stimulated the tip of the third digit supramaximally using a shock of 0.1 msec duration delivered through a pair of ring electrodes, cathode proximally. We recorded the sensory potentials over the proximal palm and distal forearm, using rectangular electrodes placed at +4 through +12 in increments of 1.5 cm (figure 1-5). The ground electrode was placed across the palm between the stimulating and recording electrodes.



**Figure 1-6.** Sensory nerve potentials over the proximal palm and distal forearm in a normal subject recorded orthodromically after stimulation of the digital branch of the median nerve. The site of recording is indicated (figure 1-4). A gradual shift in latency of the traveling peak,  $N_1$ , is linear along the course of the nerve in a bipolar recording (bottom). In contrast, the near-field peaks,  $P_1$ - $N_1$ , in a referential recording were distorted by two stationary potentials,  $P_1$  and  $P_{II}$ , that occurred concomitant with the arrival of the propagating impulse at the base of the digit and the wrist, respectively.

A bipolar recording consisted of a series of two adjacent leads,  $G_1$  distal to  $G_2$ , i.e., +4 to +5 through +11 to +12. Recorded potentials were biphasic with a major negative peak,  $N_1$ , and subsequent positive peaks,  $P_2$ , over the proximal palm and distal forearm, although a small initial positivity,  $P_1$  sometimes preceded  $N_1$  (figure 1-6, bottom). The onset latencies on  $N_1$  increased almost linearly from +4 to +11 at a rate of 0.25 to 0.35 msec per unit distance

of 1.5 cm. The latency differences between two successive recording sites were significantly ( $P < 0.01$ ) smaller proximally. The maximal conduction velocity of each 1.5 cm segment ranged from 42 to 63 msec. The amplitude of  $N_1$  showed slight variability from one recording site to the next along the course of the nerve, presumably reflecting different depths of the nerve from the surface. The potential generally decreased in amplitude beyond +9 to +10.

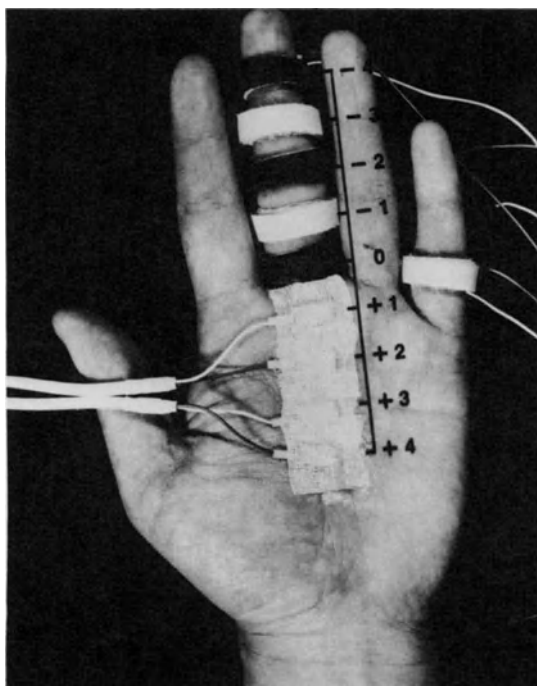
A referential recording combined the eight active electrodes, +4 through +11, to a common indifferent ring electrode around the fifth digit. The recorded potentials over the palm and distal forearm consisted of an initial positivity,  $P_1$ , followed by a negativity  $N_1$  and subsequent positivity,  $P_2$  (figure 1-6, top). The peak latencies of  $P_1$  and  $N_1$  increased linearly almost at the same rate as the corresponding peaks recorded bipolarly. However, the onset latency of  $P_1$  was stationary and coincident with the arrival of the traveling impulse at the base of the digit, indicating contribution of a far-field activity, PI. When recorded from +4 through +5, PI merged into  $P_1$  but at +6 and on, the propagating near-field peak,  $P_1$ , was usually distinct from the stationary component, PI, which then appeared as a separate standing potential.

The peak latencies of  $P_1$  and  $N_1$  continued to increase further proximally over the distal forearm. However, the onset latency of  $P_1$  changed minimally, from +7 to +11, indicating the presence of a second stationary component, PII, which occurred coincident with the arrival of the traveling volleys at the wrist. The standing far-field component, PII, merged into the propagating near-field peak,  $P_1$ , although a close inspection often disclosed a notch, suggesting a transition point. Since PII was stationary, whereas  $P_1$  was propagating, the overall duration of the initial positive peak increased progressively towards more proximal recording sites.

### **Median nerve—antidromic potential**

For antidromic study of the median nerve, we placed the cathode 3 cm above the distal crease at the wrist, and the anode 3 cm proximally. The stimulus was 0.1 msec in duration, and of just maximal intensity such that a further increase resulted in no change in amplitude of the sensory evoked potential. A ground strap was on the palm between the stimulating and recording electrodes. Some motor axons have thresholds similar to those of large myelinated sensory axons, and muscle contraction was unavoidable. However, unintended activation of motor fibers rarely interfered with the analysis of the antidromic sensory potential, which preceded the muscle action potential by a few milliseconds. For analysis of sensory potentials in 1.5 cm increments (figure 1-7), we used rectangular electrodes at +1 through +4 for palmar potential, and ring electrodes at 0 through -4 for digital potential.

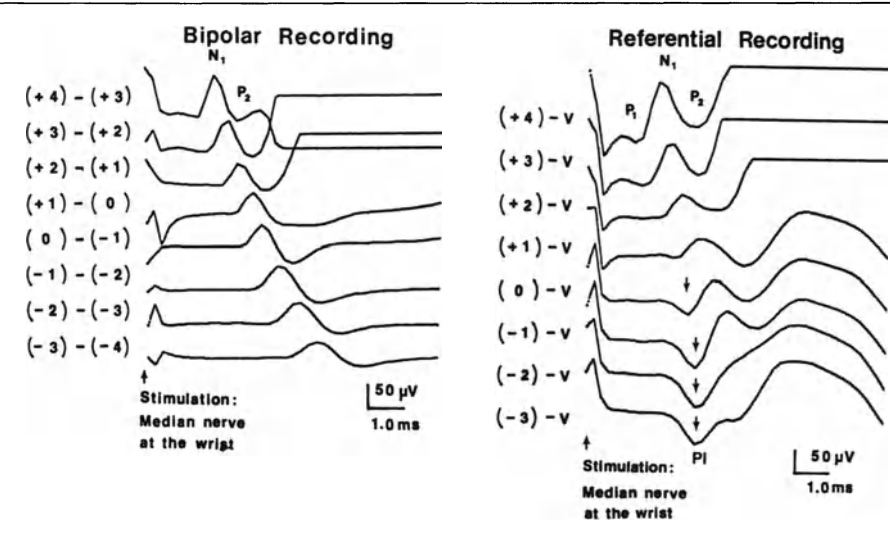
A bipolar derivation consisted of either pairs of recording electrodes, connecting two adjacent leads, with  $G_1$  proximal to  $G_2$  in each channel, i.e., +4 to +3 through -3 to -4. Both palmar and digital potentials were biphasic,



**Figure 1-7.** Eight recording sites in 1.5 cm increments along the length of the median nerve. The 0 level was at the base of the third digit where the volume conduction changes abruptly. The ring electrode around the fifth digit is an indifferent electrode for referential recordings. Sensory nerve action potentials were recorded antidromically following stimulation of the median nerve at the wrist. From Kimura et al. [24].

with a major negative peak,  $N_1$ , and subsequent positive peak,  $P_2$ . A small initial positivity,  $P_1$ , occasionally preceded  $N_1$  in the former (figure 1-8, left). The onset and peak latency of  $N_1$  increased progressively from +4 to -3 across the palm and along the length of the digit (table 1-1). The latency differences between two successive recording sites were significantly ( $P < 0.01$ ) greater distally along the digit than across the palm, indicating slowing of the sensory conduction toward the tip of the third digit. The maximal conduction velocity for each 1.5 cm segment ranged from 42 to 63 msec across the palm, and 32 to 47 msec along the digit.

For referential recording, the input from each of the eight active electrodes, +4 through -3, was led to  $G_1$  and each channel and was referenced to a common indifferent ring electrode  $G_2$  around the fifth digit, an area not innervated by the median nerve. Regardless of the recording site, the palmar potentials were triphasic with an initial positivity,  $P_1$ , and subsequent negative and positive peaks,  $N_1$  and  $P_2$  (figure 1-8, right). The latencies measured either at the onset or peak of  $P_1$  increased almost linearly at a rate of 0.21 to



**Figure 1-8.** Sensory nerve potentials across the palm and along the third digit in a normal subject recorded after stimulation of the median nerve at the wrist (arrow pointing up). The site of recording is indicated (figure 1-7). In a bipolar recording (left), shift in latency per unit distance was greater along the digit than across the palm. In contrast, the referential recording (right) showed nearly stationary positivity along the digit (arrows pointing down). These positive peaks were free of motor interference by the muscle potential that began approximately 1 msec later as indicated by saturation of the top three tracings (flat lines). From Kimura et al. [24].

0.38 msec per 1.5 cm from +4 to 0 (table 1-1). The palmar conduction velocities based on the latency of  $P_1$  were consistent with the values obtained in the bipolar derivation described above. The average onset latency of the muscle potential was 3.4 msec compared with the peak latency of  $P_1$  that ranged from 1.3 to 2.2 msec. Thus,  $P_1$  was free of motor interference, which partially buried  $P_2$  and  $N_1$  in the distal palm.

The digital potentials were also triphasic in a referential derivation. In contrast to the palmar potential, however, the onset latency of  $PI$  was identical along the length of the third digit (figure 1-8, right). Similarly, the peak latency of  $PI$  changed only 0.03 to 0.05 msec per 1.5 cm from -1 to -3 (table 1-1). Thus, the positivity generated near the base of the digit spread nearly instantaneously along the digit. In addition,  $PI$  peaks recorded near the base of the digit were significantly ( $P > 0.01$ ) smaller in amplitude and duration than those registered further distally. The muscle potential, with an average onset latency of 3.4 msec, distorted  $N_1$  and  $P_2$  but not  $PI$  of the digital potential, which had an average peak latency of only 2.9 msec.

### Radial nerve—antidromic potential

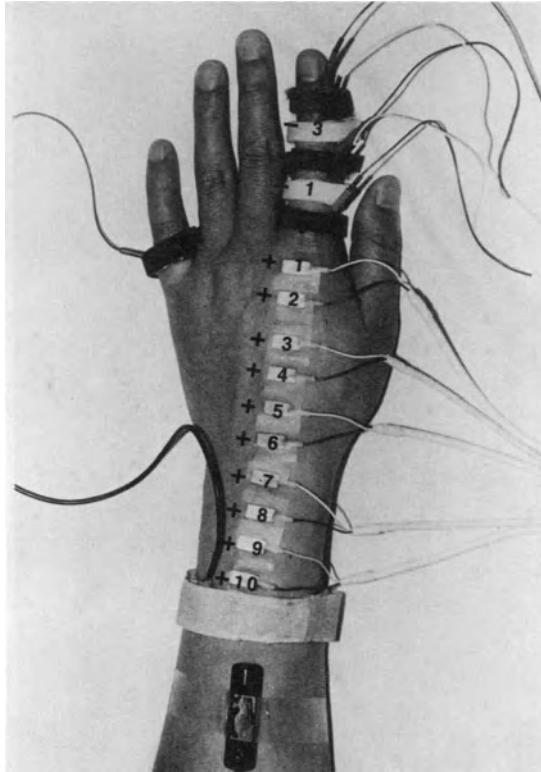
For antidromic stimulation of the radial nerve we placed the cathode 10 cm proximal to the styloid process of the radius, and anode 2 cm further proxi-

**Table 1-1.** Median sensory potentials recorded in 1.5 cm increments across the palm and along the digit (mean  $\pm$  standard deviation)  
Bipolar recording

Electrode G1 G2	Onset latency Of N <sub>1</sub> (msec)	Latency increase per 1.5 cm (msec)	Peak latency of N <sub>1</sub> (msec)	Latency increase per 1.5 cm (msec)	Amplitude of N <sub>1</sub> onset to peak ( $\mu$ V)	Duration of N <sub>1</sub> onset to peak (msec)
+4 +3	1.32 $\pm$ 0.19	0.24 $\pm$ 0.06	1.80 $\pm$ 0.20	0.31 $\pm$ 0.06	70.7 $\pm$ 31.8	0.46 $\pm$ 0.05
+3 +2	1.57 $\pm$ 0.20	0.36 $\pm$ 0.09	2.11 $\pm$ 0.24	0.33 $\pm$ 0.06	59.1 $\pm$ 20.2	0.53 $\pm$ 0.07
+2 +1	1.94 $\pm$ 0.23	0.32 $\pm$ 0.05	2.45 $\pm$ 0.25	0.34 $\pm$ 0.07	35.8 $\pm$ 18.2	0.50 $\pm$ 0.07
+1 0	2.26 $\pm$ 0.24	0.24 $\pm$ 0.07	2.79 $\pm$ 0.29	0.28 $\pm$ 0.05	26.9 $\pm$ 14.5	0.52 $\pm$ 0.08
0 -1	2.46 $\pm$ 0.41	0.32 $\pm$ 0.05	3.07 $\pm$ 0.30	0.39 $\pm$ 0.07	31.1 $\pm$ 11.2	0.55 $\pm$ 0.09
-1 -2	2.83 $\pm$ 0.28	0.34 $\pm$ 0.09	3.46 $\pm$ 0.35	0.47 $\pm$ 0.09	27.9 $\pm$ 13.5	0.63 $\pm$ 0.10
-2 -3	3.17 $\pm$ 0.32	0.47 $\pm$ 0.12	3.92 $\pm$ 0.40	0.51 $\pm$ 0.09	31.2 $\pm$ 12.1	0.74 $\pm$ 0.16
-3 -4	3.64 $\pm$ 0.34		4.46 $\pm$ 0.45		26.4 $\pm$ 13.2	0.80 $\pm$ 0.17

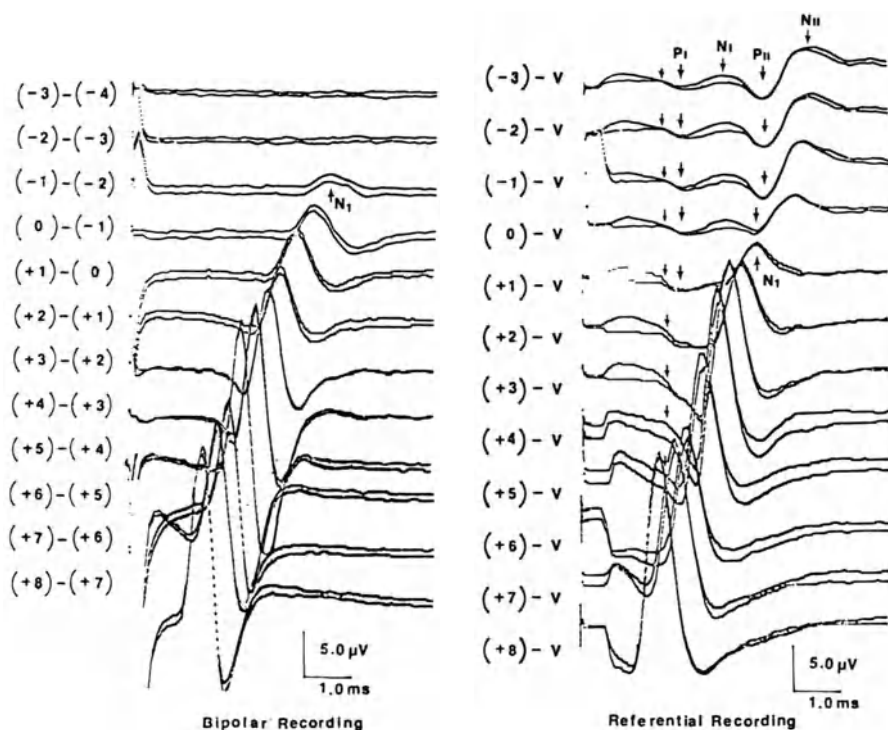
Referential recording						
Electrode G1 G2	Onset latency Of P <sub>1</sub> (msec)	Latency increase per 1.5 cm (msec)	Peak latency of P <sub>1</sub> (msec)	Latency increase per 1.5 cm (msec)	Amplitude of P <sub>1</sub> onset to peak ( $\mu$ V)	Duration of P <sub>1</sub> onset to peak (msec)
+4 V	1.02 $\pm$ 0.14	0.21 $\pm$ 0.04	1.34 $\pm$ 0.16	0.22 $\pm$ 0.08	16.1 $\pm$ 15.6	0.31 $\pm$ 0.11
+3 V	1.21 $\pm$ 0.16	0.26 $\pm$ 0.10	1.56 $\pm$ 0.19	0.32 $\pm$ 0.09	12.7 $\pm$ 9.9	0.35 $\pm$ 0.17
+2 V	1.43 $\pm$ 0.36	0.34 $\pm$ 0.12	1.89 $\pm$ 0.19	0.34 $\pm$ 0.11	8.6 $\pm$ 6.4	0.37 $\pm$ 0.12
+1 V	1.87 $\pm$ 0.21	0.26 $\pm$ 0.20	2.22 $\pm$ 0.21	0.38 $\pm$ 0.13	8.0 $\pm$ 7.4	0.41 $\pm$ 0.10
0 V	2.15 $\pm$ 0.16	0.01 $\pm$ 0.04	2.61 $\pm$ 0.23	0.23 $\pm$ 0.08	10.4 $\pm$ 7.9	0.49 $\pm$ 0.14
-1 V	2.18 $\pm$ 0.15	0.00 $\pm$ 0.00	2.85 $\pm$ 0.22	0.05 $\pm$ 0.04	23.7 $\pm$ 13.1	0.71 $\pm$ 0.14
-2 V	2.18 $\pm$ 0.15	0.00 $\pm$ 0.00	2.91 $\pm$ 0.24	0.03 $\pm$ 0.02	30.4 $\pm$ 15.6	0.77 $\pm$ 0.16
-3 V	2.18 $\pm$ 0.15		2.94 $\pm$ 0.25		30.7 $\pm$ 15.1	0.79 $\pm$ 0.16



**Figure 1-9.** Stimulation of the radial nerve 10 cm proximal to the styloid process of the radius and serial recording of antidromic sensory potentials in 1.5 cm increments along the length of the radial nerve. The 0 level was at the base of the second digit where the volume conductor changes abruptly. In most hands, +6 was near the distal crease of the wrist, where another, less obvious, transition of volume conductor geometry takes place. The ring electrode around the fifth digit is an indifferent lead for referential recordings. From Kimura et al. [25].

mally. A ground strap was on the distal forearm between the stimulating and recording electrodes. The stimulus was 0.1 msec in duration, and of just maximal intensity such that a further increase produced no change in amplitude of the recorded response. Shocks of higher intensity often resulted in an inadvertent excitation of the forearm extensors, which interfered with selective recording of intended sensory nerve potentials. To record the sensory nerve potentials we used rectangular electrodes at +1 through +10 over the dorsum of the hand and distal forearm, and ring electrodes placed at 0 through -4 around the second digit (figure 1-9).

A bipolar derivation consisted of 14 pairs of pick-up electrodes connecting two adjacent leads, with  $G_1$  proximal to  $G_2$  in each channel, i.e., +10 to +9 through -3 to -4. The near-field potentials showed a major negative peak,



**Figure 1-10.** Sensory nerve potentials across the hand and along the second digit in a normal subject recorded antidromically after stimulation of the superficial sensory branch of the radial nerve 10 cm proximal to the styloid process of the radius. The site of recording is indicated (figure 1-9). In a bipolar recording (left), the initial negative peaks,  $N_1$  (arrow pointing up), showed a progressive increase in latency and reduction in amplitude distally and no response was recorded beyond  $-1$ . In a referential recording (right), biphasic peaks,  $P_1-N_1$  and  $PII-N_{II}$  (arrows pointing down) showed greater amplitude distally, with a stationary latency irrespective of the recording sites along the digit. The onset of  $P_1$  extended proximally to the recording electrodes near the wrist (small arrows pointing down), whereas  $PII$  first appeared at the base of the digit. From Kimura et al. [25].

$N_1$ , and a subsequent positive peak, although another small positivity often preceded  $N_1$  (figure 1-10, left). The field distribution differed considerably from one subject to the next, reflecting the anatomic variability of radial nerve innervation. In all hands tested, the amplitude of  $N_1$  showed gradual reduction distally across the dorsum of the hand, from  $+10$  to  $0$ , and along the second digit, from  $0$  to  $-1$  or  $-2$ , with no response thereafter (table 1-2). The onset and peak latencies of  $N_1$  increased progressively at a rate of  $0.22$  to  $0.45$  msec per unit distance. The maximal conduction velocity for each  $1.5$  cm segment ranged from  $40$  to  $68$  msec.

A referential derivation recorded the input from each of the 14 active electrodes,  $+10$  through  $-3$ , as  $G_1$  of each channel, and a common, indifferent



**Table 1-2.** Radial nerve sensory potentials recorded in 1.5 cm increments across the dorsum of the hand and along the second digit (mean  $\pm$  standard deviation) Bipolar recording (N<sub>1</sub>)

Electrode G1 G2	# Recorded		Onset Latency (msec)	Latency Increase per 1.5 cm (msec)	Peak Latency (msec)	Latency Increase per 1.5 cm (msec)	Amplitude Onset to Peak (uV)	Duration Onset to Peak (msec)
	# Tested							
-3 -4	5/20		4.24 $\pm$ 0.23	0.38 $\pm$ 0.06	4.91 $\pm$ 0.15	0.39 $\pm$ 0.09	0.5 $\pm$ 1.0	0.66 $\pm$ 0.18
-2 -3	7/20		4.03 $\pm$ 0.44	0.34 $\pm$ 0.10	4.73 $\pm$ 0.52	0.43 $\pm$ 0.13	0.9 $\pm$ 1.6	0.70 $\pm$ 0.13
-1 -2	13/20		3.82 $\pm$ 0.36	0.32 $\pm$ 0.09	4.35 $\pm$ 0.49	0.35 $\pm$ 0.09	2.0 $\pm$ 2.4	0.58 $\pm$ 0.10
0 -1	14/20		3.48 $\pm$ 0.37	0.38 $\pm$ 0.08	4.03 $\pm$ 0.41	0.29 $\pm$ 0.11	2.5 $\pm$ 2.5	0.53 $\pm$ 0.12
+1 0	20/20		3.12 $\pm$ 0.28	0.30 $\pm$ 0.09	3.78 $\pm$ 0.35	0.45 $\pm$ 0.09	7.7 $\pm$ 4.0	0.65 $\pm$ 0.11
+2 +1	20/20		2.82 $\pm$ 0.21	0.31 $\pm$ 0.07	3.31 $\pm$ 0.26	0.33 $\pm$ 0.07	11.5 $\pm$ 6.3	0.48 $\pm$ 0.08
+3 +2	20/20		2.47 $\pm$ 0.23	0.22 $\pm$ 0.07	2.97 $\pm$ 0.26	0.29 $\pm$ 0.07	16.6 $\pm$ 9.6	0.47 $\pm$ 0.10
+4 +3	20/20		2.26 $\pm$ 0.22		2.68 $\pm$ 0.23		17.9 $\pm$ 9.8	0.42 $\pm$ 0.06
Referential recording (PI)								
-3 V	20/20		1.75 $\pm$ 0.24	0.01 $\pm$ 0.02	2.22 $\pm$ 0.26	0.01 $\pm$ 0.02	1.1 $\pm$ 0.8	0.48 $\pm$ 0.12
-2 V	20/20		1.74 $\pm$ 0.23	0.01 $\pm$ 0.02	2.22 $\pm$ 0.26	0.03 $\pm$ 0.05	1.1 $\pm$ 0.8	0.47 $\pm$ 0.13
-1 V	20/20		1.71 $\pm$ 0.22	0.01 $\pm$ 0.02	2.19 $\pm$ 0.25	0.03 $\pm$ 0.03	1.0 $\pm$ 0.7	0.46 $\pm$ 0.11
0 V	20/20		1.68 $\pm$ 0.29	0.03 $\pm$ 0.06	2.15 $\pm$ 0.24		0.9 $\pm$ 0.5	0.44 $\pm$ 0.11
+1 V	17/20		1.65 $\pm$ 0.16	0.01 $\pm$ 0.01				
+2 V	17/20		1.64 $\pm$ 0.16	0.01 $\pm$ 0.01				
+3 V	17/20		1.63 $\pm$ 0.17	0.01 $\pm$ 0.01				
+4 V	17/20		1.62 $\pm$ 0.18	0.01 $\pm$ 0.02				
Referential recording (PII)								
-3 V	20/20		3.28 $\pm$ 0.40	0.01 $\pm$ 0.02	3.92 $\pm$ 0.31	0.02 $\pm$ 0.02	3.9 $\pm$ 3.4	0.61 $\pm$ 0.15
-2 V	20/20		3.27 $\pm$ 0.39	0.01 $\pm$ 0.03	3.95 $\pm$ 0.29	0.05 $\pm$ 0.01	3.9 $\pm$ 3.1	0.60 $\pm$ 0.15
-1 V	20/20		3.25 $\pm$ 0.39	0.01 $\pm$ 0.04	3.87 $\pm$ 0.30	0.11 $\pm$ 0.07	3.3 $\pm$ 2.7	0.57 $\pm$ 0.15
0 V	20/20		3.24 $\pm$ 0.39		3.71 $\pm$ 0.32		2.0 $\pm$ 1.4	0.47 $\pm$ 0.17

Unable to measure because of the overlap with succeeding near-field potentials, P<sub>1</sub> and N<sub>1</sub>.

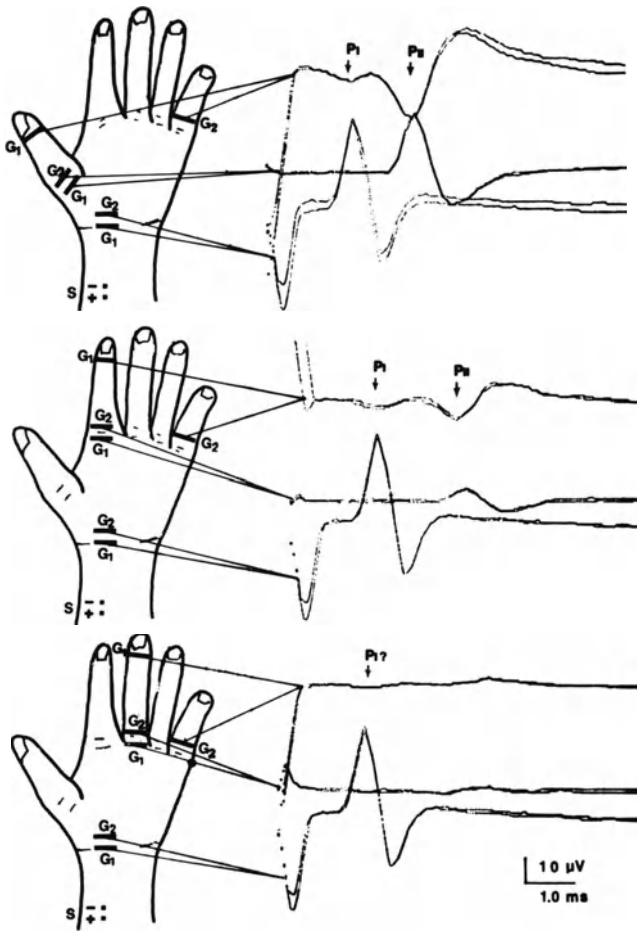
ring electrode around the fifth digit as  $G_2$ . The recorded potentials over the dorsum of the hand were triphasic, with an initial positive peak, a subsequent negative peak,  $N_1$ , and another positive peak (figure 1-10, right). The amplitude of  $N_1$  declined distally across the hand from +10 to 0. The peak latencies of  $N_1$  increased almost linearly at a rate of 0.21 to 0.38 msec per unit distance of 1.5 cm, showing the characteristics of a traveling potential with the initial positivity representing the moving front of depolarization (table 1-2). The conduction velocities based on the latency changes of  $N_1$  were consistent with the values obtained in bipolar derivation described above. In contrast, the onset latency remained nearly stationary from +5 to 0, suggesting a substantial contribution of a far-field activity, PI, preceding the propagating near-field potential.

Referential recording along the second digit showed two diphasic potentials, PI-NI and PII-NII, although NI was often small and at times absent (figure 1-10, right). Of the two positive peaks, PI was approximately one-fourth to one-half of PII in amplitude, but similar in duration. Neither PI nor PII changed significantly in onset or peak latency from 0 to -3 ( $P > 0.1$ ). The onset latency of PI along the second digit was identical to that of the corresponding peak recorded over the dorsum of the hand described above, both being concomitant with the arrival of the sensory impulse at the wrist as determined by the latency of the near-field potential. Unlike PI, PII was recorded only along the digit. When compared to the propagating potential recorded by bipolar derivation, the onset of PII was time-locked with the arrival of the sensory impulse at the base of the second digit.

### **Factors that determine the latency and amplitude of far-field peaks**

The electrode over the wrist and the base of the first digit registered the near-field potential in all 20 hands, as expected from the pattern of radial nerve innervation. This was in contrast to the recording of the potential at the base of the second and third digit in 17 and 4 hands, respectively, and at the base of the fourth and fifth digits in none. Referential recording from the tip of the first, second, third and fourth digits gave rise to PI-NI in 14, 14, 10 and 8 hands, and PII-NII in 20, 19, 12 and 1 hand, respectively. Of the two stationary positivities, PI was coincident with the entry of the impulse into the wrist (figure 1-11) showing an identical latency irrespective of the digit tested. In contrast, PII occurred when the traveling source reached the base of each digit. Therefore, the onset latency of PII was significantly ( $P < 0.01$ ) shorter for the first digit than the others, reflecting the relative distance from the stimulus point (figure 1-12).

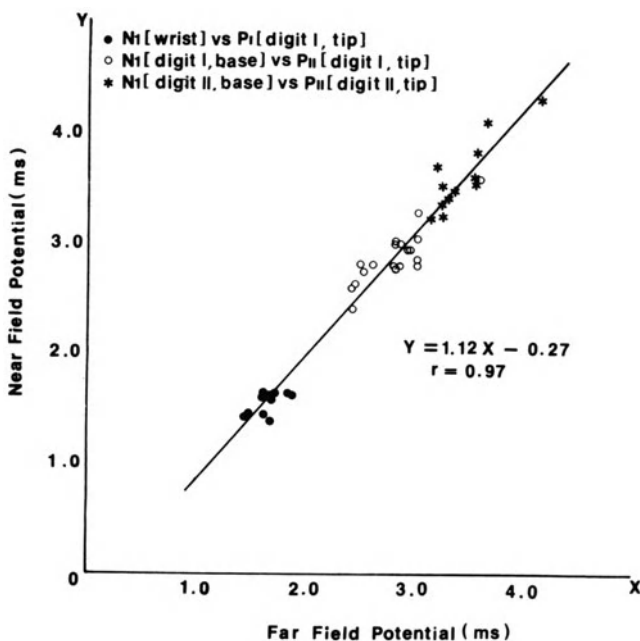
Regardless of the digit tested, PI and PII were significantly ( $P < 0.01$ ) smaller in amplitude and shorter in duration near the base of the digit than further distally (table 1-2, figure 1-10, right). A statistical analysis showed a linear correlation between the amplitude of PII recorded referentially near the tip and that of the near-field potential,  $N_1$ , registered bipolarly at the base of



**Figure 1-11.** Referential recording of far-field potentials from the tip of the first (top), second (middle) and third digit (bottom) as compared with simultaneously registered near-field potential at the wrist and the base of the respective digit. Of the two stationary peaks,  $P_I$  was identical in latency irrespective of the digit tested, whereas  $P_{II}$  was significantly shorter for the first than the second digit. Recording from the third digit showed a questionable  $P_I$  and no  $P_{II}$  in the absence of a near-field potential detectable at the base of the digit. From Kimura et al. [25].

the digit (figure 1-13). Thus, a well defined  $P_{II}$  accompanied a large  $N_1$  at the base of the digit whereas  $P_{II}$  was usually small if  $N_1$  recorded at the palm-digit junction in question is equivocal. In 8 hands, however,  $P_{II}$  was clearly present when recorded from the tip of the third digit despite the absence of  $N_1$  at the base of the digit with  $G_1$  and  $G_2$  placed at 0 and  $-1$ , respectively.

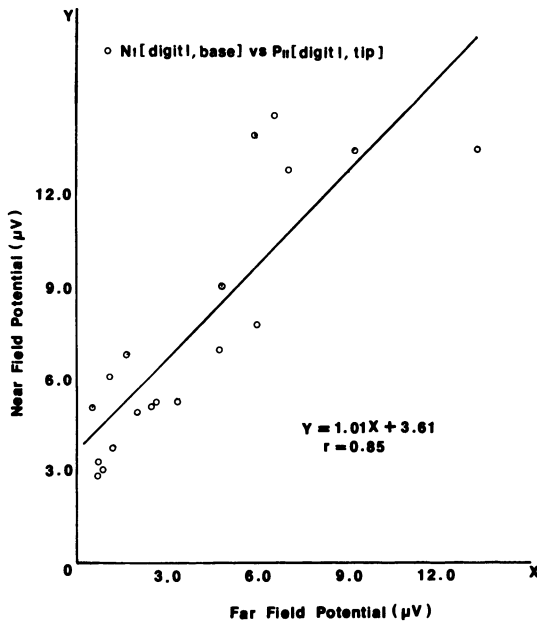
To compare the amplitude of far-field and near-field potentials elicited by various stimulus intensities, we recorded  $P_{II}$  using two referential channels:



**Figure 1-12.** Latency comparison between the near-field peak,  $N_1$ , and the far-field peaks,  $P_1$  and  $P_{II}$ , of the antidromically activated radial nerve sensory potential. Of the two far-field peaks,  $P_1$  recorded referentially from the tip of the first digit corresponded in latency to  $N_1$  recorded bipolarly at the wrist (closed circle), and  $P_{II}$  recorded from the tip of the first (open circle) and second (star) digits corresponded to  $N_1$  registered at the base of the respective digit. A high coefficient factor indicates a temporal relationship of the stationary peaks,  $P_1$  and  $P_{II}$ , with the propagating volley,  $N_1$ , at the wrist and the base of the digits. From Kimura et al. [25].

with  $G_1$  around the tip of the first or second digit and  $G_2$  around the fifth digit; and  $N_1$  by two channels of bipolar derivation, with  $G_1$  1 cm proximal to the distal crease at the base of the first or second digit, and  $G_2$  1 cm distally. A four channel averager recorded all responses simultaneously at each level of stimulus intensity. The amplitude of  $N_1$  and  $P_{II}$ , measured baseline to peak, varied considerably among individuals. For a group analysis, therefore, we converted the measurement into a percentage of the maximal potential in each hand, and plotted the percent values of corresponding responses to determine the degree of correlation between the two.

With progressive reduction in stimulus intensity from a maximal to a just threshold level in 10 step,  $N_1$  gradually decreased in size from a full response to zero (figure 1-14). This is accompanied by a concomitant reduction in size of the  $P_{II}$  recorded referentially at the tip of the respective digit in all subjects tested. Statistical analyses revealed a linear correlation in amplitude between the two responses whether tested individually or collectively. In occasional hands, a decrease in stimulus intensity resulted in a nonlinear reduction in size

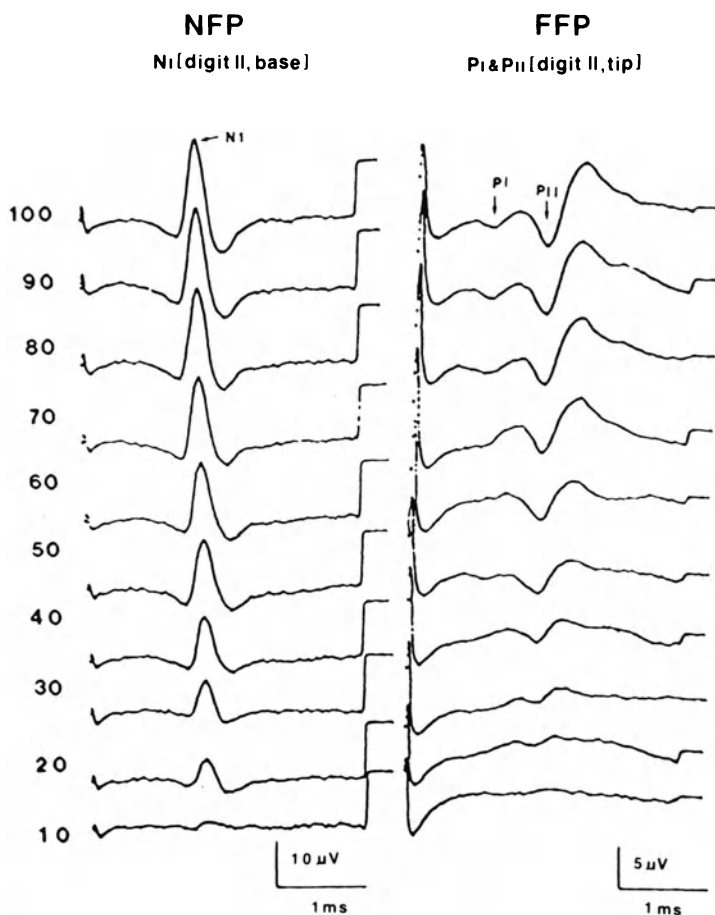


**Figure 1-13.** Amplitude comparison between the far-field peak, PII, and the near-field peak, N<sub>1</sub>, of the antidromically activated radial nerve sensory potential. The abscissa indicates the amplitude of PII recorded referentially with G<sub>1</sub> near the tip of the second digit, and G<sub>2</sub>, around the fifth digit. The ordinate shows the amplitude of N<sub>1</sub> recorded bipolarly with G<sub>1</sub> at the base of the second digit, and G<sub>2</sub>, 1.5 cm distally. As indicated by a linear relationship, PII occurred in proportion to the propagating volley, N<sub>1</sub>, approaching the base of the digit. From Kimura et al. [25].

of N<sub>1</sub>, presumably because the stimulus current spread unevenly to the radial nerve fibers. In these hands, the amplitude of PII correlated better to the size of the corresponding N<sub>1</sub> than to the stimulus intensity.

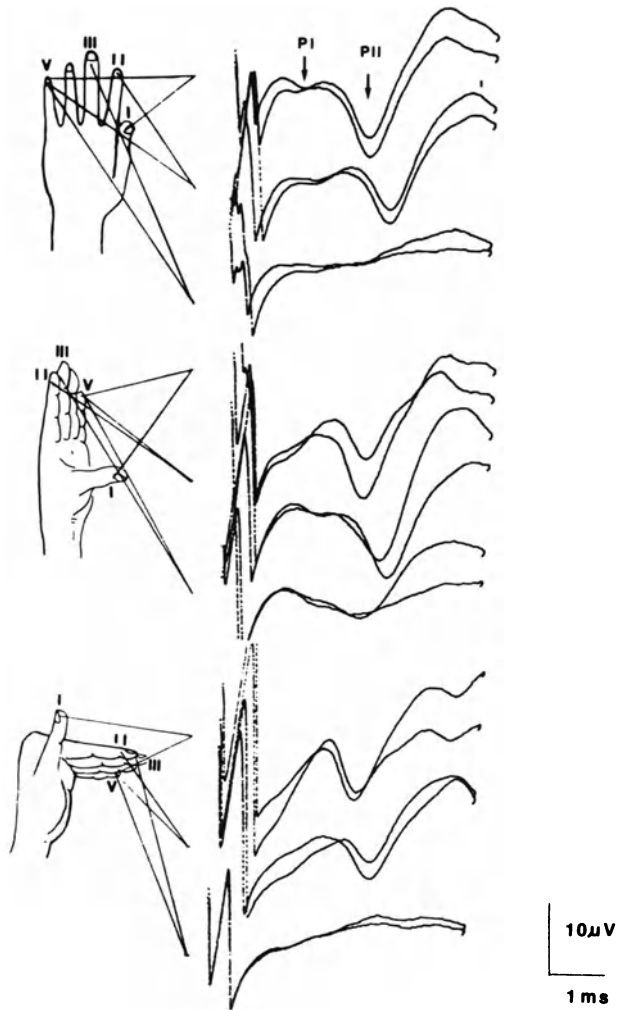
We also evaluated changes in latency, amplitude and waveform of PII induced by altering the spatial relationship between the adjoining volume conductors (figure 1-15). The PII was recorded from the first through third digits, using G<sub>1</sub> at the tip of the respective digit and G<sub>2</sub> around the fifth digit. After establishing the control values with the first digit adducted and the other digits extended at the metacarpophalangeal joint, we analyzed the effect of 90 degrees abduction for the first digit and 90 degrees flexion for the second and third digits. At least two trials confirmed the degree of reproducibility of the observed change in waveform.

Repeated trials showed consistent far-field potentials with the first digit adducted and the other digits extended. Abduction of the first digit or flexion of the second digit often caused notable muscle artifacts which distorted the small sensory potentials, despite averaging. In ten hands, where the record-



**Figure 1-14.** The far-field potential (right) recorded referentially with G1 at the tip of the second digit and G2 at the fifth digit, and near-field potential (left) registered bipolarly with G2 at the base of the digit and G1 1 cm proximally, after stimulation of the radial nerve. With reduction of stimulus from a maximal (top) to a threshold intensity (bottom) in 10 steps, the amplitude of far-field potential, P1 and PII, declined in proportion to that of near-field potential, N<sub>1</sub>. From Kimura et al. [26].

ing was relatively free of interference, PII changed in waveform following a shift of anatomical orientation between the digit and the palm (figure 1-15). However, the observed alteration varied from one hand to the next, showing no consistent pattern. Hence, we were unable to characterize the change attributable to the direction of the traveling volley at the junction of the volume conductor. Distortion of the waveform often caused a small latency shift as well, but the change was unpredictable and difficult to define.



**Figure 1-15.** The far-field potential recorded from the tip of the first (top tracing in each frame), second (middle) and third digit (bottom), referenced to the fifth digit. The top figure shows a control response obtained with the first digit adducted and the other digits extended. The center and bottom figures illustrate changes in waveform and, to a lesser extent, latency of far-field potential associated with adduction of the first digit and flexion of the second and third digits, respectively. From Kimura et al. [26].

#### FAR-FIELD POTENTIAL IN THE CLINICAL DOMAIN

One cannot attribute the standing peaks described above to an axon branching because the major divisions of the median and radial nerves lie distal to the wrist and proximal to the base of the digit, whereas the far-field peaks occur at the boundaries. Selective recording of PII, primarily from the digits innervated

by the radial nerve, refutes an alternative explanation that it represents a propagating negativity under the reference electrode around the fifth digit. Besides, a single traveling impulse under the reference could not account for two positive peaks with different latencies recorded at the tip of the first and second digits. The “killed end effect” theory does not apply to our observation since the amplitude of PII is proportional to the propagating radial nerve potential recorded at the base of the digit. Further, with orthodromic or antidromic activation of the median nerve, the far-field peaks occur coincident with the arrival of the impulses at certain fixed points along the nerve rather than at the nerve terminal. Thus, these far-field peaks most likely relate to the traveling volley approaching the borders of the volume conductor. We postulate that at the moment the source arrives at the boundary, an apparent standing potential results because of a sudden change in current density distribution from one volume conductor to the other.

The stationary far-field potentials, secondary to a traveling impulse as described above, are reminiscent of the early components of the median and tibial SEPs (figure 3-4). Here, the short latency peaks recorded over the scalp must represent axonal volleys of the first order afferents, yet they appear as standing potentials in far-field recording. We postulate that some of these peaks also result from an abrupt alteration in current flow at various boundaries of the volume conductor. For example, the initial positive peaks of the median ( $P_9$ ) and tibial SEPs ( $P_{17}$ ) may arise when the propagating volleys enter the shoulder and pelvic girdles, respectively. Similarly, the second positive peaks of the median ( $P_{11}$ ) and tibial SEPs ( $P_{24}$ ) may be in part attributable to changes in geometry as the impulses reach the cervical cord and conus medullaris, respectively. We have previously shown that the latencies of these early components are consistent with this view [11, 15–17].

We conclude that, in far-field recording, stationary potentials result primarily from a change in current flow within the surrounding tissue at the moment the afferent volleys approach a geometric transition in the volume conductor. A traveling impulse also gives rise to standing potentials concomitant with an abrupt change in tissue resistance [28, 30]. Further, the latency of far-field peaks depends to a certain degree on the anatomic orientation of the propagating impulse [18]. Although not yet proven, standing potentials may also arise as the propagating impulse reaches a branching point of the nerve axon. These findings indicate that the physical relationships between the nerve and the volume conductor dictate the field distribution of the propagating current, and consequently the complex waveform of far-field potentials. We believe that a change in geometry of the volume conductor plays a major role in the generation of some stationary peaks in far-field recording.

One traditionally regards far-field potential as a monophasic positivity from an approaching wavefront of depolarization [19, 45, 46]. Our findings indicate, however, that stationary activity from a moving source often contains a major negative component that sometimes far exceeds the preceding positivity in amplitude and duration (figures 1-1, 1-2, 1-10). The direction of the



traveling impulse in relation to the size of the volumes being left and entered may determine the onset polarity. The computer model of Stegman and his associates [47] indeed predicts that the volume entered becomes initially positive or negative compared to the volume departed, depending on the relative size of the adjoining conductors. Cunningham and his colleagues [48], however, maintain that the propagating impulse crossing the geometric junction always makes the new conductor initially positive, regardless of the type of dimensional change. The available data in humans [17, 24, 26, 32, 34, 48] tend to support the latter view, although further studies are necessary to prove or disprove such contention and to elucidate the underlying physiologic mechanisms.

### **MATHEMATICAL MODELS**

Various investigators [47, 48] have attempted to elucidate the mechanisms which could generate stationary far-field potentials from propagating axonal volleys by using mathematical models.

Stegman, Van Oosteron and Colon (47) examined the potential distributions in cylinders of infinite length with a neuronal generator model propagating along the center line. Variable conditions included: 1) an abrupt change in conductivity with uniform geometry, 2) an abrupt change in cylinder diameter with uniform conductivity, and 3) a change in the direction of propagation with uniform geometry and conductivity. All three conditions produced stationary (and essentially uniform) potential peaks in the volume between points on opposite sides of, and distant from, the site of change. The latency and duration of these peaks correspond to the time when the neuronal generator crosses the site of change.

In the case of a conductivity change with uniform geometry, the models show a positive far-field peak in the volume being entered if the volume being entered has lower conductivity; and a negative peak in the volume being entered if it has a higher conductivity. In the case of a diameter change with uniform conductivity, the model shows a positive peak in the volume being entered when the generator goes from a larger volume into a smaller volume. Unfortunately (for the polarity question), these authors did not present results for the case of a volley going from a smaller volume into a larger volume. However, they conclude [47] that the polarity is always positive in the volume of higher resistance, independent of the direction of propagation. Higher resistance is used here as a general term to denote a volume of either lower conductivity or smaller dimensions.

Cunningham, Halliday, and Jones [48] examined potential distributions in two-dimensional finite models with uniform conductivity. Rectangular models included: 1) the hand with one finger, 2) the arm, wrist, and hand with three fingers, and 3) the arms, trunk, neck and head. Variable conditions were: 1) the different geometries of the models, 2) different spatial and temporal variations of the neuronal generator model, and 3) the directions of nerve propagation in the case of arm, trunk and head models.

The results from these hand models compare well with the data recorded from real hands [25]. The model calculations predict the traveling biphasic peaks in bipolar derivation across the palm and digit quite accurately. The models predict stationary positive potential peaks in a digit from an antidromic sensory nerve volley across the palm and into the digit, with reference to either the base of the palm or on an indifferent digit. Further postulates about the mode of decline of the sources in the generator model led to calculations in the model which predict the stationary negative after-potential peaks (NII) observed in the digit of real hands [25]. However, inferences from these models fail to predict the negative far-field potential peaks observed in the forearm with orthodromic stimulation of the median sensory nerve at the digit [27].

In all of these two-dimensional, finite models with uniform conductivity, the volume entered becomes initially positive relative to the volume exited at the time of transition through the boundary, regardless of the relative sizes of the volumes. The authors explained this in terms of the preferred paths for the depolarizing and the hyperpolarizing currents as affected by the geometric limitations. These results are consistent with all of the available data recorded in humans [24–27, 32, 34]. The results from Cunningham, Halliday, and Jones [48] on models of the arm, trunk, neck and head also corroborate that the anatomical path of the nerve volley has an effect on the waveform of the junctional potential that occurs during transition between the arm and the neck (recorded between the vertex and a distant reference on the trunk.)

Considering the modeling results and the data in humans, it appears that the effects of a conductivity difference between the volumes is of lesser importance in explaining the far-field potential peaks observed in humans. It is probably reasonable to assume that the volume conductivity throughout most of the regions of the body is about the same, and that if volume conductivity effects are a significant component of the mechanism, the areas of conductivity difference should probably be modeling as narrow bands between volumes of different size and equal conductivity. More sophisticated mathematical modeling, considering the third-dimension, considering regions of conductivity difference such as bone and ligaments, and more accurately approximating the dimensions of the human body, may lead to additional clarification of the various mechanisms involved in far-field potential generation.

## SUMMARY

In referential recording of the orthodromic median sensory potential, the propagating near-field peak,  $P_1$ , was distorted by two stationary far-field activities, PI and PII, signaling the arrival of the traveling impulse at the base of the digit and wrist, respectively. The referentially recorded antidromic median sensory potentials showed a stationary positive peak along the third digit, coincident with the entry of the propagating sensory potential into the palm-digit junction. In referential recording of antidromic radial sensory potentials, the digital electrodes detected two stationary far-field peaks, PI-NI and PII-NII. When compared to a bipolar recording of the traveling source,

the PI and PII occurred with the passage of the propagating sensory impulse across the wrist and the base of the digit, respectively. Thus, PI was identical in latency irrespective of the digits tested, whereas PII varied in latency from one digit to another, reflecting different arrival times of the traveling source at the base of the respective digit.

A bipolar recording registers a near-field potential over the sensory fibers along the length of the nerve. In contrast, a referential recording represents a mixture of the near-field and far-field potentials with the latter frequently producing major distortions of the classical triphasic wave. The present findings document a temporal relationship between the standing peaks of far-field activity and the entry of the traveling volleys into major borders of the volume conductor. In far-field recording, stationary potentials can result from an abrupt change in current flow, that is based on the geometry of the volume conductor. An apparent standing potential occurs at the moment the source arrives at the boundary, probably reflecting a sudden change in current density distribution between the two adjacent volume conductors. The same mechanism may play an important role in the generation of some of the short latency peaks in the scalp recorded SEPs. The designation, junctional or intercompartmental potential, differentiates this type of far-field potential from fixed neural generators and helps specify the source of the voltage step by location.

## REFERENCES

1. Jewett DL: Volume-conducted potentials in response to auditory stimuli as detected by averaging in the cat. *Electroencephalogr Clin Neurophysiol* 28:609–618, 1970.
2. Sohmer H and Feinmesser M: Cochlear and cortical audiometry conveniently recorded in the same subject. *Isr J Med Sci*, 6:219–223, 1970.
3. Jewett DL and Williston JS: Auditory-evoked far fields averaged from the scalp of humans. *Brain* 94:681–696, 1971.
4. Cracco RO: The initial positive potential of the human scalp-recorded somatosensory evoked response. *Electroencephalogr Clin Neurophysiol* 32:623–629, 1972.
5. Cracco RQ and Cracco JB: Somatosensory evoked potential in man: far field potentials. *Electroencephalogr Clin Neurophysiol* 41:460–466, 1976.
6. Jones SJ: Short latency potentials recorded from the neck and scalp following median nerve stimulation in man. *Electroencephalogr Clin Neurophysiol* 43:853–863, 1977.
7. Wiederholt WC and Iragui-Madoz VJ: Far field somatosensory potentials in the rat. *Electroencephalogr Clin Neurophysiol* 42:456–465, 1977.
8. Chiappa KH, Choi SK and Young RR: Short-latency somatosensory evoked potentials following median nerve stimulation in patients with neurological lesions. In Desmedt JE (ed) *Clinical Uses of Cerebral Brainstem and Spinal Somatosensory Evoked Potentials*, Vol. 7. Prog Clin Neurophysiol Basel: Karger, 264–281, 1980.
9. Desmedt JE and Cheron G: Central somatosensory conduction in man: neural generators and interpeak latencies of the far-field components recorded from neck and right or left scalp and earlobes. *Electroencephalogr Clin Neurophysiol* 50:382–403, 1980.
10. Noel P and Desmedt JE: Cerebral and far-field somatosensory potentials in neurological disorders involving the cervical spinal cord, brainstem, thalamus and cortex. In Desmedt JE (ed) *Clinical Uses of Cerebral Brainstem and Spinal Somatosensory Evoked Potentials*, Vol. 7. Progressive Clinical Neurophysiology, Basel: Karger 205–230, 1980.
11. Yamada T, Kimura J and Nitz DN: Short latency somatosensory evoked potentials following median nerve stimulation in man. *Electroencephalogr Clin Neurophysiol* 48:367–376, 1980.
12. Desmedt JE and Cheron G: Prevertebral (Oesophageal) recording of subcortical somatosensory evoked potentials in man: The spinal P<sub>13</sub> component and the dual nature of the spinal

- generators. *Electroencephalogr Clin Neurophysiol* 52:257–275, 1981.
13. Eisen A: The somatosensory evoked potential. *Canadian Journal of Neurological Science*, 9:65–77, 1982.
  14. Kakigi R, Shibasaki H, Hashizume A and Kuroiwa Y: Short latency somatosensory evoked spinal and scalp-recorded potentials following posterior tibial nerve stimulation in man. *Electroencephalogr Clin Neurophysiol* 53:602–611, 1982.
  15. Kimura J and Yamada T: Short-latency somatosensory evoked potentials following median nerve stimulation. *Ann NY Acad Sci* 388:689–694, 1982.
  16. Kimura J, Yamada T, Shivapour E and Dickins QS: Neural pathways of somatosensory evoked potentials: Clinical implication. In Buser PA, Cobb WA and Okuma T (eds.) *Kyoto Symposium (EEG Suppl 36)*, Amsterdam, Elsevier, pp 328–335, 1982.
  17. Yamada T, Machida M and Kimura J: Far-field somatosensory evoked potentials after stimulation of the tibial nerve. *Neurology* 32:1151–1158, 1982.
  18. Desmedt JE, Huy NT and Carmeliet J: Unexpected latency shifts of the stationary P<sub>o</sub> somatosensory evoked potential far field with changes in shoulder position. *Electroencephalogr Clin Neurophysiol* 56:623–627, 1983.
  19. Lorente de No R: A study of nerve physiology. *Studies from the Rockefeller Institute* 132: Chapter 16, 1947.
  20. Dawson GD and Scott JW: The recording of nerve action potentials through skin on man. *Neurol Neurosurg Psychiatry* 12:259–267, 1949.
  21. Sears TA: Action potentials evoked in digital nerves by stimulation of mechanoreceptors in the human finger. *Physiol* 148:30–31, 1959.
  22. Buchthal F and Rosenfalck A: Evoked action potentials and conduction velocity in human sensory nerves. *Brain Res* 3:1–122, 1966.
  23. Lin JT, Phillips II LH and Daube JR: Far-field potentials recorded from peripheral nerves. *Electroencephalogr Clin Neurophysiol* 50:174, 1980.
  24. Kimura J, Mitsudome A, Beck DO Yamada T and Dickins QS: Field distributions of antidromically activated digital nerve potentials: Model for far-field recording. *Neurology* 33: 1164–1169, 1983.
  25. Kimura J, Mitsudome A, Yamada T and Dickins QS: Stationary peaks from a moving source in far-field recording. *Electroencephalogr Clin Neurophysiol* 58:351–361, 1984.
  26. Kimura J, Kimura A, Ishida T, Kudo Y, Suzuki S, Machida M, Yamada T: What determines the latency and the amplitude of stationary peaks in far-field recordings? *Ann Neurol* (in press).
  27. Kimura J, Ishida T, Suzuki S, Kudo Y, Matsuoka H Yamada T: Far-field recording of the junctional potentials generated by median nerve volleys at the wrist. *Neurology* (in press).
  28. Nakanishi T: Action potentials recorded by fluid electrodes. *Electroencephalogr Clin Neurophysiol* 53:343–345, 1982
  29. Komizo K: Analysis of the nerve action potential recorded by fluid electrodes. *J Physiol Soc Jap* 6:103–112, 1941.
  30. Nakanishi T: Origin of action potential recorded by fluid electrodes. *Electroencephalogr Clin Neurophysiol* 55:114–115, 1983.
  31. Nakanishi T, Tamaki M, Arasaki K and Kudo N: Origins of the scalp-recorded somatosensory far field potentials in man and cat. In Buser PA, Cobb WA and Okuma T (eds) *Kyoto Symposium (EEG Suppl 36)*, Amsterdam, Elsevier 336–348, 1982.
  32. Frith RW, Benstead TB, Daube JR: The SEP standing waveform at the shoulder due to a change in volume conductor. *Electroencephalogr Clin Neurophysiol* (abstract) 61:S272, 1985.
  33. Yamada T, Machida M, Oishi M, Kimura A, Kimura J Rodnitzky RL: Stationary negative potentials near the source vs positive far-field potentials at a distance. *Electroencephalogr Clin Neurophysiol* 60:509–524, 1985.
  34. Eisen A, Odusote K, Bozek C Hoirch M: Far-field potentials from peripheral nerve: generated at sites of muscle mass change. *Neurology* (in press) 1985.
  35. Nakanishi T, Tamaki M, Kudo K: Possible mechanism of generation of SEP far-field component in the brachial plexus in the cat. *Electroencephalogr Clin Neurophysiol* 63:68–74, 1986.
  36. Anziska B, Cracco RQ, Cook AW Field EW: Somatosensory far-field potentials: studies in normal subjects and in patients with multiple sclerosis. *Electroencephalogr Clin Neurophysiol* 45:602–610, 1978.
  37. Anziska B Cracco RQ: Short latency somatosensory evoked potentials: studies in patients

- with focal neurological diseases. *Electroencephalogr Clin Neurophysiol* 49:227–239, 1980.
38. Kritchovsky M Wiederholt WC: Short-latency somatosensory evoked potentials. *Arch Neuro (Chicago)* 35:706–711, 1978.
  39. El-Nagamy E, Sedgwick EM: Properties of spinal somatosensory evoked potential recorded in man. *Neuro Neurosurg Psychiat* 41:762–768, 1978.
  40. Hume AL, Cant BR: Conduction time in central somatosensory pathways in man. *Electroencephalogr Clin Neurophysiol* 45:361–375, 1978.
  41. Kimura J, Yamada T Kawamura H: Central latencies of somatosensory evoked potentials. *Arch Neurol (Chicago)* 35:683–688, 1978.
  42. Lueders H, Andrish J, Gurd A, Weiner G and Klem G; Origin of far field subcortical potentials evoked by stimulation of the posterior tibial nerve. *EEG Clin Neurophysiol* 52:336–344, 1981.
  43. Lueders G, Lesser R, Hahn J, Little J Klem G. Subcortical somatosensory evoked potentials to median nerve stimulation. *Brain* 106:341–372, 1983.
  44. Walker DD, and Kimura J: A fast-recovery electrode amplifier for electrophysiology. *Electroencephalogr Clin Neurophysiol* 45:789–792, 1978.
  45. Woodbury JW: Potentials in a volume conductor. In: Ruch TC, Patton HD, Woodbury JW, Towe AL, (eds) *Neurophysiology*. Philadelphia: WB Saunders Co., 1965:85–91.
  46. Wood CC Allison T: Interpretation of evoked potentials: a neurophysiological perspective. *Canad J Psychol/Rev Canad Psychol* 35(2):113–135, 1981.
  47. Stegeman DF, Oosterom AV and Colon EJ: Far-field evoked potential components induced by a propagating generator: computational evidence. *Electroencephalogr Clin Neurophysiol* 67:176–187, 1987.
  48. Cunningham K, Halliday AM and Jones SJ: Simulation of “stationary” SAP and SEP phenomena by 2-dimensional potential field modelling. *Electroencephalogr Clin Neurophysiol* 65:416–428, 1986.

---

## **2. CRITICAL ANALYSIS OF THE METHODS USED TO IDENTIFY GENERATOR SOURCES OF EVOKED POTENTIAL (EP) PEAKS**

HANS LÜDERS, RONALD P. LESSER,  
DUDLEY S. DINNER, HAROLD H. MORRIS, III,  
ELAINE WYLLIE

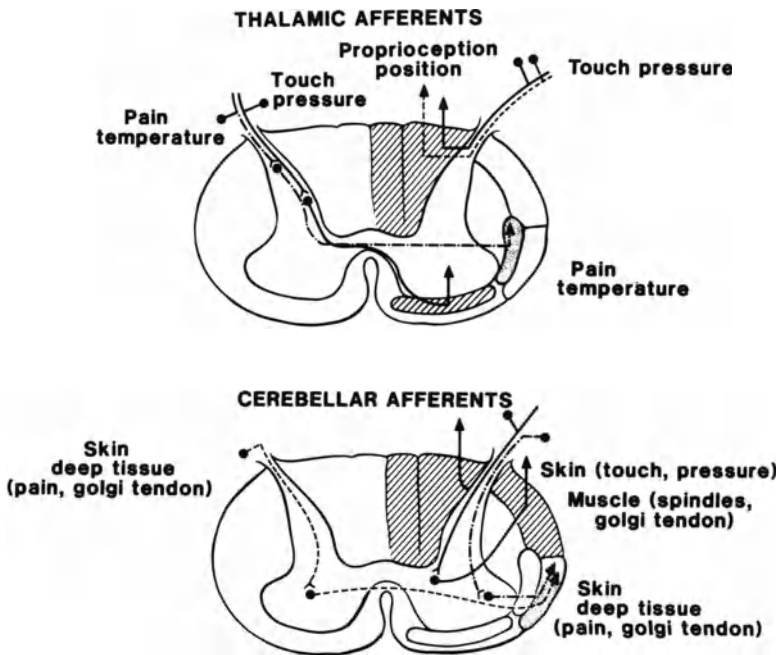
Optimal use of evoked potentials (EP) for clinical studies requires a good understanding of its generator sources. Numerous methodologies, many of them interrelated and all with significant limitations, have been used to define the generators of evoked potential peaks. In this chapter, we will discuss and analyze critically these different approaches.

### **ANATOMY**

A careful analysis of the anatomy of the system being stimulated has always been the basis for identification of the main nervous structures that could generate a given EP peak. Anatomical studies usually identify numerous afferent pathways and, therefore, numerous nervous structures that could potentially generate a given EP peak. Intelligent use of other methodologies is necessary, then to define which structures are essential generator sources and which are not.

A typical example is provided by the somatosensory evoked potentials which are mainly generated by the afferent volleys traveling in the posterior columns and spino-cerebellar pathways. Anatomical studies would have attached similar importance to the spino-thalamic afferent pathway carrying pain and temperature information (figure 2-1). Clinical correlation studies of patients with spinal cord lesions have established, however, that cortical SEPs are not affected by lesions of the spinothalamic tract [13–15, 17, 25].

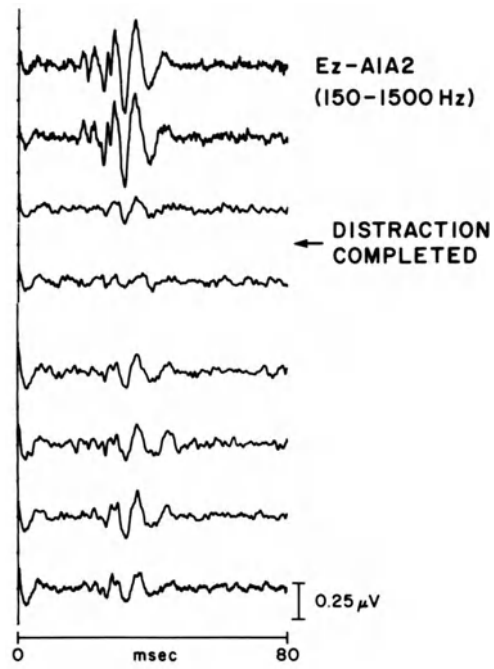
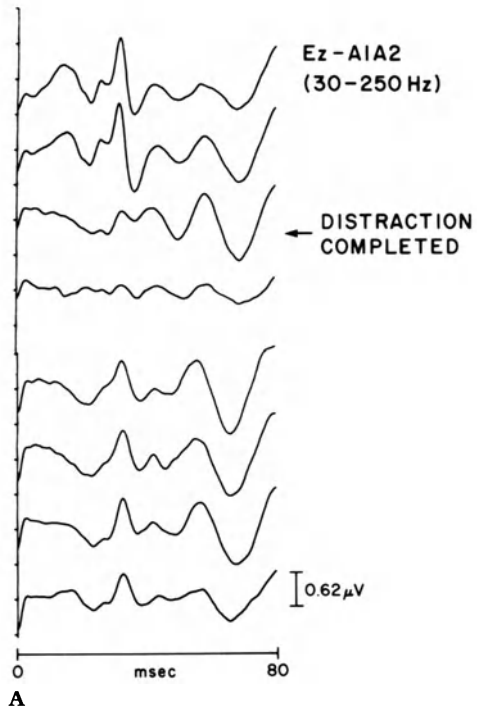
In addition, there is also evidence that different pathways participate in the



**Figure 2-1.** Diagram showing the main ascending spinal tracts.

generation of cortical and subcortical somatosensory evoked. So, for example, figure 2-2A illustrates a case of scoliosis surgery that following distraction had a temporary disappearance of all components for five to ten minutes with almost complete recovery, except a slightly decreased amplitude of the early components. Figure 2-2B shows simultaneously obtained recordings but using a filter setting of 150-1500 which selectively enhances short latency components including particularly the early afferent action potentials (see recording parameters). In this figure, the disappearance of potentials following the distraction is not followed by a recovery indicating a clear dissociation between the late cortical and early subcortical components. The patient woke up with a severe paraplegia following the surgery. This suggests that he most probably suffered from an anterior spinal artery occlusion which produced a lesion of the corticospinal pathway but spared the posterior columns necessary for the genera-

**Figure 2-2A, 2-2B.** Results of surgical monitoring during scoliosis surgery. Analysis time in Figure 2A and 2B was 80 msec, but the filter settings were different. In Figure 2A, filter settings of 30-250 Hz were used to enhance the cortical components, whereas in Figure 2B a filter window of 150-1500 Hz filtered out selectively the faster subcortical components. The figure illustrates well the dissociation of the cortical components (which were affected only temporarily after the distraction) and the subcortical components which were greatly reduced after the distraction. Ez=electrode placed between Cz and Pz (10-20 International System).





tion of cortical potentials. It is possible that the relative permanent diminution of the early potentials demonstrated in figure 2-2B was an expression of a lesion of the spino-cerebellar pathway which is also supplied by the anterior spinal artery.

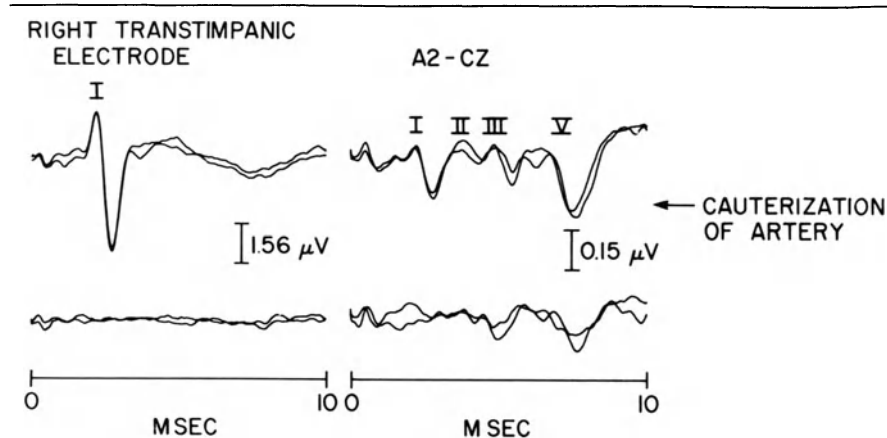
A detailed understanding of the anatomy, including, for example, its blood supply, is essential for adequate identification of generators. Figure 2-3 illustrates monitoring of auditory evoked potentials in a case who was being operated on an acoustic neurinoma. During dissection of the tumor at the internal auditory meatus almost all the responses disappeared including a complete abolition of wave I of the brainstem auditory evoked potentials and of the electrocochleogram. It is now generally recognized that wave I of the auditory evoked potentials is generated distally with respect to the internal auditory meatus. Therefore, it would be difficult to explain the disappearance of all the auditory evoked potentials components unless we know that the distal auditory nerve is actually supplied by the internal auditory artery, which is a branch either of the basilar artery or of the anterior inferior cerebellar artery and reaches the nerve through the internal auditory canal. A careful review of the videotape recording of the surgical procedure revealed that the surgeon had actually cauterized an artery at the internal auditory meatus immediately before the sudden disappearance of all auditory evoked potentials.

### **LATENCY**

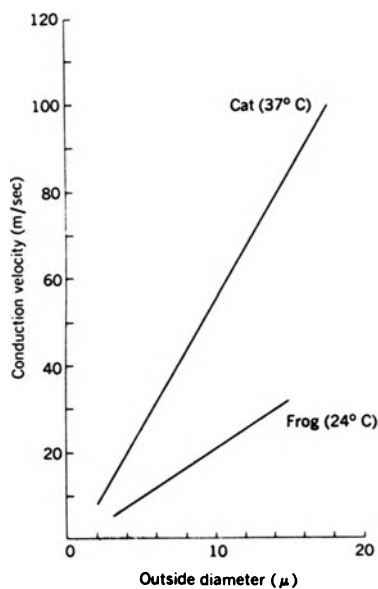
Precise knowledge of the fiber size and of the length of the afferent pathways should actually permit us to estimate with precision the latency at which the afferent volley arrives at different neural structures (figure 2-4). This information can then be used to determine the generator source of an EP occurring with a certain latency.

There are, however, two major limitations to this strategy. The anatomical knowledge is usually not precise enough to permit accurate conclusions, and not infrequently the existence of parallel afferent pathways of similar fiber size and length makes it difficult to choose the correct generator source.

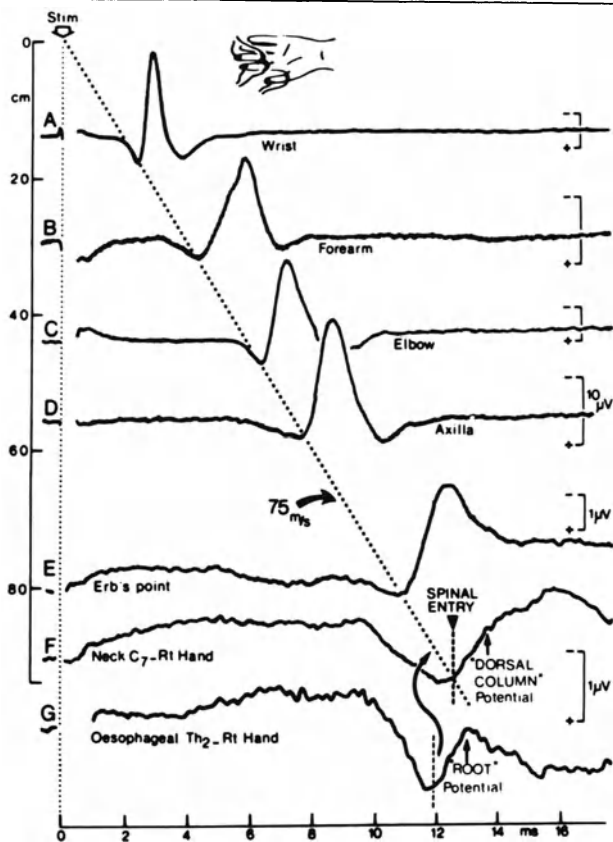
The accuracy of this methodology is greatly increased by directly measuring the afferent volley at least at one point of the afferent pathway. This permits a relatively precise definition of the conduction velocity or transit velocity of the afferent volley in the distal segment of the afferent pathway. Extrapolation and intelligent use of available anatomical information allows us also to estimate with relative precision the time of arrival of the afferent volley at other neural structures. This can then be correlated with recorded EP peaks. This method is fairly precise when we estimate the arrival of the afferent volley at a point relatively close to where the actual measurement was obtained (figure 2-5). As the distance from the reference point increases the accuracy deteriorates progressively. So, for example, measurements of the action potential in the peripheral nerve at Erb's point can be used very effectively to estimate the time of entry of the afferent volley into the spinal canal or even spinal cord, but will



**Figure 2-3.** Surgical monitoring during cerebello-pontine angle (CPA) tumor. Traces shown in the upper line were obtained immediately before cauterization of a small artery (most likely the internal auditory artery) at the level of the internal auditory meatus. Traces shown in the lower line were obtained immediately following cauterization of the artery. The surgery was recorded on videotape to establish the exact time correlation between the occurrence of an EP change and any given surgical procedure. This method allowed the investigator to establish with precision that the abrupt disappearance of EPs occurred immediately after cauterization of an artery at the internal auditory meatus.

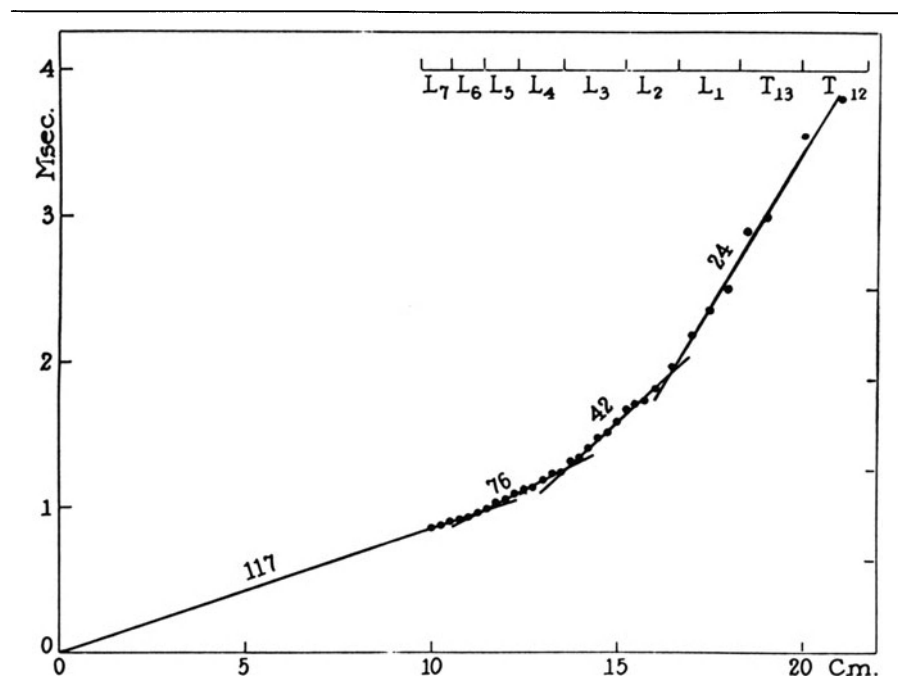


**Figure 2-4.** Relationship between outside diameter and conduction velocity at two temperature levels for myelinated nerve fibers of cat and frog. Reproduced by permission from Brinley, FJ: Excitation and conduction in nerve fibers. In Mountcastle, Vernon B, editor: Medical physiology, ed. 14, St. Louis, 1980, The C.V. Mosby Co.



**Figure 2-5.** Recording of the afferent volley to median nerve stimulation at the wrist, forearm, elbow, axilla, and Erbs point. These measurements permit a good estimate of the entry time of the afferent volley into the spinal cord. This corresponds with a broad positive deflection at a neck-non-cephalic reference recording. The Y axis shows the distance from the stimulating point. The last channel shows a simultaneously obtained esophageal recording. Reprinted with permission from, "Prevertebral (oesophageal) recording of subcortical SEPs in man: the spinal P13 component and the dual nature of the spinal generators," Desmedt and Cheron, *Electroenceph Clin Neurophysiol*, 52:257-275, 1981, Elsevier Scientific Publishers, Inc.

be useless to decide if the afferent volley at a given point in time is still in the upper cervical dorsal columns or has already entered the medial lemniscal pathways. The inaccuracy of these estimates is due to a change of conduction velocity in different segments of the afferent volley. Figure 2-6 illustrates the case of an afferent volley in a somatosensory pathway. In this example, it becomes evident that the velocity of the afferent volley decreases dramatically from 117 msec to 24 msec as the afferent volley enters the spinal cord. In other words, to accurately measure where the afferent volley is at any given point in time additional information that cannot be extrapolated from peripheral measurements of conduction velocity will be necessary.

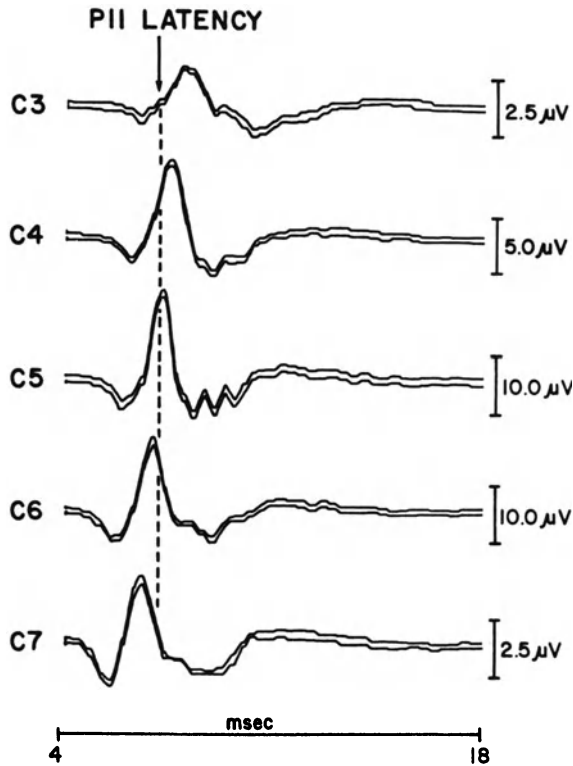


**Figure 2-6.** Conduction velocity of intramedullary portion of Group I afferent fibers. It can be seen that the conduction velocity falls off at progressively more proximal spinal cord levels (from a peripheral conduction velocity of 117 msec to 24 msec at the low thoracic—high lumbar level). X axis = distance from stimulating electrode. Y axis = latency of afferent volley. Reprinted with permission from "Dorsal column conduction of Group I muscle afferent impulses and their relay through Clarke's column," *J Neurophysiol*, 13:13-54, 1950.

These estimates can be improved by actually measuring the afferent volley at two points and then estimating where it would be at what time between these two points. In the example given above, this would correspond with measuring the afferent volley at the periphery and as it arrives at the cortex, and then trying to define when it passed through the foramen magnum. This method provides us with good approximations but does not permit definition of the source of generators with the precision we need for clinical applications. Other methodologies described below, when used in conjunction with anatomical and latency estimates, give a much better estimate of the generator sources.

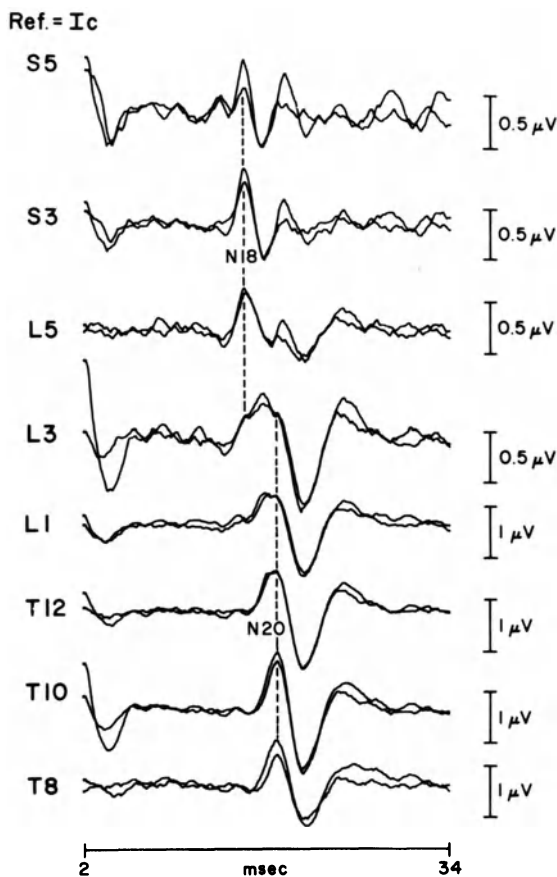
#### DISTRIBUTION

This certainly has been the most widely used methodology to locate a generator source. For a long time it was simply assumed that the generator source must be close to the point where the maximum potential is recorded. Potentials were simply subdivided into traveling and stationary waves. Traveling waves were presumably the result of an action potential moving along an



**Figure 2-7.** Afferent volley elicited by stimulation of the right median nerve and recorded intrasurgically directly from the dorsal surface of the spinal cord. The dotted line shows the latency of the presurgically recorded P11 peak. All the recordings were referential to a needle electrode at the skin at the level of C5.

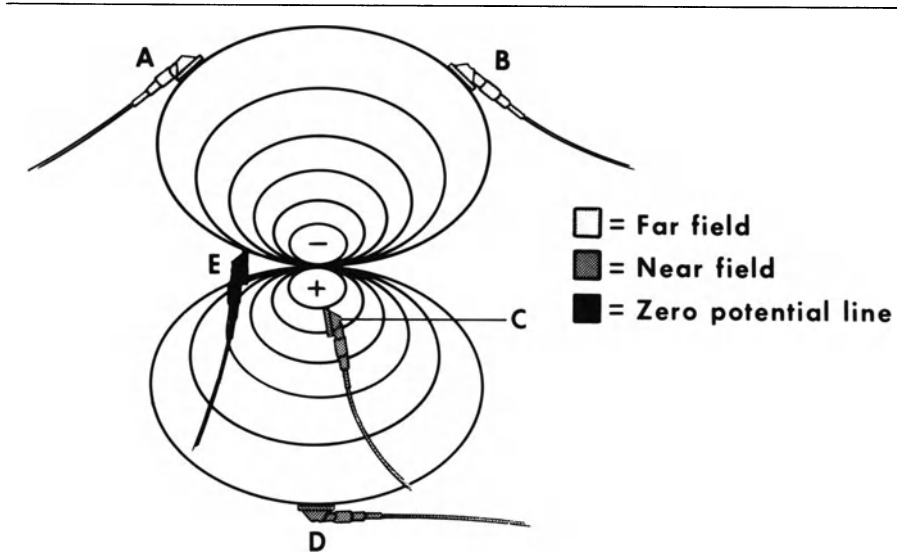
afferent pathway, whereas stationary potentials would be produced by EPSPs and/or IPSPs at a relay station. Figure 2-7 illustrates a traveling wave elicited by stimulation of the median nerve and recorded directly from the posterior surface of the spinal cord between C7 and C3. It shows a relatively typical triphasic wave of progressively longer latency at more proximal segments. Figure 2-8 shows the recordings of an afferent volley to left posterior tibial nerve stimulation. The recordings were obtained by surface cup electrodes placed over the spinous process of selected sacral, lumbar, and thoracic vertebrae. Two stationary potentials labeled respectively N18 and N20 can be recognized. N18 is most probably a reflection of the afferent volley before it enters the spinal canal, and N20 reflects the postsynaptic activity generated by the afferent volley when it enters the spinal cord. In addition, between L3 and T12 a small peak can be recognized which has an intermediate latency between N18 and N20, that progressively decreases at more proximal segments. This peak represents a traveling wave and is most probably the expression of the afferent volley as it travels in the cauda equina. The above mentioned sub-



**Figure 2-8.** Surface recordings of the afferent volley to left posterior tibial nerve stimulation. All the recordings were referential the right iliac crest. Reprinted with permission from, "Subcortical and cortical somatosensory potentials evoked by posterior tibial nerve stimulation: normative values," *Electroenceph Clin Neurophysiol*; 59:214–228, 1984.

division of potentials into traveling and stationary waves is still applicable when recording relatively close to the generator source, as, for example, with a surface electrode directly over a peripheral nerve (near-field recording).

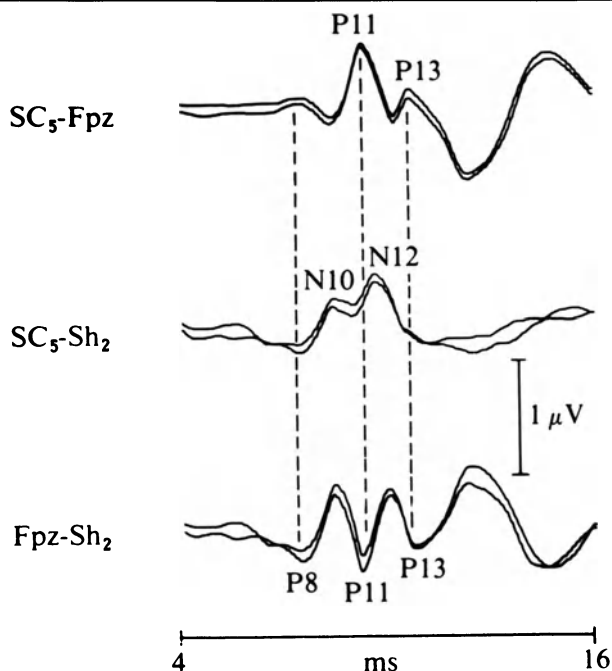
At an early stage it was also realized that generator sources did not behave as monopoles, but preferentially as dipoles or tripoles. The concept of a triphasic traveling wave was created, and the complication of bipolar or tripolar voltage distribution was introduced as an essential feature in the distribution of near-field potentials. In other words, in addition to distance to a generator, the spatial orientation of the exploring electrode, with respect to the generator source, would determine the polarity and amplitude of the potential detected. In the extreme case, an exploring electrode lying beside a bipole generator source could not record any potential at all, if it happens to lie on a zero



**Figure 2-9.** Diagram illustrating some of the basic concepts related to near-field and far-field potentials. Electrodes A and B are relatively distant with respect to the source. In spite of being relatively far apart, both electrodes record the same potential which will cancel if a recording between A and B is obtained. Electrodes C and D are at approximately the same distance as A and B. However, when recording between C and D a relatively big potential difference is detected. This is because electrode C is close to the generator and therefore picks up a so-called near-field potential. It is clear also from this diagram that the potentials at the far-field electrodes A and B can only be detected if we choose another indifferent electrode that is clearly outside the electrical field of this generator. Finally, the figure also illustrates that in the case of a bipolar generator an electrode (E) can be extremely close to the source and still not register any potential.

isopotential line between the two poles of opposite polarity. This is illustrated in figure 2-9 by electrode, E, which is located in the immediate vicinity of a bipolar generator, but is at a zero potential line. No potentials will be recorded if the reference electrode is at sufficient distance from the bipole and, therefore, also relatively inactive. This is in clear contrast with electrode C which is at a similar distance from the generator bipole than electrode E, but because of its position in the electrical field is highly positive with respect to a more distant relatively inactive electrode (as for example electrode D).

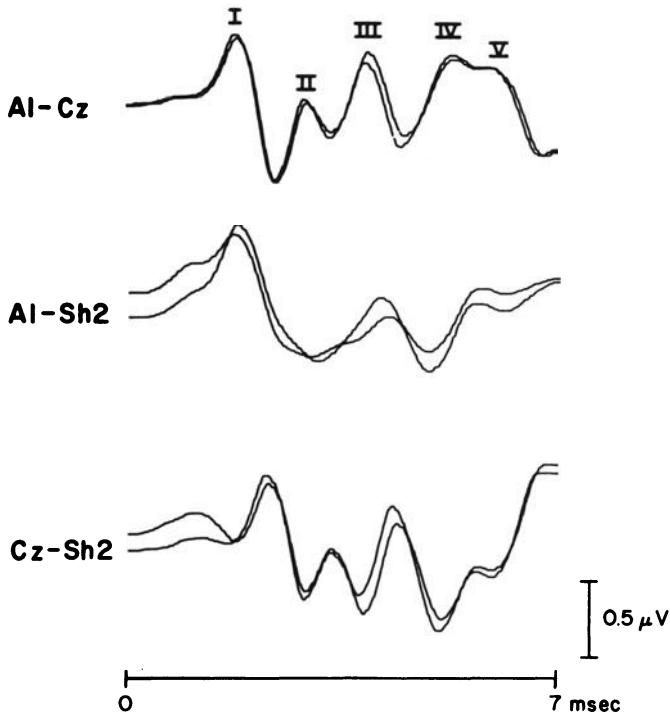
When recording EPs, produced in the central nervous system with non-invasive techniques, the recording electrode is usually at a considerable distance from the generator source. Under these conditions, the potential generated relatively closer to the recording electrode may still behave like a near-field potential with relatively fast fall-off at adjacent sites, but is of considerably smaller amplitude than when recording near-field potentials intrasurgically or from peripheral nerves (where the generator source is immediately next to the exploring electrode). When the near-field potentials are negligible or relatively small, another type of potentials called far-field potentials can dominate the



**Figure 2-10.** Comparison of neck-scalp (SC5-Fpz), neck-noncephalic reference (SC5-Sh2) and scalp-noncephalic (far-field) potentials evoked by left median nerve stimulation. SC5 = surface electrode placed over the spinous process of the fifth cervical vertebrae. Fpz = mid frontopolar electrode. Sh2 = right shoulder. Reprinted with permission from "Subcortical SEPs to median nerve stimulation," Lüders et al., *Brain* 106:341-372, 1983.

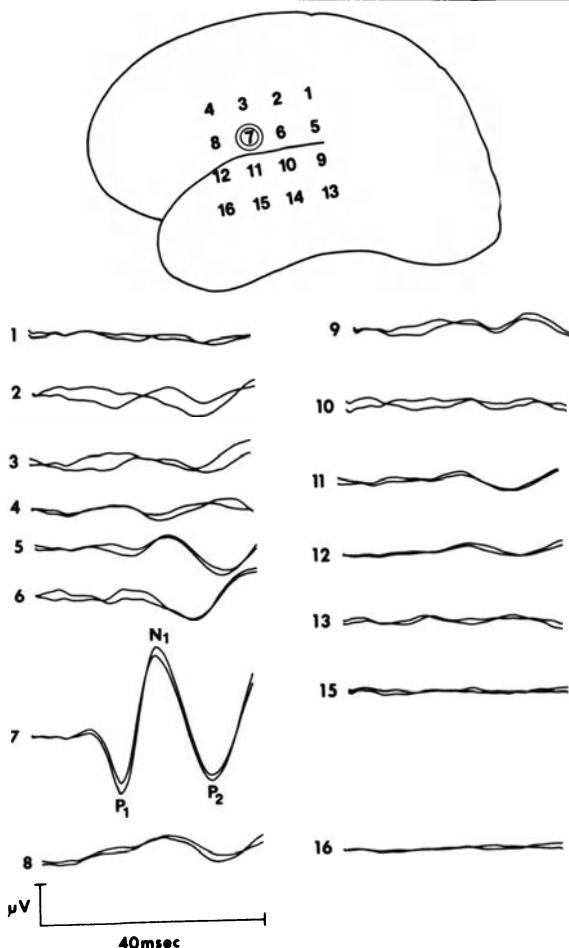
recording or contribute a significant part to it. A characteristic example is somatosensory EPs obtained in neck to scalp montages, which consist of a mixture of near-field potentials recorded from the neck and far-field potential recorded from the scalp [3, 19]. A typical example is shown in figure 2-10. The recordings from the neck electrode SC5 to a relatively indifferent noncephalic reference (Sh2) reveals two near-field negativities labeled, respectively, N10 and N12. Noncephalic reference recordings of the mid-frontopolar electrode reveals two far-field positive potentials of similar latency which were labeled, respectively, P11 and P13. The recording obtained at SC5-Fpz is evidently the mixture of these four different potentials. It is also interesting to observe that in a neck-scalp montage usually the far-field neck potentials predominate. The auditory evoked potentials recorded with an ear-vertex montage is also a mixture of near-field and far-field potentials. Figure 2-11 shows that the ear electrode referred to a relatively inactive non-cephalic reference (Sh2 = contralateral shoulder) records a prominent near-field negativity corresponding to wave I. At the vertex (Cz), however, the following waves II-V are recorded as far-field positivities. As mentioned in the previous section, far-field potentials





**Figure 2-11.** Comparison of left car-vertex (A1-Cz), left car-right shoulder (A1-Sh2) and vertex-right shoulder (Cz-Sh2) recordings. Reprinted with permission from "Intraindividual Variability of Short Latency Somatosensory Evoked Potentials to MN Stimulation," Tsuji and Lüders, Japanese Journal of EEG and EMG, 1984.

are generated by completely different mechanisms than near-field potentials, and their distribution field also differs considerably. By definition, the most significant difference is that far-field potentials do not fall off at adjacent electrodes. This characteristic of far-field potentials can be used advantageously to obtain relatively pure recordings of near-field potentials which always have a short space constant. In other words, the far-field potential will cancel when recording between two electrodes which are: 1) at relatively identical distance and 2) similarly oriented with respect to the far-field potential generator source even when these two electrodes are relatively distant one from another. However, a good recording of a near-field potential will be obtained if one of the electrodes is close and the other is distant to the near-field potential generator source. The typical example is the recording of cortical potentials between two scalp electrodes, one near to the somatosensory strip (centro-parietal region) and one at a distance from the somatosensory strip ( $F_z$  or  $F_{pz}$ ). Both electrodes show high amplitude far-field potentials in non-cephalic references, but these cancel out when referring one electrode to another. Another example is shown in figure 2-12. Direct cortical recordings were obtained



**Figure 2-12.** Recordings to right ear stimulation obtained from subdural electrodes placed over the left supra sylvian and infrasyllian region. Reprinted with permission from "Recording of AEPs in man using chronic subdural electrodes," Lee, Lüders et al., *Brain* 107:115-131, 1984.

from the electrodes shown in the diagram using as reference another cortical electrode relative distant with respect to the most active electrode #7. With this recording methodology, all the far-field early potentials shown in figure 2-11, channel 3 are cancelled out. Only the prominent, extremely localized near-field potential P1-N1-P2 remains.

The limitation of distribution studies to elucidate the generator sources of central nervous system EPs stems from the fact that, as explained above, most EPs are a variable mixture of one and not infrequently multiple near-field and far-field potentials each of which has different mechanisms of generation and follows different rules of distribution. The consequence is that the peaks

recorded in any given case can be interpreted by different mechanism and different generator sources. This certainly introduces great uncertainty in the results of a recording and it explains the almost endless controversies in the literature regarding generator sources of subcortical evoked potentials.

### **STIMULUS PARAMETERS**

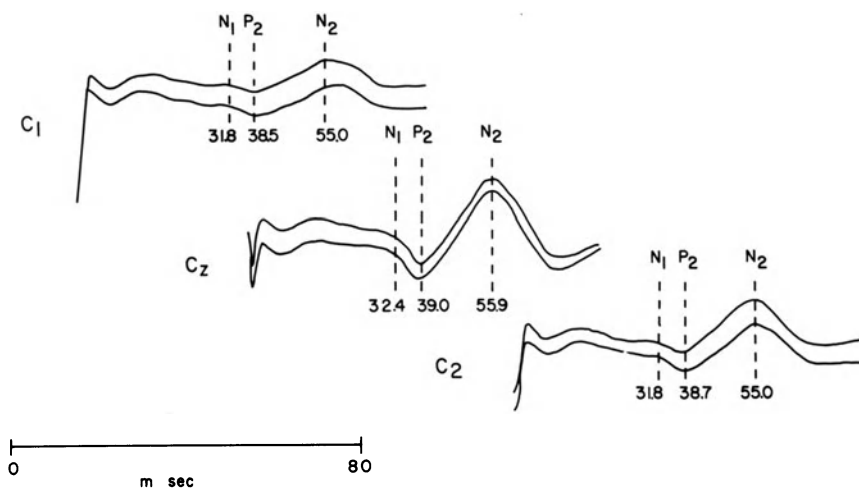
Measuring the results of varying the stimulus parameters can be of help to define the generator source of EP peaks. In general, however, these techniques are less powerful than the ones described before and so far only exceptionally have provided more than complementary information.

#### **Stimulus type**

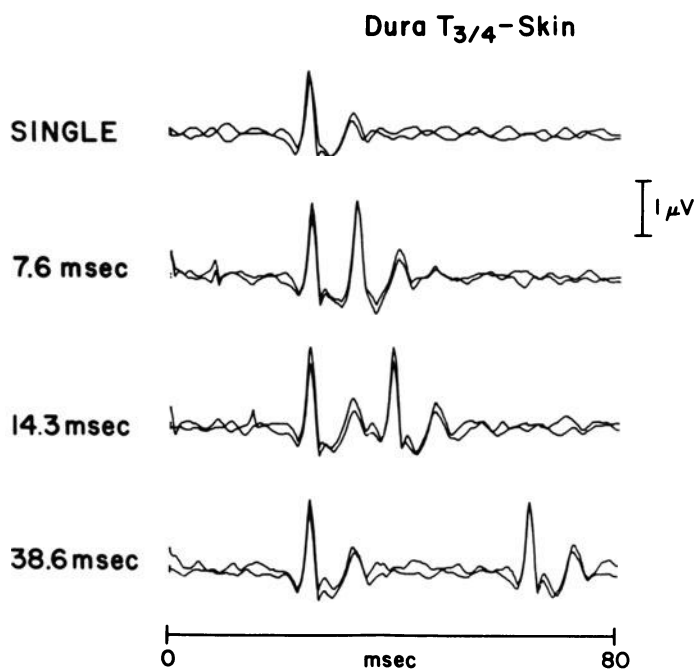
The characteristics of the stimulus can be modified to stimulate a selective afferent pathway. A typical example is comparing the peaks recorded when stimulating cutaneous afferents (which activates primarily cortical area 3b) with the peaks recorded when stimulating muscle afferent by tendon tapping (which activates primarily cortical areas 1, 2, 3a and 4). This more selective information can then be used to deduce the origin of the peaks generated by mixed nerves like the median nerve at the wrist. Another outstanding example is stimulation of the retina by hemified alternating checkerboard patterns which demonstrated an ipsilateral paradoxical distribution [7]. This observation has then been of great help in the interpretation of the generator sources of pattern evoked potentials elicited with full field stimulation. A similar example is given by the study of the scalp distribution of evoked potentials elicited by bilateral and unilateral posterior tibial nerve stimulation. Bilateral stimulation elicits potentials that are maximum at the vertex with approximately equal fall-off to both sides in more lateral derivations. Unilateral stimulation, however, elicits potentials that also are maximum at the vertex, but reflect primarily to electrodes ipsilateral to the stimulation side as shown in figure 2-13. This paradoxical distribution is most probably related to the fact that the primary cortical somatosensory response is generated as a horizontal bipole in the sagittal fissure [10].

#### **Stimulus frequency**

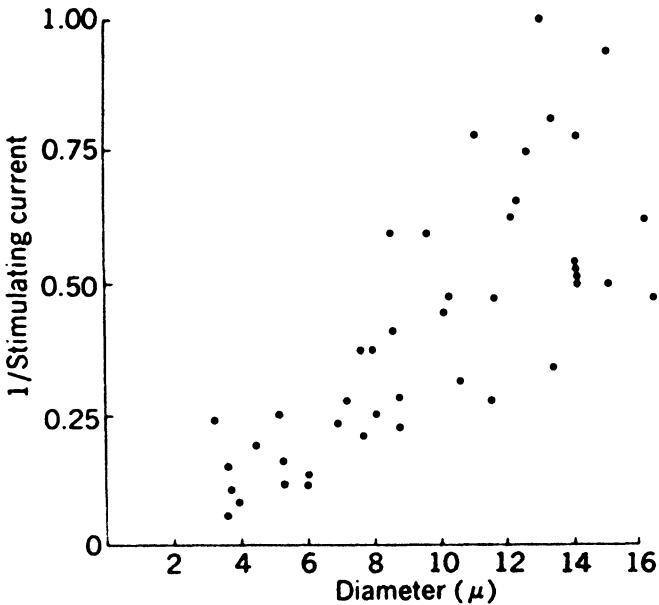
Recording of EPs to progressively increasing stimulus frequencies has been a classical neurophysiological research technique to define if a pathway is polysynaptic. Transsynaptic conduction tends to be more susceptible to high frequency repetitive stimulation than axonal conduction. With progressively increasing stimulus frequency the EP peaks which are generated by the most polysynaptic pathways will tend to disappear first. This technique was used, for example, by Wiederholt [32] and Lüders et al. [20] to deduce the origin of subcortical somatosensory evoked potentials. Figure 2-14 shows EP recorded directly from the posterior surface of the spinal cord to single and paired stimuli of the posterior tibial nerves. The figure demonstrates that the afferent



**Figure 2-13.** Recordings of scalp recordings to right posterior tibial nerve stimulation. Cz = vertex, C<sub>1</sub> = electrode placed between Cz and 10-20 International System C<sub>3</sub> electrode. C<sub>2</sub> = electrode placed between Cz and 10-20 International System C<sub>4</sub> electrode.



**Figure 2-14.** Responses obtained directly from the posterior dural surface to single and paired stimuli of both posterior tibial nerves. The interval between the pair of stimuli varied between 7.6 and 38.6 msec.



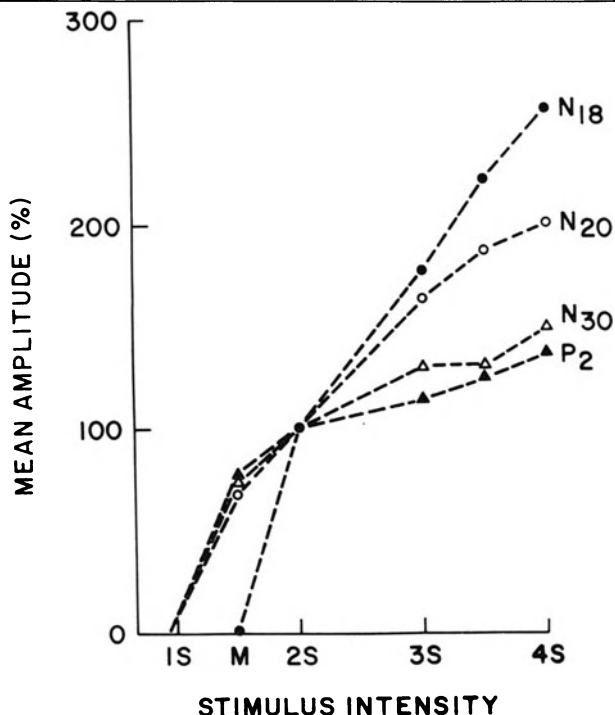
**Figure 2-15.** Relationship between stimulating current and outside diameter of single myelinated fibers isolated from sciatic nerve of frog.

volley in the posterior columns at a midthoracic level can follow stimulation frequencies of more than 100 Hz without any significant fall-off.

Besides, defining the response of any given EP peak to high frequency stimulation can be of great help for identification of peaks of similar generator source under different conditions. This has been used, for example, for identification of auditory EP peak V (which tends to be the most resistant auditory EP peak to high frequency stimulation) [29] under pathological conditions or to establish analogous peaks in different animal species.

### Stimulus intensity

Reducing the stimulus intensity usually results in stimulation of more selective afferent fiber pathways. This is illustrated in figure 2-15 for myelinated fibers of different diameter in a sciatic nerve of a frog. In transcutaneous peripheral nerve stimulation, low intensity stimulation in general will produce selective stimulation of the relatively bigger diameter sensory fibers. Therefore, this technique is just a special case of the method discussed above (stimulus type). It is widely used because of the ease with which this parameter can be manipulated. Just as with stimulus frequency, the technique can be used to identify particular peaks of an EP response. For example, at low stimulus intensities only peak V of the auditory EP persist [8]. Figure 2-16 shows how the different components of the EP elicited by stimulation of the posterior tibial nerve have significantly different stimulus-intensity curves with the components



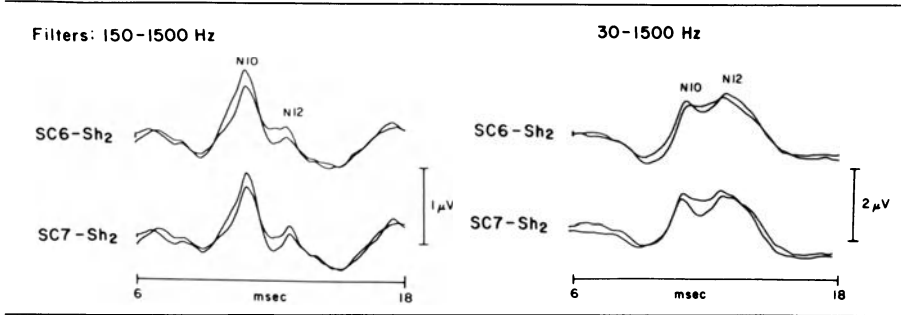
**Figure 2-16.** Stimulus-intensity curve for components N18, N20, N30, and P2 elicited by stimulation of the posterior tibial nerve. Amplitudes of these components obtained at a stimulation intensity equivalent to two times the sensory threshold was set to 100%. S = sensory threshold. M = motor threshold. Reprinted with permission from "Effect of stimuli intensity on subcortical and cortical SEPs by PTN stimulation," Tsuji, Lüders et al., *Electroenceph Clin Neurophysiol*, 59:229-237, 1984.

generated more proximally (particularly N30 and P2) reaching maximum amplitude at relatively lower stimulus intensities. From the information presented in figure 2-16, this implies that the more central components are most probably a reflection of activity in relatively larger peripheral nerve fibers.

### RECORDING PARAMETERS

There are also a number of recording parameters that can be manipulated to elucidate generator sources. The power of the techniques is similar to the alteration of stimulus parameters, providing usually only confirmatory evidence.

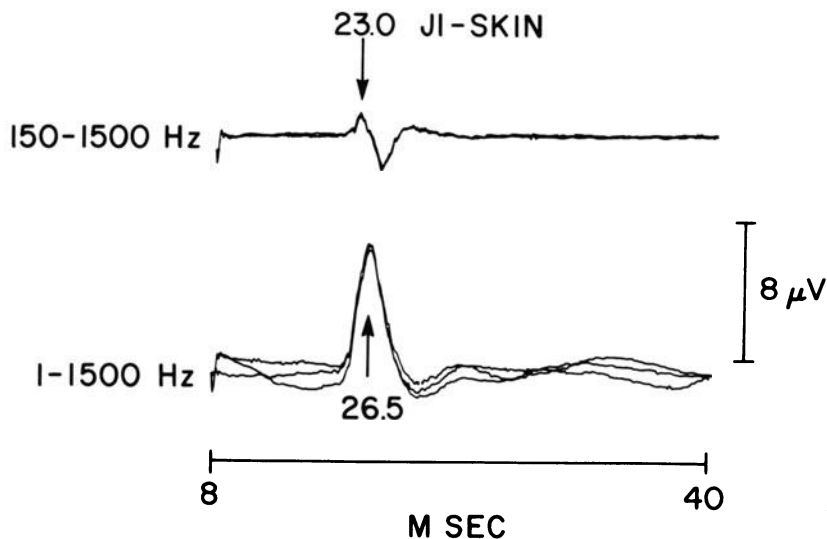
The bandpass of the amplifiers has been the recording technique most frequently modified when attempting identification of EP generators. Basic experimental neurophysiological studies have isolated two main types of potentials in electrically excitable tissue. These are the propagated action potentials and the stationary postsynaptic potentials. An essential distinction



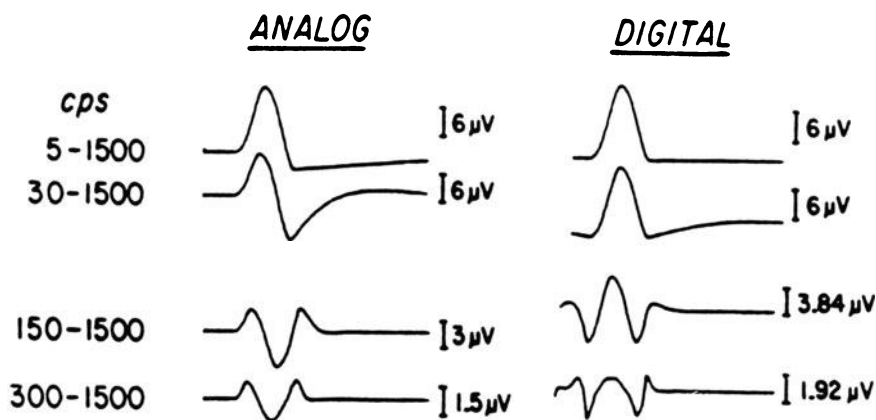
**Figure 2-17.** EP recorded in neck-noncephalic recordings (SC6-Sh2 and SC7-Sh2) after stimulation of the left median nerve. The recordings on the left were obtained with a filter window of 150–1500 Hz and the recordings on the right were obtained with a filter window of 30–1500 Hz. SC6 = surface electrode over the spinous process of the 6th cervical vertebrae. SC7 = surface electrode placed over the spinous process of the 7th cervical vertebra. Sh2 = right shoulder. Reprinted with permission from “Somatosensory Evoked Potentials,” Lüders et al., *Arch Neurol*, 40, 1983.

between these potentials is their duration, with the action potential seldomly exceeding 2 msec and the postsynaptic potentials consistently lasting more than 20 msec for central synapsis. When recording peripheral EPs the tracing usually contains only the action potentials. Central EPs, however, are almost invariably a mixture of postsynaptic and action potentials. Under these circumstances, with the use of totally open filter setting, relatively high amplitude, long duration postsynaptic potentials tend to obscure the shorter duration, lower amplitude action potentials. The use of different bandpasses can then effectively differentiate between these two types of potentials. An example is given by the recordings of EPs at the entry point into the spinal cord. Filtering out of the low frequencies permits isolation of action potential in the dorsal roots and dorsal columns, and filtering out of the high frequencies permits isolation of the postsynaptic potentials in the dorsal horn [22]. This is shown in figure 2-17 where opening of the filters selectively enhances the long duration potential N12, which most probably is a reflection of postsynaptic potentials of the dorsal horn. N10, which consists mainly of high frequency components, is most probably a reflection of the incoming afferent volley at the level it enters the spinal canal. When using these selective filtering techniques it is important to remember that analog filtering produces significant distortion of latencies (figure 2-18), and both, analog and also digital filtering, can result in the creation of artificial peaks that have no physiological meaning but are only a filtering artifact [23] (Figure 2-19).

Appropriate selection of recording montages may also assist considerably in the proper identification of EP components. So, for example, the combined use of frontopolar and linked-ear references when recording somatosensory EP to posterior tibial nerve stimulation can be extremely helpful for the differentiation between cortical and subcortical components (figure 2-20). Subcortical components will appear only in the linked-ear reference montage

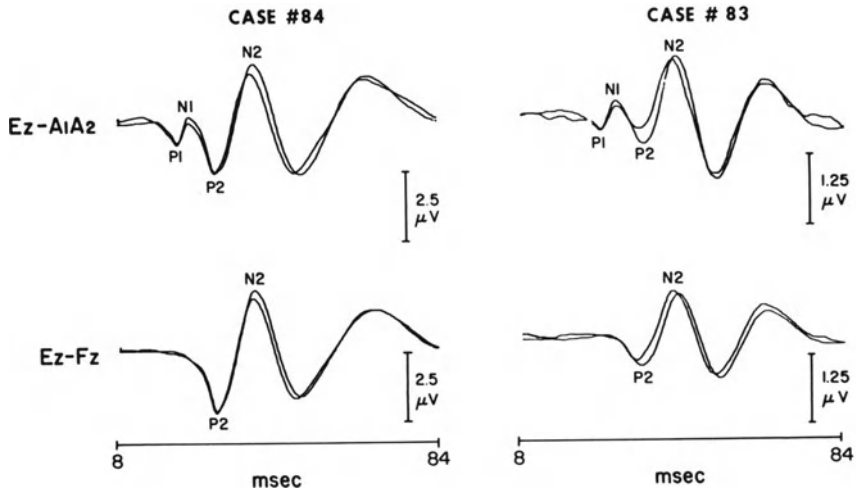


**Figure 2-18.** Epidural recordings obtained during scoliosis surgery using filter settings of 150–1500 Hz and of 1–1500 Hz. The active electrode (labeled J1) was located in the epidural space between the spinal process of the 12th thoracic vertebrae (T12) and the first lumbar vertebra (L1).



**Figure 2-19.** A quasi half-sinusoid with a slightly pronounced terminal descent was analog and digitally filtered. Analog filter recordings reveal amplitude reduction and phase lead such that the components of greatest amplitude appear to be of opposite polarity. Note that as high pass analog filtering becomes more extreme (300 csec LFF) general wave morphology of this asymmetrical half-sine visually approximates the 2nd time derivative. Digitally filtered recordings reveal relative preservation of the main upgoing deflection although it is blunted and reduced in amplitude. Latency shift is not discernible. Transition points between baseline and ascending and descending portions of the half-sine wave are markedly accentuated. Reprinted with permission from "Short latency somatosensory and spinal evoked potentials: power spectra and comparison between high pass analog and digital filter," Maccabee et al., *Electroenceph Clin Neurophysiol*, 65:177–187, 1986.





**Figure 2-20.** EP obtained from scalp recordings secondary to stimulation of the left posterior tibial nerve. Ez = electrode place between 10–20 International System electrode Cz and Pz. A1A2 = linked ears. Fz = 10–20 International System midfrontal electrode. Reprinted with permission from, “Subcortical and cortical somatosensory potentials evoked by posterior tibial nerve stimulation: normative values,” *Electroenceph and Clin Neurophysiol.* 1984, 59:214–228. Elsevier Scientific Publishers, Inc.

(P1-N1) whereas the cortical components are almost identical in both montages (P2-N2). Use of the linked-ear reference montage in isolation makes it sometimes very difficult to determine which is the first cortical component particularly because not infrequently no subcortical components may be evident in the linked-ear reference montage. This occurs particularly frequently under pathological circumstances or in elderly patients.

#### PHYSIOLOGICAL PARAMETERS

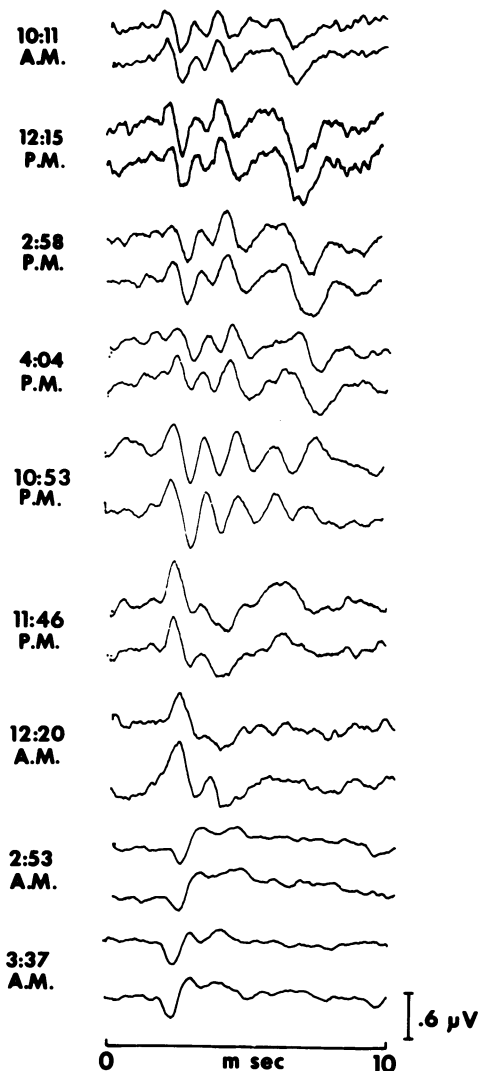
There are a number of physiological variables that can be modified to affect the EP peaks. This information can then be used to define the origin of the peaks.

#### Age

The effect of age on the waveform of the EPs has been studied in detail for all major types of EPs [6, 11, 16, 19, 30]. Usually the effects have been most marked for the first few months in life when the development of new structures and myelinization is proceeding at its fastest pace. Correlation of the anatomical changes and EPs changes has enhanced somewhat our understanding of the generation of the EP peaks most affected by maturation or aging.

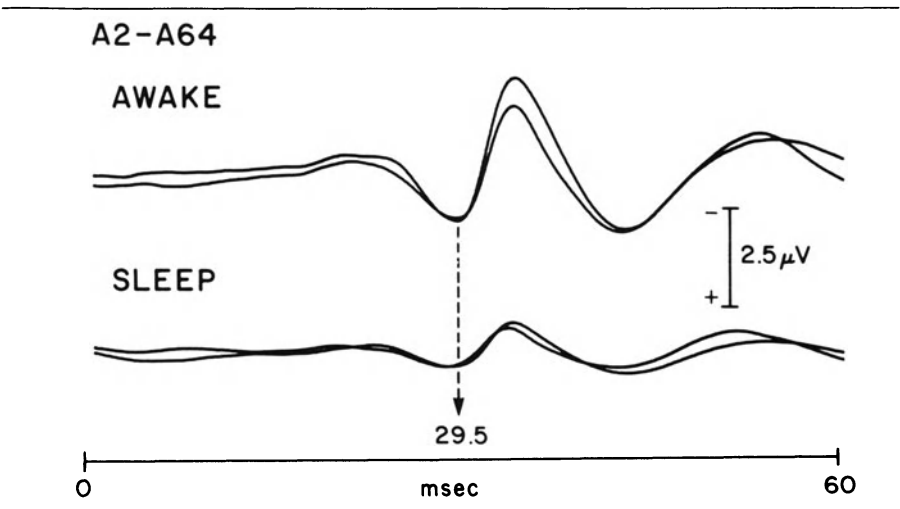
#### Anoxia

Peripheral nerve fibers of large diameter are significantly more sensitive to anoxia than smaller diameter fibers. The differential effect of tourniquet induced ischemia has been exploited to selectively study EP generated by smaller



**Figure 2-21.** Monitoring of auditory evoked potentials during surgery of posterior fossa vascular malformation. Montage: left ear—vertex. Reprinted with permission from "Brainstem AEPs in posterior circulation surgery," Little et al., *Neurosurgery*, 12:496–502, 1983.

diameter fibers [34]. The results were then used to define the origin of early and late cortical EPs. Figure 2-21 illustrates the results of intrasurgical monitoring in a case which suffered a progressive anoxia of the brainstem due to uncontrollable bleeding from a posterior fossa arteriovenous malformation. The EP studies reveal first a progressive lengthening of interpeak latencies of all brainstem components followed by disappearance of all components,



**Figure 2-22.** Recording of ipsilateral evoked potentials directly from the primary somatosensory hand area of the cortex (subdural electrodes). A2 = subdural electrode placed over the primary somatosensory hand area. A64 = subdural electrode placed at a distance from the somatosensory area.

except wave I which is unaffected. Eventually even wave I is affected with a reversal of polarity. This selective sensitivity to anoxia of the different EP components can be explained in light of their most probably generator sources. Wave I, which is most probably generated distally to the internal auditory meatus, is only affected at a late stage when progressively increasing intracranial pressure produces obliteration of the internal auditory artery which supplies the cochlear nerve in its most distal segments.

### Drugs

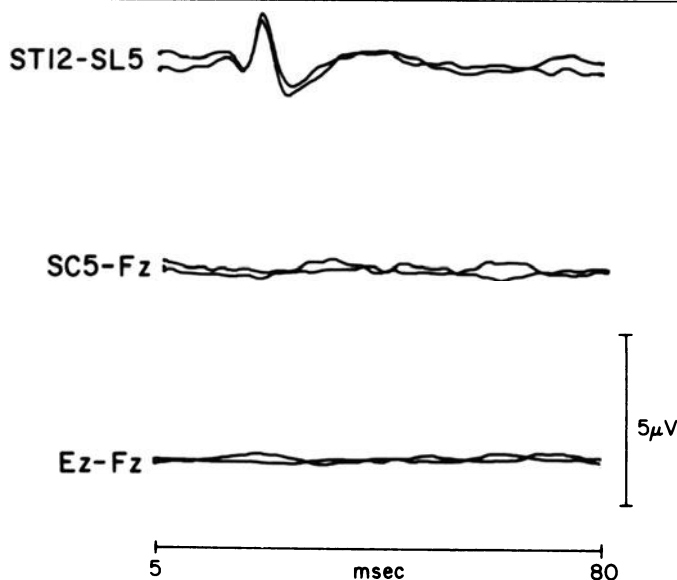
Drugs tend to have very little or no effect on subcortical, oligosynaptic pathways, but greatly alter or even abolish peaks generated by polysynaptic central pathways. This can be used then to differentiate EP peaks generated by oligosynaptic and polysynaptic pathways.

### Sleep

Sleep also tends to have selective effects on different EP components and can be used effectively for their identification. A particularly striking effect of sleep has been described for the ipsilateral somatosensory evoked potentials that tend to disappear (figure 2-22).

### PATHOLOGY

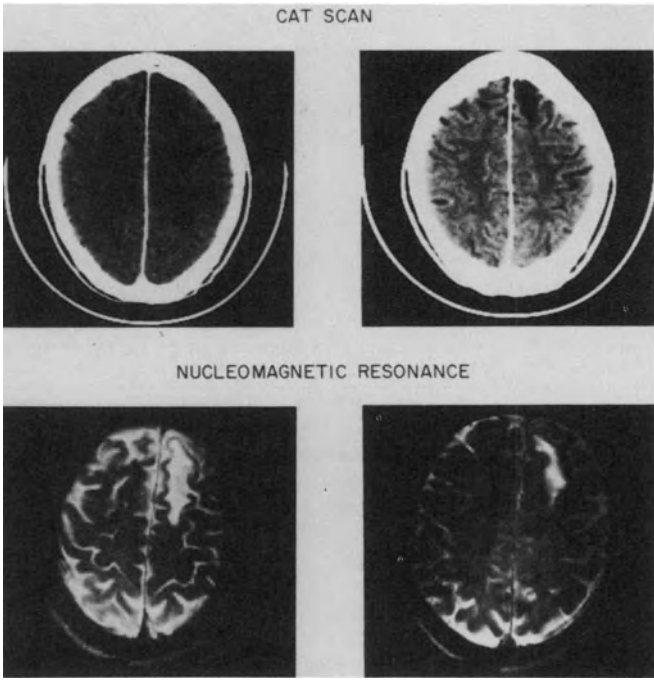
The study of the alteration of EP peaks produced by pathology of the nervous system has been one of the most powerful and most popular techniques to define the origin of EP peaks. Together with anatomy, latency and distribu-



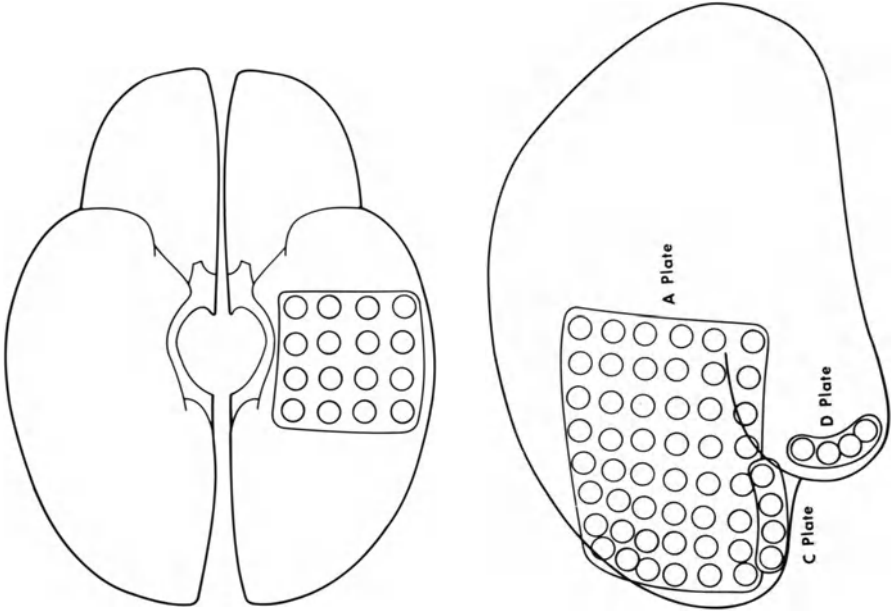
**Figure 2-23.** Somatosensory evoked potentials to bilateral posterior tibial nerve stimulation in a patient with an astrocytoma at the lower thoracic spinal cord. ST12 = surface electrode placed over the spinal process of the 12 thoracic vertebrae. SL5 = surface electrode placed over the spinous process of the fifth lumbar vertebrae. SC5 = surface electrode placed over the spinous process of the fifth cervical vertebrae. Fz = 10–20 international system mid-frontal electrode. Ez = electrode placed between 10–20 International System Cz and Pz electrode.

tion, pathology has usually provided the most reliable information for definition of generator sources. The essential strategy is simply to assume that abnormal or absent peaks are generated proximal with respect to the pathology. This is illustrated in figure 2-23 which shows the EP to posterior tibial nerve stimulation in a patient with a tumor in the lower thoracic spinal cord. It shows that all the EP with latencies longer than N20 are missing and, therefore, presumably generated proximal to the level of the lesion.

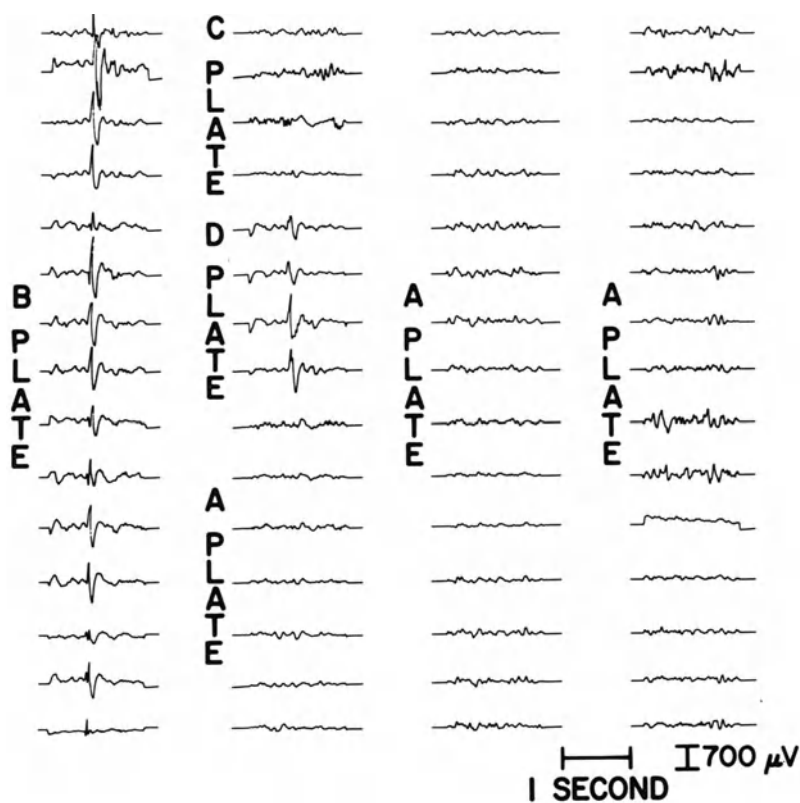
This methodology, however, has major imprecisions and occasionally may provide misleading information. The location of the pathology is usually defined by the clinical history, neurological examination and neuroimaging techniques. Occasionally this is supplemented by a surgical biopsy and/or autopsy. The precision with which these techniques define the lesion will certainly depend on how many of them are used and how sophisticated as clinicians the investigators are. In the majority of the cases, the point of maximum insult to the nervous system will be determined more or less precisely. To define, however, the anatomical extent of the lesion is significantly more difficult. The lesions of the primary cortical sensory area is a good example in which poor definition of the extent of the pathology possibly could have led to erroneous conclusions regarding the origin of the initial scalp negativity (N18). Investigators observed that N18 as also all following components were



A



B



C

**Figure 2-24.** CAT scan and nucleomagnetic resonance of patient with left frontal encephalomalacia and complex partial seizures.

absent in patients with cortical lesions limited to the primary sensory area [3, 12, 24, 26, 33]. From their observations, these investigators concluded that N18 was of cortical origin. Chiappa et al. (1980), however, pointed out that patients with lesions of the primary cortical sensory area suffer a complete retrograde degeneration of the primary thalamic nuclei 6–12 weeks after the cortical insult [28, 31]. In other words, the actual extent of the lesion was much larger than assumed in the original investigation and, therefore, a possible subcortical origin of N18 could not be excluded from these studies. We also know, from analysis of EEGs in patients with brain tumors, that the functional alterations do not remain confined to the area involved by neoplastic tissue but almost invariably extend to involve also tissue that pathologically looks normal. A good example of a dissociation between the area of maximum gross pathological damage and the area of maximum functional alteration is given in figure 2-24. This is a patient with a posttraumatic epilepsy with an extensive area of encephalomalacia in the left frontal region (CAT scan and NMR).

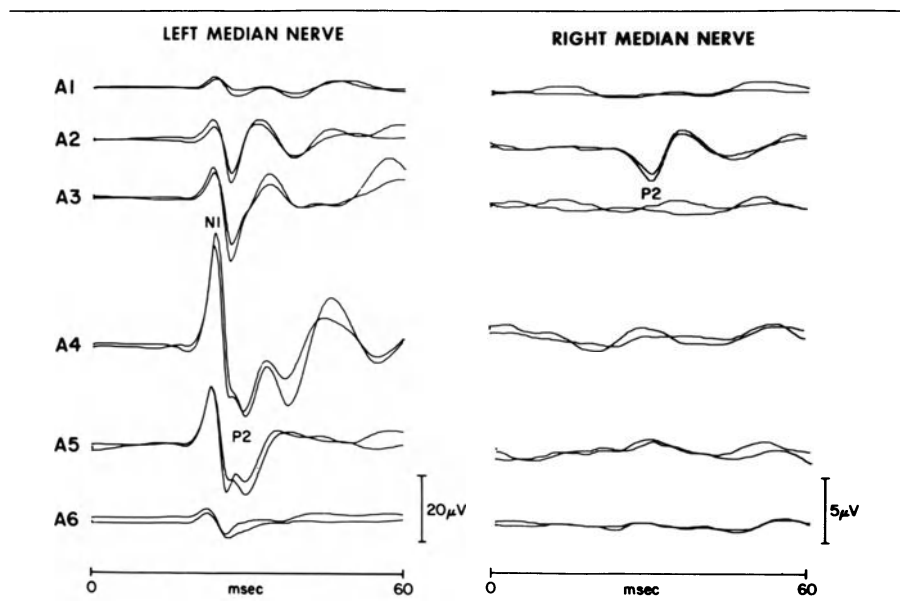
No lesion of the temporal region could be detected in spite of detailed NMR studies. The patient was investigated with subdural electrodes and, as shown in figure 2-24, the epileptogenic focus was strictly localized to the basal temporal lobe. The patient has been seizure free for over one year since resection of the temporal focus. It is also possible that some of the EP alterations could be the result of lesions located at a distance from the major pathological insult. In other words, we would need to define with precision the extent of the area of functional alterations to interpret EP abnormalities with precision. There is no known methodology which would provide us this information.

These observations lead us to the conclusion that information obtained from clinico-electrical correlation studies, like all other techniques, have major limitations. Congruent observations obtained by using some of the other techniques is essential to validate the conclusions reached by clinico-electrical correlation studies.

#### **INTRASURGICAL RECORDINGS**

This is another powerful technique to define the generator sources of EP peaks. Recording electrodes are placed immediately next to the afferent pathways to obtain optimal recording of near field potentials (far field potentials are negligible under these conditions). The active electrode is usually so close to the generator source as compared to the reference that contamination of the potentials by an active reference becomes also extremely unlikely. In other words, this technique permits precise definition of the time the afferent impulse reaches the pathways explored by the active recording electrode. This can then be correlated with the latency of occurrence of EP peaks simultaneously recorded from the surface (non-invasive), and it is generally assumed that peaks of equal latency are generated in the pathway from which the exploring technique recorded near-field potentials.

Intrasurgical recordings provide us with extremely important information but, as all the other techniques, has also major limitations. It will only define the generator source precisely when we are dealing with: 1) a well-synchronized afferent volley, 2) with no multiple parallel afferent impulses, and 3) no relay stations at which electrical activity may continue to be generated even when the afferent impulse has already moved to more proximal sites. In other words, this is the ideal technique as long as we are dealing with a single generator. This is usually the case when recording from the peripheral nervous system and determines the extreme precision of peripheral neurophysiology. In the central nervous system usually none of these conditions are met. As soon as the afferent impulses enter the spinal cord there is divergence into multiple ascending (and partially also descending) pathways of different conduction velocities, and there usually are extensive synaptic connections which will produce prolonged local electrical activity even when the afferent impulse reaches more proximal levels. Multiple generators will be active at the same time and, therefore, it is not possible anymore to define with precision which one is actually responsible for any given scalp EP peak. This was best demon-



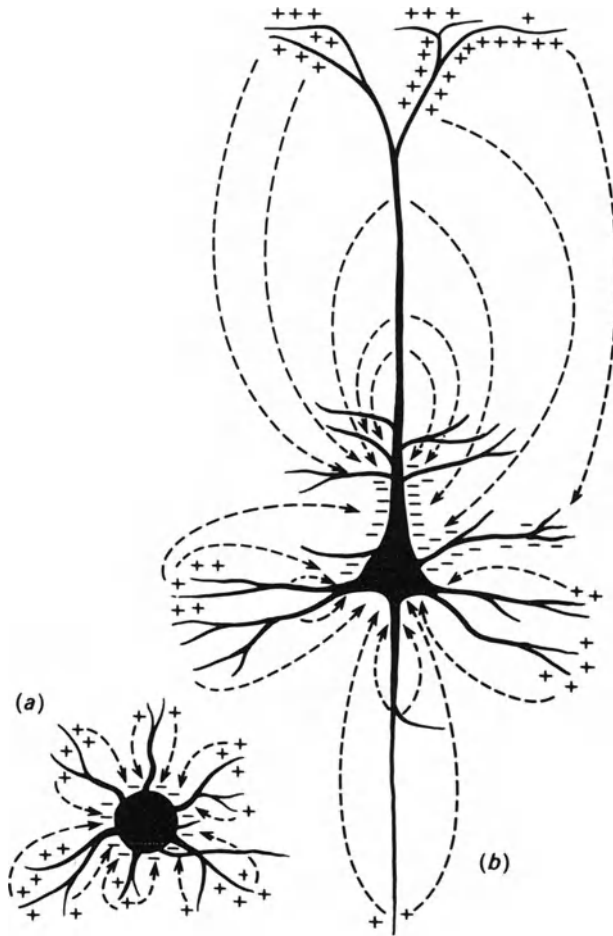
**Figure 2-25.** EP obtained to stimulation of the left (left side of the figure) and right (right side of the figure) median nerve. Recordings were obtained from subdural electrodes located over the primary somatosensory area and labelled A1-A6. Reprinted with permission from "Evoked potentials in cortical localization," Lüders et al., *J. Clin Neurophysiol*, 3:75-84, 1986.

strated by the studies of auditory EPs from depth electrodes in the brain stem of cats by Achor and Starr [1, 2].

It is reasonable to question at this point if intrasurgical recordings provide any useful information when we consider that central EP peaks will correlate always with multiple generators. Similar to all the other techniques, intrasurgical recordings do not provide the complete answer. It gives us, however, the only objective proof of which structures in the central nervous system exhibit electrical activity simultaneously with the surface recordings whose generators we are trying to establish. All these structures are candidates to represent the generator source of the peak we are interested in. It allows us also to exclude certain possible generator sources (suggested by some of the previous methods) if direct intrasurgical recordings demonstrate that they are inactive at the time of occurrence of the surface peak. So, for example, stimulation of the median nerves produces usually no recordable ipsilateral cortical responses. Only very exceptionally low amplitude, extremely localized ipsilateral responses (as shown in figure 2-25) can be seen. This indicates that the relatively prominent peaks recorded from ipsilateral scalp actually must be a volume conductor effect of a generator located either subcortically or on the contralateral hemisphere. No other method had demonstrated this fact so clearly. In other words, positive as also negative results provide valuable information.

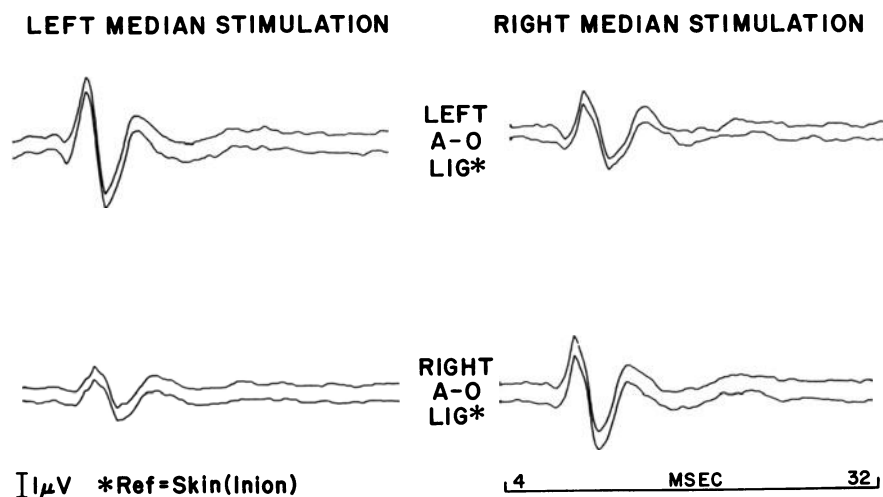
This significance of the data obtained from intrasurgical recordings can be





**Figure 2-26.** Closed (a) and open (b) electrical field generated by small stellate cell and by a large pyramidal cell, respectively.

expanded by a better theoretical knowledge of the distribution of potentials from different generator sources. Lorente de No (1947) did the pioneer work in this area. From his studies we know that generator sources can be divided into closed field and open field (figure 2-26). Closed fields are produced by nuclei in which the different neurons are oriented randomly. Simultaneous activation of the neurons will create multiple dipoles which, because of the random orientation of the dipoles, will cancel each other. Exploring electrodes placed at the nuclei itself will record potentials of high amplitude which, however, disappear almost completely as soon as the electrodes are displaced outside the nucleus. Open fields are produced by: 1) action potentials in which



**Figure 2-27.** Recordings obtained from needle electrodes inserted during surgery into the left and right atlanto-occipital ligaments. The recordings were obtained by stimulation of the left and right median nerve, respectively. The reference was a needle inserted in the skin at the level of the inion. A-O lig = atlanto-occipital ligament.

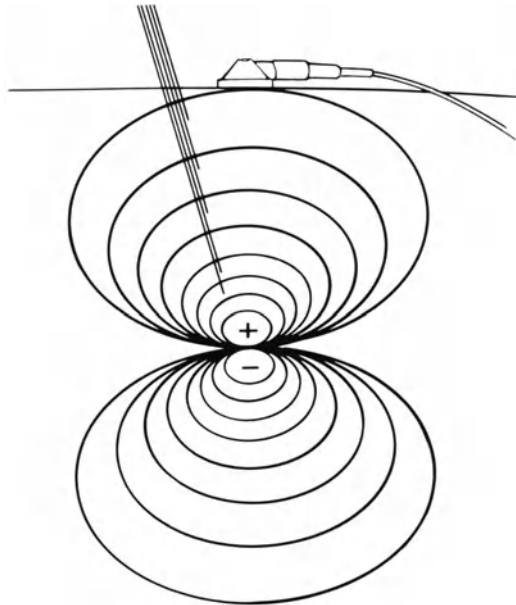
dipoles are all moving in the same direction, and by 2) nuclei in which all neurons are oriented in approximately the same direction. In both instances the result is a summation of multiple dipoles which, when located within a volume conductor, will have a potential field reflected at a considerable distance from the generator source. Only this last type of generator source can be responsible for the occurrence of surface EP peaks. Therefore, anatomical and histological knowledge of the structure from which an intrasurgical potential was recorded can be very helpful to define the underlying type of generator field (open field versus closed field).

Intrasurgical EP studies can also be of great help when trying to define some specific questions regarding the origin of certain EP peaks. Figure 2-27 shows the recordings obtained from the left and right atlanto-occipital ligaments after stimulation of the left and right median nerve. Left median nerve stimulation evoked potentials of higher amplitude at the left atlanto-occipital ligament and vice versa after stimulation of the other median nerve. This ipsilateral distribution of the afferent volley at the level of the atlanto-occipital ligament strongly supports the hypothesis that the afferent volley responsible for the generation of EP peaks is mediated by the posterior columns or spino-cerebellar pathways, both of which are uncrossed pathways at that level.

Another method to define better if an intracerebral generator participates in the generation of surface potentials is to study the distribution of its potential field between the intracerebral source and the surface potential. This technique was originally championed by Arezzo et al. (1979). Unfortunately, this tech-

---

### Single open field generator



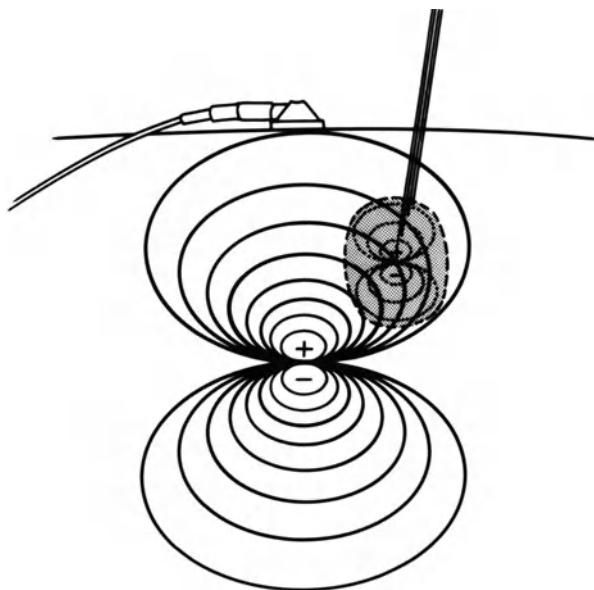
---

**Figure 2-28A.** Diagram showing the voltage distribution generated by a bipolar generator. A surface electrode and a multi-stranded depth electrode is also shown. The voltage distribution is shown by isopotential lines with the lines closest to the bipole representing a relatively higher potential.

nique can only be used to a limited degree in humans (usually not possible to place electrodes between the generator source and the surface recording site), and the extensive studies of Vaughn and collaborators in experimental animals still do not establish with certainty the intracerebral generator sources. The problem is again related to the existence of multiple generators. Recording of potentials which are larger at the surface than between the generator source and the surface indicate that this particular generator source is certainly not determining the surface potentials. The reverse, however, is not true. Potential fields may be of significantly higher amplitude at all points between a given generator source (A) and the surface recording site (B) without implying a causal relationship between the two. This is because of the existence of a second generator source (C) which actually determines the surface potential. This is illustrated in figure 2-28. Figure 2-28A shows the ideal case of a single open generator in which the multiple contacts of the depth electrode will record a progressively decreasing amplitude as we approach the surface, and the deepest contact actually records a near-field potential from the generator source itself. Figure 2-28B shows one example in which this recording technique may lead to the wrong conclusion. In this case the electrode tip is inside a

---

### Open and closed field generator




---

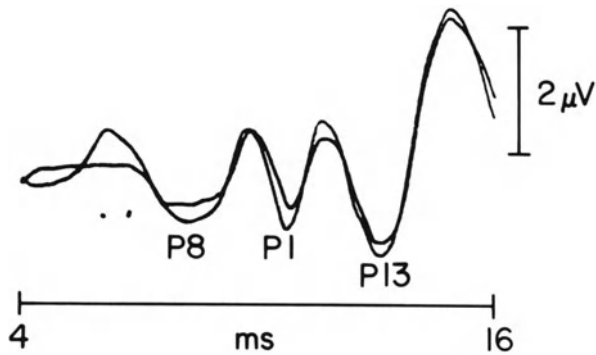
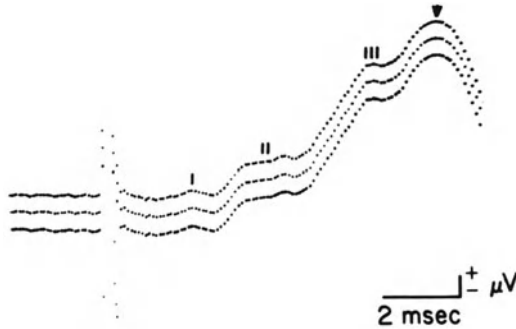
**Figure 2-28B.** Identical to figure 28A but with an additional close-field generator which generates a relatively high potential at the tip of the multistranded depth electrode.

close-field generator which does not reflect up to the surface. A progressively decreasing potential will be recorded, however, at electrodes closer to the surface because of the nearby open field generator. The potential at the surface electrode in this case is an expression of the open-field potential. This is just one example of how the existence of multiple generators may produce false conclusions when this technique is used. This explains why the experiments of Vaughn and collaborators provided extremely useful information which has greatly complemented our knowledge in the field but did not give us the final answer.

#### ANIMAL EXPERIMENTS

It seems that animal studies provide the ideal setting to answer most of the questions we have regarding EP peak origins. Detailed intracerebral recordings with exact distribution studies can be performed. Lesion experiments and extensive manipulation of physiological variables can be carried out to supplement the distribution studies. This certainly can lead to more or less precise identification of the generators of surface peaks in the animal studies. Unfortunately, these results have advanced very little our knowledge of the generator sources of surface EP peaks in humans. This is because it is difficult if

---

**HUMAN**

**RAT**


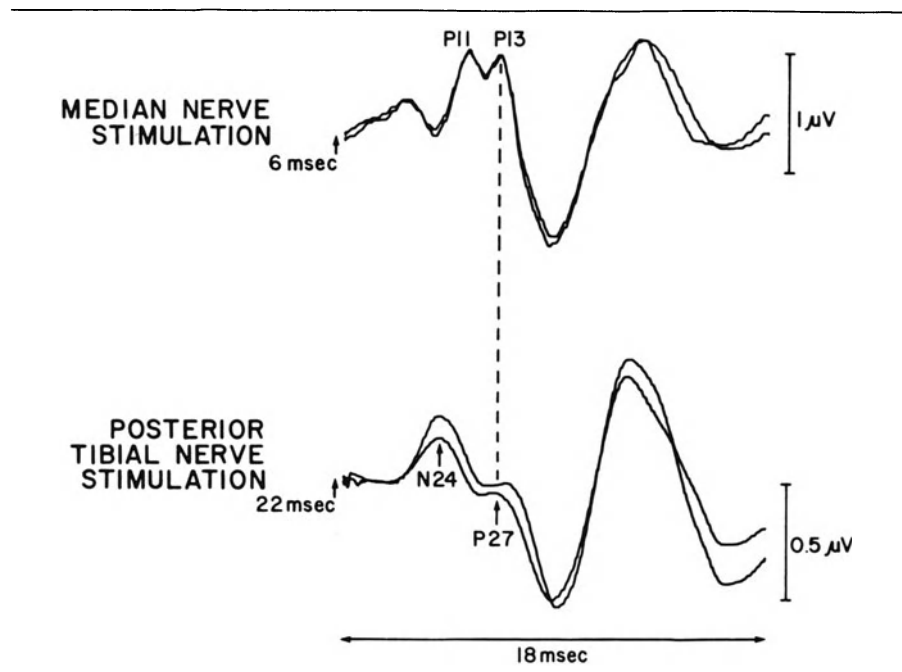

---

**Figure 2-29.** Far-field somatosensory evoked potentials recorded in humans and rats.

not impossible to establish, with precision, what surface EP peaks in different species are of the same origin. The difficulty to identify analogous EP peaks is shown in figure 2-29. This uncertainty makes conclusions drawn from animal experiments unreliable for identification of generator sources of surface EP peaks in humans. It seems that the animal experiments' main value is in establishing some general rules which can then be applied to the results obtained in human recordings.

**RECORDING OF ANALOGOUS POTENTIALS**

Another method, which has been used only to a very limited extent, is to study the distribution of other potentials generated in the same structures implicated as EP generator sources. An example of this methodology was the study of the distribution field of hippocampal sharp waves, and comparing it with the distribution of P300, which some authors had concluded was generated in the hippocampus. These comparative studies provided evidence



**Figure 2-30.** Potentials recorded from neck-scalp derivation to median nerve (MN) and posterior tibial nerve (PTN) stimulation (SC5-Fpz for MN stimulation and SC5-Cz for PTN stimulation). Analysis time was 18 msec in both cases, but time axis of response to PTN stimulation has been displaced 16 msec to left to align analogous components. Filters: 150–1500 Hz (–3 dB). Reprinted with permission from “Somatosensory Evoked Potentials,” Lüders et al., *Arch. Neurol.* 40, 1983.

that was contradictory with the theory that P300 was of hippocampal origin. This method has been used only to a very limited degree.

Another example in which analogy of potentials can be used effectively to define the origin of EP peak generators is shown in figure 2-30. In this case the investigators took advantage of the fact that the pathways carrying the afferent volley to median nerve and posterior tibial nerve stimulation are essentially contiguous to each other at the level of the cervical spinal cord and brain stem. Therefore, it seems reasonable to expect that at that level analogous waves should be recorded when stimulating the posterior tibial nerve and the median nerve. Figure 2-30 shows that this is actually the case.

## CONCLUSION

This discussion analyzes critically the different techniques which have been used to define the surface EP-peaks. It is interesting to notice how many techniques can be used for the same objective, and that all of them provide useful information, but also, without exception, have major limitations. Reliable

identification of the generator sources of surface EP-peaks can only be expected when the information collected with the different methods is congruent and consistent.

## REFERENCES

1. Achor LJ and Starr A: Auditory brain stem responses in the cat. I. Intracranial and extracranial recordings. *Electroencephalogr Clin Neurophysiol* 48:154–173, 1980a.
2. Achor LJ and Starr A: Auditory brain stem responses in the cat. II. Effects of lesions. *Electroencephalogr Clin Neurophysiol* 48:174–190, 1980b.
3. Anziska B and Bracco RO: Short latency somatosensory evoked potentials: Studies in patients with focal neurological disease. *Electroencephalogr Clin Neurophysiol* 49:227–239, 1980a.
4. Anziska BJ and Cracco RO: Short latency SEPs to median nerve stimulation: comparison of recording methods and origin of components. *Electroencephalogr Clin Neurophysiol* 52:531–539, 1981.
5. Arezzo J, Legatt AD, and Vaughan HG Jr: Topography and intracranial sources of somatosensory evoked potentials in monkey. I. Early components. *Electroencephalogr Clin Neurophysiol* 46:155–173, 1979.
6. Asselman P, Chadwick DW, and Marsden CD: Visual evoked responses in the diagnosis and management of patients suspected of multiple sclerosis. *Brain* 98:261–282, 1975.
7. Barrett G, Blumhardt L, Halliday AM, Halliday E, and Kriss A: paradox in the lateralization of the visual evoked response. *Nature (Lond.)* 261:253–255, 1976.
8. Chiappa KH. Utility of lowering click intensity in neurologic applications of brainstem auditory evoked potentials. Presented at Conference on Standards in Clinical BAEP testing, Laguna Beach, California, February 1982 (in press).
9. Chiappa KH, Choi S, and Young RR. Short latency somatosensory evoked potentials following median nerve stimulation in patients with neurological lesions. *Prog Clin Neurophysiol*, In: J. E. Desmedt (ed) Vol. 7, Karger, Basel, 264–281, 1980.
10. Cruse R, Klem G, Lesser RP, Lueders H. Paradoxical lateralization of cortical potentials evoked by stimulation of posterior tibial nerve. *Arch Neurol*; 39:222–225, 1982.
11. Desmedt JE, Brunko E, and Debecker J. Maturation of the somatosensory evoked potentials in normal infants and children, with special reference to the early N1 component. *Electroencephalogr Clin Neurophysiol* 40:43–58, 1976.
12. Desmedt JE and Noel P. Average cerebral evoked potentials in the evaluation of lesions of the sensory nerves and of the central somatosensory pathway. In: JE Desmedt (ed) *New Developments in Electromyography and Clinical Neurophysiology*, Vol. 2, Karger, Basel, 352–371, 1973
13. Fukushima T and Mayanagi Y. Neurophysiological examination (SEP) for the objective diagnosis of spinal lesions. In: Klug W, Brock M, Klager M, and Spoerri O (eds) *Advances in Neurosurgery*, Vol. 2, Springer-Verlag, Berlin, 158–168, 1975.
14. Giblin DR. Somatosensory evoked potentials in healthy subjects and in patients with lesions of the nervous system. *Ann NY Acad Sci* 112:93–142, 1964.
15. Halliday AM and Wakefield GS: Cerebral evoked potentials in patients with dissociated sensory loss. *J Neurol Neurosurg Psychiat* 26:211–219, 1963.
16. Hecox K and Galambos R: Brain stem auditory evoked responses in human infants and adults. *Arch Otolaryngol* 99:30–33, 1974.
17. Larson SJ, Sances A, and Christenson PC: Evoked somatosensory potentials in man. *Arch Neurol (Chicago)* 15:88–93, 1966b.
18. Lorente de No R: A study of nerve: physiology studies from the Rockefeller Institute 132, Chapter 16, 1947.
19. Lueders H: The effects of aging on the wave form of the somatosensory cortical evoked potential. *Electroencephalogr Clin Neurophysiol* 29:450–460, 1970.
20. Lueders H, Lesser R, Gurd A, and Klem G: Recovery functions of spinal cord and subcortical somatosensory evoked potentials to posterior tibial nerve stimulation: intrasurgical recordings. *Brain Res* 309:27–34, 1984.
21. Lueders H, Lesser RP, Dinner DS, Morris HH, and Klem G: Ipsilateral somatosensory evoked potentials recorded directly from the human cortex. 11th International Congress of EEG and Clinical Neurophysiology, London 1985.

22. Lüders H, Lesser RP, Hahn J, Little J, and Klem G: Subcortical somatosensory evoked potentials to median nerve stimulation. *Brain* 106:341–372, 1983.
23. MacCabee PJ, Hassan NF, Cracco RA, and Schiff J: Short latency somatosensory and spinal evoked potential: power spectra and comparison between high pass analog and digital filter. *Electroencephalogr Clin Neurophysiol*, 1986 (in press).
24. Maguère F, Brunon AM, Echallier JF, and Courjon J: Early somatosensory evoked potentials in lesions of the lemniscal pathway in humans. In: J Courjon, F Maguère and M Revol (eds), *Clinical Applications of Evoked Potentials in Neurology*, Raven press, New York, 321–338, 1982.
25. Namerow NS: Somatosensory evoked responses following cervical cordotomy. *Bull Los Angeles Neurol Soc* 34:184–188, 1969.
26. Noel P and Desmedt JE: Somatosensory cerebral evoked potentials after vascular lesions of the brain stem and diencephalon. *Brain* 98:113–128, 1975.
27. Noel P and Desmedt JE: Cerebral and far-field somatosensory evoked potentials in neurological disorders involving the cervical spinal cord, brainstem, thalamus and cortex. *Prog Clin Neurophysiol* 7:205–230, 1980.
28. Powell TPS: Residual neurons in the human thalamus following decortication. *Brain* 75:571–584, 1952.
29. Robinson K and Rudge P: The early components of the auditory evoked potential in multiple sclerosis. In: Desmedt JE (ed) *Auditory Evoked Potentials in Man. Psychopharmacology Correlates of EP's*. Progress Clinical Neurophysiology, Vol. 2, Karger, Basel, 58–67, 1977a.
30. Rowe MJ III: Normal variability of the brain-stem auditory evoked response in young and old adult subjects. *Electroencephalogr Clin Neurophysiol* 44:459–470, 1978.
31. Russell GV: Histologic alterations in thalamic nuclei of man following cortical lesions. *Texas Rep Biol Med* 16:483–492, 1958.
32. Wiederholt WC: Recovery function of short latency components of surface and depth recorded somatosensory evoked potentials in the cat. *Electroencephalogr Clin Neurophysiol* 45:259–267, 1978.
33. Williamson PD, Goff WR, and Allison T: Somatosensory evoked responses in patients with unilateral cerebral lesions. *Electroencephalogr Clin Neurophysiol* 28:566–575, 1970.
34. Yamada T, Muroga T, and Kimura J: Tourniquet-induced ischemia and somatosensory evoked potentials. *Neurology* 31:1524–1529, 1981.



---

### 3. CRITICAL ANALYSIS OF SOMATOSENSORY EVOKED POTENTIAL RECORDING TECHNIQUES

JOHN E. DESMEDT

Studies of cerebral evoked potentials are vigorously developing, and somatosensory evoked potentials (SEP) appear to attract a major share of interest. The remarkable length of the somatosensory pathway from peripheral skin to cerebral cortex makes it vulnerable at many different points to a variety of pathological conditions. Neural generators all along this pathway can be revealed through appropriate SEP recordings methodologies and a variety of electrode montages can be used to resolve diagnostic issues in neurological patients.

It is now accepted that the SEP profile averaged results from the interaction of many component potentials of different latencies. Each component that has been adequately isolated and documented has been found to reflect one or more neural generators. This feature is interesting since it makes it possible to concurrently assess several distinct SEP generators in a single or at least a few appropriately recorded traces. It also represents a challenge of securing the adequate background data for the proper identification of the different components and their significance. Any notch on the SEP profile need not be a genuine component and overinterpretation of data represents a definite pitfall. On the other hand, some SEP components are inconstant and may indeed be missing from a particular trace even through the recording technique

The work reported has been supported by grants from the Fonds de la Recherche Scientifique Médicale, Belgium

is adequate. Knowledge of the consistent features and their parametric sets for the standard components appears to be a prerequisite for efficient SEP interpretations.

This chapter considers several problems in conjunction with the recording and interpretation of early SEP components evoked by electrical stimulation of the median or posterior tibial nerve in man. Details of methods can be found elsewhere [9, 18]. The nomenclature of each SEP component uses P (positive) or N (negative) followed by its modal peak latency in normal adults of standard body size, even in the individual case where the component latency may be different for various reasons (e.g., different limb lengths or stimulation at different levels along the limb) [22]. For well documented SEP components, the label has indeed become a name (e.g., P9, P11, P14, N18, N20, P22) rather than an indication of the particular peak latencies in a given study, and this facilitates discussions while it helps avoid misunderstandings.

#### **PRINCIPLES UNDERLYING THE RECORDING OF SEP**

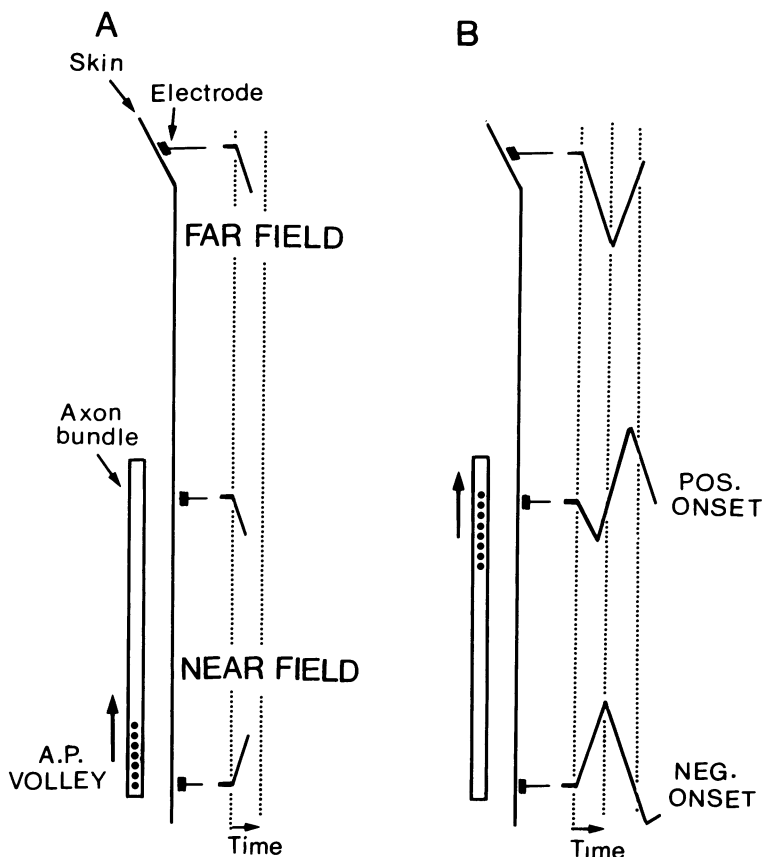
All recordings are in fact bipolar and measure the potential difference between the active electrode connected to grid 1 and the reference electrode connected to grid 2 of the amplifier. Differential amplifiers are routinely used to reject in-phase (common mode) interference that appear at both leads of each amplifier. The problem of optimizing recordings from the head is important and cannot avoid the issue of how to choose appropriate reference electrodes.

#### **VOLUME CONDUCTION OF BRAIN POTENTIALS**

Spinal and brain potentials recorded from the body surface are small (one microvolt or less) and present complex distributions. They must be interpreted in conjunction with the properties of potential fields in conductive media.

Phasic changes of extracellular potential fields are produced by volume-conduction either of a synchronized volley of action potentials in nerve trunk or corticospinal tract (Lorente de No, 1947), or postsynaptic potentials generated in the geometrically coherent dendrites of cortical neurons [23]. Lorente de No (1947) distinguished several pertinent sets of geometric parameters. A spike volley in a tract of parallel nerve fibers can be viewed as equivalent to a propagated dipole: it is a good example of an open-field system that generates in the volume conductor a coherent extracellular field at a distance. When an active recording electrode is close to the axon (near-field recording), it picks up an extracellular positivity produced by the outward current flow associated with the local circuits produced by the membrane depolarization of the action potential propagating from a distant part of the axon (figure 3-1A).

This approach positivity is followed by a larger negative potential reflecting the inward (sodium) current flow through the membrane underneath the recording electrode when it is involved by the action potential (figure 3-1B). Then, as the action potential passes further along the axon and gets beyond the



**Figure 3-1A, Figure 3-1B.** Cartoon contrasting near-field recordings over a bundle of axons (such as the dorsal column) with finite dimensions are far-field recordings beyond the termination of the bundle. The region of the axons bundle generating action potentials is pictured by heavy dots. Negativity of the recording electrode registers upwards. The vertical dotted lines help identify time relationships. A: the spike volley is initiated at the bottom end of the bundle. The adjacent near-field electrode records a negative-going deflexion while electrodes further up record an approach positively. B: slightly after, the spike volley produces a negativity at the upper near-field electrode. The far-field electrode only records a monophasic positive wave [18].

level of the recording site, the membrane repolarizes (outward current flow), which can produce a small extracellular positivity. This sequence of events seen by the electrode in the volume conductor results in the classical triphasic waveform of the extracellular potential.

Another pertinent situation is when the active recording electrode is located in the volume conductor beyond the termination of the axon (or tract), as this corresponds to the far-field recording conditions for EPs. Then the electrode picks up a positive extracellular potential representing the local circuits spreading ahead of the membrane depolarization, but no subsequent negativity

since the action potentials never get up to the recording site (figure 3-1). Thus, beyond the termination of a tract, volume-conduction of the dipole is recorded as a positive-going approach wave without subsequent negativity (this condition is similar to classical killed-end recording [11, 18, 26].

The above applies not only for single axons, but also for nerves or central tracts. The coherent geometrical orientation of the individual axons in the tract ensures cooperative summation of the individual extracellular fields. Another factor for sizeable volume-conduction at a distance is that the individual action potentials propagate roughly synchronously and this is true for at least a group of the largest axons in the tract.

Noncoherent geometry, however, prevails in many central nuclei and it corresponds to the closed-field system of Lorente de No (1947). For example, depolarization of neurons in a nuclear structure with dendrites radiating different directions from the center will produce inward flows of current toward the center of the nucleus, but virtually no recordable potential difference outside its anatomical boundaries [28].

Early discussions of brain waves in electroencephalography (EEG) considered summation of action potentials as their generators. Eccles [23] made an essential contribution when he proposed that cortical EEG potentials rather related to postsynaptic potentials in geometrically coherent apical dendrites of cortical pyramidal neurons. These form an open-field system (Lorente de No, 1947) and can indeed generate volume-conducted potentials at a distance [7, 25, 28, 33].

### **Near-field and far-field recordings**

In near-field recording, the active electrode is placed relatively close to the neural generator (say, a nerve). Distance from the generator is critical in near-field recording and a sharp attenuation of the recorded potential occurs when the electrode is moved away by even small distances. In the case of cortical generators, any scalp electrode is located at a distance of 12 to 30 mm from the generators: the cortical potentials are attenuated by a factor of about 10 to 30 at scalp electrodes as compared with electrodes placed on the cortex itself [5, 21]. Also, the potential gradients over the scalp are smoothed out because of the distance from electrode to neural generators, but this does not prevent distinct cortical generators to be mapped out over the scalp [13].

In far-field recording [26] of subcortical generators with scalp electrodes, the recorded potential are of course much attenuated by the larger distance from the actual generator. Another feature is that it changes much less with recording position on the scalp than is the case for near-field recordings of cortical potentials. In spite of their very small voltage, the volume-conducted farfields can be easily detected through electronic averaging which considerably increases the signal-to-noise ratio [11]. Familiar examples are the brainstem auditory responses which are about 1 mV in focal brainstem recordings in cats, but attenuate to about 1 $\mu$ V when averaged from the scalp [26].

Our use of the terms near field and far field does not imply any strict dichotomy between two distinct sets. They relate in fact to the two sides of a continuum of recording conditions picking up potentials from different levels of the volume-conductor of the head.

Thus, the scalp-recorded brain potentials relate to a variety of open-field generators that are either cortical (relatively near-field) or subcortical and even in the peripheral nerve (far-field). The extent to which any of the SEP neural generators will be represented in the averaged response depends on several factors: geometry of the simultaneously active neural units [28], temporal synchronization, duration and spatial distribution of the transmembrane currents in population of similar neural units (say, in a fiber bundle or in a set of neurons) which affect the size of the equivalent dipole [25]; and amount of summation or cancellation of the various field potentials that are volume-conducted from different sources that can be overlapping in time to different extents [11].

## DATA ACQUISITION AND ANALYSIS

### Stimulation

SEPs are generated by the brain or spinal cord in response to transient stimulation of sensory axons, whereby synchronized volleys of sensory impulses are elicited at known instants that serve as a reference point in time for averaging. In most cases brief (0.1 or 0.2 msec) square electric pulses are delivered to sensory or mixed nerves. Provided the electrodes establish stable contact, a consistent set of sensory axons is thus stimulated. So-called constant current stimulators should not be used as they involve a direct connexion of the subject to the output circuit of the stimulator. The electrodes should rather be connected to the stimulator via an output transformer, whereby a potential electric hazard to the subject is avoided and electric interference is minimized. It is recommended to monitor actual current flow through the stimulating electrodes (numerical display to tenths of mA) to be able to rapidly identify any change in stimulating conditions.

The electric stimuli can be delivered to digital nerves through ring electrodes around fingers or toes, or to any chosen restricted area of skin through fine needle electrodes (dermatomal or focal stimulation). This is useful in patients with restricted sensory symptoms and allows comparison of SEPs to either hypoesthetic or normal skin in the same subject. Intensities are then adjusted in relation to the subjective sensory threshold which can be estimated by the method of limits. Usually an intensity (in mA) at 150 or 300% of subjective threshold is found to elicit convenient responses.

Electric stimuli can also be delivered to mixed nerves such as the median or ulnar at the wrist, or the posterior tibial at the ankle. In this case one can choose the stimulus intensity in relation to the threshold twitch elicited by concomitantly activating the motor axons in the nerve. Such stimuli to mixed

nerve also involve the muscle group I afferents which may have a separate contribution to the recorded SEP response [4, 6]. Natural stimulation by mechanical taps on the skin surface or tendons, as well as by displacement of joints, have been recently shown to elicit measurable SEP responses. However these procedures are less easily standardized under clinical conditions and have not yet been shown to provide uniquely useful data as compared with more convenient electric stimulations.

The selective stimulation of sensory axons of small diameter, such as those related to pain, can be achieved by CO<sub>2</sub> laser radiant heat pulses, and ultralate SEP (about one second latency) elicited by such pain stimuli can be detected after pressure block of the larger-diameter alpha axons [3].

### **Electronic averaging**

SEP components generated by subcortical or cortical neurons systems have a rather small voltage, about 0.02 to 5 microvolts, so that they cannot be identified in direct recording. Under special conditions, single trials can be used, as when the SEP response is considerably enhanced in patients with myoclonic epilepsy. Therefore, SEPs recorded from the scalp or neck skin are displayed after electronic averaging which involves the analog-to-digital conversion and algebraic summation of many (say, 1,024) samples of responses to the transient sensory stimulus, which is thus repeated as many times at appropriate intervals. The averaging method has proved efficient and no concurrent method has gained widespread uses. During averaging, the random noise, without consistent temporal relationship with the sensory stimulus, tends to cancel out, while the brain responses time-locked to the sensory stimulus add up coherently.

The high sensitivity of this method makes it vulnerable to any large interfering potentials that cannot be averaged out because they are infrequent or not truly random [9]. Recognition of such limitations of averaging leads to appropriate precautions for reducing intermittent electric interferences by extraneous electrical equipment (shielding from radiological equipment, elevators, fluorescent lights, radio TV, etc.) or by large extraneous potentials in the subject (EMG of cephalic muscle, eye movements, eyeblinks or EKG). This cannot be achieved through mere filtering or smoothing of the signals which would introduce severe distortions while not actually eliminating the unwanted junk.

The recommended procedure is to maintain the subject in a relaxed state with little or no eye movements, and with cephalic muscles fully relaxed. If necessary, a tranquilizer drug can be used, namely in the case of uncooperative patients or children. Monitoring single trials is useful to identify eyeblinks or EMG bursts of swallowing, teeth clenching, frowning or neck tensing: reinforcing instructions to the subject can then be given. Also the averaging computer program can include a checking procedure of all recorded channels

with provision for rejection from the current average when any potential level exceeds set limits.

The EKG interference is best dealt with by triggering the sensory stimuli at appropriate times outside the major EKG peaks (between T and P waves) through an electronic delay circuit [18]. When used with proper care, the method proves invaluable for constantly upgrading the detailed objective evidence on specific brain functions, even under the somewhat adverse conditions of intensive care units or operating theaters.

#### **DISPLAY OF SEP RESPONSE**

The usual procedure is to average and display SEPs recorded on several channels concomitantly. Taking as an example SEPs to upper limb stimulation, one compares traces of Erb's point (brachial plexus), Cv6 spine at posterior neck with noncephalic reference (spinal components), and contralateral parietal and frontal scalp sites with earlobe reference.

Spinal responses cannot be assessed with an earlobe or scalp reference which records concomitant activities generated above foramen magnum [14, 15, 18]. Contralateral parietal responses should be differentiated from the concomitant frontal responses so that a frontal scalp reference must be excluded while an earlobe reference is acceptable [13]. The scalp SEPs can also be recorded with a noncephalic reference when a full display of subcortical components is desirable (see below).

A more comprehensive display of SEP response fields over the scalp or around the neck can be achieved by using more channels. However this rapidly raises problems of data management and analysis, unless a consistent computerized display of the spatiotemporal information therein embedded can be created as in the recent bit-mapped color imaging method. SEP imaging raises a special problem because of the fast rise times of several of the early components (bandpass fidelity required) and of the extensive coverage required by the spatial differentiation of the different SEP potential fields [13, 18]. We are currently using 28 electrodes positioned to survey comprehensively the various brain regions.

For map creation, an interpolation method was used to define potential levels at about 5,000 pixels and voltage values were imaged by a scale of discrete hues with blue for positive values and red for negative values. The bit-mapped imaging has been recently discussed [19].

Color imaging of SEP fields reveals a wealth of unsuspected detail of response features in health and disease, and allows SEP components to be analyzed into underlying neural generators. This comprehensive database calls for reassessing conclusions that could be biased or distorted because they only involved a limited number of concomitant channels. Also the imaging data suggest updated and more meaningful placements of the recording electrodes in tests where fewer channels are more convenient for some practical uses.

### EVALUATION OF SEP RESPONSE

A global description of the averaged response in terms of amplitude is no longer acceptable. It is necessary to identify specific components and their possible deviations from normal controls matched for age. Identifying SEP components in turn requires the use of appropriate recording electrode montages. For any particular application one has to choose the more useful montages, taking into account its efficiency in terms of both anticipated level of interference and optimal acquisition of adequate information.

Waveforms do vary from subject to subject, and particular SEP features need be documented as being consistent in any one subject. It is thus advisable to obtain two separate averages under similar stimulation and recording conditions in order to evaluate consistency of response features. This may also check on the possible incidence of transient interference (as this is unlikely to affect either samples in the same manner).

Latencies of SEP components can vary between subjects on account of a variety of factors which should be made explicit. The onset latencies of early spinal or cerebral responses largely reflect conduction times along afferent somatosensory pathways and they will be delayed: 1) in subjects with longer limbs and larger body size; 2) if the tissue temperature of the stimulated limb is below 36°C as this slows down nerve conduction; 3) as a factor of the subject's age; 4) if the nerve stimulated has disordered conduction due to mechanical entrapments or neuropathy.

SEPs actually have an important area of clinical uses for documenting sensory nerve conduction slowing in neuropathies [8, 10]. When this is not the issue considered, it is nevertheless recommended to document the peripheral nerve conduction time by noticing the latency of the Erb's point nerve response or of the P9 far-field that reflects activity in brachial plexus.

When estimating SEP components latencies, the time from stimulus to the peak of the component considered has frequently been estimated. However a more meaningful estimate is the component onset latency which reflects the time at which the neural generator(s) involved are activated. Improved techniques and better understanding of components features make it possible to reliably identify components onsets in most cases. In this relation, it must be stressed that electrode montages do affect the actual latency measures, namely when inappropriate montages involve algebraic addition of distinct components with different features [13, 14].

Amplitudes of SEP components do vary between subjects and it may be a problem to decide about abnormal deviations in patients unless the disorder is focal, whereby the opposite side can be used for documenting control responses. Early SEP components have rather stable latencies in any given subject, while late components can display so-called latency jitter, which in turn can blur the component's profile in the averaged trace. Special methods involving single trials latency adjustments can be used in this case.



## SELECTED SEP FEATURES

### Spinal entry time of the somatosensory volley

A useful data for interpreting subcortical SEP far fields is actual time of arrival of the afferent volley at the spinal cord. This can be documented by direct recordings of sensory nerve action potentials along the limb. The conduction velocity (CV) of afferent axons in median nerve is  $71.1 \pm 4.0$  (s.d.) msec (mean for 25 healthy adults of mean age 22 years). These axons travel in the Cv6 and Cv7 spinal roots which enter into the spinal cord at the junction of the fourth and fifth vertebrae [14]. Extrapolation of the afferent CV regression line to that level roughly estimate the spinal entry time of the afferent volley: this fits with the onset of either the N11 near field component recorded at low posterior neck or of the P11 scalp far field (figure 3-2). Both N11 and P11 are thought to reflect the action potentials volley which ascend the dorsal column [14, 15, 18].

For posterior tibial nerve, the mean afferent CV is  $59.2 \pm 3.3$  msec (mean for 18 healthy young adults). The posterior tibial nerve depends mainly on spinal segments S1-S2 and partly on S3, which correspond to the level of the D12 spine at the skin. Extrapolation of the peripheral CV to the D12 spine gives a mean spinal entry time of  $19.7 \pm 1.4$  msec which coincides with onset of the N21 near field thought to be the first spinal response in dorsal column after the P17 far field (figure 3-3) [17].

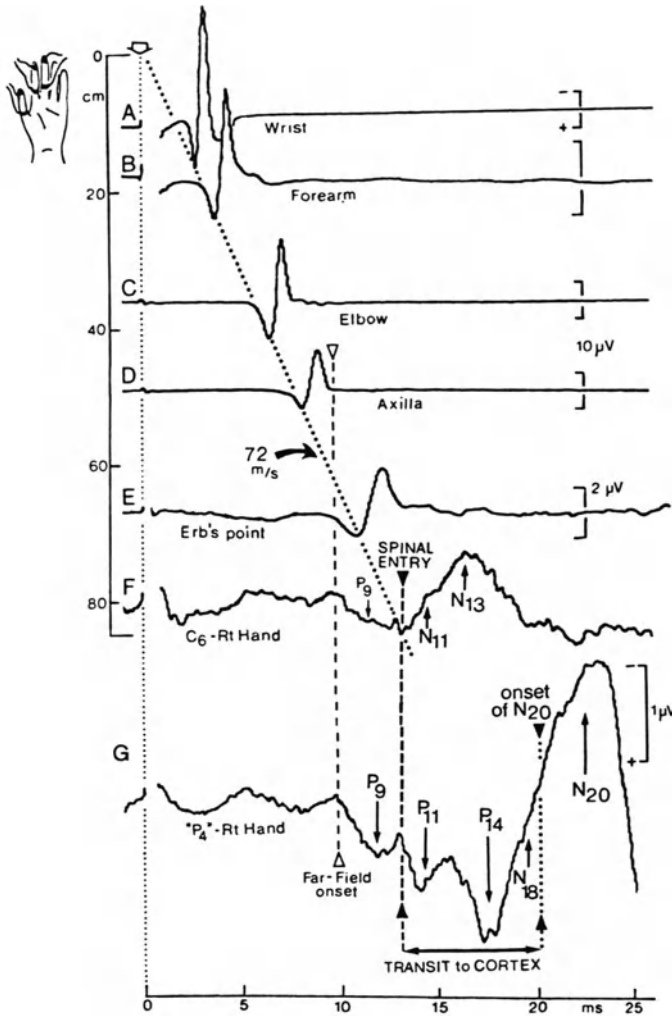
### Peripheral nerve far field

With noncephalic reference, the first SEP event over the spine or head is a widespread far-field positivity identified as P9 for median nerve or as P17 for posterior tibial nerve stimulation. P9 reflects a volume-conducted potential generated in the brachial plexus as the afferent volley reaches a site under the lateral part of the clavicle [20, 27]. P17 reflects the afferent volley in the lumbosacral plexus as it reaches the upper third of the buttock [17, 34].

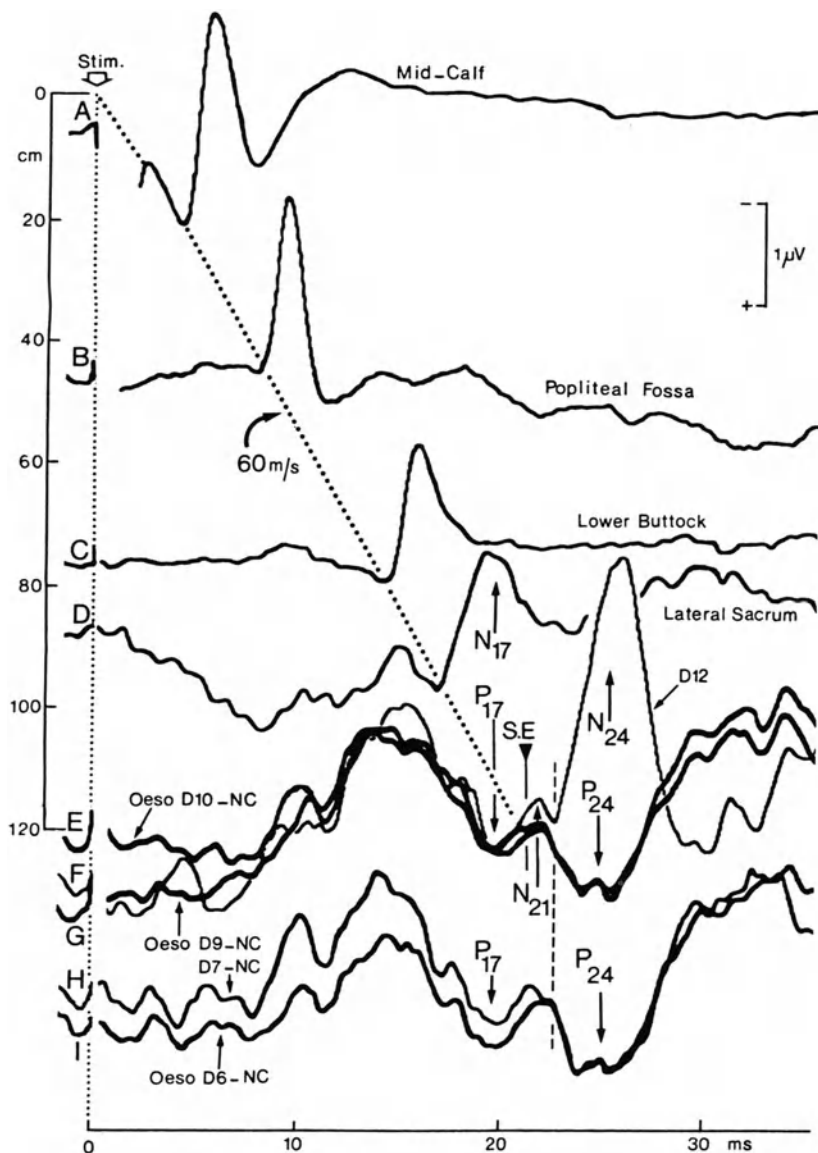
### Dorsal column propagated volley

In the median nerve SEP recorded from the neck with noncephalic reference, the N11 near field shows an increase of its onset latency from lower to upper neck that is thought to reflect the dorsal column volley propagated along a caudo-rostral axis [1, 14, 29]. The high neck electrode registers an approach positivity before the negative-going response. Scalp electrodes beyond pathway termination only register a P11 far field (figures 3-1, 3-4) [18] The mean maximum CV of N11 along the cord was calculated as 58 msec [11].

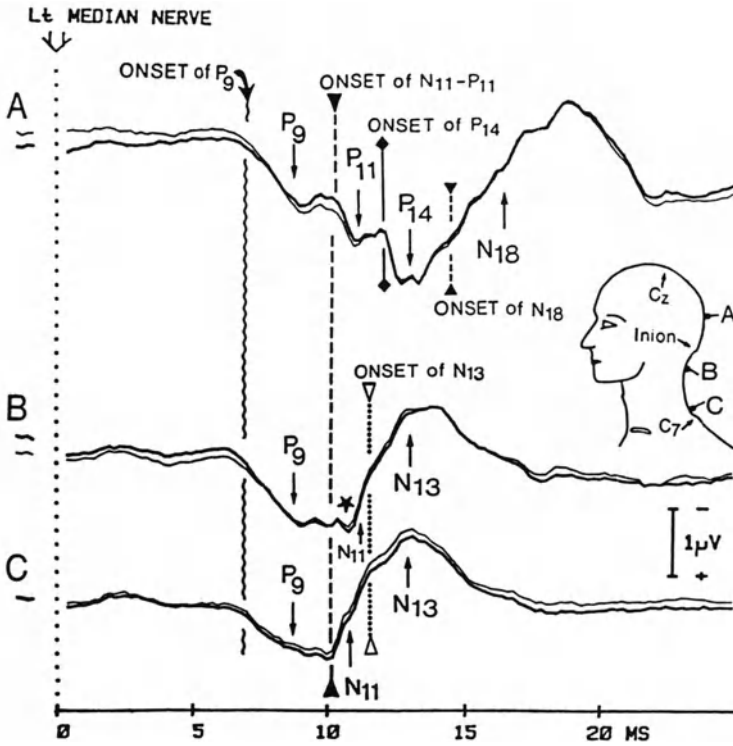
The posterior tibial nerve SEP is larger at D12 spine than higher up over the dorsal region. Published data on CV from D12 to C7 tended to exceed peripheral nerve CV even though it is highly unlikely that the CV would suddenly accelerate over the dorsal cord. This difficulty was partly resolved by showing



**Figure 3-2.** Estimation of spinal entry time of an afferent volley elicited in median nerve by stimulation (3 times sensory threshold) of left fingers I-II-III. Thumb stimulus delayed by 0.5 msec to achieve a synchronized sensory nerve volley. The volley is recorded by subcutaneous steel needles (active close to the nerve; reference inserted 3 cm at right angle to the nerve course) at the wrist (A), mid-forearm (B), elbow (C), axilla (D) and Erb's point at mid-clavicle (E). The vertical separation of the (averaged) traces is proportional to distances between electrode sites along the nerve. Calculated linear regression traced obliquely through onsets of the first negative phase of sensory nerve potentials. The neck SEP is picked up over the spinous process of the Cv7 vertebra is recorded with noncephalic reference on the dorsum of the right hand dorsum (F). The contralateral parietal scalp SEP is shown in G (noncephalic reference). Vertical interrupted line with white triangles shows onset of P<sub>9</sub> far field. Vertical interrupted line with black triangles shows spinal entry time extrapolated from peripheral condition; this coincides with the onset of the neck N<sub>11</sub> and of the P<sub>11</sub> scalp far field. The transit from spinal entry (onset of P<sub>11</sub>) to arrival at the cortex (onset of N<sub>20</sub>) is indicated. Negativity of the active electrode records upwards [14].



**Figure 3-3.** SEPs to posterior tibial nerve stimulation in a normal adult. Recordings from peripheral nerve at mid-calf (A), popliteal fossa (B), lower buttock (C) and lateral sacrum (D), with calculated linear regression indicating a conduction velocity of 60 msec (dotted line through the negative-going onset of nerve potentials). E, response at the D12 spine with the P17 far field, N21 and N24 components. Spinal entry corresponds to onset of N21. F-I, esophageal recordings at the level of D10, D9, D7 and D6 respectively which show a P24 response after the P17 far field. The esophageal P24 is a phase-reversal of the D12 spine N24 and both reflect the dorsal horn generator [17].



**Figure 3-4.** SEPs to stimulation of the left median nerve at the wrist. The two traces superimposed represent a separate average of different runs to show consistency of waveform for the same recording electrode. Noncephalic reference (NC) on the right hand dorsum. A: recording from posterior scalp above the inion (figurine). B: recording from upper posterior neck at the Cv2 spine. C: recording from the lower posterior neck at the Cv6 spine. Negativity of the active electrode registers upwards. The vertical wavy line identifies onset of P9 far field. The vertical interrupted line identifies onset of neck N11 or scalp P11. The vertical large dotted line identifies onset of spinal N13. Notice that N13 onset (B-C) occurs nearly one msec before P14 onset (A) and that P13 has a longer duration than P14 [18].

**Figure 3-5.** Bit-mapped color imaging of neck potential fields. Stimulation of the left median nerve at the wrist. Noncephalic reference on the dorsum of the right hand. Voltage increments are represented by different hues in blue-purple for positive or red for negative. A: spatiotemporal imaging of the changes in SEP fields along time. The map is based on 8 electrodes in a horizontal plane at mid-neck (ordinate). The time along the abscissa is from 5 to 20 msec after the left median nerve stimulus. After the deep blue valley of positivity at 9 msec (P9 far field), a negativity develops at the back of the neck while a concomitant positivity develops at the anterior part. B: spatiotemporal imaging of the changes in evoked potentials fields along the midline.

The map is based on 12 skin electrodes placed from upper back up to the tip of the nose (figurine). The 3 blue sources of positivity of the P9, P11 and P14 far fields have a vertical axis that indicates stationary latency throughout the head and neck. While P9 extends down to lower neck, P11 only encroaches down to the upper neck (see figure 3-4A) and P14 only extends to the inion. From 10 msec after the stimulus the onset of the neck negative field (red) is seen to extend progressively from lower to upper neck (propagation of N11). After 15 msec, the whole scalp goes negative (widespread N18 brainstem response) [8].

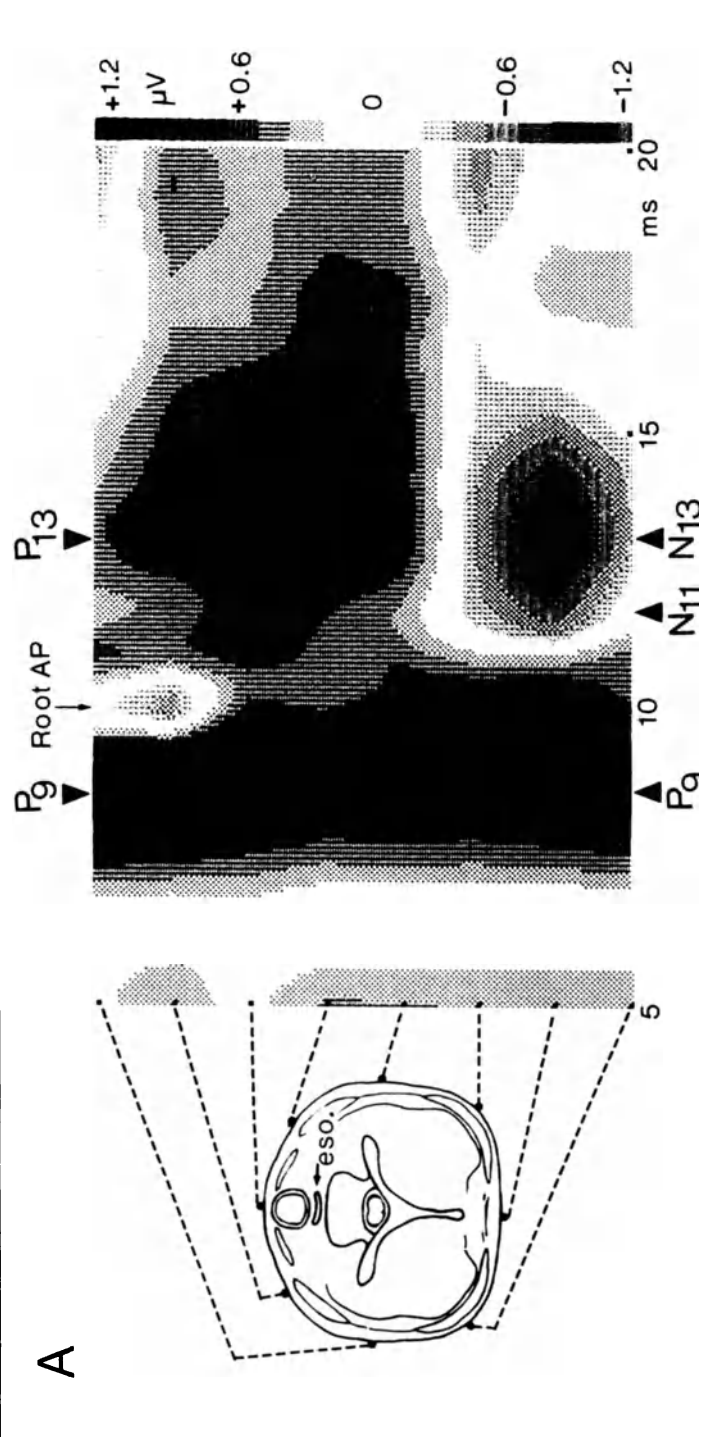


Figure 3-5A.

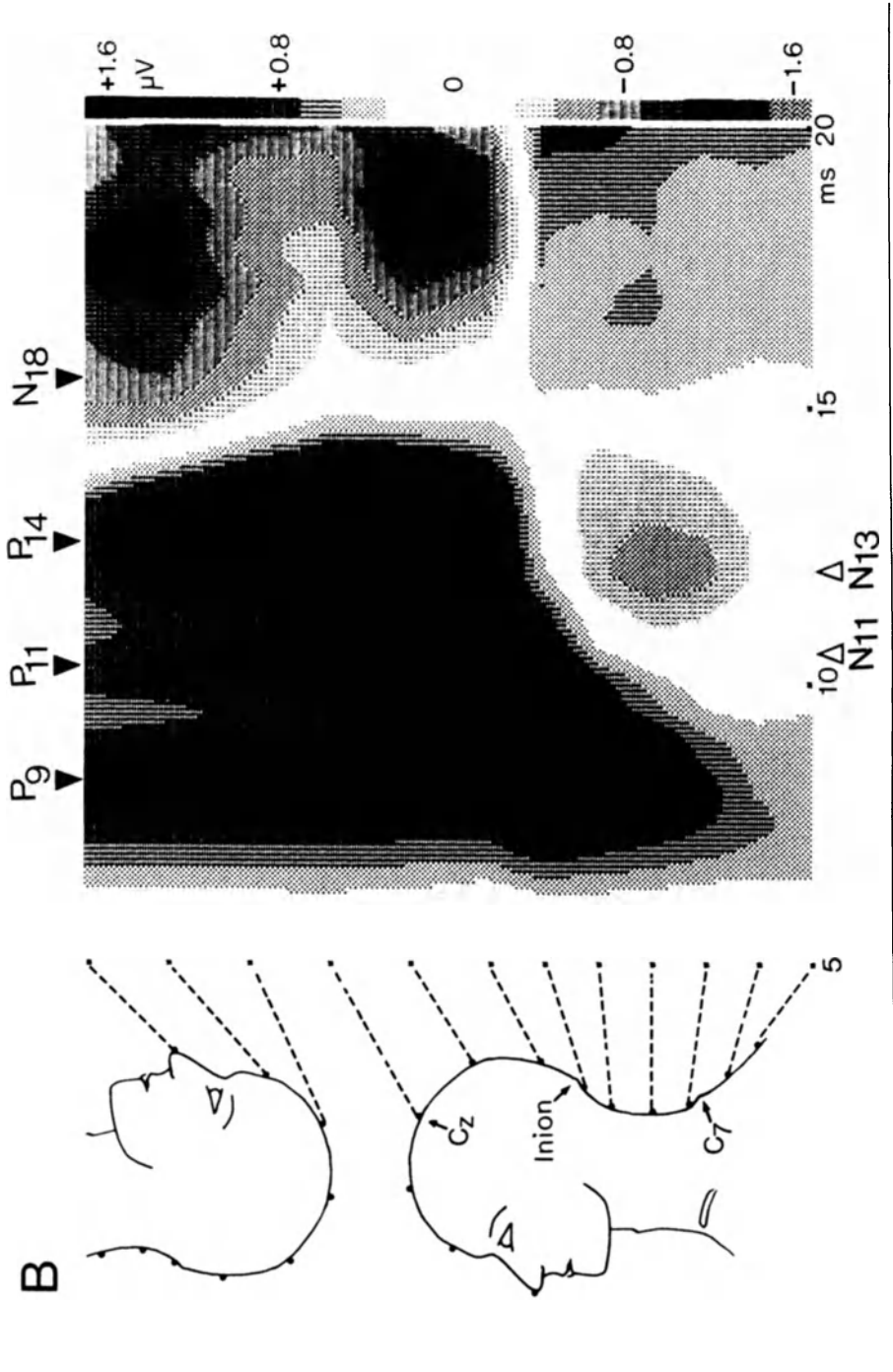


Figure 3-5B.

that surface measures along the back convexity overestimated the actual conduction distance because the cord tends to take a more or less straight course in the rather wide dorsal canal. When applying a correction factor of 13% for conduction length, the mean CV from D12 to C7 spines is found as 57 msec [17].

### **Dorsal horn segmental generator**

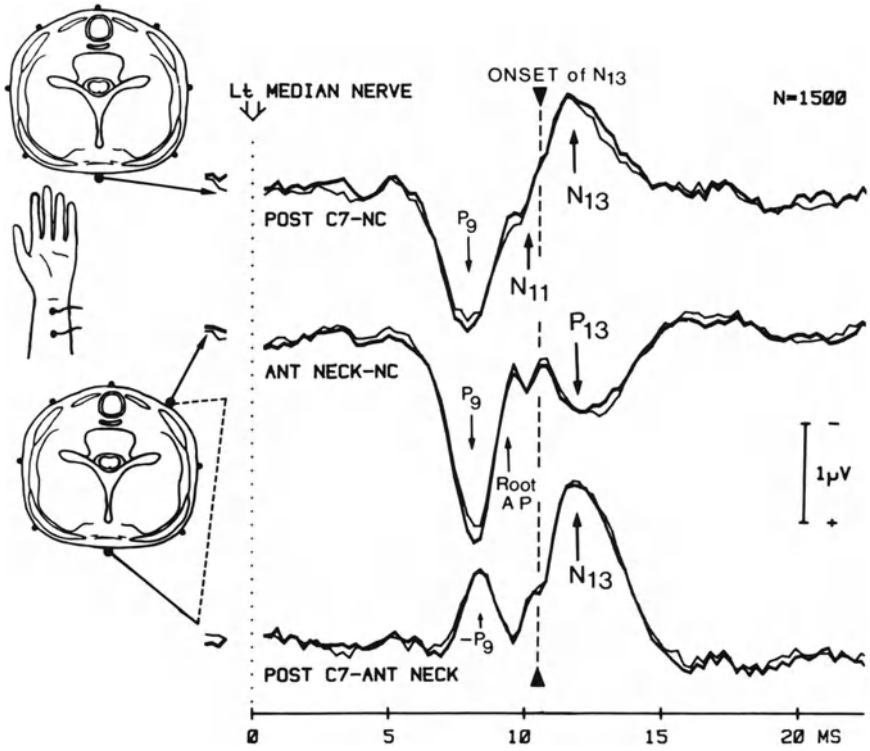
In the neck SEP to median nerve (noncephalic reference) the N11 near field is superimposed by a second negativity N13 which phase-reverses into a positive P13 at esophageal recording sites in front of the spinal cord. The actual longitudinal extent of the spinal P13 generator (charted by electrodes along the esophagus lumen) is from Cv7 to Cv4 spinal cord levels [11, 15].

Bit-mapped color imaging of SEP fields around the neck documented a genuine phase reversal between the posterior neck N13 and anterior neck P13, both sharing identical onset, peak and offset times (figure 3-5A) [18]. N13 reflects postsynaptic potentials at interneurons in layers IV-V of dorsal horn [11]. Because the N13 near field recorded at posterior neck and the P13 near field recorded at anterior neck reflect two opposite sides of the same dorsal horn generator, we introduced a new electrode montage referring a Cv6 neck electrode to an electrode at the center of the bit-mapped P13 field (above the hyoid bone and 3 cm contralateral to the anterior neck midline) so as to selectively enhance recording of this generator (figure 3-6) [18]. In neuro-monitoring this new montage will no doubt prove important for titrating spinal cord interneurons, [12].

The N24 nearfield to posterior tibial stimulation recorded at D12 is always larger than higher up along the spine and this is related to the existence of dual generators whereby the N21 dorsal column potential summates with a N24 dorsal horn potential. Recording from an esophageal probe inserted to the level of the D10 vertebra discloses a typical phase reversal of the dorsal N24 SEP response into a P24 potential prevertebrally (figure 3-3E-I) [17]. The P24-N24 is thought to reflect postsynaptic excitatory potentials in dorsal horn interneurons of the sacral spinal cord and is homologous to the N13-P13 of the median nerve neck SEP.

### **Lemniscal generator and scalp farfields**

The median SEP recorded from the scalp discloses a P14 far field that is recorded as far back as theinion, but not at posterior neck [14, 15]. P14 persists in patients with thalamic lesions. It is lost in patients with high spinal lesion [31]. It is thought to reflect the ascending volley in the medial lemniscus. The question whether subcomponents with distinct generators in brainstem can be identified in P14 is still pending. The homologous far field for posterior tibial SEP is P30 [17, 30]. This is usually preceded by a P26 far field that is concomitant with an upper dorsal N26 response.



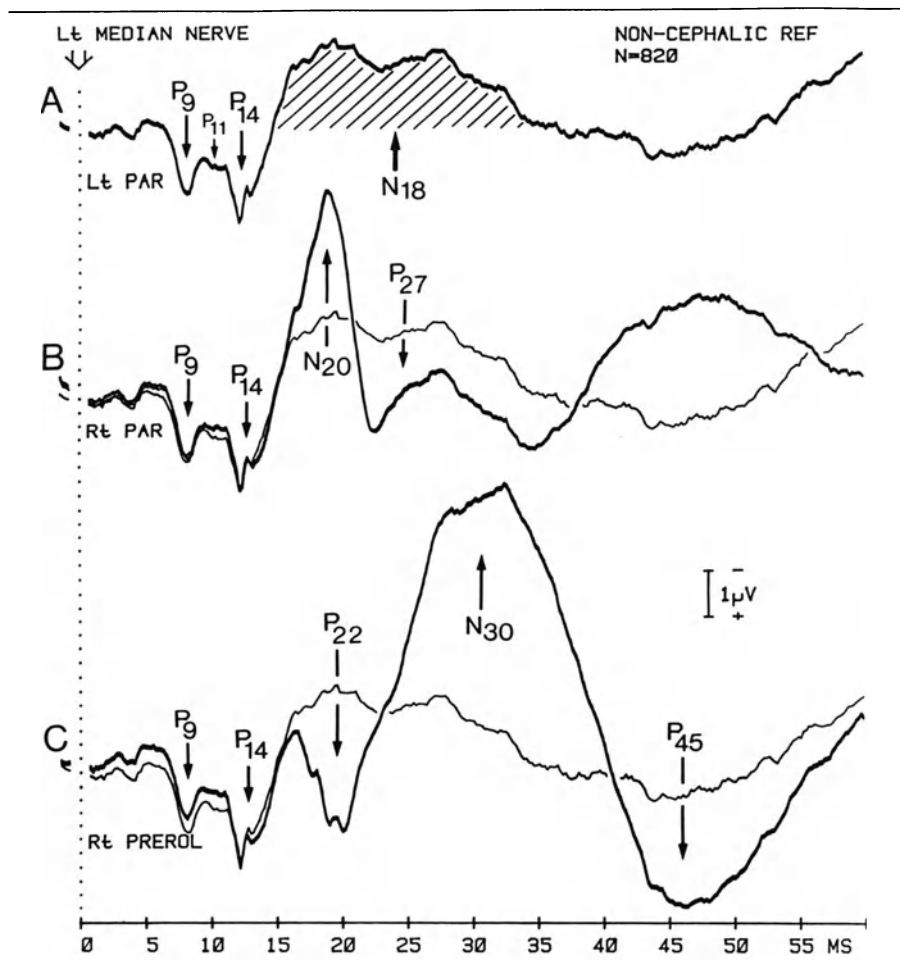
**Figure 3-6.** SEPs to stimulation of the left median nerve. A-B, recordings with noncephalic reference on right hand dorsum from the Cv7 spine (A) or from the skin at the level of the hyoid bone, 4 cm to the right of midline (B). C, montage referring the Cv7 spine to the anterior neck. Vertical interrupted line, N13-P13 onset. The -P9 in C results from subtraction of the larger anterior P9 from the smaller posterior P9 [18].

**Brainstem and cortical components**

When recording with noncephalic reference, two distinct negativities can be distinguished in the early scalp-recorded SEP response to median nerve stimulation, namely a widespread and prolonged N18 reflecting brainstem generator, and a focal N20 reflecting the early response of the contralateral parietal receiving cortex [16]. N18 appears virtually in isolation at the parietal scalp ipsilateral to the upper limb stimulated (figure 3-7A). At the contralateral parietal scalp, the N20 and P27 focal responses are seen to diverge from this N18 baseline (figure 3-7B).

At the contralateral frontal scalp, the P22 and N30 responses similarly diverge on the N18 baseline (figure 3-7C). N18 is reduced or absent when recording with an earlobe reference because the latter picks up much of the N18 activity itself [16]. The actual onset latency of the focal parietal N20 is an important SEP measure that is now taken as the point in time when the con-





**Figure 3-7.** Scalp-recorded SEP responses. Stimulation of the left median nerve at the wrist. Noncephalic reference on the dorsum of the right hand. Negativity of the active electrode registers upwards. A: at the left (ipsilateral) parietal scalp, the P<sub>9</sub>, P<sub>11</sub> and P<sub>14</sub> far fields are followed by the prolonged negativity of the N<sub>18</sub> brainstem response (hatched). This trace is superimposed (fine trace) on the contralateral responses recorded at the parietal (B) or frontal (C) scalp. There is a clear distinction between the prerolandic P<sub>22</sub>-N<sub>30</sub> and the postrolandic N<sub>20</sub>-P<sub>27</sub> SEP components which are seen to diverge from the N<sub>18</sub> baseline at these sites [12].

tralateral parietal trace diverges in the negative direction from the ipsilateral parietal trace (figure 3-7B). This corresponds to the time when contralateral parietal cortical generators start adding negativity upon the N<sub>18</sub> baseline. Detailed issues about the N<sub>20</sub> and P<sub>22</sub> respective generators and whether they are genuinely distinct are discussed elsewhere [13, 19].

N<sub>18</sub> must clearly be set apart from the positive far fields P<sub>9</sub>, P<sub>11</sub> and P<sub>14</sub> which have brief durations and reflect synchronized volleys of action poten-

tials conducted in bundles of nerve fibers. Bit-mapped imaging over the head discloses the blue sources of positivity of P9-P11-P14 with distinct and characteristic boundaries between inion and low neck, while N18 appears as a wide red sea of negativity all over the head (figure 3-5B). That N18 is actually generated subcortically is evidenced by patients with a unilateral thalamic lesion in whom stimulation on the affected side elicits bilateral N18 (mean total duration 19 msec), while all subsequent SEP components are lost [32]. Depth recordings also suggest that N18 is generated in brainstem nuclei [24].

Considering the profile and long duration of N18, we think that it reflects postsynaptic potentials in brainstem nuclei with open-field geometry that receive branches of the somatosensory lemniscal axons. Thus N18 emerges as a major SEP response that can be used for brainstem titration in diagnosis and neuromonitoring [12].

### Central somatosensory conduction

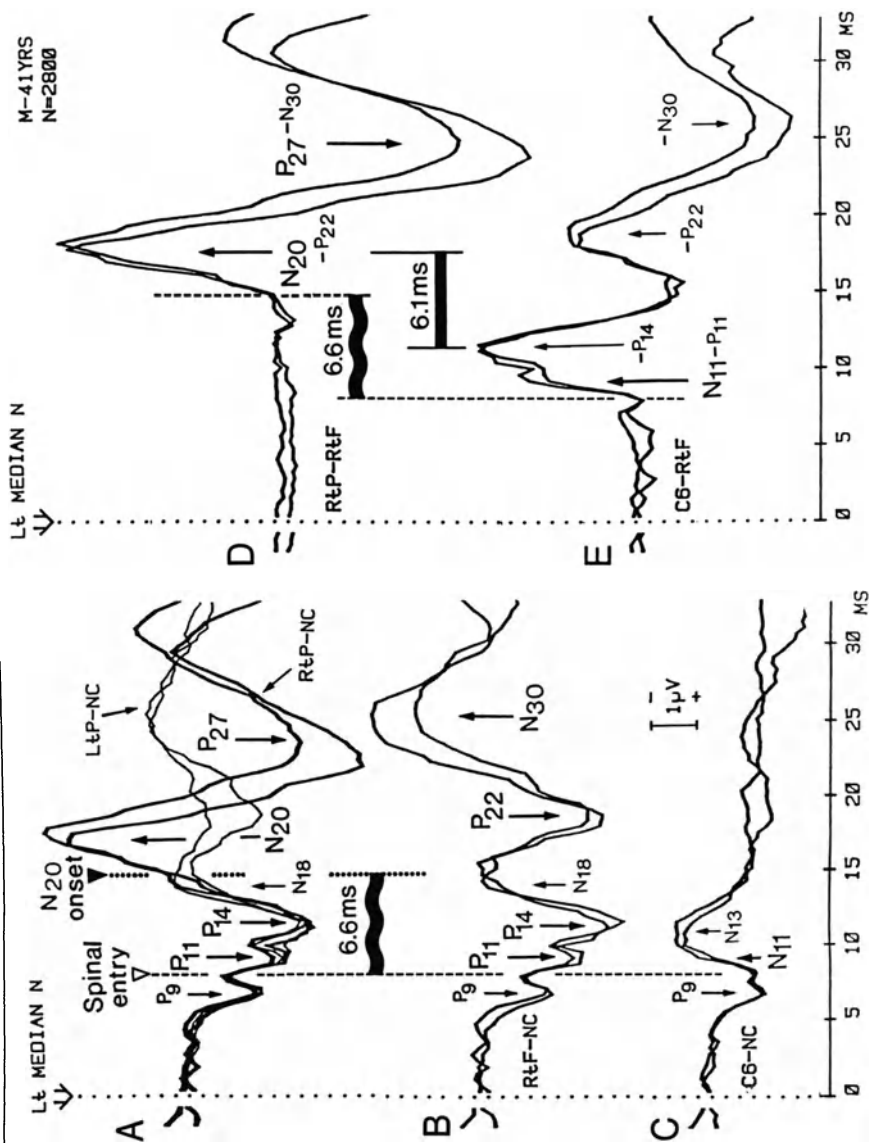
On the basis of the foregoing data, appropriate electrode montages can be selected for monitoring central somatosensory conduction [12]. Two measures are required for this to be done. The first is spinal entry time of the afferent volley which can be estimated from the onset of either the low-neck N11 near field response or the scalp P11 farfield (figure 3-8A-C). One difficulty with the latter measure is that, for unknown reasons, P11 fails to be clearly recorded in certain subjects. The N11 profile at low neck is faithfully recorded with a noncephalic reference (figure 3-8C) but it is distorted with a front scalp reference, namely by the addition of P14 far field and later brain components (figure 3-8E). It is true though that, with the latter montage, the P11 far field (recorded by the front reference) can be algebraically added to the N11 recorded by the neck electrode whereby the onset latency of the rising phase of N11 may be better defined. Thus, estimating the onset of the N11 rising limb in neck-to-front montages is considered a valid measure of spinal entry time [18].

The second measure required is time of arrival at cortex, best estimated at

---

**Figure 3-8.** Methods of estimation of the central conduction time. SEPs to stimulation of the left median nerve at the wrist. Two traces obtained in separate runs are superimposed to show consistency of responses. Negativity of the active electrode registers upwards. A-C: noncephalic reference recording from the contralateral parietal (A) or frontal (B) scalp, or from the lower posterior neck (C).

In A, the ipsilateral parietal response is superimposed (fine traces) to show the N18 baseline. The N20 onset (vertical dotted line) is taken as the point of divergence of the upgoing negativity at contralateral parietal scalp from the N18 seen at the ipsilateral parietal scalp. The spinal entry time is taken from the onset of the P11 scalp far field or the spinal N11 neck near field. D-E: same data presented with the front electrode (thus trace B) used as reference. This cancels most far field responses as well as the N18 while it distorts the waveforms by algebraic addition of the components recorded by the front reference. The central conduction time estimated from onset latencies is not distorted. However the transit between the peaks is more ambiguous and may be misleading [12].



the upward divergence of the parietal N20 from N18 baseline in a montage of the contralateral parietal scalp electrode and noncephalic reference (figures 3-7B 3-8A). It can also be estimated with a montage with the contralateral parietal electrode referred to the front (figure 3-8D), in which case the N18 is cancelled while the frontal P22 is subtracted from the parietal N20. While this definitely distorts the N20 profile, it should not alter its onset latency which gives a measure of the time of arrival at cortex.

These recommended measures [12] differ from what has been used in many estimates of central conduction, namely the time difference between the peak latencies of neck-to-front and parietal-to-front responses (figure 3-8D-E). The peak of the neck-to-front response does not relate to any spinal component, but to the peak of the P14 far field (recorded by the front reference) that is seen as a N14 after algebraic addition. This spurious N14 peak bears no relationship to the actual spinal entry time as it reflects activities in the medial lemniscus [14, 15].

On the other hand, the peak of the parietal-to-front response occurs later than the time of arrival of the afferent volley at the cortex and it misleadingly compounds interactions between the distinct N20 and P22 responses. One indeed has to call for a reassessment of what has in fact been measured with the difference in peak times of SEP profiles recorded with front reference because the latter is anything but neutral (figures 3-7C, 3-8B). The measured peak difference must reflect afferent conduction time between some level in upper medial lemniscus and some stage of intracortical activation in pericentral cortex [13]. It can be noticed that the values for central conduction time are shorter for the peak difference measure than for the onset difference measure (figure 3-8).

## REFERENCES

1. Anziska B and Cracco RQ: Short latency SEPs to median nerve stimulation: comparison of recording methods and origin of components. *Electroenceph Clin Neurophysiol* 52:531-539, 1981.
2. Beall JE, Applebaum AE, Foreman, RD and Willis WD: Spinal cord potentials evoked by cutaneous afferents in the monkey. *J Neurophysiol* 40:199-211, 1977.
3. Bromm B, Neitzel H, Tecklenburg A and Treede RD: Evoked cerebral potential correlates of C-fibre activity in man. *Neuroscience Lett* 43:109-114, 1983.
4. Burke D, Gandevia SC, McKeon B and Skuse NF: Interactions between cutaneous and muscle afferent projections to cerebral cortex in man. *Electroencephalogr Clin Neurophysiol* 53:349-360, 1982.
5. Celesia GG: Somatosensory evoked potentials recorded directly from the human thalamus and Sml cortical area. *Arch Neurol* 36:399-405, 1979.
6. Cohen L and Starr AD: About the origin of cerebral somatosensory potentials evoked by Achilles tendon taps in humans. *Electroencephalogr Clin Neurophysiol*, 62:108-116, 1985.
7. Creuzfeldt OD, Watanabe S and Lux HD: Relations between EEG phenomena and potentials in single cells. *Electroencephalogr Clin Neurophysiol* 20:1-18, 1969.
8. Desmedt JE: Somatosensory cerebral evoked potentials in man. In: A Rémond (ed) *Handbook of Electroencephalography and Clinical Neurophysiology*. Vol. 9. Elsevier, Amsterdam 55-82, 1971.
9. Desmedt JE: Some observations on the methodology of cerebral evoked potentials in man. In:

- JE Desmedt (ed) *Attention, Voluntary Contraction and Event-Related Cerebral Potentials*, Progr Clin Neurophysiol, Vol. 1, Karger, Basel 12–29, 1977.
10. Desmedt JE: Evoked potentials. In: PJ Dyck PK Thomas, EH Lambert and R Bunge (eds) *Peripheral Neuropathy*. Second edition. Chapter 46, Saunders, Philadelphia, 1045–1066, 1984a.
  11. Desmedt JE: Noninvasive analysis of the spinal cord generators activated by somatosensory input in man: near-field and far-field components. *Exper Brain Res suppl* 9:45–62, 1984.
  12. Desmedt JE: Critical neuromonitoring at spinal and brainstem levels by somatosensory evoked potentials (SEP), *CNS Trauma*, 2:169–186, 1985.
  13. Desmedt JE and Bourguet M: Color imaging of scalp topography of parietal and frontal components of somatosensory evoked potentials to stimulation of median or posterior tibial nerve in man. *Electroencephalogr Clin Neurophysiol* 62:1–17, 1986.
  14. Desmedt JE and Cheron C: Central somatosensory conduction in man: neural generators and interpeak latencies of the far-field components recorded from neck and right or left scalp and earlobes. *Electroencephalogr Clin Neurophysiol* 50:382–403, 1980.
  15. Desmedt JE and Cheron C: Prevertebral (oesophageal) recording of subcortical somatosensory evoked potentials in man: the spinal P13 component and the dual nature of the spinal generators. *Electroencephalogr Clin Neurophysiol* 52:257–275, 1981.
  16. Desmedt JE and Cheron C: Non-cephalic reference recording of early somatosensory potentials to finger stimulation in adult or aging man: differentiation of widespread N18 and contralateral N20 from the prerolandic P22 and N30 components. *Electroencephalogr Clin Neurophysiol* 52:553–570, 1981B.
  17. Desmedt JE and Cheron C: Spinal and far-field components of human somatosensory evoked potentials to posterior tibial nerve stimulation analysed with oesophageal derivations and non-cephalic reference recording. *Electroencephalogr Clin Neurophysiol* 56:635–651, 1983.
  18. Desmedt JE and Nguyen TH: Bit-mapped color imaging of the potential fields of propagated and segmental subcortical components of somatosensory evoked potentials in man. *Electroencephalogr Clin Neurophysiol* 58:481–497, 1984.
  19. Desmedt JE, Nguyen TH and Bourguet M: Bit-mapped color imaging of human evoked potentials with reference to the N20, P22, P27 and N30 somatosensory response. *Electroencephalogr Clin Neurophysiol* 68:1–19, 1987.
  20. Desmedt JE, Nguyen TH and Carmeliet J: Unexpected latency shifts of the stationary P9 somatosensory evoked potential far field with changes in shoulder position. *Electroencephalogr Clin Neurophysiol* 56:628–634, 1983.
  21. Domino EF, Matsuoka S, Waltz J and Cooper I: Simultaneous recordings from scalp and epidural somatosensory evoked response in man. *Science* 145:1199–1200, 1964.
  22. Donchin E, Callaway E, Cooper R, Desmedt JE, Goff WR, Hillyard SA and Sutton S: Publication criteria for studies of evoked potentials in man. In: JE Desmedt (ed) *Attention, Voluntary Contraction and Event-Related Cerebral Potentials*, Progr Clin Neurophysiol Vol. 1, Karger, Basel, 1–11, 1977.
  23. Eccles JC: Interpretation of action potentials evoked in the cerebral cortex. *Electroencephalogr Clin Neurophysiol*, 3:449–464, 1951.
  24. Hashimoto I: Somatosensory evoked potentials from the human brainstem: origins of short-latency potentials. *Electroencephalogr Clin Neurophysiol* 57:221–227, 1984.
  25. Humphrey DR: Re-analysis of the antidromic cortical response: contribution of cell discharge and PSPs to evoked potentials. *Electroencephalogr Clin Neurophysiol* 25:421–442, 1968.
  26. Jewett DL and Williston JS: Auditory evoked far-fields averaged from the scalp in humans. *Brain* 94:681–696, 1971.
  27. Kimura J, Mitsudome A, Beck Do, Yamada T and Dickins QS: Field distribution of antidromically activated digital nerve potentials: model for far-field recording. *Neurology* 33:1164–1169, 1983.
  28. Klee M and Rall W: Computed potentials of cortically arranged populations of neurons. *J Neurophysiol* 40:647–666, 1977.
  29. Lüders H, Lesser R, Hahn J, Little J and Klem C: Subcortical somatosensory evoked potentials to median nerve stimulation. *Brain* 106:341–372, 1983A.
  30. Lüders H, Dinner DS, Lesser RP and Klem G: Origin of far-field subcortical evoked potentials to posterior tibial nerve stimulation. *Arch Neurol* 40:93–97, 1983B.
  31. Mauguière F, Courjon J and Schott B: Dissociation of early SEP components in unilateral

- traumatic section of the low medulla. *Ann Neurol* 13:309–313, 1983.
32. Mauguière F, Desmedt JE and Courjon J: Neural generators of N18 and P14 far-field somatosensory evoked potentials: patients with lesion of thalamus or thalamo-cortical radiations. *Electroencephalogr Clin Neurophysiol* 56:283–292, 1983B.
  33. Towe AL: On the nature of the primary evoked response. *Exp Neurol* 15:113–139, 1966.
  34. Yamada T, Machida M and Kimura J: Far-field somatosensory evoked potentials after stimulation of the tibial nerve. *Neurology* 32:1151–1158, 1982.

---

#### **4. CRITICAL ANALYSIS OF PATTERN EVOKED POTENTIAL RECORDING TECHNIQUES**

IVAN BODIS-WOLLNER

In the last decade, it has become increasingly apparent that demyelination is not the only cause of an abnormal Visual Evoked Potential (VEP), but that among other things, pathology of the intraretinal optic nerve as in glaucoma (1), axonal neuropathy (2) and synaptic neurotransmitter deficiency (3) may cause delayed VEPs. Maculopathy also induces VEP delays, [4, 5, 6]. Several of these studies have shown that stimulus “details” such as element size, orientation and luminance, influence VEP diagnosis. From these and other unquoted studies, it is becoming evident that making that simple distinction between flash vs. pattern stimulation is not sufficient: one has to differentiate between one pattern and another. Selecting stimuli and appropriate analytical methods has become more important in clinical EP practice. In this chapter no attempt will be made to review all of the different EP techniques currently in use, but, rather advanced aspects of the foveal VEP will be discussed. The relevant physiology will be summarized. For addressing the foveal pathways, the pattern element size needs to be matched to the physiological constraints of foveal vision in humans. Several properties of human foveal vision are known from spatial contrast sensitivity (C.S.) measurements which will be described. Clinical studies which demonstrate the importance of selecting physiologically meaningful patterns for clinical VEP diagnosis will be summarized.

## **BASIC CONSIDERATIONS OF THE FUNCTIONAL ORGANIZATION OF THE VISUAL PATHWAY**

### **Receptive field of retinal ganglion cells: “center-surround” interaction**

Signals of a large number of photoreceptors are collected by bipolar neurons, which synapse on retinal ganglion cells. The ganglion cell axons, known as the optic nerve, synapse in the lateral geniculate nucleus and then reach the cortex via the optic tract. Horizontal cells, preceding the bipolar cell organization, collect or pool signals of more receptors than do bipolars. Several laterally connected horizontal cells may create even larger pools: their interconnections are under the modulating effect of neurotransmitters. Some neurotransmitters decrease the size of the pool, with the result that retinal neurons become more selective for pattern element size. Detailed neurophysiological functions have been shown in the turtle and carp for the neurotransmitters GABA and Dopamine [7, 8, 9]. Dopaminergic interplexiform cells [10] have been found in the human retina [11]. (These physiological data are relevant to VEP studies in Parkinson’s Disease [12]). Beyond the receptors, with each subsequent synaptic organization, progressive response compression occurs and the response is not just a simple increase as a function of stimulus area or luminance [13].

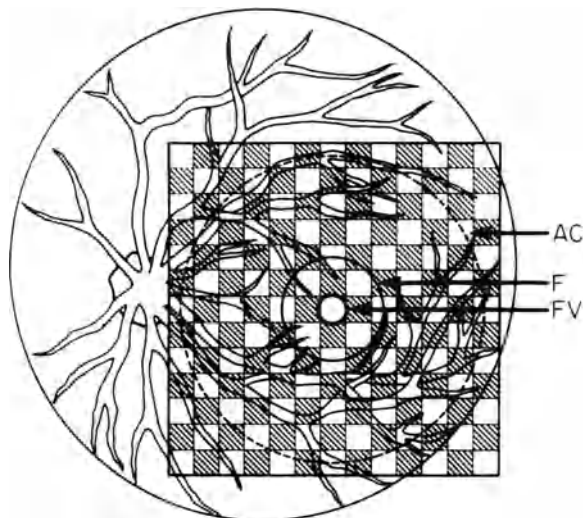
The concept of the receptive field of individual neurons [14] is crucial for appreciating why spatial contrast (i.e., pattern) is so important for VEP studies. Signals from photoreceptors of a portion of the illuminated retina converge into two separate pools of a single neuron. Because of the geometry of the receptive field, these pools are called the “center” and the “surround” [15, 16, 17]. The ganglion cell response, recorded from the appropriate single fiber of the optic nerve or tract, is a departure (a decrease or increase) from the mean firing rate (i.e., the neuronal response is a modulation around some steady level of number of spikes per unit time). When both center and surround are illuminated, the modulated response decreases compared to the illumination of the center alone. As a consequence of the antagonistic organization, the size of center relative to the surround establishes the spatial selectivity of individual neurons. For instance, if a neuron is stimulated with a small spot of light, the response of the neuron will first grow as the size of the spot is enlarged, and it will fall as soon as the spot becomes larger than the diameter of the receptive field center. This is due to surround antagonism. Due to the antagonistic organization of separate pools for center and surround portions of the receptive field of bipolar neurons and ganglion cells, the retinal output does not simply represent the total illumination of a retinal patch. Instead, the response of bipolar and ganglion cells is determined by spatial contrast, (i.e., a difference of illumination between neighboring retinal areas rather than by the sum of their separate illumination). The distinction between center and surround, and hence their interaction, is most evident in foveal ganglion cells. The more sharply defined is each mechanism, the more selective is each neuron for stimulus size. For instance, bipolar cells of the retina are less selective for



stimulus size than are ganglion cells, which in turn, are less selective than cortical neurons. Retinal and lateral geniculate neurons are radially symmetrical (i.e., show little or no orientation selectivity). A vertical or horizontal slit-like stimulus or grating pattern will be equally effective in the retina and LGN, unlike in the cortex [18].

### **Parallel pathways from retina to cortex**

Retinal ganglion cells mediating foveal vision may be broadly classified into two groups: a) so-called X; and b) so-called Y ganglion cells. The organization described above is strictly true for X ganglion cells. In Y ganglion cells, opposing forces of center and surround are never completely in balance. Nevertheless, center size of Y cells in respect to distance from the fovea follows the same rules as of X cells: it increases with distance. In Y ganglion cells, there is a particular subunit organization which contributes signals which cannot be cancelled; that is, it is not possible to bring center and surround responses into perfect functional opposition [19]. Y ganglion cells are sensitive to short lasting, small changes in illumination and to any spatial variation occurring in their receptive field. Any X and Y ganglion cell may overlap in the area of the retina sampled [17], but respond to different aspects of a complex stimulus. Studies by Shapley and his colleagues [19, 20] have established that an important quantitative difference between X and Y ganglion cells becomes evident when one considers the temporal relationship between the stimulus and the neuronal response. For instance, a spot which is modulated sinusoidally with some temporal frequency around some level of luminance in the center of the receptive field will induce a response which follows the frequency of the input signal. In Y cells, however, a distortion of the output will be noticeable. The simple distortion which characterizes Y ganglion cells in the frequency domain is frequency doubling (i.e., 4 Hz input yields both 4 and 8 Hz output). This is a nonlinear distortion, and it is characteristic of Y cells. Furthermore, Y cells (mostly large neurons) in the lateral geniculate nucleus are more sensitive to low contrast stimuli than are small cells [21]. In the LGN, as in the retina, individual ganglion cells differ in the size of their receptive fields (i.e., their spatial selectivity). In general, the closer a neuron is to the anatomical fovea, the smaller its receptive field. However, each region of the retina is subserved by a range of ganglion cells with different receptive field sizes. The population of parafoveally located ganglion cells has larger receptive field centers than the foveal population. From spatial contrast sensitivity studies in man and monkey and single cell studies in the monkey [22], it is estimated that the center size of human foveal ganglion cells is considerably smaller than  $14'$ . Based on an understanding of these physiological principles we can appreciate the importance of pattern element size of the VEP stimulus. By selecting the appropriate pattern element size, one can stimulate the fovea or predominantly peripheral retinal neurons.



ANATOMIST	CLINICIAN	
Area Centralis 6.0 mm (AC)	Posterior Pole	⊙
Fovea 1.5 mm (F)	Macula	○
Foveola .35 mm (FV)	Fovea	●

**Figure 4-1.** A schematic diagram of the human retinal surface. Superimposed is a checkerboard pattern with 50 ft. checks, drawn to scale, to illustrate its relationship to the fovea.

**The subdivision between foveal and extrafoveal processing**

Receptor density and the number of neurons per unit area of the visual field is largest in the foveal region. Roughly speaking, a circular central 1 degree of the visual field can be considered as the foveal window. This is used by most mammals for foveating (i.e., looking at targets to be scrutinized). Foveal magnification factor refers to the ratio of foveal versus eccentric receptor and neuronal density per unit area. Because of the anatomy and physiology of foveal cortical representations, much of the pattern VEP amplitude derives from stimulating the central 8 degrees [23]. The larger the pattern element size (in respect to foveal processing) the less reliable the VEP latency, given a foveal 2 degrees stimulus field. This odd result occurs because a 2 degree field, with large checks, is a very odd stimulus. With a customary 50' checksize stimulus, recommended for routine use by some authors, the fovea does not receive a real spatial contrast stimulus but predominantly a flickering 50' rectangle (figure 4-1). In addition, if the number of checks is odd, which is the case with 50' checks in a 2 degree foveal field (i.e., 2.4 checks per field), there is

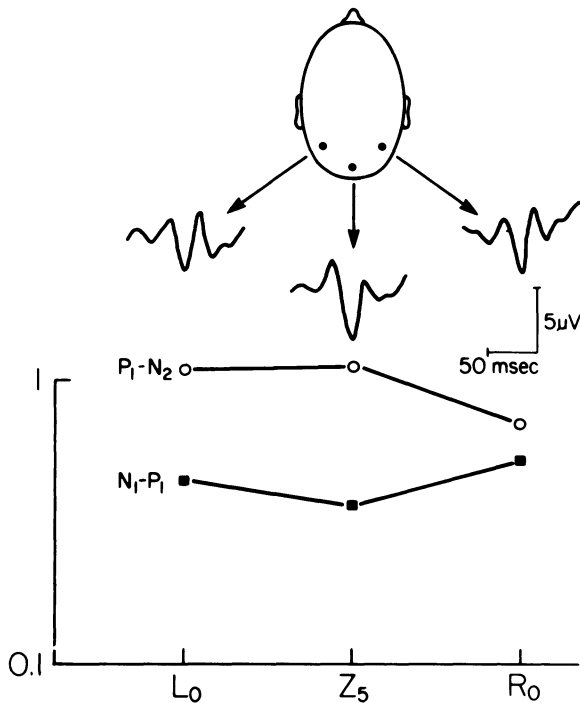
overall luminance flicker. With an odd number of checks, there is a basic asymmetry between the two pattern-shift positions. In one position, there are more bright, and in the other, there are more dark elements. These are important considerations. It is best to avoid the unknown, but most likely complex, effects of combined pattern and luminance stimulation of both the fovea and parafovea on the VEP.

### **Lateral electrodes reflect on foveal and parafoveal processing**

Blumhardt and his colleagues [24], and several other studies [25, 26, 27], suggest that laterally (more laterally than O<sub>1</sub> and O<sub>2</sub>) placed occipital electrodes are useful for diagnosing visual field defects. It was shown that an ipsilateral, paradoxical response to a large field stimulus in patients with hemianopic defects is consistent with the effects of half field stimulation in normals. Our studies [26], in hemianopic patients and patients with chiasmal syndromes showed a diagnostic yield similar to those reported by others. The surprising fact is that our stimulus is only 9 degrees in diameter (i.e., 4.5 degrees for each half field). Apparently, VEP diagnosis of visual field defects using 2.3 cycles per degree (cpd) gratings reflects the organization of the central 9 degree visual field. Recently, we studied the response to increasing spatial frequencies (finer and finer patterns) over midline and lateral occipital electrodes. Our data (figure 4-2) confirm a report by Skrandies [28] that the response to increasing spatial frequency does not fall off any more rapidly at the lateral electrodes than at the central electrode. Since the higher (6.0 cpd) spatial frequencies stimulate much less of the parafoveal than foveal organization, these data show that laterally placed electrodes record significant foveal responses. In view of this finding, it is unlikely that placement of the active electrode alone provides sufficient separation to study foveal and parafoveal cortical topography. Rather, precise stimulus size control as we described earlier and multiple referential or bipolar montages may need further attention.

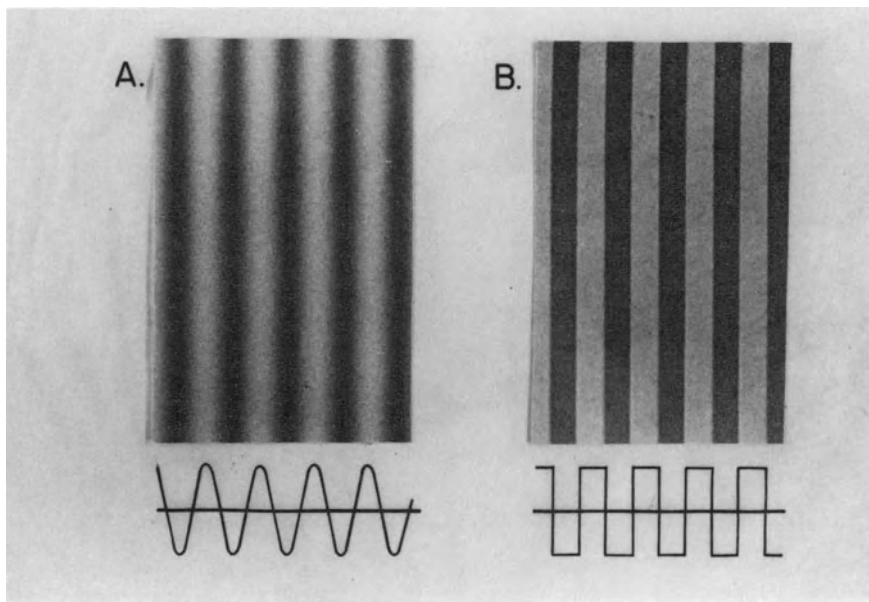
### **Spatial tuning in the human fovea**

The stimuli used in clinical contrast sensitivity [29, 30] and in our VEP studies consist of sinusoidal grating patterns [31, 32] (figure 4-3). Pattern element size in a grating pattern is specified by the variable, spatial frequency ( $f$ ), which is the number of bars subtended in an angle of one degree at the eye. The width ( $W$ ) of a bar, or rather band of a grating, can be calculated (in minutes of arc) by the formula  $w = 60/2f$ , where  $w$  is in minutes of arc and  $f$  is spatial frequency in cycles per degree (cpd). Conversely, the fundamental spatial frequency of a check pattern can be expressed as  $f = 60/1.4w$ , where  $f$  is measured in cpd and  $w$  is the width of the check in minutes of arc. A more accurate description of the relationship of sinusoidal gratings to checkerboard patterns will be detailed later. Contrast ( $C$ ) is the luminance difference of adjacent dark and bright



**Figure 4-2.** This figure illustrates that lateral occipital electrodes record significant foveal responses. The location of the electrodes is displayed in the upper part of the figure: they were placed at lateral left (L0), central (Z5) and lateral right (R0) occipital areas. They all were referred to 263 (63%) ofinion to nasion distance. For each electrode location, the averaged (based on 4 observations) VEP traces to transient modulation of a 6 cpd sinusoidal grating are shown. In the lower part, the graph represents, in a logarithmic scale, the amplitude ratios of the VEP to 1 cpd and to 6 cpd. Solid squares represent the amplitude ratios of N1P1 (measured as first negative to first positive wave) for L0, Z5 and R0. N1P1 amplitude is clearly larger using a 6 cpd than 1 cpd stimulus; for P1N2, the ratios are close to 1. The noteworthy feature of this figure is that nearly the same ratio is seen for all the three recording sites. Compare in figure 4-4 contrast sensitivity to 1 cpd and 6 cpd for foveal and parafoveal vision: higher selectivity to 6 cpd occurs only at the fovea, while for the parafovea the corresponding sensitivities are nearly equal. These data suggest that laterally placed electrodes record foveal responses as well as do central electrodes.

bands given a constant level of luminance where  $C = L_{max} - L_{min} / L_{max} + L_{min}$ . The mean luminance of the pattern should be the average uniform luminance of the patterned screen. Routinely, in our laboratory we use  $170 \text{ cd/m}^2$  as a mean luminance. Spatial contrast sensitivity is defined as the inverse of the minimum contrast which is needed for an observer to detect a given spatial frequency. The general shape of a normal contrast sensitivity curve varies as a function of mean luminance [33]. Several aspects of the contrast sensitivity function such as the cut-off frequency (which is another way to measure a visual acuity score), the spatial frequency at which peak sensitivity occurs, and the peak contrast sensitivity value depend on the average luminance.

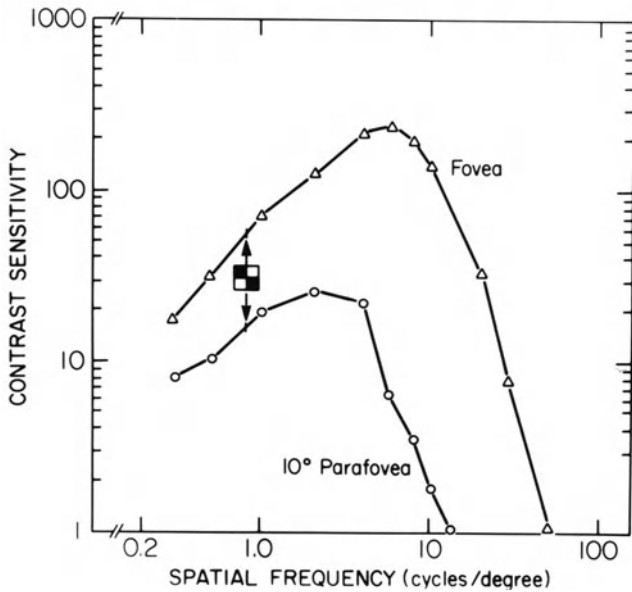


**Figure 4-3.** A: The luminance profile of sinusoidal grating pattern is a one dimensional sinusoid. Complex pattern such as checks can be synthesized from a series of sinusoidal gratings of different spatial frequency, contrast and orientation (see later figures). B: A square wave grating pattern. It contains the sinusoidal pattern, shown on the left (A) and higher spatial frequencies.

ance. However, in a wide photopic range between 6 cd/m<sup>2</sup> and 600 cd/m<sup>2</sup>, there is little change in contrast sensitivity. In this range normal human vision is most sensitive to pattern element sizes near 10'. Highest contrast sensitivity occurs at the fovea. The curve representing foveal vision has a broad peak (maximum sensitivity) around 5 cpd (figure 4-4). This corresponds to a check size having a diagonal of 12 minutes of arc. Figure 4-5 demonstrates the mismatch which occurs when one tries to stimulate the fovea with 50 ft. checks, (i.e., 0.83 cpd). Properly conducted VEP studies show that VEP amplitude in adults is largest to pattern elements sizes somewhere between 10' and 15' of arc [34] and to a spatial frequency near 5 cpd [28, 35, 36, 37].

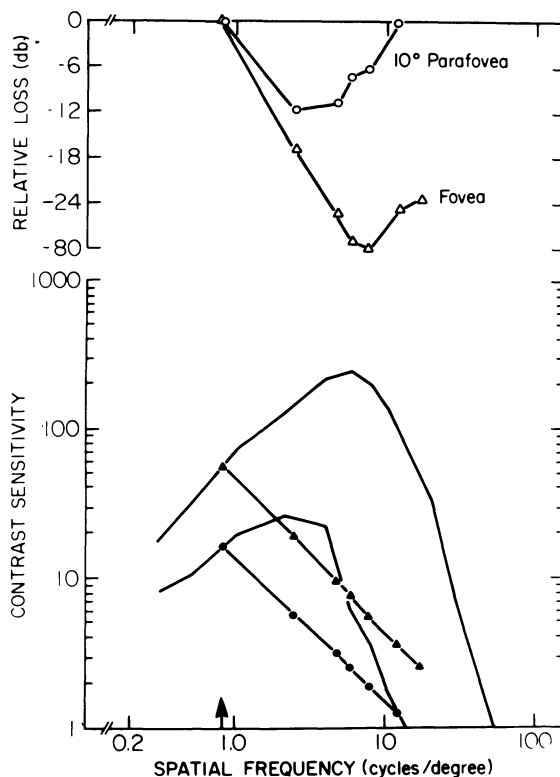
#### **Checkerboard patterns versus sinusoidal gratings**

In terms of Fourier analysis, a pattern with a one-dimensional sinusoidal luminance profile is the simplest visual pattern. By this analysis, any two-dimensional visual pattern can be decomposed into a series of sine waves. A checkerboard could be synthesized from sinusoidal gratings by properly arranging a range of sinusoidal gratings of specific spatial frequencies and orientations whose contrasts (amplitudes) show a regular, fixed sequence.



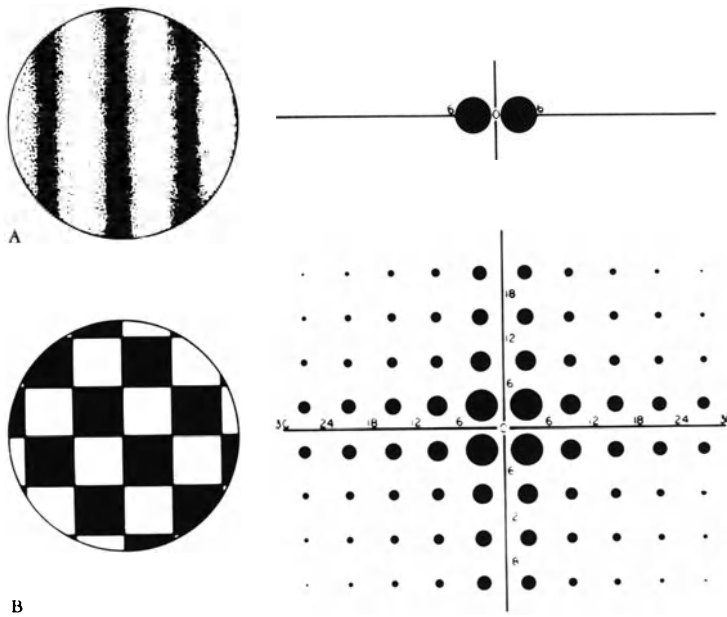
**Figure 4-4.** The contrast sensitivity (CS) curves are shown: one for foveal (triangles), and one for the parafoveal region at 10 deg eccentricity (circles). Note that the parafoveal CS curve is shifted down and to the left compared to the foveal curve. The maximum sensitivity for the fovea is around 5 cpd, and for the parafovea is around 2 cpd. Therefore, the best stimulus for the fovea and parafovea are element sizes of 8 and 21 min of arc (corresponding to 5 and 2 cpd). The checkerboard symbol represents the commonly used clinical checkboard stimulus with a pattern element of 50 ft. checks corresponding to the fundamental spatial frequency of .85 cpd. See text for comparing check and grating spatial frequencies.

Their ratios are constant and their absolute magnitudes depend on the magnitude of the fundamental component. Figure 4-6A illustrates a vertical sine wave grating on the left; to the right, its amplitude spectrum. Notice that all the amplitude is in one spatial frequency and one orientation. This is the simplest spectrum possible for a two-dimensional pattern. The diagram below, in figure 4-6B, represents the amplitude spectrum of a checkerboard pattern with its edges aligned normally (horizontal and vertical). The fundamental spatial frequency of this checkerboard pattern is represented by the largest dot on the amplitude spectrum and it is located at the 45 degree diagonal. Smaller and smaller dots represent the decreasing contribution of higher spatial frequencies to the checkerboard pattern. From the spectrum illustrated in figure 4-6, it is evident that the major power of a checkerboard pattern is concentrated at 45 degrees and at 135 degrees, with power dropping to zero as one moves toward 0 degrees or 90 degrees. A checkerboard with its edges aligned along the major axes has neither vertical nor horizontal components [38]. Consideration of the power spectrum analysis of checkerboard patterns



**Figure 4-5.** The relationship of a 50 min of arc stimulus to foveal and parafoveal contrast sensitivities. The foveal and the parafoveal contrast sensitivity (CS) curves are displayed in the lower part of the illustration (see figure 4-4). The significant spatial frequency components of a 50 min of arc checkerboard are presented in scale to the foveal (solid triangles) and parafoveal (solid circles) CS curves. 50 min of arc corresponds to a fundamental spatial frequency of .85 cpd. The other components of this pattern are odd harmonics, i.e. third (2.5 cpd), fifth (4.2 cpd), seventh (5.9 cpd), which have respectively 1/3, 1/5 and 1/7 of the energy of the fundamental component. In the upper part, the loss of contrast (in dB), for components of a 50 min of arc stimulus, is shown relative to foveal (open triangles) and for parafoveal (open circles) CS. The loss for the peak of the foveal and parafoveal curves is evident. Thus, this stimulus size is not optimal for the fovea or 10 degree parafoveally, but as can be seen is better suited for parafoveal sensitivity than for foveal vision. This graph presents all components of a check pattern without regard to their relative orientation.

reveals two simple but clinically relevant facts. One is that when the edges of a checkerboard are aligned vertically and horizontally, all the power is concentrated in oblique orientations. The other is that in order to equate the fundamental spatial frequency of the check pattern with that of a grating, the appropriate measure to use is the grating cycle length, which equals the check diagonal.



**Figure 4-6.** A: A sinusoidal grating pattern. B: a checkerboard pattern, with the Fourier spectrum of each. The numbers indicate spatial frequency and the radial dimensions, the orientation of the spatial frequency components of each pattern. Note that the sinusoidal grating contains energy only at the fundamental frequency (3 cycles per degree), while the checkerboard contains energy at a number of frequencies. The relative contribution of each harmonic to the total amplitude of the pattern is indicated by the size of the dot at each spatial frequency. The orientation of the sinusoidal components of the check pattern is all oblique, with no energy at either the vertical or the horizontal meridian.

## MANIPULATION OF STIMULUS PARAMETERS IN CLINICAL PRACTICE

### Spatial frequency and check size

Gambi et al. [39] recorded VEPs of multiple sclerosis patients to checkerboard patterns of different check sizes. Abnormalities of the VEP occurred most often with a check size of 40 minutes (which corresponds to 1.06 cpd). These authors were able to increase their diagnostic yield in all categories of MS by exploring more than one spatial frequency. Neima and Regan [40] also reported that some MS patients may show a normal response to one while an abnormal response to another size of the pattern. Hennerici et al. [41], originally reported that a small foveal rectangular stimulus provides the best diagnostic yield in MS. The stimulus is, however, not a true spatial contrast pattern for the fovea. Nevertheless, at this point, these and other data suggest that one cannot predict which stimulus is optimal for detecting VEP abnormalities in MS. On the other hand, in Parkinson's disease, it is crucial to select a



medium spatial frequency for demonstrating VEP abnormalities; an abnormality becomes evident only to patterns above 2 cpd [42, 43, 44].

Abnormal VEP latency to smaller than 28 ft. checks is not diagnostic, but it is consistent with early macular pathology [45]. In maculopathy, even when visual acuity is relatively intact (20/30), a VEP loss may become evident with a stimulus of 14 ft. or smaller (i.e., nearer to the spatial frequency peak), and a VEP abnormality may not be apparent to 50 ft. checks.

### **Stimulus orientation**

Camisa, Mylin and Bodis-Wollner [3] reported that while the specific orientation of a grating stimulus did not appreciably influence VEP latency of control observers, over half of MS patients exhibited orientation-dependent delays of the VEP. Thus, the diagnostic yield is higher if one employs more than one stimulus orientation. An orientation dependent VEP change suggests cortical rather than retinal pathology. In patients with maculopathy, an abnormal VEP does not depend on pattern orientation [4]. Orientation-specific effects in MS have been originally demonstrated with psychophysical determination of contrast sensitivity as a function of grating orientation. Orientation-specific losses were commonly observed at medium spatial frequencies [46]. Kuper-smith and his colleagues [47] estimated contrast sensitivity functions based on VEP amplitude for 15 MS patients. Four different orientations (0, 45, 90 and 135 degrees) and three spatial frequencies (low, medium and high) were explored. On the whole, more orientation-specific rather than spatial frequency-specific VEP abnormalities exist in MS; moreover, orientation and spatial frequency abnormalities do not covary (i.e., they can be independently abnormal in different MS patients). It is a well established fact that orientation selectivity occurs for only cortical neurons and not for or LGN cells in primate [18]. The explanation as to why orientation selective processes are affected by the demyelinating process, is possibly related to intracortical organization of myelinated axonal branches between orientation columns [48]. In patients with maculopathy an abnormal VEP does not depend on pattern orientation [4, 68].

### **Contrast**

Typically, VEP testing is performed at high levels of contrast. In some MS patients, whose visual acuity is within the normal range, psychophysical techniques reveal an elevated contrast threshold even when the VEP is classified as normal [49]. Several studies [50, 51] suggest that low contrast VEPs are diagnostically useful in MS, presumably by revealing early foveal defects. Low versus high contrast VEPs probably represent the response of different groups of neurons [52]. Single cell data suggest that low contrast stimuli trigger responses from the population of those neurons that provide the input to the magnocellular layer of the LGN (21).

### **Transient Versus Steady-State Stimulation**

VEP latency is measured on traces which represent signals arising from stimulation rates below 3.5 Hz (so-called transient VEPs). Amplitude and phase measurements are performed using Fourier analysis on VEPs arising from sinusoidal temporal modulation rates above 3.5 Hz (so called steady-state VEPs). With rates above 4 Hz the response is quasi-sinusoidal. There are two common errors in measuring steady-state signals. Because the response is only quasi-sinusoidal (i.e., it contains several harmonically related frequencies), it can be misleading to measure peak-to-through amplitudes. Secondly, the timing of the response should not be measured on raw traces from trigger to peak as time. Properly, the phase of each frequency response needs to be established, and delay measured from the slope of the phase plot [53]. Amplitude and phase measurements are objective when Fourier analysis [54] or a tuned lock-in amplifier [53] is used. The average VEP can be subjected to Fourier analysis with appropriate care (sufficient number of cycles) to avoid aliasing. Also, with sufficient computer memory, the EEG can be subjected to Fourier analysis. Transient and steady-state VEPs do not always provide the same information. One unestablished but likely reason may be that transient VEPs induce strong neuronal non-linearities, due to the sudden stimulus change.

### **Glaucoma: A clinical example of the importance of steady-state analysis and spatial contrast**

Glaucoma, a pathology of retinal ganglion cells, may subject certain sizes of ganglion cells to damage at its earliest stages, while other sizes are left intact. Early glaucoma and ocular hypertension predominantly affects central vision in a manner consistent with the notion that large ganglion cells may be vulnerable. In general, it is assumed that Y ganglion cells, which have larger cell bodies, also have larger receptive fields than X ganglion cells. Synaptic transmission, conduction velocity and axoplasmic flow are, on the average, different for X and Y cells; Y cells are slightly faster than X cells. In glaucoma and ocular hypertension, degraded vision is characterized by a spatial contrast sensitivity loss which is most evident to low spatial frequencies (including homogenous field targets) flickering at fast rates [55, 56]. Some findings are consistent with our proposition that glaucoma (at least in its initial stages) may predominantly affect large ganglion cells of the retina. For diagnostic applications of the VEP in glaucoma, steady-state stimulation is most useful. VEP and PERG studies [57, 58, 59, 60] agree that low (1–2 cpd) targets modulated above 5 Hz are the most useful for glaucoma diagnosis. This stimulus dependence is understandable in view of recent anatomical data. Quigley and Hendrickson [61] studied retinal and LGN properties following laser induced glaucoma in the monkey. They demonstrated morphological evidence of a selective magnocellular loss in this glaucoma model. In the primate, some

large X cells, in addition to Y cells, synapse in the magnocellular layer. Thus, one might conclude that in glaucoma, while there must be both X and Y cell loss, the damage is to large cells. Pattern evoked retinal responses (PERGs) are obtained with direct ocular recordings in the glaucomatous monkey eye [1]. These studies demonstrate retinal defects to low spatial frequencies, providing functional evidence for the selectivity of the glaucomatous process. It was suggested by several pathophysiological studies, starting with the seminal work of Maffei and his colleagues [62], that PERG is dominated by the retinal ganglion cell response (i.e., the intraretinal activity which generates optic nerve impulses) [63, 64]. A study by Bobak et al. [58] suggests that in some eyes with glaucoma the VEP has the higher signal to noise ratio and higher diagnostic yield than the PERG—even though they were simultaneously obtained. This result argues for a possible qualitative difference between PERG and VEP, and may imply a filtering function interposed between retina and cortex. The neuronal organization which may underlie this function is unknown. Although there is increasing popularity of pattern ERG recordings (PERG), the clinical value of simultaneous PERG and VEP has yet to be established.

A major difference between the magno and parvocellular populations is their different contrast sensitivity. Contrast segregation may be reflected in the normal VEP: the amplitude functions of the steady-state plateaus around 10–14% contrast, then grows again [52]. However, at present, there are no published studies in glaucoma addressing, either linear versus non-linear retinal ERG response properties, nor contrast dependent abnormalities of the VEP.

## **METHODOLOGICAL CONSIDERATIONS OF OBTAINING THE FOVEAL VEP**

### **The stimulus**

To obtain a foveal VEP, the stimulus field does not need to be restricted: however, as has been mentioned earlier, pattern element size is crucial since pattern elements coarser than 14' are more efficient to stimulate parafoveal rather than foveal neurons. Figures 4-4 and 4-5 provide useful information to select pattern element size for a particular diagnostic problem. Our method of foveal stimulation differs from other proposed techniques, such as stimulating with a small foveal rectangle [41] or providing a small central stimulus area [65]. We recommend using a large screen cathode ray tube (CRT) display which subtends 9 degrees of visual angle from a 1.44 meter viewing distance. This longer distance is needed to minimize accommodation errors by the patient. An appropriate CRT provides high luminance, high pattern contrast and superior resolution so that medium (2–10 cpd) spatial frequencies can be generated without loss of contrast. The frame rate of the CRT is either 100 or 200 per second. This ensures 10 or 5 msec (200 ps frame rate) reversal time across the screen. The orientation of the pattern can be continuously varied with a CRT,

as opposed to TV or projection screen. CRT picture presentation is based on X/Y rasters. One other problem with the slow interlaced TV raster presentation of patterns [66] is flicker. Therefore, if a large CRT is not available, oscillating mirror projection is still preferable to most TV screens. One problem with any screen is that luminance asymmetry at the edges of the display (so-called edge flicker) becomes very noticeable once the pattern element size becomes large, thus flicker contaminates the pattern VEP. Flicker is a problem in reference to clinical diagnosis. For instance, we, as well as others, have shown that flicker responses may be normal while pattern responses are abnormal. A continuously illuminated surround is needed to minimize edge flicker.

### **Calibrations: Flicker and contrast**

As mentioned in various places earlier on, flicker is an unwanted concomitant when pattern VEP diagnosis is pursued. One of the simplest ways to check for flicker is to put a diffusing screen in front of the modulated pattern display and watch. If nothing else is available, even a few pages of a newspaper will do as a diffusing screen. The eye is a very good judge for flicker.

A more precise calibration is needed for luminance gradients across the screen. A photocell, with an aperture small enough, should be positioned in front of a pattern element, and then the pattern shifted or modulated. The maximum and minimum photocell output can be measured in any arbitrary unit and contrast calculated according to the formula  $C = \frac{L_{max} - L_{min}}{L_{max} + L_{min}}$ . (In this case, L can stand for any unit of measure).

### **Accommodation, acuity and adaptation**

Visual acuity should be checked prior to EP testing. Appropriate refraction is mandatory. If the patient did not bring glasses, one should provide a trial frame with appropriate corrective lenses. Very precise correction is hardly needed: A range of  $\pm$  diopter best correction will be sufficient. It is also easy to test for astigmatism, and the patient should be both questioned and tested for its presence in particular if orientation dependent VEPs are desired for differential diagnosis of maculopathy and neuropathy.

Pupil size should be estimated. If the results indicate, the monocular test should be repeated with an artificial pupil. This is particularly important for foveal VEPs.

Covering the non tested eye with a patch which blurs spatial detail but keeps the nontested eye in a light adapted condition is preferable. The room should be moderately lighted to avoid luminance transients when the patient looks around the room.

### **FUTURE DIRECTIONS**

From this short review chapter, it should be apparent that there is more to the VEP than the latency of the major positive wave. In the past, it has been

assumed that the N70 is unreliable (i.e., has large inter-observer variability). This may be a somewhat premature conclusion; probably true when the pattern element size is coarse. Pattern ERG is not yet perfected to be a routine clinical tool. Steady-state analysis has not yet developed into a diagnostic tool of clinical VEP practice. However, some novel methods, tapping non-linear components of the steady-state VEP, have been used with promise in evaluating the site of VEP abnormality as in Parkinson's disease [67].

## SUMMARY

The purpose of this chapter has been to distinguish stimulus parameters related to the physiological properties of the visual system, and which are important in differential diagnostic applications of VEPs. There are many ways to manipulate stimuli. Haphazardly varying parameters will only lead to greater complexity of interpretation without pathophysiological insights. The clinical evidence suggests that foveal VEPs provide a more specific tool in clinical electrophysiology than large field coarse patterns. The importance of pattern orientation in distinguishing retinal from demyelinating retrobulbar pathology is considered. Furthermore, it is discussed that spatial frequency needs to be low and temporal frequency high in the diagnosis of glaucomatous optic nerve. A more widespread awareness and consequent use of stimulus control in clinical VEP studies is recommended.

## REFERENCES

1. Marx MS, Bodis-Wollner I, Teitelbaum CS, Podos SM: The pattern ERG and VEP in glaucomatous optic nerve disease in the monkey and human. In: Evoked Potentials, eds RQ Cracco and I Bodis-Wollner, Alan R, Liss, New York, in press.
2. Kriss A, Carrol WM, Blumhardt LD, Halliday AM: Pattern and flash evoked potential changes in toxic (nutritional) optic neuropathy. In: J Courjon, F Mauguière and M Revol (eds) Clinical Applications of Evoked Potentials in Neurology. Raven Press, New York pp. 11–19, 1982.
3. Bodis-Wollner I, Yahr MD: Measurement of Visual Evoked Potentials in Parkinson's Disease. *Brain* 101:661–671, 1978.
4. Bodis-Wollner I, Feldman R: Old perimacular pathology causes VEP delays in man. *Electroencephalogr Clin Neurophysiol* 53:38p–39p, 1982.
5. Lennerstrand G: Delayed Visual Evoked Cortical Potentials in retinal disease. *Acta Ophthalmologica* 60:497–504, 1982.
6. Papakostopoulos D, Hart CD, Cooper R, Natsikos V: Combined electrophysiological assessment of the visual system in central serious retinopathy. *Electroencephalogr Clin Neurophysiol* 59:77–80, 1984.
7. Cohen JL, Dowling JE: The role of the retinal interplexiform cell: Effects of 6-hydroxydopamine on the spatial properties of carp horizontal cells. *Brain Res* 264:307–310, 1983.
8. Piccolino M, Neyton J, Gerschenfeld HM: Decrease of gap junction permeability induced by dopamine and cyclic AMP in horizontal cells of turtle retina. *J Neurosci* 4:2477–2488, 1984.
9. Teranishi T, Negishi K, Kato S: Regulatory effect of dopamine on spatial properties of horizontal cells in carp retina. *J Neurosci* 4:1271–1280, 1984.
10. Dowling JE, Ehinger B, Hedden WL: The interplexiform cell: A new type of retinal neuron. *Invest Ophthalmol Vis Sci* 15:916–926, 1976.
11. Frederick DW, Rayborn F, Laties A, Lam D, Hollyfield C: Dopamine containing neurons in the human retina *J Comp Neurol* 210:65–79, 1982.
12. Bodis-Wollner I, Yahr MD, Mylin L and Thornton J: Dopaminergic deficiency and delayed visual evoked potentials in humans. *Ann Neurol* 11:478–483, 1982.

13. Werblin FS and Dowling JE: Organization of the retina of the mudpuppy *Necturus Maculosus* II. Intracellular recording. *J Neurophysiol* 32:339–354, 1969.
14. Fischer B: Overlap of receptive field centers and representation of the visual field in the cat's optic tract. *Vision Res* 13:2113–2120, 1973.
15. Kuffler SW: Discharge pattern and functional organization of the mammalian retina. *J Neurophysiol* 16:37–68, 1953.
16. Rodieck RW, Stone J: Analysis of receptive fields of cat retinal ganglion cells. *J Neurophysiol* 28:833–849, 1965.
17. Enroth-Cugell C, Robson JG: The contrast sensitivity of retinal ganglion cells of the cat. *J Physiol* 187:517–552, 1966.
18. Hubel DH, Wiesel TN: Receptive fields and functional architecture of monkey striate cortex. *J Physiol* 195:215–243, 1968.
19. Hochstein S, Shapley RM: Quantitative analysis of retinal ganglion cell classification. *J Physiol* 262:237–264, 1976.
20. Victor JD, Shapley RM: The nonlinear pathway of Y ganglion cells in the cat retina. *J Gen Physiol* 74:671–789, 1979.
21. Kaplan E, Shapley RM: X- and Y- cells in the lateral geniculate nucleus of macaque monkeys. *J Physiol* 330:125–143, 1982.
22. Foster KH, Gaska OP, Nagler M and Pollen DA: Spatial and temporal frequency selectivity of neurons in visual cortical areas V1 and V2 of the macaque monkey. *J Physiol* 365: 331–363, 1985.
23. Yiannikas C, and Walsh DC: The variation of the pattern shift visual evoked response with the size of the stimulus field. *Electroencephalogr and Clin Neurophysiol* 55:427–435, 1983.
24. Blumhardt LD, Barrett G, Halliday AM, Kriss A: The asymmetrical visual evoked potential to pattern reversal in one half field and its significance for the analysis of visual field defects. *Br J Ophthalmol* 61:454–461, 1977.
25. Celesia GG, Meredith JT, Pluff, K: Perimetry, visual evoked potentials and visual spectrum array in homonymous hemianopsia. *Electroencephalogr Clin Neurophysiol* 56:16–30, 1983.
26. Onofrj M, Bodis-Wollner I, Mylin LH: Visual evoked potential diagnosis of field defects in patients with chiasmatic and retrochiasmatic lesions. *J Neurol Neurosurg Psychiatry* 45: 294–302, 1982.
27. Rowe M J III: The clinical utility of half field pattern reversal visual evoked potential testing. *Electroencephalogr Clin Neurophysiol* 53:73–77, 1982.
28. Skrandies W: Scalp potential fields evoked by grating stimuli: effect of spatial frequency and orientation. *Electroencephalogr Clin Neurophysiol* 58:325–332, 1984.
29. Bodis-Wollner I, Diamond S: The measurement of spatial contrast sensitivity in cases of blurred vision associated with cerebral lesions. *Brain* 99:695–710, 1976.
30. Bodis-Wollner I: Methodological aspects of contrast sensitivity measurements in the diagnosis of optic neuropathy and maculopathy. In: *Fifth International Visual Field Symposium* ed EL Greve and A Heijl. The Hague: Dr. W. Junk Publishers, pp. 225–237, 1983.
31. Campbell FW, Green DC: Optical and retinal factors affecting visual resolution. *J Physiol* 181:576–593, 1965.
32. Campbell FW, Gubisch RW: Optical quality of the human eye. *J Physiol* 186:558–578, 1966.
33. Van Ness FL, Bauman MA: Spatial modulation transfer in the human eye. *J Opt Soc Am* 47:401–406, 1967.
34. Spekreijse H: Maturation of contrast EP-s and development of visual resolution. *Arch Ital Biol* 116:358–369, 1978.
35. Jones R, Keck MI: Visual evoked response as a function of grating spatial frequency. *Invest Ophthalmol Vis Sci* 17:652–659, 1978.
36. Parker DM, Salzen EA: Latency changes in the human visual evoked responses to sinusoidal gratings. *Vis Res* 17:1201–1204, 1977.
37. Plant GT, Zimmern RT, Durdan K: Transient visual evoked potentials to the pattern reversal and onset of sinusoidal gratings. *Electroencephalogr Clin Neurophys* 56:147–158, 1983.
38. Camisa J, Mylin L, Bodis-Wollner I: The effect of stimulus orientation on the visual evoked potential in Multiple Sclerosis. *Ann Neurol* 10:532–539, 1981.
39. Gambi D, Rossini PM, Onofrj M, Marchionno L: Visual Evoked Cortical Potentials (VECP) by television presentation of different patterned stimuli to patients with Multiple Sclerosis. *Ital J Neurol Sci* 2:101–106, 1980.

40. Neima D, Regan D: Pattern visual evoked potentials and spatial vision in retrobulbar neuritis and multiple sclerosis. *Arch Neurol* 41:198–201, 1984.
41. Hennerici M, Wenzel D, Freund HJ: The comparison of small-size rectangle and checkerboard stimulation for the evaluation of delayed visual evoked responses in patients suspected of Multiple Sclerosis. *Brain* 100:119–136, 1977.
42. Onofrij M, Ghilardi MF, Basciani M, Gambi D: Visual Evoked Potentials in Parkinsonism and dopamine blockade reveal a stimulus-dependent dopamine function in humans. *J Neurol Neurosurg Psychiatry* 49:1150–1159, 1986.
43. Tartaglione A, Pizio N, Bino G, Spadavecchia L, Favale E: VEP changes in Parkinson's Disease are stimulus specific. *J Neurol Neurosurg Psychiatry* 47:305–307, 1984.
44. Tartaglione A, Pizio N, Bino G, Spadavecchia L, Favale E: Spatial properties of patterns as determinants of visual evoked potential changes in Parkinson's syndrome. M: "Evoked Potentials" Eds. Morocutti C and Rizzo PA, Elsevier, Amsterdam p. 321–328, 1985.
45. Bass SJ, Sherman J, Bodis-Wollner I and Nath S: Visual evoked potentials in macular disease. *Invest Ophthalmol Vis Sci* 26:1071–1074, 1985.
46. Regan D, Whitlock JA, Murray TJ, Beverly KI: Orientation-specific losses of contrast sensitivity in multiple sclerosis. *Invest Ophthalmol Vis Sci* 19:324–328, 1980.
47. Kupersmith MJ, Seiple WH, Nelson JI, Carr RE: Contrast sensitivity loss in multiple sclerosis: selectivity lay eye, orientation and spectral frequency measured with the evoked potential. *Invest Ophthalmol Vis Sci Suppl* 25:632–639, 1984.
48. Gilbert CD, Wiesel TN: Clustered intrinsic connections in cat visual cortex. *J Neuroscience* 3:1116–1133, 1983.
49. Regan D: Visual evoked potentials and visual perception in Multiple Sclerosis. *Proceedings of the San Diego Biomedical Symposium* 16:87–95, 1977.
50. Siegel I, Kupersmith MJ: Electrophysiological evaluation of visual loss in ophthalmology, In: *Evoked Potentials*, eds RQ Cracco and I Bodis-Wollner, Alan R, Liss, New York, chapter 29, p. 333–342, 1986.
51. Robinson NL, Robinson PM, Bayliss SG and Powell R: Contrast sensitive changes in visual evoked potentials. In "Evoked Potentials" eds Morocutti C and Rizzo P. Elsevier, Amsterdam p 267–272, 1985.
52. Bobak P, Bodis-Wollner I, Harnois C: VEPs in humans reveal high and low spatial contrast mechanisms. *Invest Ophthalmol Vis Sci* 25:104–107, 1984.
53. Regan D: *Evoked Potentials in Psychology, Sensory Physiology and Clinical Medicine*, London: Chapman and Hall, 1972.
54. Bodis-Wollner I, Harnois C, Bobak P, Mylin LH: On the possible role of temporal delays of afferent processing in Parkinson's Disease, *J Neural Transmission, Suppl* 19:243–252, 1983.
55. Atkin A, Bodis-Wollner I, Wolkstein M, Moss A, Podos S: Abnormalities of central contrast sensitivity in glaucoma. *Am J Ophthalmol* 88:205–211, 1979.
56. Atkin A, Wolkstein M, Bodis-Wollner I, Anders M, Kels B, Podos S: Interocular comparison of contrast sensitivities in glaucoma patients and suspects. *Br J Ophthalmol* 64:858–862, 1980.
57. Atkin A, Bodis-Wollner I, Podos S M, Wolkstein M, Mylin L H, Nitzberg S: Flicker threshold and pattern VEP latency in ocular hypertension and glaucoma. *Invest Ophthalmol Vis Sci* 24:1524–1528, 1983.
58. Bobak P, Bodis-Wollner I, Harnois C, Maffei L, Mylin LH, Podos S, Thornton J: Pattern electroretinograms and visual-evoked potentials in glaucoma and multiple sclerosis. *Am J Ophthalmol* 96:72–83, 1983.
59. Bodis-Wollner K: Differences in low and high spatial frequency vulnerabilities in ocular and cerebral lesions. In: *Pathophysiology of the Visual System*, ed L Maffei, The Hague; Dr W Junk, pp 195–204, 1981.
60. Towle VL, Moskowitz A, Sokol S, Schwartz, B: The visual evoked potential in glaucoma and ocular hypertension: effects of check size, field size and stimulation rate. *Invest Ophthalmol Vis Sci* 24:175–183, 1983.
61. Quigley HA, Hendrickson A: Chronic experimental glaucoma in primates: blood flow study with iodantipyrine and pattern of selective ganglion cell loss. *Invest Ophthalmol Vis Sci Suppl* 24:225, 1984.
62. Maffei L, Fiorentini A, Hollander H: Pattern ERG in the monkey after section of the optic nerve. *Exp Brain Res* 59:423–425, 1985.
63. Korth M: Pattern evoked responses and luminance-evoked responses in the human electroretinogram. *J Physiol* 337:451–469, 1983.

64. Korth M, Rix R, Sembritzki O: Spatial contrast transfer functions of the pattern evoked electretinogram. *Invest Ophthalmol Vis Sci* 26:303–308, 1985.
65. Rover J, Schaubele G, Berndt K: Macula and periphery: their contribution to the visual evoked potential (VEP) in humans. *Albrecht Von Graefes Arch Klin Ophthalmol* 214:47–51, 1980.
66. van Lith GHH, van Marle GW, van Dok—Mak GTM: Variation in latency times of visually evoked cortical potentials. *Br J Ophthalmol* 62:220–222, 1978.
67. Marx M, Bodis-Wollner I, Bobak PH, Harnois C, Mylin L and Yahr MD: Temporal frequency-dependent VEP changes in Parkinson's Disease. *Vis Res* 26:185–193, 1986.
68. Bodis-Wollner I, Feldman RG, Quillory SL, Mylin L: Delayed visual evoked potentials are independent of pattern orientation in macular disease. *Electroencephalogr Clin Neurophys* 68:172–179, 1987.



---

## 5. CRITICAL ANALYSIS OF SHORT-LATENCY AUDITORY EVOKED POTENTIALS RECORDING TECHNIQUES

ISAO HASHIMOTO

The short-latency auditory evoked potentials (SAEPs) are the sum of responses time-locked to high intensity click stimulations occurring within 10 msec. The remarkable stability of the SAEP waveforms and latencies across repeated recording sessions and varying arousal levels suggests that they originate in an extremely secure and highly synchronized generator system. It is hypothesized that synchronized neuronal discharges may summate to produce specific components of the SAEPs. Recording of such discharges in the auditory system from the surface of the scalp would require (1) that a sufficient number of neurons and fibers fire in synchrony, (2) that the neurons and fibers are relatively large and, therefore, the impulse is conducted fast, producing large extracellular potential fields and (3) that individual neurons and fibers have an orderly and parallel arrangement so that individual extracellular fields summate.

It has long been argued that extracellular field potentials generated by summed neural activity are due to current flows produced by postsynaptic potentials (PSPs) rather than action potentials (APs). In the context of generator of the SAEPs, it is extremely difficult to record selectively PSPs of the cell bodies and dendrites or APs of the nerve fibers since the brainstem auditory pathways are densely packed within a small area. Hence, the relative contribution of the two components to the SAEPs is not yet well understood.

**BASIC CONSIDERATIONS ON ANATOMY AND PHYSIOLOGY OF THE AUDITORY SYSTEM**

The purpose of this section is to briefly review the fundamental anatomical and physiological background of the SAEPs. The auditory system consists of the peripheral and the central ascending auditory system.

**Peripheral auditory system**

The peripheral auditory system includes the outer ear, middle ear, and inner ear, and the first-order afferents of the auditory nervous system.

*Outer ear and middle ear*

The tympanic membrane which separates the middle ear from the outer ear is extremely flexible and its acoustic impedance almost matches that of the medium of air. The sound waves, when transmitted from the tympanic membrane to the inner ear, are amplified by about 30 dB by a lever action of the middle ear ossicles. The significant attenuation of sound energy when transferred from the air to the inner ear fluid (about 30 dB) is thus offset by the natural amplification system. In other words, the sound energy which arrives at the tympanic membrane is conveyed to the cochlea almost without loss of energy.

There are two middle ear muscles; the tensor tympani and the stapedius. The tensor tympani is innervated by the trigeminal nerve and its action is to tense the tympanic membrane so as to dampen sound vibrations. The stapedius, which is innervated by the facial nerve, pulls the stapes away from the oval window and also dampens the input to the inner ear when it contracts.

Thus, to high intensity acoustic stimuli, both middle ear muscles are activated and protect the inner ear from an exceedingly high intensity input by increasing the acoustic impedance of the middle ear. The dampening effect, however, is of no more than 5–10 dB.

*Inner ear*

Within the inner ear cavity, there are the cochlear and the vestibular organs subserving, respectively, audition and equilibrium. The oval and round windows separate the inner ear from the middle ear cavity. The cochlea is essentially a fluid-filled coiled structure containing the basilar membrane (or cochlear partition to be more exact) in the center of the fluid cavity. The most significant feature contributing to frequency analysis of sounds is the fact that the membrane is narrower at the basal turn of the cochlea and wider toward the apical turn. Higher frequency sounds have a point of maximum displacement of the membrane near the base of the cochlea, and lower frequency sounds produce maximal displacement towards the apex.

The hair cells on the basilar membrane are responsible for the transduction of the mechanical information into electrical signals. There are two types of

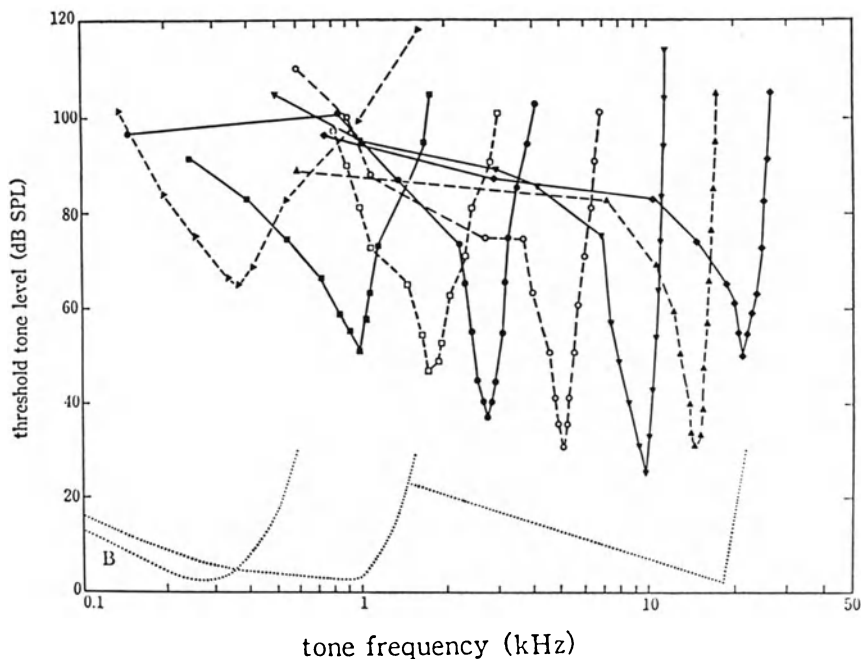
hair cells: the inner hair cells, which are arranged medially in a single row; and the outer hair cells, which are arranged laterally in three rows. When sounds are applied, the vibration of the basilar membrane causes hairs of the hair cells to bend against the tectorial membrane, which in turn distorts the membrane of the cells altering its ionic permeability. This leads to the generation of receptor potentials, i.e., the cochlear microphonic potentials (CM) and summing potentials (SP). CM are the oscillating analog potentials to sounds and SP, a sustained DC potential, the duration of which coincides with that of the acoustic stimuli. These receptor potentials of the hair cells are capable of exciting or inhibiting the auditory neurons which innervate them. The total number of inner and outer hair cells is 3,500 and 12,000 respectively.

The peripheral fibers from the ganglion cells lose the myelin sheath after passing through the habenula perforata and synapse on the hair cells as unmyelinated terminal fibers. In man, the majority of these fibers have been found to be 2 to 7  $\mu\text{m}$  in diameter [39, 83, 108]. There are two types of spiral ganglion cells which send fibers to the hair cells: type I cells, which comprise approximately 95 percent of the total spiral ganglion cells, innervate the inner hair cells; and type II cells, which project to the outer hair cells. Thus, a number of type I fibers converge on a single inner hair cell (a ratio of 20 to 1), while type II fibers send off many branches that synapse on many outer hair cells (a ratio of 1 to 10) [126].

#### *Cochlear nerve*

The cochlear nerve consists of both afferent fibers from the spiral ganglion cells and efferent fibers from the superior olivary complex (the olivocochlear bundle). There are about 31,000 afferent fibers in the cochlear nerve, corresponding to the total number of spiral ganglion cells [108]. The afferent fibers have a spiral arrangement within the cochlear nerve corresponding to the systematic arrangement of the hair cells on the basilar membrane. Thus, the fibers from the basal turn of the cochlea run in the periphery of the cochlear nerve, and those from the apical turn run in the central portion of the nerve [118]. A single afferent nerve fiber is limited in response to acoustic stimuli in terms of frequency and sound pressure. In other words, each fiber has its specific frequency threshold curve (tuning curve) defined as a plot of the stimulus level for eliciting threshold response as a function of stimulus frequency (figure 5-1). The characteristic frequency (CF) is the frequency of the turning curve to which a unit responds with the lowest threshold. In agreement with the anatomical arrangement described above, single-unit studies of the cochlear nerve fibers demonstrated that high CF units are located relatively more externally in the nerve trunk as compared to low CF units.

The bandwidth of a turning curve is narrow (tip) when the stimulus intensity is low, and becomes wider with greater spread toward low-frequencies (tail) when the stimulus intensity is increased. Therefore, increasing the stimulus intensity of a pure tone results in the activation of units with CF above

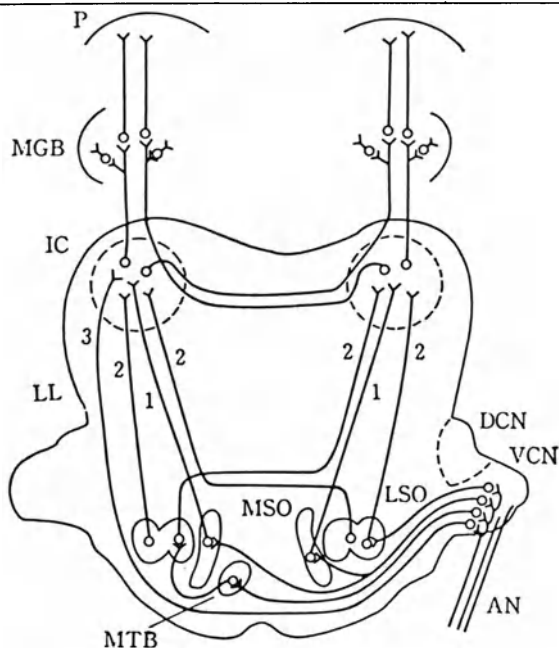


**Figure 5-1.** Frequency-threshold (tuning) curves of the acoustic nerve units. The stimulus level required to elicit a discharge above the spontaneous rate is plotted as a function of stimulus tone frequency. The shapes of high characteristic frequency (CF) units have a sharply tuned tip segment and a more broadly tuned low frequency tail region. Low CF units, on the other hand, exhibit tails on both low and high sides of the tip. Dotted lines indicate tuning curves of the basilar membrane [41].

the frequency for that tone because the stimulus intensity exceeds the threshold of their low frequency tail segment. This has significant implications when trying to obtain frequency-specific responses to high intensity stimuli using SAEPs (see section “Basic considerations on frequency specificity in the recording, SAEPs”).

The displacement of the basilar membrane toward the scala vestibuli depolarizes the receptor cells. As a consequence, cochlear nerve fibers are activated at a particular phase of acoustic input (phase-locking). The rarefaction click by producing the stapes displacement out of the oval window, and displacement of the basilar membrane toward the scala vestibuli, evokes spike discharges at a shorter latency than the condensation click by a factor of  $(2F)^{-1}$  second ( $F$ : center frequency of the click).

The click-evoked discharges of cochlear nerve units show a systematic increase in latency with decreasing CF reflecting the traveling time along the basilar membrane from its base to the apex. However, at high click intensities, units with the CF above 2–4 KHz respond in relative synchrony with a similar



**Figure 5-2.** Principal ascending connections of the auditory system with respect to the acoustic nerve (AN) on the right side. Axons projecting to the inferior colliculus (IC) numbered 1 and 2 arise from nerve cells in the medial superior olivary nucleus (MSO) and lateral superior olivary nucleus (LSO) where a high degree of bilateral innervation has already occurred.

DCN = the dorsal cochlear nucleus; VCN = the ventral cochlear nucleus; MTB = the medial nucleus of the trapezoid body; LL = the lateral lemniscus; MGB = the medial geniculate body; and P = the principal auditory cortex [58a].

latency to wave I in SAEPs [6]. Based on the above unit studies, as well as correlative studies between surface SAEPs, depth macro-electrode recordings [1, 68, 74, 85], and lesion experiments [9, 15], there is general agreement that the initial component of the SAEPs (wave I) is generated by the peripheral portion of the cochlear nerve. Wave I appears as a small positivity over the vertex which inverts to a larger negativity around the ear, ipsilateral to stimuli [64, 101, 119, 134]. Polarity inversion of wave I around the ear is consistent with an acoustic nerve dipole as its generator model.

The efferent fibers of the cochlear nerve are considerably smaller in number (1,700–1,800) than the afferent fibers [147] and have an inhibitory influence on the hair cells innervated by efferent fiber of a specific CF.

### Central auditory system

The central auditory system consists of various nuclei and tracts extending from the cochlear nucleus in the brainstem to the auditory cortex (figure 5-2).

*Cochlear nucleus*

When the cochlear nerve enters the cochlear nucleus in the ponto-medullary junction, it forms ascending and descending branches. The cochlear nucleus (CN) is divided into dorsal and ventral nuclei; and the latter further subdivided into anteroventral (AV) and posteroventral (PV) nuclei. The ascending branches synapse in the AV, and the descending branches in the PV and dorsal nuclei. Moreover, the types and configurations of their synaptic connections differ in that the ascending branches terminate on the cell bodies as large end-bulbs, and the descending branches end as pericellular nests of terminal boutons [11]. The cochlear nerve fibers that innervate the apical turn of the cochlea project to the periphery of the CN, while fibers that innervate the basal turn project to the central portion of the nuclei. This orderly spatial representation in the CN of the peripheral receptors is called tonotopic organization.

The axons of the CN form three ascending tracts; the trapezoid body (TB) from the ventral nucleus, the intermediate acoustic stria from the PV, and the dorsal acoustic stria from the dorsal nucleus. The dorsal and intermediate acoustic striae are vestigial in man. Although the majority of the secondary auditory neurons cross in the TB and project to the contralateral superior olivary complex, one-third of them project to the ipsilateral superior olivary complex. The CN units are activated by acoustic input only from the ipsilateral ear. On the basis of post-stimulus onset (PST) histograms of discharges to short tone-bursts, the CN units have been classified into 3 types with specific response characteristics: 1) primary-like type, which resembles cochlear nerve units with little adaptation, 2) chopper type, and 3) on type, characterized by a brief discharge sharply time-locked to stimulus onset.

The primary-like units are found most frequently in the AV where neurons (bushy cells) are enveloped by large end-bulbs of the ascending branches of the cochlear nerve fibers. The primary-like units are often preceded by a small positive presynaptic potentials believed to be generated by the large end-bulbs. On-units, on the other hand, tend to be located in the central area of the PV (octopus cell area) where fibers from the basal turn of the cochlea terminate.

Correspondence between anatomical and physiological cell types in the ventral nucleus can be summarized as follows: 1) bushy cells exhibit primary-like pattern, 2) octopus cells produce an onset pattern, and 3) stellate cells, chopper pattern [110]. The on-units exhibit short and uniform latency to high intensity click stimuli [72]. Thus it is likely that both the primary-like units of the AV and the on-units of the PV are capable of producing summed responses synchronized to click stimuli.

When SAEPs are recorded from the vertex with noncephalic reference, wave II consists of two distinct peaks separated by 0.5 msec (IIa and IIb). This has been described in animals [1, 122] and in man [103]. It has been suggested that the presynaptic potentials in the central terminals of the cochlear nerve generate wave IIa [1]. Wave IIb, on the other hand, has a latency similar to the

PSPs of the second-order neurons in the CN and the AP voltage fields in the TB [1, 17].

In correlative recordings between surface SAEPs and single units in the CN, the mean latency of the highly synchronized onset units ( $2.6 \pm 0.4$  msec) corresponds closely with the surface wave II ( $2.3 \pm 0.4$  msec) [72]. Lesion studies indicate also that wave II is generated in the vicinity of the CN [2, 15, 51, 145]. However, the available data from different experiments have failed to pinpoint whether the primary anatomic and physiologic substrate of wave II is presynaptic or postsynaptic potentials of the CN neurons or APs of the TB fibers.

#### *Superior olivary complex*

The superior olivary complex (SOC) which occupies the ventral region of the pons is a conglomerate of various nuclei, including the superior olivary nuclei, the nuclei of the TB and periolivary nuclei. In man, the medial superior olivary nucleus (MSO) is the largest nucleus in the SOC [135]. Each nucleus is tonotopically organized. The SOC is the initial relay nuclei where the inputs from both sides of the auditory system converge and is involved in the processing of the binaural inputs. The MSO has a unique anatomical arrangement of its neurons with their bipolar dendrites extending medially and laterally. The MSO receives projections from the ventral CN of both sides: fibers from the ipsilateral CN synapse on the lateral dendrites and fibers from the contralateral CN end on the medial dendrites of the same neurons [59, 133].

In agreement with the anatomical studies, the units located medial to the MSO are activated by the contralateral input, and units located lateral to the MSO are excited by the ipsilateral input [23, 49, 56, 57, 141, 143]. Within the MSO, there are many primary-like and chopper units, as in the CN, but there are fewer on-units [142]. The MSO units are capable of producing discharges synchronized with low CF tones and are also capable of responding to variations in interaural time differences. Most of the high CF units, when binaurally stimulated, produce higher output than when monaurally stimulated, and are thus sensitive to interaural intensity differences [16, 54, 124]. From these observations it has been concluded that MSO neurons are most probably integrating binaural inputs for localization of sounds in space.

A group of neurons in the SOC is activated by click stimuli with short uniform latencies ( $3.2 \pm 0.8$  msec) that correspond approximately to those of wave III at the scalp ( $3.1 \pm 0.3$  msec) [72]. Correlative studies of the surface SAEPs and depth field potentials have shown that a field potential of maximum amplitude in the contralateral as well as ipsilateral SOC has a latency similar to that of the surface wave III [1, 74, 85, 144]. Other intracranial mapping studies, however, also recorded from TB a field potential of similar latency to surface wave III [1, 17]. Lesion studies provide additional support to the hypothesis that SOC and TB are the main generators of surface wave III [2, 15, 51, 144–146].

Some MSO neurons receive descending inputs and send axons to the contralateral cochlea with synapses on the hair cells or on the fibers innervating hair cells (crossed-olivocochlear tract), and some neurons in the vicinity of the lateral superior olivary nucleus (LSO) send axons to the ipsilateral cochlea (uncrossed-olivocochlear tract). Thus the olivocochlear tracts function as the final common pathway in the descending auditory system that provide a feedback system to modulate the amplitude of its inputs.

#### *Nuclei of the lateral lemniscus*

The nuclei of the lateral lemniscus are located within the fibers of the lateral lemniscus (LL). The nuclei are divided into ventral and dorsal nuclei. The ventral nucleus receives primarily contralateral input and the dorsal nucleus receives bilateral input [3]. Although the nuclei of the LL provide a major input to the inferior colliculus, little is known about its anatomy and physiology. In a correlative single-unit study, a subpopulation of early onset units in the LL showed a latency ( $4.5 \pm 0.9$  msec) corresponding approximately to that of wave IV of SAEPs [72].

Similarly, depth mapping study revealed that field potentials with the latency of wave IV were found within the contralateral LL and also within the SOC bilaterally [1]. Caird et al. [17] suggested bilateral MSO fibers ascending in the LL as the main source for wave IV. Lesion experiments have yielded rather conflicting results that are difficult to reconcile. For example, unilateral lesion of the LL including the nucleus of the LL abolished the uncrossed component of wave IV which remained after TB transection [15], while bilateral complete transection of the LL had no effect on wave IV in other experiment [146].

#### *Inferior colliculus*

The inferior colliculus (IC) is a prominent auditory relay nucleus in the mid-brain. The central nucleus is the core of the IC and is surrounded by pericentral and external nucleus.

On the basis of cell size and innervation, the central nucleus has been divided into the ventrolateral division (VL) and the dorsomedial division (DM). The laminated arrangement of the fibers and cells within the VL is tonotopically organized in which the posterodorsal layer represents the apical turn and the anteroventral layer represents the basal turn of the cochlea [115]. The VL receives ascending projections only from the LL and sends axons to medial geniculate body via brachium of the IC [114]. The DM receives fibers not only from the LL but also from primary auditory cortex and the contralateral IC. The pericentral nucleus receives input from the auditory cortex, and the external nucleus receives projection from the central nucleus as well as from the ascending somatosensory system.

The majority of units in the central nucleus are excited by input from the contralateral ear, and a few units are excited by the stimulation of the ipsilateral



ear. Many binaural units are suppressed by the ipsilateral stimulation and a few binaural units are suppressed by the contralateral stimulation [143]. The response characteristics of the IC units differ from those of the CN units, i.e., sustained discharge patterns are infrequently found, and onset and pause type discharge patterns are more common in the IC. A subpopulation of the central nucleus units responds to monaural clicks with short latencies (4–5 msec) [7]. This latency range may correspond closely with that of wave V. Correlative studies of single units and surface SAEPs indicate a similarity of latency between unit activity in the ventral part of the IC and the surface Wave V [78, 100].

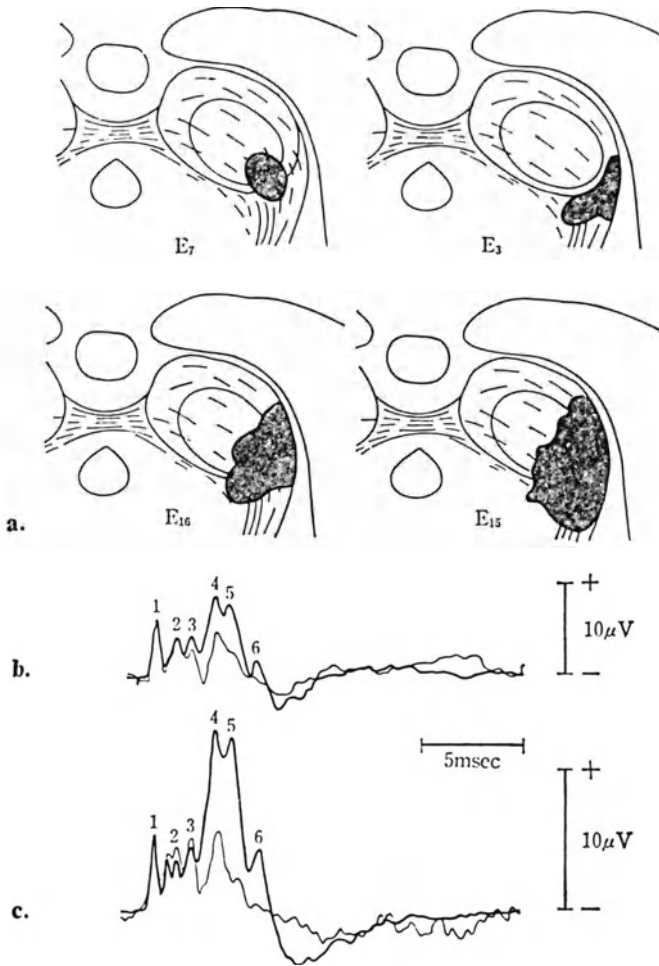
However, the majority of the central nucleus units are less synchronized and respond with longer latencies [72, 78, 100]. These slower onset units are assumed to correspond to a slow negative wave (SN10) following wave V [60–63]. Depth field potential studies provided additional support for the importance of the IC contributions (primarily contralateral and secondarily ipsilateral) to surface wave V [46, 71, 74, 85].

Extensive bilateral IC lesions, including the ventrolateral extent of the nuclei, resulted in marked reduction or loss of wave V (figure 5-3) [15, 46, 71]. Similarly, lesions which interrupted lemniscal input to the IC eliminated wave V [46, 71, 85]. The preceding correlative and lesion studies clearly demonstrate that the deep ventrolateral portion of the IC is particularly important in the generation of wave V. However, the resolution of these methods has been insufficient to define if wave V is generated by PSPs of the cell bodies and dendrites within the VL or by APs of the input fibers from the LL.

#### *Medial geniculate body*

The medial geniculate body (MGB) of the thalamus is the final relay nucleus in the ascending auditory system. The MGB includes the ventral, dorsal and medial divisions. The ventral division contains fibers and multipolar cells that are densely and regularly arranged. The lateral layer is related to lower auditory frequencies and the medial layer to higher frequencies. The ventral division is the major thalamic receiving area from the central nucleus of the IC and sends projections to the primary auditory cortex via auditory radiation. The dorsal and medial divisions receive auditory as well as somatosensory, and visual inputs. The discharge pattern of the MGB units is extremely complex and variable [34, 47]. Some of the units respond to clicks within 10 msec with a uniform latency [4]. These short-latency units follow click rates above  $20 \text{ sec}^{-1}$ .

Correlative extracranial and intracranial field potential studies indicate that surface wave VI occurs with a similar latency (6–8 msec) as the activity of the MGB and that it follows repetition rates up to  $20 \text{ sec}^{-1}$  with only minor decrements in amplitude [14]. Following complete transection of the brainstem rostral to the IC wave VI disappeared [15]. These data suggest that wave VI largely reflects neural activity of the MGB.



**Figure 5-3.** Short-latency auditory evoked potentials after various lesions of the ventrolateral part of the inferior colliculus. Waves 5 and 6 disappear (b and c) in all cases after lesions of the inferior colliculus as illustrated in a [46].

#### *Auditory cortex*

The cortical areas responsive to auditory stimuli are the primary auditory cortex located in the dorsal surface of the superior temporal gyrus. The auditory cortex receives and integrates acoustic information already processed in the ventral division of the MGB. The majority of the primary auditory cortex units are binaurally excited; the response to contralateral stimulation is greater than that to ipsilateral stimulation. Some units produce a short latency onset response (9–11 msec) to binaural clicks, although they represent a small proportion of acoustically driven units [111]. Correlative surface SAEPs and depth

recordings in cats have shown that a potential field of maximum amplitude in the primary auditory cortex has a latency (10–12 msec) which may coincide with that of wave VII [14]. These surface and depth potentials show the same parametric changes to stimulus rates. Aspiration of the primary auditory cortex has been shown to selectively abolish wave VII [14]. These results suggest that wave VII reflects direct activation of the primary auditory cortex.

#### **BASIC CONSIDERATIONS ON GENERATORS OF SAEP WAVES IN MAN**

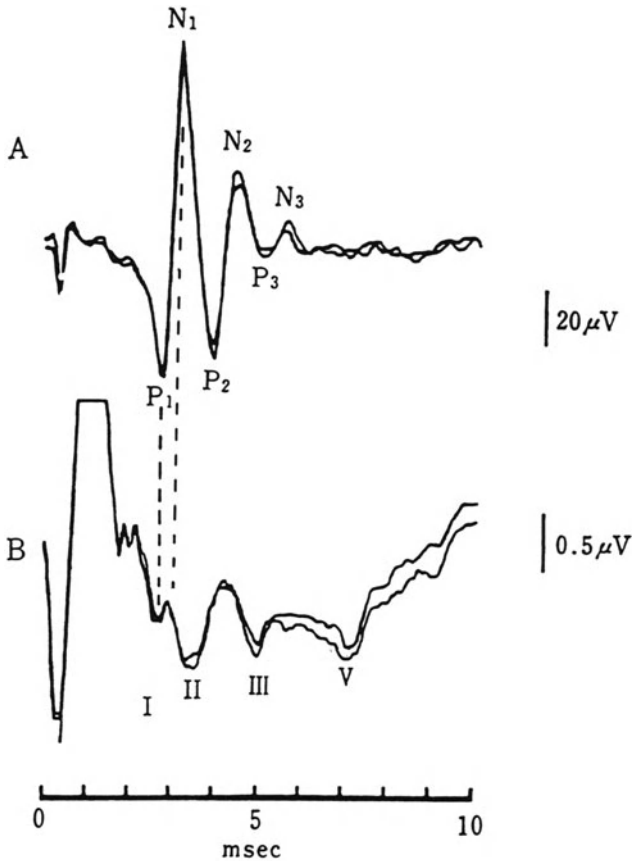
In the last few years, SAEPs have become an integral part of the neurological diagnostic tools. It is well documented that SAEPs can identify a variety of focal brainstem lesions [13, 66, 127, 129, 131]. However, the power of SAEPs as a localizing techniques is greatly dependent on the accuracy of our knowledge regarding the origin of each SAEP component. The present section surveys some basic data about the neural generators of SAEP components in man derived from intrasurgical recordings [60, 61, 65, 67, 68, 90–92, 125]. Relevant pathophysiological data will also be presented to assess the validity of the conclusions drawn from intrasurgical recordings of SAEPs.

The slow negative wave (SN10), an early middle latency component of the auditory evoked potentials, will also be included in the present analysis since from direct recordings this component appears to originate from the midbrain auditory structure, namely the inferior colliculus [61, 62].

#### **Action potentials of the cochlear nerve fibers (Wave I)**

Compound action potentials recorded directly from the cochlear nerve both distally, within the porus acousticus, and proximally, within the cerebello-pontine angle region, have a triphasic shape similar to sensory nerve action potentials (APs) recorded along peripheral nerves (figure 5–4) [68, 92, 125]. The onset of the negative phase (N1) of the triphasic action potentials reflects the arrival of the earliest nerve volley under the recording electrode. The fast conducting fibers subserving this early phase of the APs are likely to make a major contribution to the generation of SAEPs, and the slower conducting fibers represented by the late phase of N1 are virtually non-contributory to the SAEP generation. The recordings from the proximal part of the cochlear nerve show a similar triphasic waveform with smaller amplitudes and longer peak latencies.

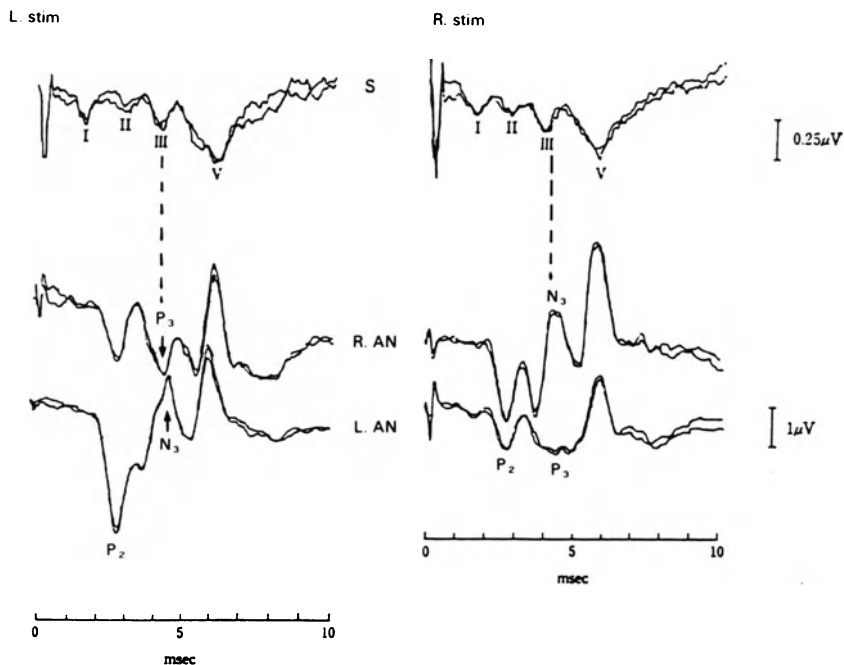
Clinically, only wave I is preserved and other waves are lost or of prolonged latency in cerebellopontine angle tumors [20, 35]. This is most probably due to conduction block of the cochlear nerve with sparing of the more distal portion of the cochlear nerve in the cochlea. This evidence clearly indicates that wave I originates from the most peripheral portion of the cochlear nerve. However, whether wave I reflects generator potentials in the unmyelinated dendritic terminals in the cochlea, or APs in the myelinated terminal portion of the cochlear nerve, is not yet settled [13].



**Figure 5-4.** Action potentials of the cochlear nerve fibers (A) and far-field SAEPs (B). Fast conducting nerve volley represented by the onset (peak of P1) of the negative phase (N1) of the triphasic action potentials makes a major contribution to the generation of SAEPs. The onset and peak of the P1 component recorded distally from the intrameatal portion of the cochlear nerve are synchronous with those of wave I at the scalp, while the following large N1 component occurs later than the peak of wave I [60].

### Brainstem entry time of the acoustic nerve volley

Critical data for interpretation of the subsequent waves involve the accurate time of arrival of the earliest afferent volley at the brainstem. Cochlear nerve fibers in man have a length of 20 to 25 mm [81, 125] and a diameter of 2 to 7  $\mu\text{m}$  [39, 83, 108]. From these data, as well as from the actual measurements of the conduction velocity along the cochlear nerve (10 to 24  $\text{ms}^{-1}$ ), the conduction time between the cochlea and the cochlear nucleus can be reasonably estimated to be about 1 msec [68, 125].



**Figure 5-5.** Recordings from the dorsal surface of the pons in the vicinity of the auditory nuclei (AN) of the lower brainstem (the cochlear nucleus and superior olivary complex). The potentials recorded over the ipsilateral auditory nuclei have a prominent positive peak (P2) which shows almost a perfect match with the scalp recorded wave II. A negative wave (N3) following the P2 starts and ends in time with wave III. However the recording from the contralateral nuclei shows this component as a positive wave (P3) indicating a horizontal dipole field in the lower pontine region. L = left, R = right, Stim = stimulation, S = scalp [62a].

### Early brainstem component (Wave II)

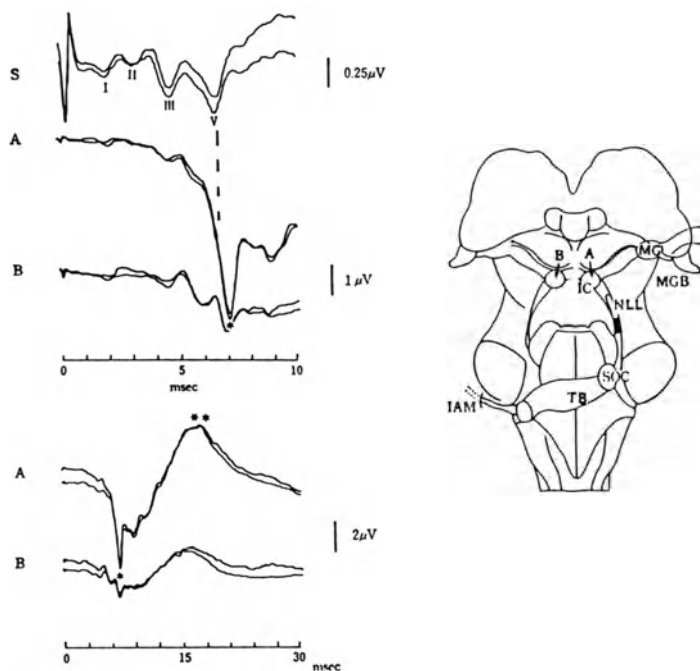
Since the auditory nuclei of the lower brainstem, i.e., the cochlear nucleus (CN) and superior olivary complex (SOC), are not directly accessible in man, recordings are made from the surface of the dorsal pons in the vicinity of these nuclei (figure 5-5). The potentials recorded over the ipsilateral cochlear nuclei have a prominent initial positive peak (P2) which shows almost a perfect match with the scalp recorded wave II. Møller and Jannetta [90] also recorded evoked potentials from the identical locus in the brainstem that are similar in morphology to the recordings presented in figure 5-5. Surface potential field distribution studies have shown that wave II is negative at the earlobe and positive at the vertex and this earlobe negativity (N2) occurs slightly earlier than the vertex positivity [63, 101]. Therefore, wave II recorded from the vertex to the ipsilateral earlobe may consist of two temporally overlapping but separate components; the cochlear nerve APs and the ipsilateral CN activities.

### **Horizontal dipole field in the pontine region (Wave III)**

In recordings from the dorsal pons in the vicinity of the cochlear nuclei a negative wave (N3) following the positive wave (P2) is seen in responses to ipsilateral auditory stimulation. This wave N3 starts and ends in time with surface wave III (figure 5-5). However, recording from the contralateral nuclei shows that this component is phase reversed, appearing as a positive wave (P3). This is in agreement with surface potential distribution studies that show that surface wave III is positive in contralateral scalp recordings and negative or only slightly positive in ipsilateral ear recordings. [64, 101, 128, 130, 134, 139]. The medial superior olivary nucleus (MSO) is generally accepted as the largest nucleus in the superior olivary complex (SOC) in man [73, 93, 135]. The MSO receives direct projections from the CN of both sides, with fibers from the ipsilateral CN projecting to the lateral dendrites and those from the contralateral CN ending on the medial dendrites of the same cells [59, 133]. It can therefore be speculated that with contralateral stimulation, EPSPs on the medial dendrites produce a negative field at the medial edge of the MSO and that the potential is inverted to a positivity at the lateral edge of the nucleus [8, 17, 23, 49, 143]. Conversely with ipsilateral stimulation, depolarization on the lateral dendrites produces a negative field at the lateral border and a positive field at the medial border of the MSO. These field potential data in animal experiments resemble closely the mirror-image dipole field in the recordings from the human brainstem. The potentials recorded from the midline of the dorsal surface of the pons in the vicinity of the trapezoid body (TB) have 3 positive components—P2, P3 and P4—separated by 2 negative deflections. The P3 component which temporally coincides with surface wave III shows a rapid change both in polarity and amplitude when the recording electrode within the brainstem is displaced slightly [68]. From these observations no brainstem auditory nucleus or tract can be specified with certainty as the generator for wave III in man, although the findings in these intrasurgical recordings do indicate that the MSO can be a good candidate for the neural generator of wave III. The P4 component from the midpons corresponds to wave IV and is maximal at this level with rapid attenuation by rostral electrode displacement, suggesting a pontine auditory structure as the generator source for this component [68].

### **Vertical dipole field in the midbrain (Wave V)**

In recordings from the midbrain, a slow positive wave—P5—was the most predominant potential, whereas the earlier wavelets were poorly defined. The P5 component from the midbrain has a closetime relationship with the scalp wave V, although a small but consistent peak latency difference between the two is present [68]. The P5 from the midbrain is the virtual mirror-image of the slow negative component (N5) in the recordings from the pons where the P5 from the midbrain is much larger than the N5 from the pons. In contrast to



**Figure 5-6.** Potentials evoked from both ipsilateral and contralateral inferior colliculi (IC). With stimulation of the left ear, a large potential (\*) corresponding to wave V is recorded from the contralateral IC (A) but only a small potential from the ipsilateral IC (B). Similarly a large potential (\*\*), the depth correlate of SN10 is recorded from the contralateral IC (A). The physiological predominance of P5 and SN10 components in the contralateral IC is in conformity with the human and animal anatomical studies that the major part of the brainstem auditory pathway ascends contralaterally [62a].

the P3 (the depth correlate of wave III) with the horizontal dipole field in the pontine region, the P5 has a vertically-oriented dipole field within the mid-brain with a rostral-positive and caudal-negative potential field configuration.

These distinct dipole fields in the brainstem indeed suggest that the potential sources for these far-field components are close to the respective recording electrodes.

#### **Predominance of P5 component in the contralateral inferior colliculus**

Evoked potentials from the contralateral and ipsilateral inferior colliculi (IC) to monaural stimulation are presented in figure 5-6. The contralateral response corresponding to wave V is considerably larger than the ipsilateral response. The result is in conformity with the human and animal anatomical studies that the major part of the brainstem auditory pathway ascends contralaterally.

A restricted upper pontine-midbrain lesion lateralized to one side produces mounted electrodes have been helpful in defining better the relationships be-

selective abnormality in wave V with stimulation contralateral to the lesion (figure 5-7). On stimulation of the ipsilateral ear, SAEPs are completely normal. The absence of wave V in contralateral responses can be interpreted as conduction block of the presynaptic fibers of the contralateral IC with preservation of the generator substrate for wave IV in the pontine region. Whether or not this wave V reflects a postsynaptic or presynaptic neural activity in the IC is still an open question [60, 61, 65, 68, 89, 91].

### **Widespread slow negative wave (SN10) from the midbrain**

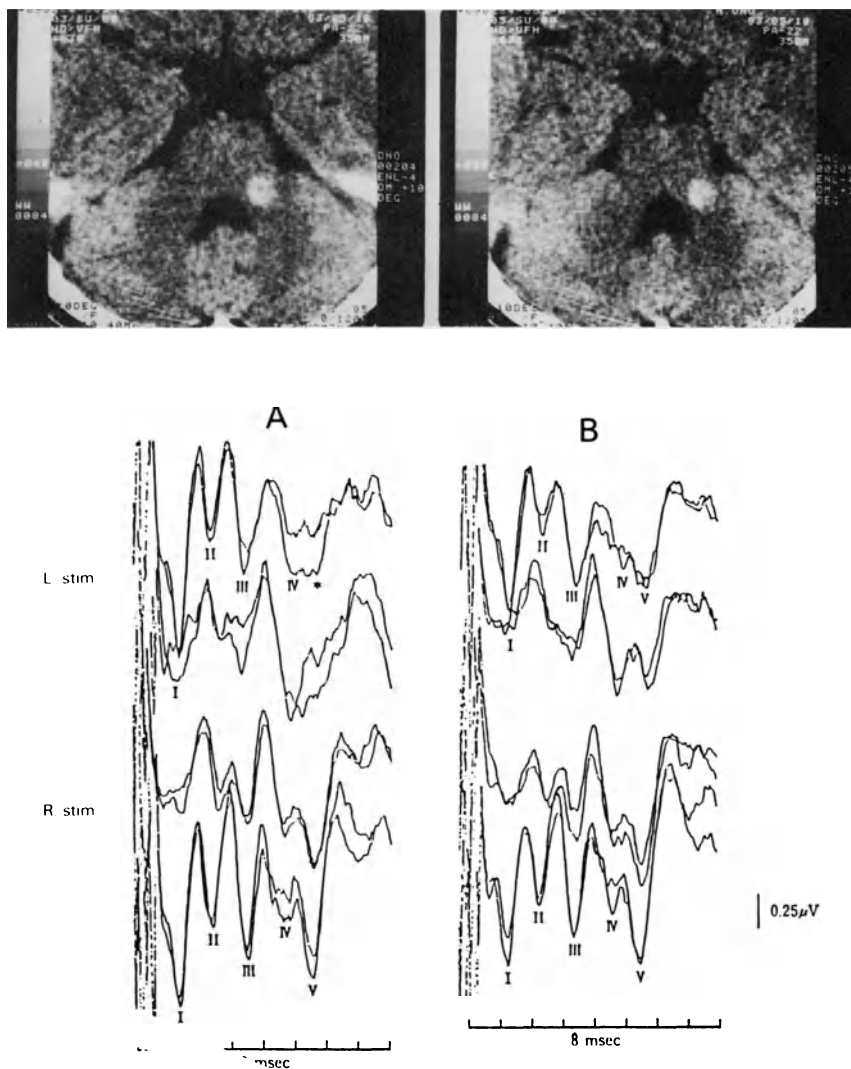
When a non-cephalic reference electrode is used, a slow negative wave is seen to follow the brief positive SAEP wavelets. This slow negative peak has a latency of about 10 msec and has been labeled SN10 [28]. This component is widely distributed over the scalp and, therefore, it is reasonable to assume that it arises from deep auditory structures [65]. Evoked potentials from ipsilateral and contralateral IC to monaural stimulations in man show brief positive peaks followed by a slow negative wave SN10 with the contralateral response being significantly larger than the ipsilateral response (figure 5-6). This slow negative potential from the IC corresponds temporally to the scalp SN10 [60, 61]. SN10 from the contralateral IC shows a steady increase in latency and decrease in amplitude as stimulus intensity is progressively decreased. However, SN10 is relatively unchanged by varying the stimulus repetition rate of stimuli from  $1 \text{ s}^{-1}$  to  $45 \text{ s}^{-1}$  [65]. The above mentioned parametric manipulations affect similarly the scalp SN10 [28]. This contrasts sharply with the following positive cortical component (Pa) which decreases in amplitude quite rapidly with an increasing stimulus rate [18, 84]. The duration of the SN10 component is about 10 msec and definitely longer than the duration of the earlier SAEP wavelets (about 1 msec). We are, therefore, tempted to speculate that this slow wave is the far-field reflection of the postsynaptic potentials (PSPs) of the IC, whereas short duration SAEP wavelets may reflect the synchronized activity (APs) of the fiber tracts in the brainstem auditory pathways.

The conclusion that may be drawn from the preceding intracranial recordings, as well as from the topographic and parametric studies, is that the SN10 reflects primarily the dendritic potentials of the contralateral IC.

### **Volume conduction of the intracranial potentials to the scalp surface**

Thus far we have discussed the intracranial sources of surface-recorded potentials taking in account of synchronously occurring high amplitude potentials seen in intrasurgical recordings. However, intracranial and scalp potentials are not always strictly concurrent in peak latencies, and often minor shifts are present between them, questioning the correspondence of a given intracranial activity with a scalp potential [60, 61, 68]. Recording of potentials all the way from its intracranial maximum to the scalp using intraventricular catheter-mounted electrodes have been helpful in defining better the relationships be-





**Figure 5-7.** Pathophysiological correlation of SAEP wave V.

A. A small right upper pontine hemorrhage on CT scan.

B. SAEPs to stimulation of the ear ipsilateral to the lesion is normal (VB-A).

On stimulation of the contralateral ear, there is a selective loss of wave V (\*). A repeat SAEPs testing after 3 months reveals that wave V has a slightly delayed latency and still clearly diminished amplitude (B-B).

tween depth and surface potentials [60, 61, 65, 68]. Sequential recordings from the electrodes in the fourth ventricle, aqueduct of Sylvius, third ventricle and lateral ventricle, clearly show amplitude reductions as well as minor but systematic latency shifts of the fast and slow SAEP components as a function of distance from their sources (figure 5-8). A similar recording technique has also been used to record short-latency brainstem somatosensory evoked potentials (SSEPs) [62]. The traveling fast positive components (P13 and P14) and slow negative component (N16) from the brainstem are considered to reflect respectively the APs in the medial lemniscus (ML) and the PSPs in the various brainstem nuclei receiving collateral projections from the ML [58].

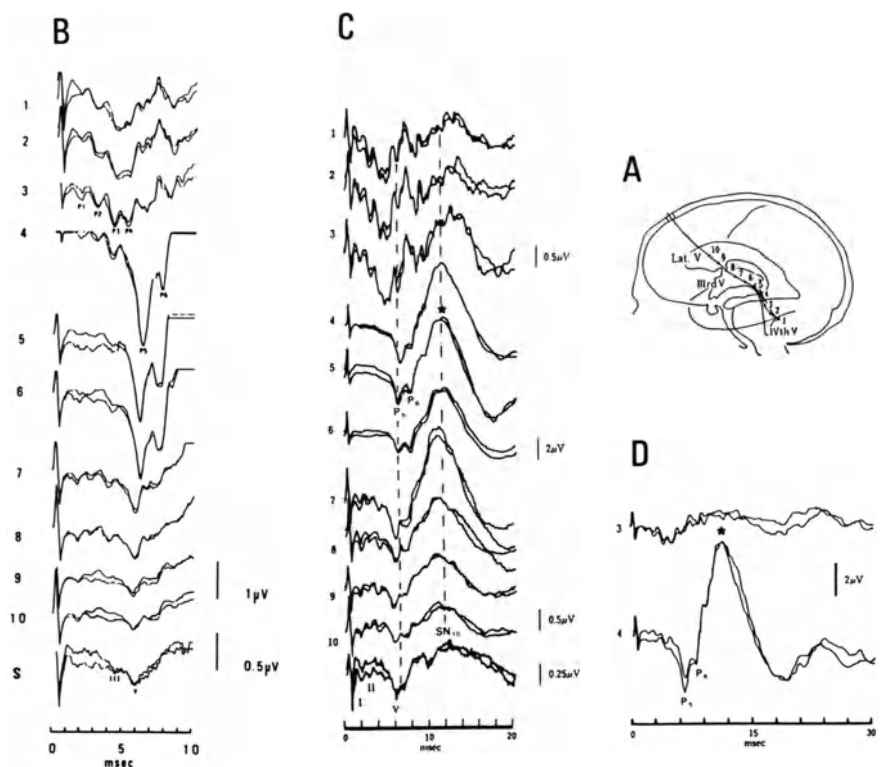
The attenuation of the slow component both in SAEPs (SN10) and SSEPs (N16) at the scalp is greater than that of the fast components in SAEPs (waves I-V) and SSEPs (P13 and P14). This differential attenuation ratio in the two distinct intracranial components may imply that: 1) the slow and fast components have different source locations (nuclei versus fiber tracts) and dipole orientations (horizontal versus vertical), 2) semiclosed PSP fields for the slow components versus open AP fields for the fast components, and/or 3) the brain as a volume conductor has a higher resistivity to a lower frequency spectrum of biological signals.

The consistent and uniform latency shifts of the near-field SAEP and SSEP peaks points to interactions of potential fields generated by multiple sources, or the brain itself, working as a low-cut filter introducing a phase lead in the signal.

#### **BASIC CONSIDERATIONS ON INCREASING SIGNAL-TO-NOISE RATIO IN THE RECORDING OF SAEPS**

Increasing the signal-to-noise ratio, i.e., 1) decreasing the amplitude of noise upon which the signal is superimposed, and 2) increasing the amplitude of the signal of interest, is the basic consideration upon which recording of evoked potential is based. SAEPs are extremely low amplitude (<1 micro-volt), far-field potentials from auditory peripheral and brain stem afferent pathways that are buried in background noise. Averaging enhances the stimulus-time-locked potentials relative to the random background noise and, thereby, permits detection of the SAEPs. Reduction in the amplitude of the noise is proportional to the square root of the number of individual responses in the average. Assuming that the SAEPs have a 1:50 signal to noise ratio in an unaveraged epoch,  $50^2 = 2,500$  signals must be averaged to improve the signal to noise ratio up to a 1:1. In addition to averaging, there are several other methods which can be applied to eliminate or reduce noise from various sources. Increasing the amplitude of the signal is another important aspect of enhancing the signal-to-noise ratio. This can be accomplished by manipulating the stimulus and recording parameters as discussed in detail in the section "Basic considerations on isolation and identification of different components in SAEPs".

The recording of SAEPs can be divided in 3 Stages: 1) generation of the acoustic stimuli, 2) amplification of the signal, and 3) processing of the signal



**Figure 5-8.** Volume conduction of the fast and slow SAEP components to the scalp surface.

**A)** Multiple recording electrodes located along the intraventricular catheter at equal intervals of 1 cm within the fourth ventricle, aqueduct of Sylvius, third and lateral ventricles. The electrodes 1, 2 and 3 are located in the fourth ventricle (vicinity of the pons); 4 and 5 in the aqueduct of Sylvius (vicinity of the midbrain); 6, 7 and 8 in the third ventricle (vicinity of the thalamus); and 9 and 10 in the lateral ventricle.

**B)** Fast SAEP waves to left monaural stimulation recorded at the various locations indicated in A. The P2, P3 and P4 components are maximal at the pontine level while P5 is largest at the midbrain level. These pontine and midbrain potentials are propagated to the scalp surface with amplitude reductions as a function of distance from the brainstem and with minor but systematic latency shifts. S = scalp recording. Intracranial and scalp recording are referenced to the left earlobe (A1).

**C)** Slow SAEP component (SN10) to left monaural stimulation recorded at the multiple locations indicated in A. The potentials recorded in the vicinity of the pons consist of brief sinusoidal components with about 1 msec duration, while the potentials from the midbrain are dominated by a large slow negative wave after the P5 component.

Note different voltage calibrations: 0.5  $\mu$ V for the upper three (1, 2, 3) and lower four (7, 8, 9, 10) traces, 2  $\mu$ V for the middle three (4, 5, 6) traces and 0.25  $\mu$ V for the scalp (S) recordings. The common reference for the intracranial and scalp recordings is the earlobe ipsilateral to stimulus. The large negative wave from the midbrain indicated by \* corresponds to SN10 at the scalp. This negative potential initially shows rapid decrement in size with distance from the midbrain (in the near-field) but the amplitude gradient becomes shallow with increasing distance from the midbrain (in the far-field).

**D)** Recordings from the same subject as in B.

Note a rapid fall off of the negative potential (\*) caudal to the midbrain. Voltage calibration is the same for the two recordings [60, 61].

obtain SAEPs. Noise is generated at each of these stages. It is therefore, convenient to organize the discussion on noise reduction following this sequence.

### **Stimulus artifact**

A click is a transient acoustic stimulus preferably used for eliciting SAEPs. The stimulus is generated by driving an acoustical transducer with the output of a waveform generator. Since the acoustic transducer is usually placed close to the recording sites, electromagnetic fields generated by the transducer are readily coupled to the recording electrodes. A large stimulus artifact can drive an amplifier beyond its linear range or block it and lead to distortion of the early components of the SAEPs. The stimulus artifact can be reduced by the following methods: 1) separating the acoustic transducer from the subject (and therefore from the recording electrodes) either by connecting the transducer to the subject by a flexible tube or by stimulation in free field, 2) shielding the transducer, 3) reversing click polarity, and 4) use of piezoelectric transducer.

With free field stimulation, a sound-isolating room is required and this is not practical in the clinical setting. When using a connecting tube between the transducer and the ear, the artifact is reduced: 1) by keeping the transducer away from the electrodes and 2) by introducing a fixed delay between the stimulus delivery and responses. Shielding the transducer usually with mu-metal is an effective way of reducing the stimulus artifact. Adding responses to reversing-polarity clicks selectively eliminates the stimulus artifact while preserving the neural responses. However, this method precludes recording of the cochlear microphonics (CM) and the frequency-following response (FFR) from the auditory system and may distort neural response waveforms theoretically by a factor of  $(2F)^{-1}$  second (F: the center frequency of the clicks). This effect of opposite-polarity clicks should be taken into account particularly when stimulating with low frequency clicks [25] or when recording from the subject with a high-frequency hearing loss [20, 24]. (Refer also to the section "Basic considerations on isolation and identification of different components in SAEPs" for further details.) Finally, the piezoelectric-transducer generates a much smaller magnetic field than the above mentioned electromagnetic transducer, and the electromagnetic stimulus artifact is essentially eliminated by its use [75]. The elimination of the stimulus artifact has revealed an early neural component prior to wave I.

### **Noise in amplification of the signal**

Differential amplifiers amplify only voltage differences between input leads, and voltages that are the same at the two inputs are cancelled, thus attenuating selectively electrical noise mainly from power lines. Amplifiers with high-input impedance reduce distortion and noise particularly when high impedance recording electrodes such as those for recording electrocochleogram (ECochG) are used. Thus, where the amplifier has an input impedance of

10 M $\Omega$  and a recording electrode impedance of 50 K $\Omega$ , for instance, an input signal is only attenuated by about 0.5 percent.

Internal noise, however, tends to be higher in high-input impedance amplifiers. This type of noise is reduced by averaging and by restricting the frequencies to those necessary for faithful reproduction of the wanted response.

### **Trade offs between noise reduction and signal distortion by the use of filters**

Since SAEPs are buried in much larger electrical noise, the quality of the record will be considerably improved when the frequency response of the filters is set to maximally reject the interfering noise. However, the frequency response of an analogue filter must not be so restrictive that the evoked potentials are distorted both in terms of amplitude attenuation and phase-shift. In general, the low-cut filters introduce phase lead, and the high-cut filters phase lag into the signal to be analyzed.

Thus, lowering the high-cut filter frequency produces an increase in latency, and increasing the low-cut frequency produces a decrease in absolute latency of all components [130] and also of I–V interpeak latency [37]. Absolute amplitudes of all components are reduced by increasing the low-cut filter frequency, this effect being most prominent for wave V [37, 97, 112, 130]. In addition to filter frequency, filter slope also leads to waveform distortion.

Increasing the low-cut filter slope produces similar effects on the waveform as increases of the low-cut filter frequency [33, 37, 97, 112]. Digital filtering with zero-phase shift does not produce such distortions [10].

The frequency distribution of SAEPs shows three peaks: low frequency (50–150 Hz), middle frequency (500–600 Hz), and high frequency (1,000–1,100 Hz) peaks [76, 138]. The main noise interfering with the SAEPs corresponds to the background EEG which has a frequency range of 0.5–30 Hz and can be considerably reduced with a low-cut filter. Other two important sources of noise contamination are muscle potentials with a 20 Hz–1 KHz frequency range and acoustic stimulus artifact with a 10 Hz–20 KHz range, both of which cannot be eliminated by filtering because their frequencies overlap those of the SAEPs. In restless, tense patients, for example, raising the low-cut filter from 30 to 100–300 Hz can attenuate significantly the EMG and movement artifact (0.05–50 Hz frequency range) but the waveform of the SAEPs will be distorted and identification of wave V becomes difficult due to the loss of the slow component on which wave V is normally superimposed [137]. A more desirable alternative to ensure muscle relaxation is sedation. Involuntary muscle activity in response to (and hence time-locked to) acoustic stimuli is not easily distinguishable from the neural response and difficult to eliminate [101]. The post-auricular muscle response (PAR) overlapping the SN10 is not abolished by voluntary relaxation or light sleep. Monitoring not only the ongoing background EEG but also the ongoing averaged waveform is worthwhile because it permits identification of this muscle response; the muscle

response usually grows much faster than the neural response. Serial intra-operative recordings of the SAEPs show that PAR grows rapidly prior to recovery from the general anesthesia and often provides the earliest sign of arousal from anesthesia (Hashimoto, unpublished observation).

### **Distortion of signal in the averaging process**

In specifying averaging system requirements for recording the SAEPs, one must consider the huge background noise with the amplitude 50–100 times that of the SAEPs. Hence only 1–2 percent of A–D amplitude resolution is available to resolve the digitized SAEP waveforms. Increasing A–D amplitude resolution widens the voltage range through which data can be accepted, and thus reduces the incidence of blocked epoch. Including such blocked epochs in an averaged waveform diminishes its amplitudes and smears the sharpness of its peaks. An averager with automatic artifact rejection circuitry rejects epochs that contain any sample exceeding the A–D converter's amplitude limit or a certain pre-specified level. The time resolution of the A–D converter must be sufficient enough to allow a good reconstruction of the waveform; 20 samples or more per msec allows reasonable resolution of the SAEP waveforms.

### **BASIC CONSIDERATIONS ON ISOLATION AND IDENTIFICATION OF DIFFERENT COMPONENTS IN SAEPS**

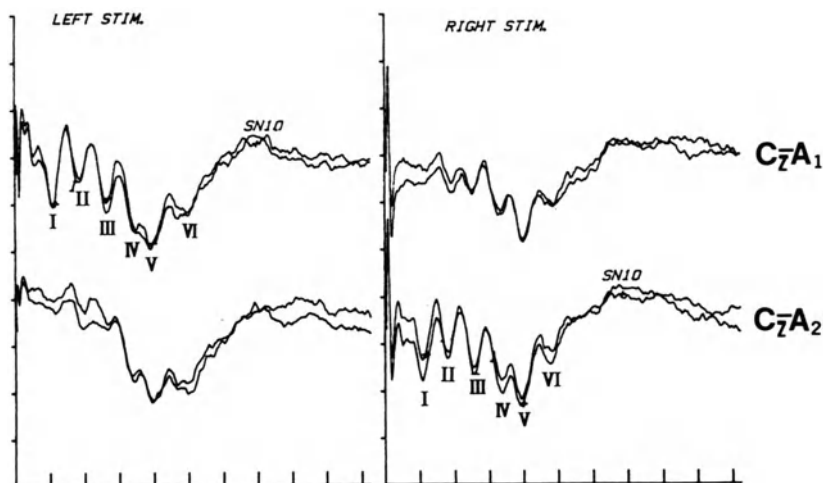
Isolation and identification of different components in the SAEPs involves the basic understanding of: 1) the anatomy and physiology underlying each component (see section on the anatomy and physiology of the auditory system), 2) general waveform, 3) parametric changes, and 4) potential field distribution of each component. In this section, a brief description of the general waveform of the SAEP components is followed by a discussion on the stimulus and recording parameters that can be manipulated to facilitate the identification of SAEP waves.

#### **General waveform**

Sinusoidal fast waves I–VII are superimposed on a slow positive wave peaking at approximately the same latency as wave V (figure 5-9). Therefore, in normals, wave V is usually the most prominent peak around 5.5–5.8 msec after the stimulus. Filtering-out the low frequency (50–150 Hz) slow wave component reduces the amplitude of wave V making its identification more difficult. With progressive decrease of stimulus intensity, wave V is the last wave to disappear. Recordings from the vertex referenced to the contralateral ear provide additional information that can be helpful to identify wave V because in this montage waves IV and V tend to be clearly separated [130].

Wave I is the initial neural response which appears at about 1.6–1.7 msec after the stimulus. In contrast to the cochlear microphonics (CM), it does not reverse polarity with reversal of the click polarity.

NAME : UKIKO YOSHIDA	L-R ABR			
AGE : 31	LEFT		RIGHT	
SEX : F	I	1.650	I	1.650
ID # :	III	3.960	III	3.780
CASE # :	V	5.880	V	5.880
DIAGNOSIS : NORMAL	SN10	10.380	SN10	10.170
PROCEDURE : ABR	I-III	2.310	I-III	2.130
DATE : 3/18/85	III-V	1.920	III-V	2.100
REMARKS :	I-V	4.230	I-V	4.230
TAG ID :				
			MSEC/DIV	μVLT/DIV
			1.500	0.31



**Figure 5-9.** Short-latency auditory evoked potentials from a normal subject. The recording montage is the vertex to left earlobe (upper traces) and the vertex to right earlobe (lower traces). Stimuli consist of alternating polarity clicks delivered monaurally to the left (left stim.) and right ear (right stim.) at 75 dBHL with masking of the contralateral ear by white noise at 40 dB less than that of the click stimulus. Vertex-positivity down.

Wave I is absent or of very low amplitude in a vertex to contralateral ear derivation so that comparison with the vertex to ipsilateral ear derivation may help in the identification of this wave. In the vertex to ipsilateral external ear canal derivation wave I is of higher amplitude than in the conventional vertex to ipsilateral earlobe derivation. Wave III appears approximately midway between waves I and V. Recordings from the vertex to contralateral ear have been suggested as an aid to the identification of wave III because it tends to be attenuated in that derivation [130]. Wave II stands equidistantly between waves I and III. Wave IV appears between waves III and V and tends to occur somewhat closer to wave V. Occasionally, wave IV may be completely fused with wave V. Waves VI and VII are superimposed on the upswing from the slow positive wave peaking approximately simultaneously with wave V. Waves II, IV, VI, and VII are usually not used in clinical interpretations of SAEPs.

## Stimulus parameters

### *Stimulus intensity*

As the intensity of the click stimulus increases, the frequency of neural firing and the number of active neurons and fibers increase progressively up to a maximum. These relationships are represented in the SAEP components as input-output amplitude functions with different intensity levels. The most abrupt changes in amplitudes are seen between 60 and 70 dBHL and then these input-output functions reach an asymptote at about 75 dBHL. Therefore a single click intensity of 75 dBHL or more is adequate for neurological applications of SAEPs where recordings of input-output function are of limited value. The latencies of the SAEP waves are increased with decreasing click intensity. Because the intensity-dependent latency-shifts of all the waves are roughly parallel, there is very little change in interpeak latencies [20, 107].

The relative constancy of the interpeak latency measurements irrespective of changes in physical or effective stimulus intensity provides the basis for neurologic applications of the SAEPs. Thus, in general, any disorder of the peripheral hearing itself (conductive or cochlear) will not prolong the interpeak latencies [35, 117]. Coats and Martin [24] even reported a slight shortening of the I–V interpeak latency in cochlear hearing loss. In conductive hearing loss, the input-output latency function is parallel to but displaced from that of a subject with normal hearing. In cochlear hearing loss, on the other hand, the slope of the input-output latency function is steeper than that of the normals. This phenomenon is considered to be the electrophysiological equivalent of loudness recruitment [48].

### *Stimulus repetition rate*

Increasing the rate of stimulation decreases the amplitude of the SAEP waves [103]. This effect is most pronounced for repetition rates greater than  $10 \text{ sec}^{-1}$  [21].

The amplitude of the action potentials (APs) recorded directly from the human cochlear nerve is extremely large and can be distinguished even in single sweeps [68]. The initial negative component (N1) maintains its maximum amplitude at stimulus repetition rate of up to  $20 \text{ sec}^{-1}$ . However, the amplitude falls to 70 and 50 percent when the repetition rate is increased to  $50 \text{ sec}^{-1}$  and  $100 \text{ sec}^{-1}$  respectively. At  $200 \text{ sec}^{-1}$  the APs tend to disappear. This results are comparable to the recordings of N1 at the round window [34] and that of wave I over the scalp [21] in response to progressively increasing click repetition rate. These observations suggest that the decrease in amplitude of wave I or N1 with increasing repetition rate is due to an adaptation phenomenon which most probably occurs at the synapses between the hair cells and the first/order neurons. The amplitude of all the SEAPs decrease by a similar magnitude with increasing click rates. The exception is wave V that decreases significantly less than waves I to IV [21, 44, 53, 75, 95, 103, 107, 121, 140].



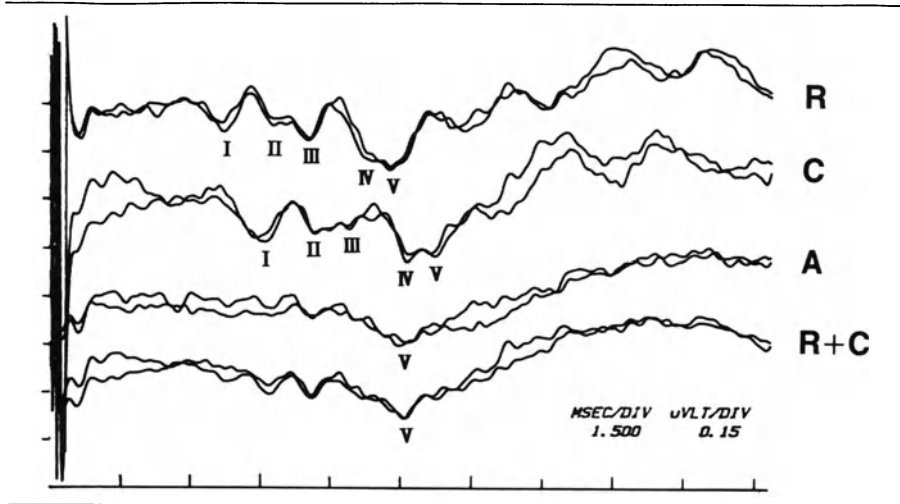
This selective sparing of wave V to increasing stimulus rate can be explained by its dual structure, i.e., fast and slow components. The fast component of wave V decreases in amplitude by roughly the same amount as the preceding fast waves I–IV. On the other hand, the slow component underlying wave V shows little or no decrement in amplitude with increasing rate of up to  $90 \text{ sec}^{-1}$  [137].

All SAEP waves show progressive increases in peak latencies with increasing stimulus repetition rate. The latency increase is greater with each successive wave. These non-parallel latency changes result in significant increases in interpeak latencies at higher stimulus rates [21, 103, 132, 148]. These rate-dependent latency increases that are greater for each successive wave suggest that an adaptation similar to the peripheral auditory system also occurs at the central auditory system. Another important aspect in respect to stimulus rate is the effect of developmental processes as myelination and synaptogenesis [138] or of pathological processes such as demyelination [112], acoustic tumors [120] and other miscellaneous disease states [70] upon the ability of the auditory system to process high repetition rate stimuli. In these developmental and pathological states, rate effects could be enhanced by stressing the auditory system with high stimulus rates. However, Chiappa et al. [19] reported that patients with multiple sclerosis did not show any pathological rate effect.

#### *Stimulus polarity*

Rarefaction clicks generally produce a larger wave I with a relatively shorter latency than condensation clicks [38, 138]. This effect is consistent with single fiber studies which show that the initial firing of the cochlear nerve coincides with movement of the basilar membrane toward the scala vestibuli at the time of the rarefaction phase of the stimulus [77]. The interpolarity latency difference for wave I has a mean value of about 0.1 msec (shorter latency for rarefaction) that is close to the predicted latency difference of one-half the cycle of the click stimulus [38]. The polarity-dependent latency shifts of the subsequent waves II–IV are of roughly the same amount [96, 130]. However, the latency of wave V does not vary with stimulus polarity [38, 130]. In subjects with normal hearing there are minor but significant polarity-dependent latency differences (as discussed above) which are, however, negligible for neurological interpretation of the SAEPs. However in patients with high frequency hearing loss, a change in click polarity can result in significant latency shifts of all components up to the point where equivalent waves may reverse polarity [20, 24].

Therefore, the use of alternating polarity clicks may eliminate some waves by out-of-phase cancellation (figure 5-10). In addition, Emerson et al., [38] found a polarity specific loss of wave V in 20 out of 600 patients consecutively studied. It is not known whether this unusual disappearance of wave V represents an abnormality or a rare normal variant.



**Figure 5-10.** Effect of changing click polarity in peripheral high-tone hearing loss. A remarkable change in latencies and morphology occurred when switching the click phase from (R) rarefaction to (C) condensation. Due to out-of-phase cancellation effect, earlier waves I-IV are difficult to identify with alternating rarefaction and condensation clicks (A). The bottom traces are the algebraic summation of responses to rarefaction and condensation clicks (R + C).

#### *Monaural versus binaural stimulation*

The response to binaural clicks is larger than that to monaural stimulation and its amplitude is about the same as the sum of the responses to monaural clicks. Hence for enhancing detectability of the SAEP waves, binaural stimulation has been used in recordings from patients with suspected brainstem lesions such as demyelinating diseases [112]. The use of only binaural stimulation, however, will result in significant loss of sensitivity since a normal response from one ear can mask an abnormal one from the other ear [19, 104]. In non-cephalic reference recordings, there is a minor but consistent difference between the two modes of stimulation (monaural versus binaural) called the binaural interaction component (BIC). The BIC is visualized by subtracting the sum of the monaural responses from that obtained by binaural stimulation [30, 86, 113]. The main peak of the BIC occurs at a constant latency about 0.5 msec later than the peak of wave V for different stimulation intensity levels [31]. That this effect is not an artifact is supported by Levine [86] and Dobie and Wilson [31] who have excluded contributions either from middle ear reflex or acoustic cross-talk to the BIC, and by animal experiments in which the BIC is abolished when crossing fibers in the trapezoid body (TB) are transected [45] or is attenuated linearly as a function of the extent of the TB section [145]. It was suggested recently that the BIC might be produced by binaural mechanisms in the medial superior olivary nucleus (MSO) [16, 17, 124]. This BIC may

become a useful clinical tool if its generator in the central auditory pathways can be defined better.

#### *Contralateral masking*

High intensity monaural clicks will stimulate both ears and, therefore, in these cases the monaural SAEPs are really the algebraic sum of the SAEPs from the ipsilateral and contralateral ears.

Interaural attenuation of clicks may vary due to differences in characteristics of the transducers but has mean values ranging from 50 dB to 70 dB [31, 86, 109]. Thus, in unilaterally deaf subjects, the SAEPs can be recorded because of the acoustic crossover. The contralateral ear is therefore masked with white noise at an intensity well below crossover levels that is 40 to 50 dB less than that of the click stimulus. Excessive white noise masking on the other hand produces a central masking effect and the latency of wave V increases in the absence of a latency shift of wave I [113, 116]. Contralateral masking is usually not necessary unless gross asymmetry of hearing function is present.

#### **Potential field distribution**

Selection of the optimal recording montages requires good understanding of the potential distribution of the different SAEP wave. Amplitude distributions to binaural stimulation are not always strictly symmetrical. One possible explanation is the usual asymmetry of the brain, skull, muscle and scalp as a volume conductor. Technical factors such as impedance variations between different recording electrodes may also affect the potential field distributions. With monaural stimulation, the potential distributions of the SAEP waves differ in their loci of maximum amplitudes.

Wave I has a wide distribution of the positivity over the scalp with a negativity localized to the ipsilateral ear [64, 66, 101, 128, 130]. The out-of-phase addition of positivity at the vertex and negativity at the ear enhances detection of wave I in the vertex to ipsilateral ear derivation. Electrode placements closer to the cochlea, such as in the external ear canal, increase the size of the negativity of wave I. Therefore, this technique is useful when wave I cannot be registered with the conventional surface montages. Wave II is positive and distributed widely over the scalp with maximum at the vertex and minimum at the contralateral ear [128]. Wave II is negative at the ipsilateral ear and this wave probably corresponds to the N2 component seen in electrocochleography (EcochG). The negative wave II at the ipsilateral ear occurs earlier than the vertex positivity [63, 101]. Therefore the recording from the vertex referenced to the ipsilateral ear is not necessarily additive because these positive and negative waves are not completely 180 degrees out-of-phase. Wave III is positive at all scalp locations with a maximum amplitude at the vertex. This

positivity tends to be lateralized to the contralateral scalp [64, 101, 128]. At the ipsilateral ear it is reflected either as a weak positivity or even a negativity [134, 139]. Therefore, the vertex to ipsilateral ear derivation produces a relatively higher amplitude wave III.

Wave IV is positive at all scalp sites and tends to be symmetrically distributed [128]. In some cases it is of slightly higher amplitude contralaterally [64]. Wave V is positive at the scalp with the maximum at the contralateral frontal area whereas the ipsilateral parietoccipital area is minimum. Thus recording from the vertex to ipsilateral ear produces lower amplitude for wave V due to cancellation of in-phase activity. Wave V recorded with a noncephalic reference shows a small but progressive shift in peak latency in the coronal plane with the shortest peak latency (less than 0.2 msec) at the contralateral temporal region. No shift is seen in the sagittal plane [64, 128]. The reason for this site-dependent peak latency shift is unknown.

There are only very limited attempts to use the potential field distribution in the clinical interpretation of SAEPs. However, Hashimoto et al. [64] have indicated that alterations in the field distributions and polarity inversions of selective waves occur in patients with mass lesions affecting brainstem structures. These changes may reflect the displacement of the generator loci by expanding lesions with a possible deviation of dipole axes and a resultant change in potential fields.

The information obtained from the potential field distribution can be used for the estimation of loci and vectors of the equivalent dipoles within the brainstem [52, 55, 119]. This approach has serious limitations because: 1) the biological noise seriously restricts the accuracy when trying to locate the dipole sources, 2) only a small variation in electrode placement produces considerable errors in the dipole estimation, 3) a unique solution is impossible if there are two or more concurrent dipoles, 4) brain is neither isotropic nor homogeneous as a volume conductor, and 5) the assumed spherical model is wrong since there are marked deviations of the human head from sphericity. However, this approach may provide a method of linking the local potential fields to the far-field potentials over the scalp.

#### **BASIC CONSIDERATIONS ON FREQUENCY SPECIFICITY IN THE RECORDING OF SAEPS**

A principle of topographic organization, i. e., an orderly spatial representation in the central nervous system of peripheral receptors is preserved at all levels of the sensory system. In the auditory system, this topographic organization is equivalent to the tonotopic organization. In other words, the auditory system has a frequency map of the cochlea at all levels of the ascending auditory pathways. Therefore, it is possible theoretically that with the use of frequency specific stimuli, the frequency specific and thus place-specific responses from periphery to each nucleus or tract of the ascending central auditory system can be obtained. In fact, there has been a great deal of interest in using the SAEPs

to approximate the behavioral audiogram and provide threshold information about specific frequencies [27, 80, 88, 136, 149].

Basically two different techniques are employed: 1) by using frequency-specific stimuli that are abrupt enough to synchronize the neuronal activity yet long enough to maintain frequency specificity (tone bursts, tone pips and filtered clicks), and 2) by combining a wide-band stimulus such as a click with various types of masking so as to derive narrow-band responses.

### **Frequency specific stimuli**

The basic problem with frequency-specific stimuli is the requirement that a stimulus should be abrupt enough to synchronize auditory neurons and yet long enough to maintain frequency specificity.

It is impossible to have an abrupt stimulus and at the same time have precision in frequency since the abrupt onset causes spectral broadening of the stimulus. Conversely, when the stimulus has an envelope with a much slower rise-decay time that is suitable for maintaining frequency specificity of the stimulus, response identification becomes more difficult due to loss of sufficient synchronicity. One solution to these problems, or rather a compromise, is the use of the tone pip or short tone burst with a 3–5 msec duration. The waveform of filtered click obtained by passing a click stimulus through a narrow band-pass filter resembles that of a brief tone burst due to the ringing of the filter. There is a fairly broad range of frequencies in those frequency specific stimuli which will result in activation of cochlear regions beyond those specific to the nominal frequency of the stimulus [12]. The frequency spread is further exaggerated by increasing the intensity levels much above normal hearing threshold since fibers innervating more basal parts of the cochlea are recruited [43]. Audiogram estimations with the SAEPs elicited by tone pips at 0.5, 1, 2, and 4 KHz have been found to be comparable to the subjective audiograms with mean threshold differences of 10–20 dB [79, 80] in which threshold difference for low frequency (0.5 KHz) is largest [69].

The frequency-following response (FFR) that can be recorded with surface electrodes has the same frequency and waveform as the acoustic stimulus [40, 87, 94]. This response has a latency of 6 msec and is recordable to lower frequency tones up to 2 KHz. Comparative surface FFR and depth recording in the cat inferior colliculus (IC) showed parallel changes with cooling and warming of the IC [123]. However, other lesion and parametric studies revealed contributions from other multiple brainstem structures, i.e., primarily from the cochlear nucleus (CN) and secondarily from the superior olivary complex (SOC) and the nucleus of lateral lemniscus (LL) [42, 51].

Since the traveling wave generated by a 500 Hz tone takes about 4 msec to traverse to the corresponding cochlear partition, there may be only 2 msec left for activation of the brainstem auditory structures to occur. Thus the question has been raised as to the earlier conclusion implicating brainstem structure as sources of the FFR [40]. Because thresholds for FFR generation in man are

commonly in the range of 40–50 dBSL and considerably higher than those for SAEPs by 20–30 dB, the recording of FFR may be less helpful for audiogram estimation.

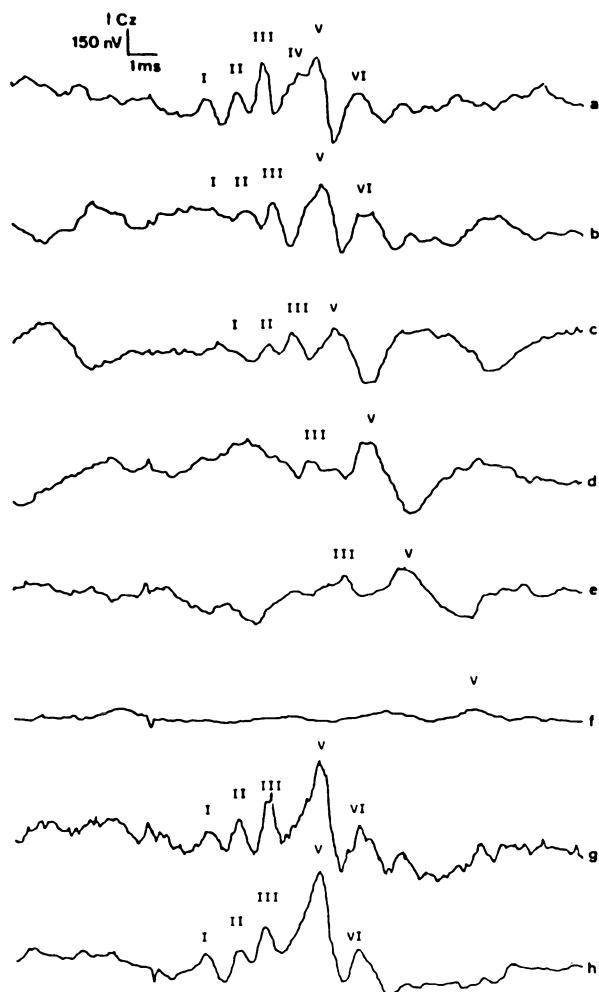
### **Combination of a wide band click with various types of masking**

At low intensities near threshold, a short tone burst elicits neural activity from a limited part of cochlear partition and can therefore be said to a truly frequency-specific stimulus. However, with increment of the short tone burst intensity, increasing number of fibers from the basal portion of the cochlea are recruited and the short tone burst no longer maintains frequency-specificity.

In this situation, the amplitude and latency of the SAEP components are predominantly determined by fibers innervating the basal portion of the cochlea. In order to restrict the spread of the neural activity toward basal portions of the cochlea, a high-pass filtered noise is presented with a click stimulus. The subtraction of the waveforms recorded in the presence of the noise filtered at two different frequencies produces the derived responses from the frequency band formed by the two filter frequencies (figure 5-11). [26, 32, 99]. Instead of using a high-pass filtered noise, a pure tone is presented with a click. Subtracting the SAEP waveforms obtained with a pure tone noise from those without noise, yields responses from the cochlear partition corresponding to the frequency of the pure tone [98]. Measurement of click thresholds in each of the narrow bands results in accurate estimates of audiograms, comparable to the results with the short tone bursts. This technique of derived response provides much more accurate information on the activity of a given restricted portion of the cochlear partition than the unmasked or compound responses. However, the technique is not practically applicable to clinical uses at present due mainly to complicated manipulations of the noise parameters that involve a considerably long test session. Presenting a notched-filtered masking noise or band eliminate noise with a click or tone pip, yields responses from the unmasked portion of the cochlear partition [82, 102, 106]. This technique is simpler and easier than that of the derived responses, and the response can be obtained online and therefore is more applicable to routine audiological and otological evaluation.

### **FUTURE DEVELOPMENTS OF SAEPS**

Anatomic and neurophysiologic studies indicate that there are numerous cell groups and fiber tracts in the central auditory system that may contribute to the generation of SAEPs. The complexity of the problem of specifying the generators of the different components of the SAEPs is obvious since all of the auditory structures are packed into a small area in the brainstem. Basically two conflicting general hypotheses on SAEP generator substrates have been explicitly proposed in recent publications: 1) all SAEP waves represent the graded PSP current fields generated at the cell soma and dendrites within the



**Figure 5-11.** Responses obtained by high-pass noise masking. Responses are derived from the frequency band of 8–10 KHz (a), 4–8 KHz (b), 2–4 KHz (c), 1–2 KHz (d), 0.5–1 KHz (e), and 0.2–0.5 KHz (f). Summation of the above derived responses (g) gives a pattern similar to the unmasked response (h). Note monotonic latency decreases as a function of stimulated frequency band [26].

nuclei [13], and 2) all SAEP waves reflect the all-or-none APs traveling along the fiber tracts [17]. More systematic correlative single-unit studies of the various cell groups or fiber tracts and the surface SAEP waves coupled with microlesion studies could be helpful to solve this discussion.

Kainic acid is a potent neurotoxic agent causing the destruction of neuronal cell bodies and dendrites while preserving axons of passage and nerve ter-

minals. This agent, when appropriately injected into the brainstem, may yield valuable information about the generator substrates for the SAEP waves and resolve the relative contributions that complex nuclei and fiber tracts make to all the waves comprising the SAEPs [50]. There have been detailed studies in animals related to SAEP generators. A controversy still exists on the correspondence of SAEP waves between humans and animals [45a, 84a, 84b, 88a].

Thus, the problem of generators in man has to be tackled separately but not exclusively as discussed in the section II on generators in man. Feasible approaches include: 1) correlative intrasurgical recording from the human brainstem and the surface SAEPs [60, 65, 67, 68, 89, 91, 92, 125] and 2) estimation of the dipole sources and their orientations of different SAEP waves from the surface potential field distributions [52, 55, 119]. Attempts should also be made to relate the SAEPs to other methods correlating brainstem structure and function such as the detailed anatomic studies in humans [92a] and nuclear magnetic resonance imaging.

Rigorous control of the stimulus and recording variables, and a knowledge of the variability of normal SAEPs, as a function of these factors are prerequisites for accurate interpretation of SAEPs. Standardization of stimuli and recording montages for measurement of the SAEPs in clinical tests has been developed and is now widely adopted. Specific applications, however, may require other methodologies. In the design of these special methods, a good understanding of the basic concepts set forth in the previous sections is essential.

Topographic or dermatomal stimulation have become increasingly important for recording place-specific responses in the somatosensory system [62b, 62c]. In the same sense, there has been a great deal of interest in using tonotopic or frequency-specific stimulations for recording frequency-specific responses in the auditory system. It is likely that with future technical refinements, finely shaped frequency-specific stimuli will become more widely used for clinical interpretation of SAEPs.

## REFERENCES

1. Achor LJ and Starr A: Auditory brain stem responses in the cat. I. Intracranial and extracranial recordings. *Electroencephalogr Clin Neurophysiol* 48:154–173, 1980a.
2. Achor LJ and Starr A: Auditory brain stem responses in the cat. II. Effect of lesions. *Electroencephalogr Clin Neurophysiol* 48:174–190, 1980b.
3. Aitkin LM, Anderson DJ and Brugge JF: Tonotopic organization and discharge characteristics of single neurons in nuclei of the lateral lemniscus of the cat. *J Neurophysiol* 33:421–440, 1970.
4. Aitkin LM, Dunlop CW and Webster WR: Click-evoked response patterns of single units in the medial geniculate body of the cat. *J Neurophysiol* 29:109–123, 1966.
5. American Electroencephalographic Society: Recommended standards for short-latency auditory evoked potentials. *J Clin Neurophysiol* 1:32–40, 1984.
6. Antoli-Candela F and Kiang NYS: Unit activity underlying the N1 potential. In: RF Naunton and C Fernandez (eds) *Evoked electrical activity in the auditory nervous system*. Academic Press, New York, 165–191, 1978.
7. Benevento LA, Coleman PD and Loe PR: Responses of single cells in cat inferior colliculus



- to binaural click stimuli. Combinations of intensity levels, time differences, and intensity differences. *Brain Res* 17:387–405, 1970.
8. Biedenbach MA and Freeman WJ: Click-evoked potential map from the superior olivary nucleus. *Am J Physiol* 206:1408–1414, 1964.
  9. Boelen HJJ: The origin of the waveform of cochlear whole action potential. *Arch Otorhinolaryngol* 222:205–209, 1979.
  10. Boston JR and Ainslie PJ: Effects of analog and digital filtering on brain stem auditory evoked potentials. *Electroencephalogr Clin Neurophysiol* 48:361–364, 1980.
  11. Brawer JR and Moreset DK: Relations between auditory nerve endings and cell types in the cat's anteroventral cochlear nucleus seen with the Golgi method and Nomarski optics. *J Comp Neurol* 160:491–506, 1975.
  12. Brinkmann RD and Scherg M: Human auditory on-and off-potentials of the brainstem. Influence of stimulus envelope characteristics. *Scand Audiol* 8:27–32, 1979.
  13. Buchwald JS: Generators. In: EJ Moore (ed) *Bases of auditory brainstem evoked responses*. Grune & Stratton, New York, 157–195, 1983.
  14. Buchwald JS, Hinman C, Norman RJ, Huang CM and Brown KA: Middle-and long-latency auditory evoked responses recorded from the vertex of normal and chronically-lesioned cats. *Brain Res.* 205:91–109, 1981.
  15. Buchwald JS and Huang CM: Far-field acoustic response: Origins in the cat. *Science*, 189: 382–384, 1975.
  16. Caird DM and Klinke R: Processing of binaural stimuli by cat superior olivary complex neurons. *Exp Brain Res* 52:385–399, 1983.
  17. Caird DM, Sontheimer, D and Klinke R: Intra-and extracranially recorded auditory evoked potentials in the cat. I. Source location and binaural interaction. *Electroencephalogr Clin Neurophysiol* 61:50–60, 1985.
  18. Celesia GG: Organization of auditory cortical areas in man. *Brain* 99:403–414, 1976.
  19. Chiappa KH: Pattern shift visual, brainstem auditory and short-latency somatosensory evoked potentials in multiple sclerosis. *Neurology* 30:110–123, 1980.
  20. Chiappa KH: Brainstem auditory evoked potentials: Methodology. In: KH Chiappa (ed) *Evoked Potentials in Clinical Medicine*. Raven Press, New York 105–143, 1983.
  21. Chiappa KH, Gladstone KJ and Young RR: Brainstem auditory evoked responses: studies of waveform variation in 50 normal human subjects. *Arch Neurol* 36:81–87, 1979.
  22. Chiappa KH, Harrison JL, Brooks EB and Young RR: Brainstem auditory evoked responses in 200 patients with multiple sclerosis. *Ann Neurol* 7:135–143, 1980.
  23. Clark GM, Dunlop CW: Field potentials in the cat medial superior olivary nucleus. *Exp Neurol* 20:31–42, 1968.
  24. Coats AC and Martin JL: Human auditory nerve action potentials and brain stem evoked responses. Effects of audiogram shape and lesion location. *Arch Otolaryngol* 103:605–622, 1977.
  25. Coats AC, Martin JL and Kidder HP: Normal short-latency electrophysiological filtered click responses recorded from vertex and external auditory meatus. *J Acoust Soc Am* 65: 747–758, 1979.
  26. Conraux C, Dauman R and Feblot P: Potentials évoqués auditifs rapides dérivés. *Audiology* 20:382–393, 1981.
  27. Davis H and Hirsh SK: The audiometric utility of brain stem response to low-frequency sounds. *Audiology* 15:181–195, 1976.
  28. Davis H and Hirsh SK: A slow brainstem responses for low-frequency audiometry. *Audiology* 18:445–461, 1979.
  29. Dawson GD: Cerebral responses to electrical stimulation of peripheral nerve in man. *J Neurol Neurosurg Psychiatry* 10:134–140, 1947.
  30. Dobie RA and Norton SJ: Binaural interaction in human auditory evoked potentials. *Electroencephalogr Clin Neurophysiol* 49:303–313, 1980.
  31. Dobie RA and Wilson MJ: Binaural interaction in auditory brain-stem responses: Effect of masking. *Electroencephalogr Clin Neurophysiol* 62:56–64, 1985.
  32. Don M and Eggermont JJ: Analysis of the click-evoked brainstem potentials in man using high-pass noise masking. *J Acoust Soc Am* 63:1084–1092, 1978.
  33. Doyle DJ and Hyde ML: Bessel filtering of brainstem auditory evoked potentials. *Electroencephalogr Clin Neurophysiol* 51:446–448, 1981.

34. Dunlop CW, Itzkowic DJ and Aitkin LM: Tone-burst response patterns of single units in the cat medial geniculate body. *Brain Res* 16:149–164, 1969.
35. Eggermont JJ, Don M and Brackmann DE: Electrocochleography and auditory brainstem electric responses in patients with pontine angle tumors. *Ann Otol Rhinol Laryngol* 89 [Suppl.] 75:1–19, 1980.
36. Eggermont JJ and Odenthal DW: Electrophysiological investigation of the human cochlea: Recruitment, masking, and adaptation. *Audiology*, 13:1–22, 1974.
37. Elton M, Scherg M and Von Cramon D: Effects of high-pass filter frequency and slope on BAEP amplitude, latency and waveform. *Electroencephalogr Clin Neurophysiol* 57:490–494, 1984.
38. Emerson RG, Brooks EB, Parker SW and Chiappa KH: Effects of click polarity on brainstem auditory evoked potentials in normal subjects and patients: Unexpected sensitivity of wave V. *Ann NY Acad Sci* 388:710–721, 1982.
39. Engström H, Rexed B: Über die kaliberverhältnisse der Nervenfasern im N. Stato-acusticus des Menschen. *Mikro-anat Forsch* 47:448–455, 1940.
40. Euler M and Kiessling J: Frequency-following potentials in man by lock-in technique. *Electroencephalogr Clin Neurophysiol* 52:400–404, 1981.
41. Evans EF: The frequency response and other properties of single fibers in the guinea-pig cochlear nerve. *J Physiol* 226:263–287, 1972.
42. Faingold CL and Caspary DM: Frequency-following responses in primary auditory and reticular formation structures. *Electroencephalogr Clin Neurophysiol* 47:12–20, 1979.
43. Folsom RC: Frequency specificity of human auditory brainstem responses as revealed by pure-tone masking profiles. *J Acoust Soc Am* 75:919–924, 1984.
44. Fowler CG and Noffsinger D: Effects of stimulus repetition rate and frequency on the auditory brainstem response in normal, cochlear-impaired, and VIII nerve/brainstem-impaired subjects. *J Speech Hear Res* 26:560–567, 1983.
45. Fullerton BC and Hosford HL: Effects of midline brain stem lesions on the short-latency auditory evoked responses. *Neurosci Abstr* 5:20, 1979.
- 45a. Fullerton BC, Levine RA, Hosford-Dunn HL and Kiang NYS: Comparison of cat and human brain-stem auditory evoked potentials. *Electroencephalogr Clin Neurophysiol* 66: 547–570, 1987.
46. Funai H and Funasaka S: Experimental study on the effect of inferior colliculus lesions upon auditory brain stem response. *Audiology* 22:9–19, 1983.
47. Galambos R: Microelectrode studies on medial geniculate body of cat. III Response to pure tones. *J Neurophysiol* 15:381–400, 1952.
48. Galambos R and Hecox K: Clinical applications of the human brainstem evoked potentials to auditory stimuli. In: JE Desmond (ed) *Progress in clinical neurophysiology*. Vol. 2, Auditory evoked potentials in man: Psychopharmacology correlates of evoked potentials. Karger, Basel 1–19, 1977.
49. Galambos R, Schwartzkopf J and Rupert A: Microelectrode study of superior olivary nuclei. *Am J Physiol* 197:527–536, 1959.
50. Gardi JN and Bledsoe SC: The use of kainic acid for studying the origins of scalp-recorded auditory brain-stem responses in the guinea pig. *Neurosci Lett* 26:143–149, 1981.
51. Gardi JN, Merzenich MM and Mckean C: Origins of the scalp-recorded frequency following response in the cat. *Audiology* 18:353–381, 1979.
52. Gaumond RP and Fried SI: Analysis of cat multichannel acoustic brainstem response data using dipole localization methods. *Electroencephalogr Clin Neurophysiol* 63:376–383, 1986.
53. Gerling IJ and Finitzo-Hieber T: Auditory brainstem response with high stimulus rates in normal and patient populations. *Ann Otol (St. Louis)* 92:119–123, 1983.
54. Goldberg JM and Brown PB: Functional organization of the dog superior olivary complex: An anatomical and electrophysiological study. *J Neurophysiol* 639–656, 1968.
55. Grandori F: Dipole localization method (DLM) and auditory evoked brainstem potentials. *Rev Laryngol (Bord)* 105:171–178, 1984.
56. Guinan JJ, Guinan SS and Norris BE: Single auditory units in the superior olivary complex. I. Responses to sounds and classification based on physiological properties. *Int J Neurosci* 4:101–120, 1972a.
57. Guinan JJ, Norris BE and Guinan SS: Single auditory units in the superior olivary complex II. Locations of unit categories and tonotopic organization. *Int J Neurosci* 4:147–166, 1972b.
58. Hand PJ and Van Winkle T: The efferent connections of the feline nucleus cuneatus. *J Comp Neurol* 171:83–110, 1976.

- 58a. Harrison JM and Howe ME: Anatomy of the afferent auditory nervous system of mammals. IN: WD Keidel and WD Neff (eds) Handbook of sensory physiology. Vol V/1, Auditory system. Springer-Verlag, Berlin 283–336, 1974.
59. Harrison JM and Irving R: Ascending connections of the anterior ventral cochlear nucleus in the rat. *J Comp Neurol* 126:51–64, 1966.
60. Hashimoto I: Auditory evoked potentials recorded directly from the human VIIIth nerve and brain stem: Origins of their fast and slow components. In: PA Buser, WA Cobb and T Okuma (eds) Kyoto-Symposia (EEG Suppl., No. 36), Elsevier, Amsterdam, 305–314, 1982a.
61. Hashimoto I: Auditory evoked potentials from the human midbrain: Slow brain stem responses. *Electroencephalogr Clin Neurophysiol* 53:652–657, 1982b.
62. Hashimoto I: Somatosensory evoked potentials from the human brain-stem: Origins of short-latency potentials. *Electroencephalogr Clin Neurophysiol* 57:221–227, 1984.
- 62a. Hashimoto I: Neural generators of early auditory evoked potential components in man. In: K Kunze, WH Zangemeister and Arlt (eds) Clinical problems of brainstem disorders, Georg Thieme, Verlag, New York 111–120, 1986.
- 62b. Hashimoto I: Somatosensory evoked potentials elicited by air-puff stimuli generated by a new high-speed air control system. *Electroencephalogr Clin Neurophysiol* 67:231–237, 1987.
- 62c. Hashimoto I: Trigeminal evoked potentials following brief air-puff: Enhanced signal-to-noise ratio. *Ann Neurol* (in press).
63. Hashimoto I and Ishiyama Y: Electric responses of the brainstem to acoustic stimuli. Basic studies and clinical applications. *Lang Sci Supple* “Current issues in neurolinguistics: Japanese contributions” 1–28, 1981.
64. Hashimoto I, Ishiyama Y, Manaka S, Ebe M and Sano K: Spatial distribution of brainstem auditory evoked potentials and their alterations in lesions of the VIIIth nerve and brainstem. *Neurol Res* 3:167–194, 1981.
65. Hashimoto I, Ishiyama Y, Nemoto S, Kuroiwa A, Yasuda K and Sekine Y: Intracranial origin and scalp distribution of slow auditory brainstem responses. In: RH Nodar and C Barber (eds) Evoked Potentials II. Butterworth Publishers, Boston 145–162, 1984.
66. Hashimoto I, Ishiyama Y and Tozuka G: Bilaterally recorded brainstem auditory evoked responses: Their asymmetric abnormalities and lesions of the brainstem. *Arch Neurol* 36:161–167, 1979.
67. Hashimoto I, Ishiyama Y, and Tozuka G and Mizutani H: Monitoring brainstem function during posterior fossa surgery with brainstem auditory evoked potentials. In: C Barber (ed) Evoked Potentials. MTP Press, Lancaster, 377–390, 1980.
68. Hashimoto I, Ishiyama Y, Yoshimoto T and Nemoto S: Brain-stem auditory evoked potentials recorded directly from human brainstem and thalamus. *Brain* 104:841–859, 1981b.
69. Hayes D and Jerger J: Auditory brainstem responses (ABR) to tone-pips: Results in normal and hearing-impaired subjects. *Scand Audiol* 11:133–142, 1982.
70. Hecox KE, Cone B and Blaw ME: Brainstem auditory evoked response in the diagnosis of pediatric neurologic disease. *Neurology*, 31:832–840, 1981.
71. Henry KR: Auditory brainstem volume conducted responses. Origins in the laboratory mouse. *J Acoust Soc Am* 4:173–178, 1979.
- 71a. Hughs JR and Fino J: Usefulness of piezoelectric earphones in recording the brainstem auditory evoked potentials: a new early deflection. *Electroencephalogr Clin Neurophysiol* 48: 357–360, 1980.
72. Huang CM and Buchwald JS: Interpretation of the vertex short latency acoustic response. A study of single neurons in the brainstem. *Brain Res* 137:291–303, 1977.
73. Irving R and Harrison JM: The superior olivary complex and audition. A comparative study. *J Comp Neurol* 130:77–86, 1967.
74. Jewett DL: Volume-conducted potentials in responses to auditory stimuli as detected by averaging in the cat. *Electroencephalogr Clin Neurophysiol* 28:609–618, 1970.
75. Jewett DL and Williston JS: Auditory-evoked far fields averaged from the scalp of humans. *Brain* 94:681–696, 1971.
76. Kevanishvili Z and Aphonchenko V: Frequency composition of brainstem auditory evoked potentials. *Scand Audiol* 8:51–55, 1979.
77. Kiang NY-S, Watanabe T, Thomas EC and Clark LF: Discharge patterns of single fibers in the cat’s auditory nerve. *Research Monograph* 35. M.I.T. Press, Cambridge, Mass., 1965.
78. Kimura H: Experimental study on the correlation between peak V of auditory brainstem

- response and unit activities of the inferior colliculus. *Jpn J EEG EMG* 13:131–141 (Jpn.), 1985.
79. Klein AJ: Properties of brain-stem response slow-wave component. I. Latency, amplitude, and threshold sensitivity, *Arch Otolaryngol* 109:6–12, 1983.
  80. Kodera K, Yamane H, Yamada O and Suzuki J: Brainstem response audiometry at speech frequencies. *Audiology*, 16:469–479, 1977.
  81. Lang J: Facial and vestibulocochlear nerve, topographic anatomy and variations. In: M Samii and PJ Jannetta (eds) *The cranial nerves*. Springer-Verlag, Berlin, 363–377, 1981.
  82. Laukli E: High-pass and notched noise masking in suprathreshold brainstem response audiometry. *Scand Audiol* 23:75–84, 1983.
  83. Lazorthes G, Lacomme Y, Gaubert J and Planet H: La constitution du nerf auditif. *Presse méd* 69:1067–1068, 1961.
  84. Lee YS, Lueders H, Dinner DS, Lesser RP and Hahn, J: Recording of auditory evoked potentials in man using chronic subdural electrodes. *Brain* 107:115–131, 1984.
  - 84a. Legatt AD, Arezzo JC and Vaughan HG: Short-latency auditory evoked potentials in the monkey. I. Wave shape and surface topography. *Electroencephalogr Clin Neurophysiol* 64:41–52, 1986a.
  - 84b. Legatt AD, Arezzo JC and Vaughan HC: Short-latency auditory evoked potentials in the monkey. II Intracranial generators. *Electroencephalogr Clin Neurophysiol* 64:53–73, 1986b.
  85. Lev A and Sohmer H: Sources of averaged neural responses recorded in animals and human subjects during cochlear audiometry (Electro-cochleogram). *Arch Ohr-, Nas.-u. kehlk.-Heilk* 201:79–90, 1972.
  86. Levine RA: Binaural interaction in brain stem potentials of human subjects. *Ann Neurol* 9:384–393, 1981.
  87. Marsh JT, Brown W and Smith J: Far-field recorded frequency-following responses: Correlates of low pitch auditory perception in humans. *Electroencephalogr Clin Neurophysiol*. 38:113–119, 1975.
  88. Maurizi M, Paludetti G, Ottaviani F and Rosingnoli M: Auditory brainstem responses to middle-and low-frequency tone pips. *Audiology*, 23:75–84, 1984.
  - 88a. Molter AR and Burgess J: Neural generators of the brain-stem auditory evoked potentials (BAEPs) in the rhesus monkey. *Electroencephalogr Clin Neurophysiol* 65:361–372, 1986.
  89. Møller AR and Jannetta PJ: Evoked potentials from the inferior colliculus in man. *Electroencephalogr Clin Neurophysiol* 53:612–620, 1982.
  90. Møller AR and Jannetta PJ: Auditory evoked potentials recorded from the cochlear nucleus and its vicinity in man. *J Neurosurg* 59:1013–1018, 1983.
  91. Møller AR and Jannetta PJ: Neural generators of the brainstem auditory evoked potentials. In: RH Nordar and C Barber (eds) *Evoked Potentials II*. Butterworth Publishers, Boston, 137–144, 1984.
  92. Møller AR, Jannetta PJ, Bennett M and Møller MB: Intracranially recorded responses from the human auditory nerve: New insights into the origin of brain stem evoked potentials (BSEPs). *Electroencephalogr Clin Neurophysiol.*, 52:18–27, 1981.
  - 92a. Moore JK: The human auditory brainstem as a generator of auditory evoked potentials. *Hear Res* 29:33–43, 1987.
  93. Moore JK and Moore RY: A comparative study of the superior olivary complex in the primate brain. *Folia Primat* 16:35–51, 1971.
  94. Moushegian G, Rupert AL, and Stillman RD: Scalp-recorded early response in man to frequencies in the speech range. *Electroencephalogr Clin Neurophysiol* 35:665–667, 1973.
  95. Olphen AF van, Rodenburg M and Verwey C: Influence of the stimulus repetition rate on brain-stem-evoked responses in man. *Audiology* 18:388–394, 1979.
  96. Ornitz EM, Mo A, Olson ST and Walter DO: Influence of click sound pressure direction on brain stem responses in children. *Audiology* 19:245–254, 1980.
  97. Osterhammel P: The unsolved problems in analogue filtering on the auditory brain stem responses. *Scand Audiol* 13:69–75, 1981.
  98. Pantev CH and Pantev M: Derived brain stem responses by means of pure-tone masking. *Scand Audiol* 11:15–22, 1982.
  99. Parker DJ and Thornton ARD: The validity of the derived cochlear nerve and brainstem evoked responses of the human auditory system. *Scand Audiol* 7:45–52, 1978.
  100. Parmer AR and Harrison RV: On the contribution of inferior collicular neurones to brainstem evoked responses in the guinea-pig. *Rev Laryngol (Board)*, 105:157–162, 1984.
  101. Picton TW, Hillyard SH, Krauz HJ and Galambos R: Human auditory evoked potentials. I.

- Evaluation of components. *Electroencephalogr Clin Neurophysiol* 36:179–190, 1974.
102. Picton TW, Quellette J, Hamel G and Smith AD: Brainstem evoked potentials to tonepips in notched noise. *J Otolaryngol* 8:289–314, 1979.
  103. Picton TW, Stapells DR and Campbell KB: Auditory evoked potentials from the human cochlea and brainstem. *J Otolaryngol* 10 (Supp. 9): 1–41, 1981.
  104. Prasher DK and Gibson WPR: Brain stem auditory evoked potentials: A comparative study of monaural versus binaural stimulation in the detection of multiple sclerosis. *Electroencephalogr Clin Neurophysiol* 50:247–253, 1980.
  105. Pratt H, Ben-David Y, Peled R, Podoshin L and Scharf B: Auditory brain stem evoked potentials: Clinical promise of increasing stimulus rate. *Electroencephalogr Clin Neurophysiol* 51:80–90, 1981.
  106. Pratt H and Bleich N: Auditory brainstem potentials evoked by clicks in notched-filtered masking noise. *Electroencephalogr Clin Neurophysiol* 53:417–426, 1982.
  107. Pratt H and Sohmer H: Intensity and rate functions of cochlear and brainstem evoked responses to click stimuli in man. *Arch Otorhinol* 211:85–92, 1976.
  108. Rasmussen AT: Studies of the VIIIth cranial nerve of man. *Laryngoscope* 50:67–83, 1940.
  109. Reid A and Thornton ARD: The effect of contralateral masking upon brainstem electric responses. *Br J Audiol* 17:155–162, 1983.
  110. Rhode WS, Oertel D and Smith PH: Physiological response properties of cells labeled intracellularly with horseradish peroxidase in cat ventral cochlear nucleus. *J Comp Neurol* 213: 448–463, 1983.
  111. de Ribaupierre F, Goldstein MH and Yeni-Komshian G: Cortical coding of repetitive acoustic pulses. *Brain Res* 48:205–225, 1972.
  112. Robinson K and Rudge P: Abnormalities of the auditory evoked potentials in patients with multiple sclerosis. *Brain* 100:19–40, 1977.
  113. Robinson K and Rudge P: Wave form analysis of the brainstem auditory evoked potential. *Electroencephalogr Clin Neurophysiol* 52:583–594, 1981.
  114. Rockel AJ and Jones EG: The neuronal organization of the inferior colliculus. I. The central nucleus. *J Comp Neurol* 147:11–60, 1973.
  115. Rose JE, Greenwood DD, Goldberg JM and Hind JF: Some discharge characteristics of single neurons in the inferior colliculus of the cat. I. Tonotopic organization, relation of spike-counts to tone intensity and firing patterns of single elements. *J Neurophysiol* 26: 294–320, 1963.
  116. Rosenhamer HJ and Holmqvist C: Will contralateral white noise interfere with the monaurally click-evoked brainstem response? *Scand Audiol* 12:11–14, 1983.
  117. Rosenhamer HJ, Lindstrom B and Lundborg T: On the use of click-evoked electric brainstem responses in audiological diagnosis. III. Latencies in cochlear hearing loss. *Scand Audiol* 10:3–11, 1981.
  118. Sando I: The anatomical interrelationships of the cochlear nerve fibers. *Acta Otolaryngol* 59:417–436, 1965.
  119. Scherg M and Cramon D: A new interpretation of the generators of BAEP waves I–V: Results of a spatio-temporal dipole model. *Electroencephalogr Clin Neurophysiol* 62:290–299, 1985.
  120. Selters WB and Brackmann DE: Acoustic tumor detection with brainstem electric response audiometry. *Arch Otolaryng* 103:181–187, 1977.
  121. Shanon E, Gold S and Himelfarb MZ: Assessment of functional integrity of brain stem auditory pathways by stimulus stress. *Audiology* 20:65–71, 1981.
  122. Shipley C, Buchwald JS, Norman R and Guthrie D: Brain stem auditory evoked response development in the kitten. *Brain Res* 182:313–326, 1980.
  123. Smith JC, Marsh JT and Brown WS: Far-field recorded frequency-following responses: Evidence for the locus of brainstem sources. *Electroencephalogr Clin Neurophysiol* 39:465–472, 1975.
  124. Sonthheimer D, Caird D and Klinke R: Intra- and extracranially recorded auditory evoked potentials in the cat. II. Effect of interaural time and intensity differences. *Electroencephalogr Clin Neurophysiol* 61:539–547, 1985.
  125. Spire JP, Dohrmann GJ and Prieto PS: Correlation of brain stem evoked response with direct acoustic nerve potential. In: J Courjon, F Mauguière and M Revol (eds) *Clinical Applications of Evoked Potentials in Neurology*. *Adv Neurol*, Vol 32. Raven Press, New York, 159–167, 1982.
  126. Spöndlin H: Primary neurons and synapses. In: I Friedmann and J Ballantyne (eds) *Ultra-*

- structural atlas of the inner ear. Butterworth, London, 133–164, 1984.
127. Starr A and Hamilton AE: Correlation between confirmed sites of neurological lesions and abnormalities of far-field auditory brainstem responses. *Electroencephalogr Clin Neurophysiol* 41:594–608, 1976.
  128. Starr A and Squires K: Distribution of auditory brain stem potentials over the scalp and nasopharynx in humans. *Ann NY Acad Sci* 388:427–442, 1982.
  129. Stockard JJ and Rossiter VS: Clinical and pathological correlates of brain stem auditory responses abnormalities. *Neurology* 27:316–325, 1977.
  130. Stockard JJ, Stockard JE and Sharbrough FW: Nonpathologic factors influencing brainstem auditory evoked potentials. *Am J EEG Technol* 18:177–209, 1978.
  131. Stockard JJ, Stockard JE and Sharbrough FW: Brainstem auditory evoked potentials in neurology: Methodology, interpretation, clinical application. In: MJ Aminoff (ed) *Electrodiagnosis in Clinical Neurology*. Churchill Livingstone, New York 370–413, 1980.
  132. Stockard JE, Stockard JJ, Westmoreland BF and Corfits JL: Brainstem auditory-evoked responses: Normal variation as a function of stimulus and subject characteristics. *Arch Neurol* 36:823–831, 1979.
  133. Stotter WA: An experimental study of the cells and connections of the superior olivary complex of the cat. *J Comp Neurol* 98:401–432, 1953.
  134. Streletz LJ, Katz L, Hohenberger M and Cracco KC: Scalp recorded auditory evoked potentials and somomotor responses: An evaluation of components and recording techniques. *Electroencephalogr Clin Neurophysiol* 43:192–206, 1977.
  135. Strominger NL and Hurwitz JL: Anatomical aspects of the superior olivary complex. *J Comp Neurol* 170:485–498, 1976.
  136. Suzuki T, Hirai Y and Horiuchi K: Auditory brain stem responses to pure tone stimuli. *Scand Audiol* 6:51–56, 1977.
  137. Suzuki T, Kobayashi K and Takagi N: Effect of stimulus repetition rate on slow and fast components of auditory brain-stem responses. *Electroencephalogr Clin Neurophysiol* 65:150–156, 1986.
  138. Suzuki T, Sakabe N and Miyashita Y: Power spectral analysis of auditory brain stem responses to pure tone stimuli. *Scand Audiol* 11:25–30, 1982.
  139. Terkildsen K, Osterhammel P and Huis in't Veld F: Recording procedures for brainstem potentials. *Scand Audiol* 3:415–428, 1974.
  140. Thornton ARD and Coleman MJ: The adaptation of cochlear and brainstem auditory evoked potentials in humans. *Electroencephalogr Clin Neurophysiol* 39:399–406, 1975.
  141. Tsuchitani C: Functional organization of lateral cell groups of the cat superior olivary complex. *J Neurophysiol* 40:296–318, 1977.
  142. Tsuchitani C: Physiology of the auditory system. In: EJ Moore (ed) *Bases of Auditory Brainstem Evoked Responses*. Grunc and Stratton, New York 67–108, 1983.
  143. Tsuchitani C and Boudreau JC: Wave activity in the superior olivary complex of the cat. *J Neurophysiol* 27:814–827, 1964.
  144. Wada S and Starr A: Generation of auditory brain stem responses (ABRs). I. Effects of injecting a local anesthetic (procaine HCl) into the trapezoid body of guinea pigs and cat. *Electroencephalogr Clin Neurophysiol* 56:326–339, 1983a.
  145. Wada S and Starr A: Generation of auditory brain stem responses (ABRs). II. Effects of surgical section of the trapezoid body on the ABR in guinea pigs and cat. *Electroencephalogr Clin Neurophysiol* 56:340–351, 1983b.
  146. Wada S and Starr A: Generation of auditory brain stem responses (ABRs). III. Effects of lesions of the superior olive, lateral lemniscus and inferior colliculus on the ABR in guinea pig. *Electroencephalogr Clin Neurophysiol* 56:352–366, 1983c.
  147. Warr WB: The olivocochlear bundle: Its origin and terminations in the cat. In: RF Naunton and C Fernandes (eds) *Evoked electrical activity in the auditory nervous system*. Academic Press, New York 43–65, 1978.
  148. Yagi T and Kaga K: The effect of the click repetition rate on the latency of the auditory evoked brain stem response and its clinical use for a neurological diagnosis. *Arch Otorhinolaryng* 222:91–97, 1979.
  149. Zöllner C and Pedersen P: Problems of a frequency-specific threshold measurement with the brainstem potentials using the otometric sound pressure signal (damped wavetrain). *Arch Otorhinolaryngol* 226:259–268, 1980.

---

## 6. CLINICAL USE OF EVOKED POTENTIALS: A REVIEW

HAROLD H. MORRIS III, HANS LÜDERS,  
DUDLEY S. DINNER, RONALD P. LESSER,  
ELAINE WYLLIE

### CLINICAL USE OF EVOKED POTENTIALS: A REVIEW

The use of evoked potentials has become widespread in the past ten years. Evoked potentials have probably been obtained in patients with virtually all neurologic diseases. Much has been learned about proper techniques, and the neuropathways involved. Recently, several articles have discussed the use and abuse of evoked potentials in clinical practice [1,2,3,4].

In this chapter I will review the use of evoked potentials in the clinical practice of neurology. For the most part, I will not discuss either the techniques required or the degree of training of the interpreter or technologist. The reader is referred to standard sources for information on these important and basic materials [5, 6].

Patients present to neurologists with multiple symptoms and signs; rather than discussing individual evoked potential tests, this chapter will approach the problem through the clinician's view point.

A not uncommon problem for the neurologist is the symptom of visual disturbance. In this setting, a pattern evoked potential (PEP) can be of significant help if the eye examination is normal or equivocal; however, if an unequivocal afferent pupillary defect is present or definite optic atrophy found, a PEP adds little to the clinical information.

A PEP abnormality is not specific for optic neuritis, or any other specific disease, and may be seen in a wide variety of neurologic problems, including glaucoma, amblyopia exanopsia, ischemic optic neuritis, compression of the

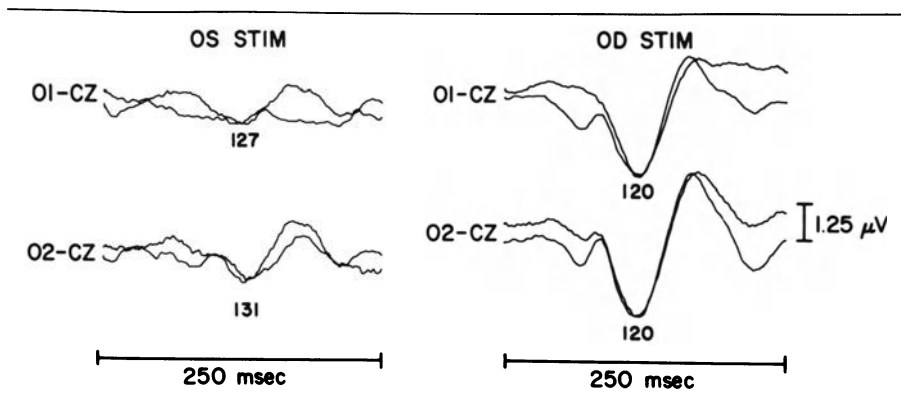


Figure 6-1.

optic nerves at the chiasm, and spinocerebellar degenerations, especially Friedreich's ataxia, and Leber's optic atrophy [5]. Marked (greater than 30 msec) prolongation of the PEP is characteristic of a demyelinating process, however.

PEPs are of greatest clinical usefulness in the evaluation of diseases affecting the optic nerves and/or chiasm.

*Case 1: A 15-year-old male was seen by a neuro-ophthalmologist because of poor vision, OS worse than OD, of one year duration. Examination revealed OD 20/20, OS 20/80 but with correction OS 20/20. There was questionable optic atrophy and a tilted disc OD with a questionable superior temporal quadrantanopsia OD.*

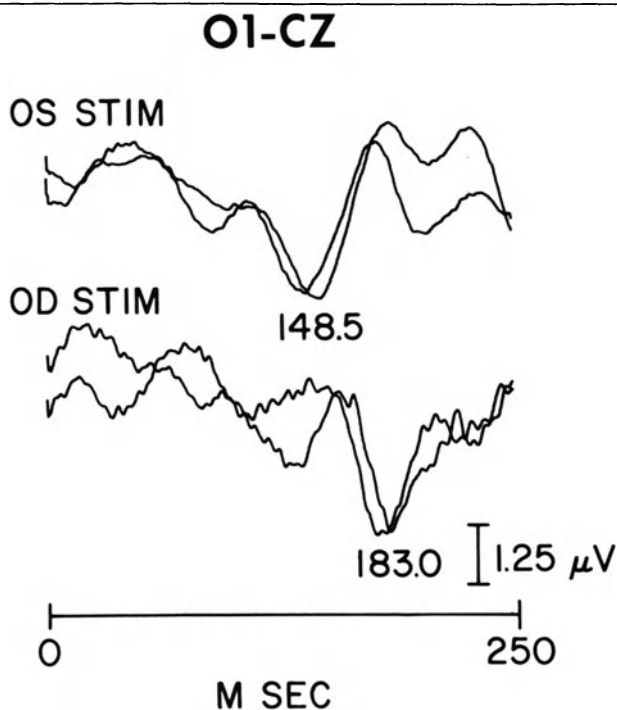
*Discussion: A PEP (figure 6-1) was abnormal showing decreased amplitude and increased P2 latency with OS stimulation strongly suggesting optic nerve pathology in addition to the anisometropia. A CT demonstrated an intrasellar tumor, which proved to be a prolactinoma. This case illustrates the usefulness of the PEP as a screening test for optic nerve pathology, but also emphasizes the nonspecificity of the test.*

While PEP abnormalities certainly occur with tumors, ischemia, and other processes affecting the optic tracts or occipital lobes, these are best evaluated with hemifield stimuli [5]. The methodology required is considerably more demanding for hemifield studies and usually adds little to the information obtained by formal visual fields and modern neuro-imaging techniques.

In Chiappa's [5] literature review, PEPs were abnormal in approximately 90% of patients with optic neuritis, while only about 5% of patients had reversion of the PEP to normal, even with complete clinical recovery. Abnormalities of PEPs were more sensitive than any aspect of a careful neuro-ophthalmologic evaluation. This fact makes the PEP helpful in either confirming the presence of optic neuritis or validating a previous occurrence.

*Case 2: 39-year-old woman was referred because of dizziness and seizures. History suggested an episode of optic neuritis OD six months previously. Examination revealed normal visual acuity,*





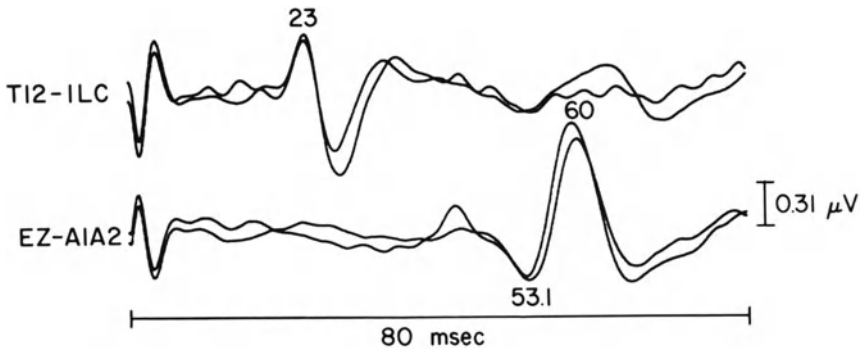
**Figure 6-2.**

*no Marcus Gunn pupil, and questionable optic atrophy OD. Speech was scanning and the gait slightly ataxic and stiff. Sensory examination and muscle stretch reflexes were normal.*

*Discussion: The patient came with a normal CT scan with special views of the posterior fossa; a pattern evoked potential was abnormal (figure 6-2) and confirmed the history of optic neuritis; an AEP was not done, because at most it only would have identified an abnormality in the posterior fossa which was definitely known from the clinical examination. Spinal fluid examination revealed increased IgG synthesis. Diagnosis: multiple sclerosis.*

However, in a very selective group of patients with unilateral (clinical and physiologically) ischemic optic neuropathy or optic neuritis, the PEP was less sensitive than the clinically determined afferent pupillary defect when evaluated six months to 11 years after the original episode. An abnormality of PEP latency was found in 64% of patients with optic neuritis and in only 21% of patients with ischemic optic neuropathy [7].

Following isolated optic neuritis, approximately 20–50% of patients will eventually develop multiple sclerosis (MS) [8]. Short latency somatosensory evoked potentials (SEPs) and brainstem auditory evoked potentials (AEPs) can be used to screen this group of patients for abnormalities in other areas of the nervous system. Tackmann et al. [9] performed SEP's, AEP's and the blink



**Figure 6-3.**

reflex in 32 patients with isolated optic neuritis. Approximately one-third of these patients had evidence of abnormalities in other pathways. Whether detecting these abnormalities is worthwhile from a clinical or a therapeutic standpoint at this time is another question.

*Case 3: A 48-year-old female was seen because of numbness in her legs of three months duration. Historically she experienced optic neuritis OS three years beforehand with full recovery. Her examination was normal except for subjective decrease in vibratory sensation in both legs. Investigations included a normal MRI and auditory evoked potential. A SEP of the posterior tibial nerves revealed slowing of central conduction (figure 6-3). The N20 (23 msec) P2 (53.1 msec) interpeak latency of 30.1 msec (normal mean + 3SD  $\leq$  21 msec) was clearly prolonged. Spinal fluid showed increased IgG synthesis with oligoclonal bands.*

*Discussion: The SEP abnormality served to confirm the sensory complaints and indicated they were of central origin. With the history of optic neuritis of CSF findings a diagnosis of multiple sclerosis was made.*

The patient who complains of blindness but has a normal fundus exam and normal pupillary reflexes poses a difficult problem. Either cortical blindness or functional disease could be present. The cortical generators for P2 are not precisely known, but undoubtedly arise in the primary visual and/or visual association cortex [5]. A lesion in the occipital cortex may be located in such a manner so as to effectively blind the patient, yet enough cortex remains to generate a normal P2 [10]. Most patients with cortical blindness have abnormal PEPs, particularly when small check sizes are utilized. However, Bodis-Wollner et al. [11] reported the case of a 6-year-old cortically blind child who had preserved flash evoked potentials (FEP) and PEPs; CT scans demonstrated destruction of visual association areas with preservation of primary visual cortex (area 17). Cclesia et al. [10] also reported a case of cortical blindness with preserved PEPs and FEPs. Preservation of FEPs in cortical blindness is not uncommon, so this procedure is of limited clinical value in this circumstance [12,13,14,15]. The absence of FEPs would strongly support an organic illness however.

Functional blindness cannot be excluded by the absence of PEPs either. Baumgartner and Epstein [16] reported that control subjects, not infrequently, could voluntarily abolish or delay the latency of the PEP by meditation, day-dreaming, or convergence. Morgan et al. [17] found 11 of 42 normal subjects were able to voluntarily either extinguish or make uninterpretable a pattern PEP; these subjects were unable to alter a FEP.

Monitoring of visual function over a period of time with serial PEPs in MS is not clinically helpful. Improvement and worsening of vision do not precisely correlate with PEP changes [18, 19, 20, 21]. The value of monitoring PEP's in experimental treatment protocols of MS is unknown at this time. The test does provide quantifiable reproducible results, however, and therefore would be expected to be of some utility in this circumstance.

On the other hand, monitoring visual function with PEPs during treatment with ethambutol has resulted in detecting subclinical deterioration of the PEP, which improved upon stopping treatment [22]. Monitoring PEP during treatment may prove beneficial for other drugs with known toxic effects on the optic nerve but this use has not been fully explored.

Another large group of patients present with complaints of vertigo, tinnitus, decreased hearing, or ataxia. Obviously the clinician is dealing with pathology in the cochlea, 8th cranial nerve, or posterior fossa.

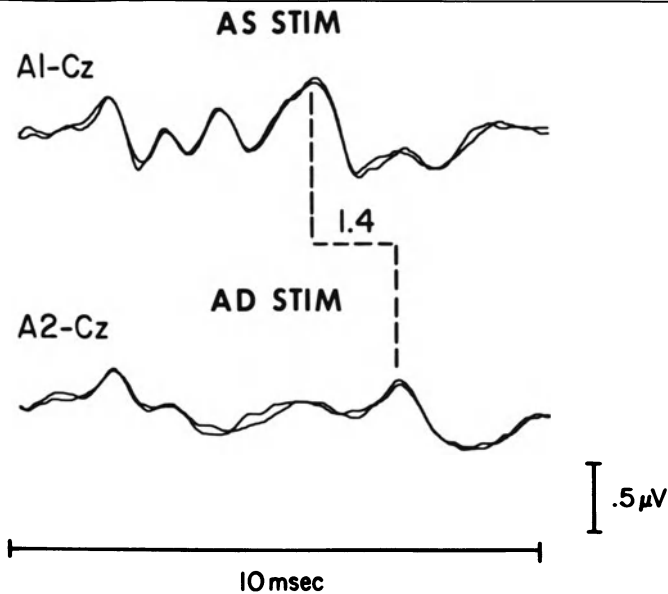
The short latency brain stem auditory evoked potential can be of help in some of these situations. As with the PEP, the AEP does not produce disease specific abnormalities but it does have good (but not exact) localizing value. For example, in the patient with vertigo and nystagmus, if the AEP demonstrates abnormalities of waves III or V, the pathology is either primarily or secondarily affecting the pons and/or the midbrain. Peripheral auditory disorders producing vertigo and nystagmus basically do not produce changes in the AEP interpeak latencies.

If the clinical problem is to exclude an acoustic neuroma, the AEP is the most sensitive nonradiographic test [23, 24, 25], with an overall abnormality rate of 96% in Hart's review.

*Case 4: A 19-year-old male complained of decreased hearing and tinnitus in the right ear. His examination was normal and there was no family history of neurofibromatosis. An audiogram was normal but auditory evoked potentials showed a clear increase in the I-V interpeak latency with right ear stimulation (figure 6-4). Magnetic resonance imaging (MRI) revealed a 1.5 cm acoustic neuroma on the right. Pathologic diagnosis was schwannoma.*

*Discussion: The auditory evoked potential is clearly abnormal demonstrating the sensitivity of the procedure in detecting acoustic neuromas. Fourth generation CT scans also are very sensitive in detecting these lesions and one would expect the MRI to be even better. The MRI provides anatomic detail and provides more specific information than does the AEP.*

Chiappa and Parker [25] found 100% of 41 patients with acoustic neuromas had abnormal AEPs while several of these patients had normal CT scans. Fourth generation CT scanners have improved the diagnostic yield to over 90% [24] and also provide a considerable degree of additional information



**Figure 6-4.**

about the posterior fossa and cerebellar pontine angle. To obtain the high yield reported by Chiappa and Parker, it is necessary to accurately identify wave I, in order to measure the interpeak latencies. They have used needle electrodes in the external auditory canal for this purpose [25].

In patients with long tract signs and cranial nerve abnormalities suggesting posterior fossa disease, the AEP can be used as a screening test. For example, a normal AEP essentially excludes a diagnosis of brainstem glioma [23].

*Case 5: A 7-year-old was seen with a two year history of right facial weakness and occasional vomiting. His examination revealed decreased sensation on the right side of his face, a decreased gag reflex on the right, and left hyperreflexia. Neuroimaging revealed a brainstem lesion. AEP (figure 6-5) showed absence of waves II-V with right ear stimulation. Biopsy of the lesion yielded a diagnosis of a low grade astrocytoma.*

*Discussion: This AEP was interesting but basically contributed very little to the patient's diagnosis or management. While the AEP is invariably abnormal in patients with brainstem gliomas (see text) it clearly is not as helpful as the MRI in this situation.*

On the other hand, since the AEP is nonspecific, it adds little to the clinical evaluation with the patient with a known brainstem pathology (for example, in a patient with definite internuclear ophthalmoplegia). In the author's opinion, an MRI would provide more useful diagnostic information in this clinical circumstance. If the patient with the brainstem abnormalities is suspected of having multiple sclerosis, more useful information would be

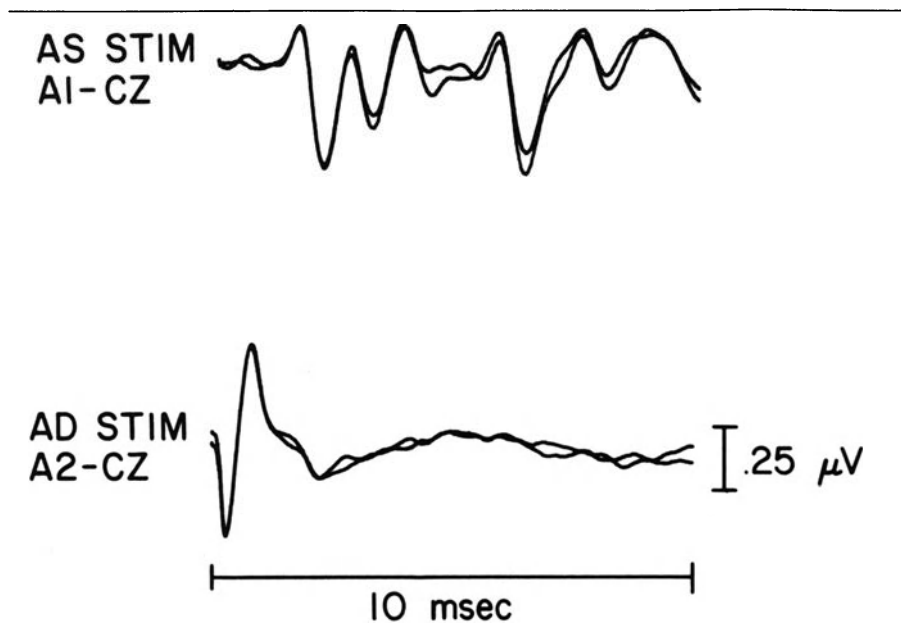


Figure 6-5.

gained from a PEP and/or a SEP; since an abnormality in these studies would demonstrate a second lesion.

*Case 6: 37-year-old female with a 3 year history of "tic-like" facial pain and paresthesias. There was also a previous history of an episode of blurred vision six months previously. Her examination was normal except for questionable optic atrophy OS. A pattern evoked potential was markedly abnormal with a delayed P2 bilaterally (figure 6-6) and CSF examination revealed increased IgG synthesis and oligoclonal bands.*

*Discussion: An AEP in this instance would have supported the clinical history suggesting a posterior fossa abnormality but a PEP was of more clinical usefulness as it documented the history of optic neuritis.*

In patients with brainstem infarcts, central pontine myelinolysis and other disease affecting the pons and/or the midbrain the AEP or SEP frequently is abnormal; this information, however, since it is nondiagnostic, is of limited clinical use.

Conversely in the patient with suspected multiple sclerosis who has no clinical evidence of brainstem abnormality an AEP may be useful but will show abnormalities in only 20% of patients with probable or possible multiple sclerosis [23].

Strange sensory symptoms are common complaints heard by neurologists. Usually the clinician can decide by history and examination if the complaints

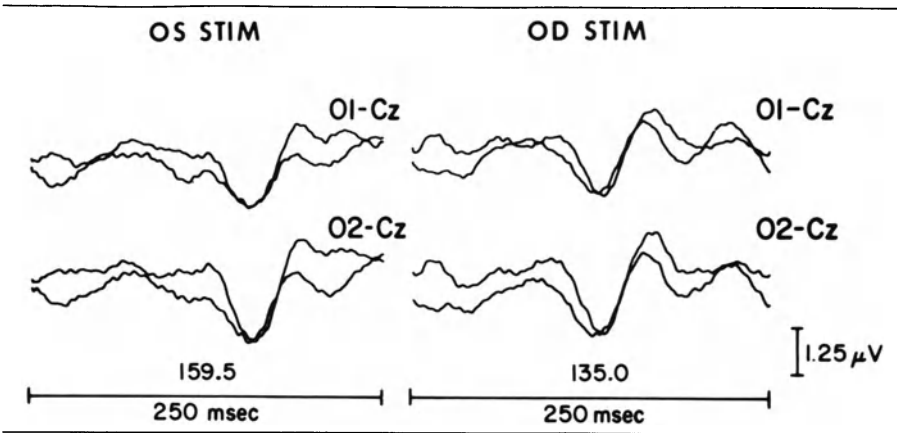


Figure 6-6.

reflect pathology in the peripheral nervous system, the central nervous system, or are functional. SEPs are of value when the presence or site of pathology are unknown.

As with other evoked potentials, changes in SEPs are not disease specific. They are of value in localizing pathology. Diseases affecting myelin tend to produce greater abnormalities in latency and axonal pathology usually is reflected in amplitude changes. As currently practiced clinically, SEPs are obtained by electrical stimulation of peripheral nerves, most commonly the median and posterior tibial. Investigations into more specific sensory stimuli, such as tendon taps, touch, etc., is being done and may prove to be of clinical benefit in the future [26].

The N20 (posterior tibial nerve) and N12 (median nerve) waves are the dorsal cord negative potentials in the appropriate cord segments. P27 (posterior tibial nerve) and P13 (posterior median nerve) are the standing waves originating from the cervical medullary junction. N1 and P2 are the potentials generated by arrival of the signal at the primary sensory cortex. Knowing the inter-peak latency differences may allow localization to peripheral nervous system, spinal cord, brain stem, and cortex. The primary pathway for conduction of somatosensory potentials in the spinal cord is the dorsal column.

A patient's sensory complaints are not necessarily invalidated by a normal SEP since the pathway is via large myelinated peripheral axones and the dorsal columns. On the other hand, an abnormal study does, without question, add validity and localization to the symptoms.

*Case 7: 10-year-old male had progressively severe ataxia and scoliosis of five years duration. Neurologic examination revealed scoliosis, areflexia, decreased vibratory sensation, ataxia, and pes cavus. Nerve conduction measurements were normal except for decreased sensory, action potential amplitude. A SEP (figure 6-7) revealed a normal N20 (21.9 msec, dorsal cord potential) and P27 (29.1 msec, arrival of impulse at foramen magnum) and delayed cortical potentials.*

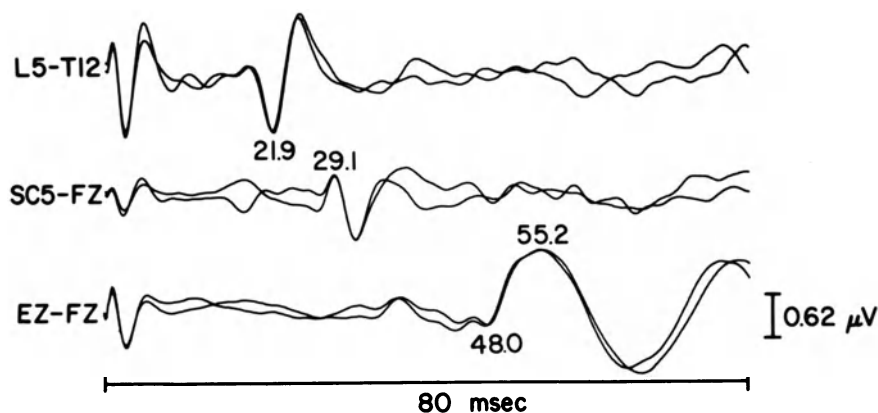


Figure 6-7.

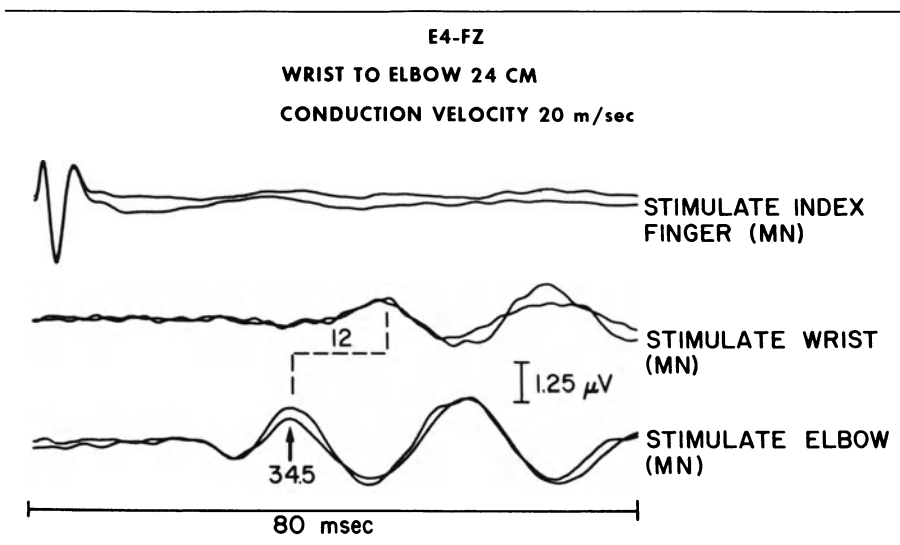
(P2 48.0; N2 55.2 msec). This study confirmed an abnormality in the central somatosensory pathways and supported a diagnosis of spinocerebellar degeneration.

While SEPs may be of occasional benefit in the evaluation of diseases of the peripheral nervous system, for the most part, the information gained has been disappointing. Theoretically, SEPs should provide information on proximal conduction velocity in the Guillain-Barre Syndrome. In actuality, however, the degree of information over and above that from conventional electromyography is small. In a similar vein, the routine use of SEPs for radiculopathies and thoracic outlet syndrome is also of limited value [27].

In patients with neuropathies, sensory conduction velocity can be estimated even when no sensory action potential can be seen with standard nerve conduction measurements. To measure this, the differences in latency of the central waves (P2, N2) are measured following stimulation at proximal and distal locations in the extremity being tested. The distance between the two stimulation sites is divided by the latency difference to obtain conduction velocity. This technique is made possible without being able to record peripheral sensory action potentials because of central amplification of the signal.

*Case 8: A 52-year-old male had sensory complaints of two years duration. Examination demonstrated distal sensory loss. Motor nerve conductions were normal; sensory showed either an absent or reduced amplitude sensory action potential. Median nerve SEPs (figure 6-8) obtained by stimulating the median nerve at the wrist and elbow allowed the conduction velocity to be calculated and was 20 msec. No potentials were recorded with stimulating the median nerve at the finger.*

Clinically, in the patient with a known myelopathy, SEP, abnormalities are probably of limited practical value, and more useful information obtained with a PEP or AEP if one is trying to exclude MS. Obviously a MRI scan of the



**Figure 6-8.**

brain and spinal cord would provide considerably more information if a structural abnormality was in question.

*Case 9:* 72-year-old female experienced a progressive gait disturbance of two years duration. Her examination revealed impaired vibratory sense, brisk knee jerks, absent ankle jerks, and bilateral Babinski reflexes. CBC, B12, folic acid levels and myelogram were normal. PEP (figure 6-9) showed P2 to be significantly delayed bilaterally. CSF examination showed increased IgG synthesis.

*Discussion:* An SEP would have only confirmed the clinical findings. The abnormal PEP provided the clinician with a second lesion and supported a diagnosis of multiple sclerosis.

SEPs certainly demonstrate abnormalities in patients with tumors, infarcts, and other structural abnormalities of the brain stem or cerebral hemisphere. For the most part however, they only support the information available from other clinical and neuroimaging techniques.

*Case 10:* 29-year-old male with von Hippel-Lindau syndrome complained of left arm and leg numbness of one year duration. Six years previously a cerebellar hemangioblastoma was removed. Examination revealed decreased sensation of the left arm and leg and mild left dysmetria. MRI identified a cystic cavity at C6; angiography showed multiple hemangioblastomas of both cerebellar hemispheres and the cervical spinal cord. Median nerve SEP (figure 6-10) revealed marked decrease in amplitude of P13 and the cortical components with left median nerve stimulation.

*Discussion:* The SEP did not add localizing information to the neuroimaging studies but gave a baseline record for SEP monitoring during removal of the cervical cord lesions. No adverse changes in the SEP occurred while monitoring and the patient's neurological status was unchanged after the operation.



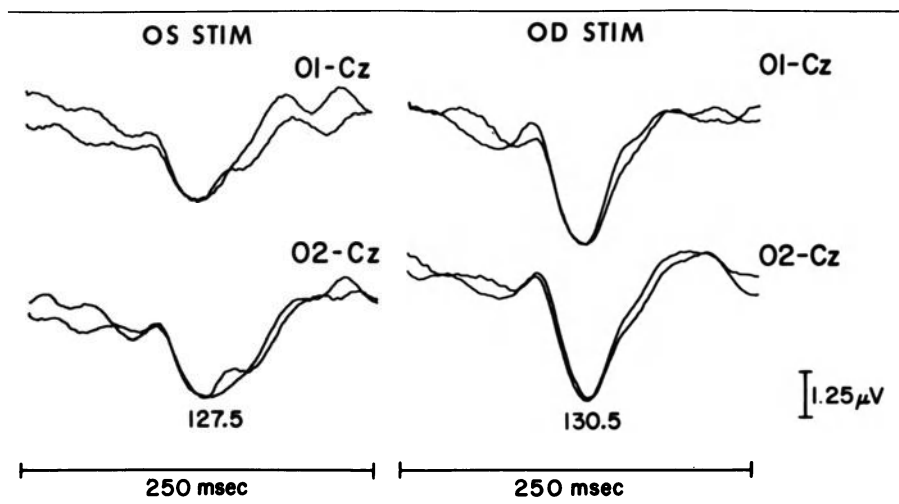


Figure 6-9.

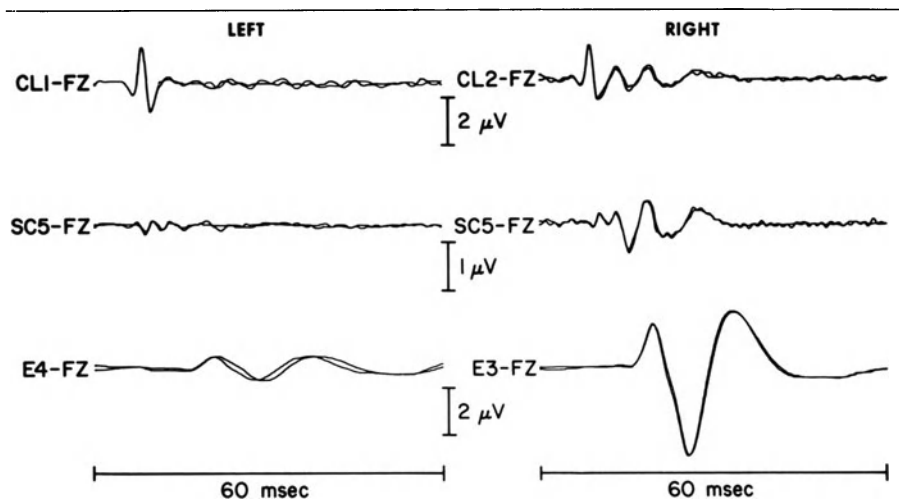


Figure 6-10.

One exception, however, might be the differential diagnosis of primary lateral sclerosis (SEPs usually normal) and the patient with progressive myelopathy due to MS when the symptoms and signs are purely motor (SEPs frequently abnormal). SEPs may be abnormal in pernicious anemia and would not help to clinically distinguish that process from MS (neither would PEPs!).

Monitoring sensory function with serial PEPs over time in patients with

known MS is of limited clinical value because the clinical course of patients does not closely correlate with changes in SEPs [18, 21, 28]. As previously mentioned, serial SEPs may provide useful data in experimental treatment protocols of multiple sclerosis. They are almost the only method of quantifying sensory abnormalities.

The detection of asymptomatic lesions in patients suspected of having MS has been an important indication for evoked potential studies. Recent studies have been published [29, 30] comparing MRI, CSF examination, and evoked potential data, in patients with definite, probable, and possible multiple sclerosis. In both studies, a total of 65 patients, the single most sensitive test in detecting an abnormality was the MRI which showed lesions in 94% of these patients. Unfortunately, MRI findings in multiple sclerosis are also nonspecific. Which and how many diagnostic tests are appropriate to obtain in the evaluation of a patient suspected of having multiple sclerosis is not answerable at this time.

The ability to monitor neurologic function in anesthetized patients would be of definite clinical usefulness. Ideally, the data could be easily obtained, be free of electrical and other operating room artifact; be quickly collectible, and give the surgeon advanced warning of potential neurologic complications in time for the procedure to be altered and the complication avoided. Unfortunately these goals have not been achieved with current evoked potential technology and procedures.

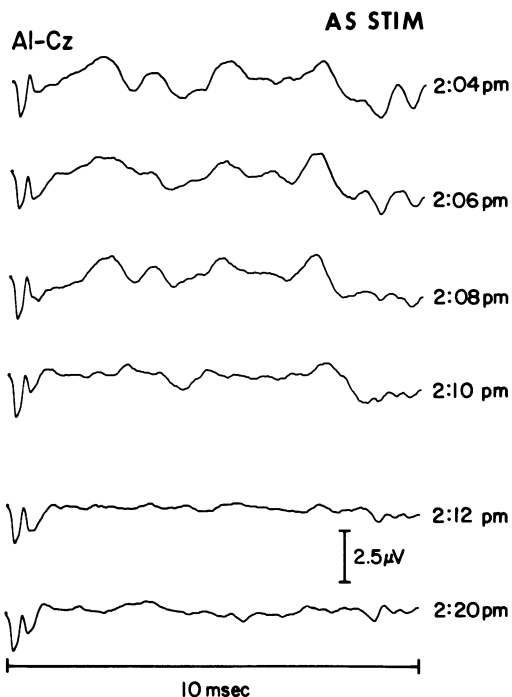
Monitoring visual function during neurosurgical procedures near the optic nerves and/or chiasm utilizing FEPs has been studied, but marked instability, false positive and false negative results make the value of this technique suspect at this time [31].

Raudzens [31] monitored brainstem and auditory function with AEPs in 66 patients undergoing posterior fossa surgery for a variety of lesions. In no case were significant hearing problems present postoperatively when there had been no significant AEP change. Conversely, all patients with significant AEP change during the procedure had definite hearing impairment postoperatively.

Our experience has been similar, a significant intraoperative change in the AEP (e.g., loss of all waves) accurately predicts loss of neurologic function (e.g., deafness). Only rarely does the monitoring give immediate information to the surgeon allowing alteration of the procedure in time to prevent hearing loss.

*Case 11: A 36-year-old female presented with numbness of the left side of her face. Examination revealed only decreased sensation over the left trigeminal nerve distribution. CT scan revealed a left tentorial tumor. Intraoperative monitoring of the AEP (figure 6-11) was done during removal of the tumor (a meningioma). During the procedure, the AEP suddenly vanished (2:12PM) and did not return. Postoperatively the patient had left sided deafness.*

*Discussion: As is frequently the case, the AEP was easily recorded during the surgical procedure and did indicate an adverse change and correctly predicted a postoperative hearing loss.*



**Figure 6-11.**

*Commonly, however, this change occurs suddenly and irreversibly and therefore is of limited immediate benefit to the surgeon.*

Monitoring spinal cord function can be done with SEPs. Again, the theory is that if significant changes occur, the surgeon can alter the operation (e.g., release distraction in scoliosis surgery) and prevent neurologic complications. The problem is that changes in anesthesia and other parameters also affect SEPs in terms of both latency and amplitude producing false positives. In our retrospective study [32] of 121 patients undergoing surgery for scoliosis, two patients had significant alteration of SEPs; in one patient, no change in the operation was made by the surgeon and the patient was without neurologic deficit afterwards; the other patient became paraplegic postoperatively despite immediate release of distraction by the surgeon.

*Case 12: 15-year-old male experienced progressive scoliosis and dystonia. Neurologic examination was normal except for the dystonia and scoliosis. SEP with posterior tibial nerve stimulation monitoring (figure 6-12) was done during surgical scoliosis correction. At time of distraction there was a sudden loss of spinal cord potentials (11:16AM) at T1/T2 (needle electrodes inserted intraoperatively) and cortical potentials at EZ; the spinal potential below the distraction at*

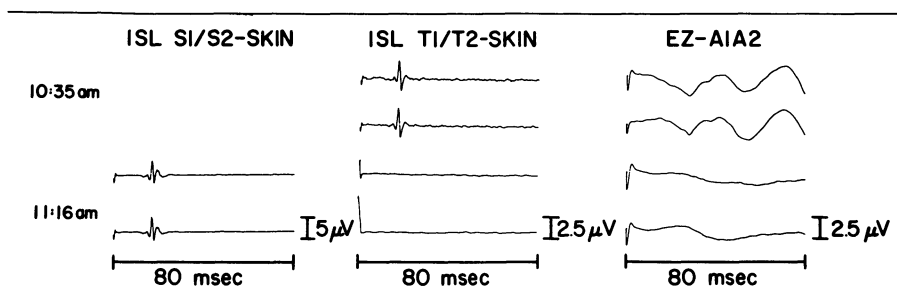


Figure 6-12.

*S1/S2 (intraoperative needle electrode) could still be recorded. The potentials did not return despite release of the distraction and the patient was paraplegic postoperatively.*

*Discussion: The adverse evoked potential change occurred suddenly and was not reversible. Even though the surgeon immediately released the distraction, the damage had been done and occurred without apparent warning. This sequence of events illustrates one of the problems with surgical monitoring of SEPs as it is currently practiced.*

Raudzens [31] noted considerable technical difficulty in monitoring SEPs during surgical procedures. One of the 31 cases possibly had a neurological complication prevented by monitoring during cervical cord decompression. Overall, the yield from SEP monitoring is low and the degree of benefit unproven.

These criticisms of evoked potential monitoring do not mean the technique is of no value. No other technique has the capability of monitoring neural structures in the anesthetized patient. Prevention of a devastating deficit such as paraplegia in even a few cases is worthwhile. The shortcomings indicate the need for improving and extending monitoring procedures so that: 1) information can be more quickly gathered (i.e., fewer stimuli) thereby allowing adverse change to be detected almost immediately, and 2) by monitoring additional pathways (e.g., motor pathways in the spinal cord).

Evaluation of the comatose patient with evoked potentials can, in certain instances, provide clinically useful information. AEPs are resistant to alteration with anesthetics and metabolic disturbances; this fact makes the test valuable in selected patients with coma when the differential diagnosis is between a metabolic/toxic etiology or a structural brainstem lesion [33].

*Case 13: 13-year-old female admitted for status epilepticus. Thiopentothal coma was required to stop the seizures. During the coma, the EEG revealed low amplitude burst suppression. An AEP (figure 6-13) revealed presence of waves I and V bilaterally.*

*Discussion: This AEP was done for interest only and demonstrates the persistence of the AEP in the face of deep metabolic coma.*

In brain death wave I of the AEP is absent in approximately 77% of the patients [34]. In this situation, no conclusions about brainstem integrity can

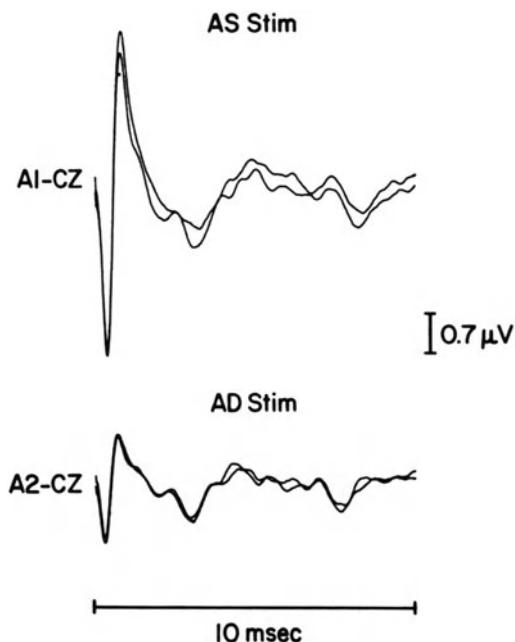


Figure 6-13.

be made because one cannot determine whether or not the auditory signal actually reached the brainstem.

As with AEPs, SEPs are markedly resistant to toxic and metabolic disturbances severe enough to produce deep coma. Because of this fact, they may also be used to evaluate the somatosensory pathways in comatose individuals as well as give prognostic information. In brain death, SEPs are absent above the medulla in all cases, but the P13 is present in 69% of brain dead individuals [34]. These findings indicate the stimulus reached the cervicomedullary region before transmission ceased. In Goldie's study, all patients with N1 and P2 absent bilaterally either died or entered into a chronic vegetative state. All 8 patients died in Hume's and Cant's study [35] with bilaterally absent N1, P2 after median nerve stimulation. Similar results were found in the Frank et al. [36] study of 5 anoxic children. All children who had absent N1, P2 waves with median nerve stimulation and preserved AEPs entered into a chronic vegetative state.

Severely abnormal or absent FEPs are also good predictions of poor outcome from severe closed head injury and correlated well with known clinical parameters of poor outcome [37]. Under circumstances such as barbiturate coma or neuromuscular blockade, this information may prove to be of value.

There are certain general principles which address the clinical utility of evoked potentials: The first concept is to think of the evoked potential as an extension of the neurological examination. If a definite abnormality is found

on examination, an evoked potential can only confirm its presence and thereby adds little information. The exception to this statement is the somatosensory pathway in which the SEP may be able to help localize the lesion responsible for the signs or symptoms.

The second guideline is applicable to those circumstances in which an anatomical lesion (e.g., tumor) should be excluded. In this situation radiographic studies such as MRI and CT give more information about location, site, and the nature of the lesion, and should be done before evoked potentials are obtained.

Thirdly, the fact that an evoked potential study is likely to be abnormal in a clinical circumstance (e.g., AEP in brainstem glioma or PEP in optic atrophy) does not imply that the study should be done.

Lastly, it should be realized that when obtaining tests with normality based on statistical parameters, the more tests ordered, the more likely one is to obtain an abnormal result—even in a normal population.

In closing, evoked potentials can provide reproducible measurements of neurophysiologic function. When obtained appropriately, they give information not currently available by other techniques. However, the practice of obtaining a routine evoked potential battery in the evaluation of patients with neurologic disease must be condemned.

## REFERENCES

1. Eisen A, Cracco RQ: Overuse of evoked potentials: Caution. *Neurology* 33:618–621, 1983.
2. Menken M: Consequences of an oversupply of medical specialists: The care of neurology. *N Engl J Med* 308:1224–1226, 1983.
3. Chiappa HK, Young RR: Evoked responses: Overused, underused, or misused. *Arch Neurol* 42:76–77, 1985.
4. Kimura J: Abuse and misuse of evoked potentials as a diagnostic test. *Arch Neurol* 42:78–79, 1985.
5. Chiappa K: *Evoked Potentials in Clinical Medicine*. New York, Raven Press, 1983.
6. American Electroencephalographic Society. Guidelines for clinical evoked potential studies. *J Clin Neurophysiol* 1:3–53, 1984.
7. Cox TA, Thompson HS, Hayreh SS, Snyder JE: Visual evoked potential and papillary signs: A comparison in optic nerve disease. *Arch Ophthalmol* 100:1603–1607, 1982.
8. Miller NR: Optic Neuritis in Walsh and Hoyt's *Clinical Neuro-ophthalmology*, 4th ed Vol. 1; Williams and Wilkins, Baltimore, pp 227–248, 1982.
9. Tackmann W, Ettl TH, Strenge H: Multimodality evoked potentials and electrically elicited blink reflex in optic neuritis. *J Neurol* 227:157–163, 1982.
10. Celesia GC, Polcyn RD, Holden JE, Nickles RJ, Gatley JS, Koeppel RA: Visual evoked potentials and positron emission tomographic mapping of regional cerebral blood flow and cerebral metabolism: Can the neuronal potential generators be visualized? *Electroencephalogr Clin Neurophysiol* 54:243–256, 1982.
11. Bodis-Wollner I, Atkin A, Raab E, Wolkstein M: Visual association cortex and vision in man: Pattern-evoked occipital potentials in a blind boy. *Science* 198:629–630, 1977.
12. Duchowney MS, Weiss IP, Majlessi H, Barnett AB: 1974 Visual evoked responses in childhood cortical blindness after head trauma and meningitis. *Neurology* 24:933–940, 1974.
13. Hess CW, Meienberg O, Ludin HP: Visual evoked potentials in acute occipital blindness. *J Neurol* 277:193–200, 1982.
14. Spehlmann R, Cross RA, Ho SU, Leestma JE, Norcross KA: Visual evoked potentials and postmortem findings in a case of cortical blindness. *Ann Neurol* 2:531–534, 1977.
15. Frank Y, Torres F: Visual evoked potentials in the evaluation of "cortical blindness" in children. *Ann Neurol* 6:126–129, 1979.

16. Baumgartner J, Epstein CM: Voluntary alteration of visual evoked potentials. *Ann Neurol* 12:475–478, 1982.
17. Morgan RK, Nugent B, Harrison JM, O'Conner PS: Voluntary alteration of pattern visual evoked responses. *Ophthalmology* 92:1356–1363, 1985.
18. DeWeerd AW, Jonkman EG: Changes in visual and short latency somatosensory evoked potentials in patients with multiple sclerosis. In: *Clinical Applications of Evoked Potentials in Neurology*. Raven Press, New York, pp 527–534, 1982.
19. Confavreux C, Maugviere F, Courjon J, Aimand G, Devic M: Course of visual evoked potentials in multiple sclerosis: Electroclinical correlations and pathophysiological considerations in 25 patients. In: J Courjon, F Mauguière and M Revol (eds): *Clinical Applications of Evoked Potentials in Neurology*. Raven Press, New York, pp 541–550, 1982.
20. Cohen SN, Sydulko K, Hansch E, Tourtellotte WE, Potvin AR: Variability on serial testing of visual evoked potentials in patients with multiple sclerosis. In: *Clinical Applications of Evoked Potentials in Neurology*. Raven Press, New York, pp 559–565, 1982.
21. Aminoff MJ, Davis SL, Panitch HS: Serial evoked potential studies in patients with definite multiple sclerosis: Clinical relevance. *Arch Neurol* 41:1197–1202, 1984.
22. Yannikas C, Walsh JC, McLeod JG: Visual evoked potentials in the detection of subclinical optic toxic effects secondary to ethambutol. *Arch Neurol* 40:645–648, 1983.
23. Chiappa K: Brainstem auditory evoked potentials: Interpretation. In *Evoked Potentials in Clinical Medicine*. New York, Raven Press, pp 144–202, 1983.
24. Hart RG, Gardner DP, Howieson J: Acoustic tumors: Abnormal features and recent diagnostic tests. *Neurology* 33:211–221, 1983.
25. Chiappa KH, Parker SW: Diagnosis of acoustic tumors. *Neurology* 34:131, 1984.
26. Cohen LG, Starr A, Pratt H: Cerebral somatosensory potentials evoked by muscle stretch, cutaneous taps and electrical stimulation of peripheral nerves in the lower limbs in man. *Brain* 108:103–121, 1985.
27. Yiannikas C, Plexopathies and radiculopathies. In Chiappa K (ed): *Evoked Potentials in Clinical Medicine*. New York, Raven Press, 1983, pp 278–286.
28. Matthews WB, Small DG: Serial recordings of visual and somatosensory evoked potentials in multiple sclerosis. *J Neurol Sci* 40:11–21, 1979.
29. Kirshner HS, Tsai SI, Runge VM, Price AC: Magnetic resonance imaging and other techniques in the diagnosis of multiple sclerosis. *Arch Neurol* 42:859–863, 1985.
30. Gebarski SS, Gabrielsen TO, Gilman S, Knare JE, Latack JT, Aisen AM: The initial diagnosis of multiple sclerosis: clinical impact of magnetic resonance imaging. *Ann Neurol* 17:469–474, 1985.
31. Raudzens PA: Intraoperative monitoring of evoked potentials. *Ann NY Acad Sci* 388:308–326, 1982.
32. Dinner DS, Lüders H, Lesser RP, Morris HH: Invasive methods of somatosensory evoked potential monitoring. *J Clin Neurophysiol* 3:113–130, 1986.
33. Starr A, Achor LJ: Auditory brainstem responses in neurological diseases. *Arch Neurol* 32:761–768, 1975.
34. Goldie WD, Chiappa KH, Young RR, Brooks EG: Brainstem auditory and short-latency somatosensory evoked responses in brain death. *Neurology* 31:248–256, 1981.
35. Hume AL, Cant BR: Central somatosensory condition after head injury. *Ann Neurol* 10:411–419, 1981.
36. Frank LM, Furgivele TL, Etheridge JE: Prediction of clinic vegetative state in children using evoked potentials. *Neurology* 35:931–934, 1985.
37. Anderson DC, Bundlic S, Rockswold GL: Multimodality evoked potentials in closed head trauma. *Arch Neurol* 41:369–374, 1984.

---

## 7. EVOKED POTENTIALS IN MULTIPLE SCLEROSIS AND OPTIC NEURITIS

KEITH H. CHIAPPA

Multiple Sclerosis (MS) is a demyelinating disease of the CNS characterized by foci of myelin destruction with relative preservation of axons and nerve cell bodies. Central myelin is formed by extensions of the cytoplasmic membrane of oligodendrocytes which wrap around the axon, resulting in concentric layers of lipid and protein. The acute MS plaque shows myelin breakdown and inflammation with perivenous infiltrates of mononuclear cells and lymphocytes; older lesions contain microglial phagocytes and reactive astrocytes. Inactive lesions (sclerotic plaques) contain relatively acellular fibroglial tissue (gliosis) and show loss of axis cylinders [53]. The pathogenesis of MS is unknown although this is a very active research area [62].

The biochemistry and electrophysiology of nerve conduction with normal and abnormal myelination have been well-studied. Waxman [107], Waxman and Ritchie [108], Rasminsky [83], Sears and Bostock [92], and Sedgwick [93] provide excellent reviews of pertinent topics. Although these principles provide a starting point for understanding EP abnormalities seen in patients with demyelinating diseases the generation of evoked potentials (EPs) often involves complex physiologic mechanisms whose response to partial anatomic and physiologic lesions is difficult, if not impossible, to predict or understand. These considerations will be discussed as they pertain to each EP modality.

The clinical utility of EPs in MS is based on their ability: 1) to demonstrate abnormal sensory system function when the history and/or neurological examination are equivocal, 2) to reveal the presence of clinically-unsuspected



malfunction in a sensory system when demyelinating disease is suspected because of symptoms and/or signs in another area of the central nervous system (CNS), 3) to help define the anatomic distribution of a disease process, and 4) to monitor objective changes in a patient's status. Although some of the information they provide is similar to that elicitable at the bedside by an experienced clinician, these tests are very helpful in the evaluation of patients with suspected demyelinating disease because: 1) they provide data unobtainable without the use of amplifiers and oscilloscopes, 2) they quantify and objectify data which the clinician may only sense, and 3) they can localize lesions within a pathway whereas clinicians often cannot.

Pattern-shift visual (PSVEP), brainstem auditory (BAEP) and short-latency somatosensory evoked potentials (SEPs) are the EP tests most commonly studied in patients suspected of having demyelinating disease. Latencies and amplitudes of the various waves provide numerical data; sometimes the absence of a wave or an abnormal configuration of its potential field also provides useful information.

#### **PATTERN-SHIFT VISUAL EVOKED POTENTIALS (PSVEPS)**

The PSVEP is obtained with a reversing checkerboard pattern and recorded from the scalp overlying visual cortex where a prominent positive peak, appearing at about 100 msec in normal subjects (P100), is used for clinical interpretation. The major change associated with optic nerve demyelination is prolongation of P100 latency. The mean latency in MS patients in a representative study exceeded the normal mean by about 10 msec (possible MS) to 30 msec (definite MS) [9], while delays exceeding 100 msec have also been reported [94].

Interocular latency difference is probably the most sensitive indicator of optic nerve dysfunction in the PSVEP and has been used to provide evidence of optic nerve pathology [37, 94]. Failure to utilize this parameter in a comparative study of flight of colors (FOC) testing versus PSVEPs [101] resulted in erroneously low sensitivity of the PSVEP. Rolak [89] used the interocular latency difference parameter and found that although FOC testing compared favourably with PSVEPs, it was less sensitive. Shahrohki et al. [94] found that 8 of 100 ON and MS patients had abnormal PSVEPs based on this parameter alone.

Amplitude of P100 has not proven to be a reliable measure, presumably because of the relatively large normal variability of amplitude. Matthews et al. [57] reported that 3 of 110 definite MS patients had abnormal PSVEPs on the basis of amplitudes less than 4 mv. Shahrohki et al. [94] found only 1% of 149 patients who were abnormal in this measure. Halliday et al. [32] and Halliday and McDonald [33] noted that amplitude was correlated with visual acuity whereas latency was not.

The duration and shape of P100 has also been investigated [15, 37, 94]. Isolated abnormalities in these parameters are relatively uncommon, and when

present are usually associated with P100 latency abnormalities. An explanation for these findings has been provided by Riemslog et al. [85] who stimulated different segments of the visual field with varying time separations between stimuli. When the stimulus onset asynchrony was 40 msec or less, no contribution from the second stimulus could be identified in the recorded response. This suggests that the relative preservation of P100 shape and duration in partial optic nerve demyelination is due to inhibition of the late arriving impulses which had traversed the abnormally conducting segments. In the experimental situation, even when the initial stimulus comprised only 25% of the visual field and the later stimulus comprised 75%, the first suppressed the second. Thus, in the partially demyelinated optic nerve, the healthiest fibers determine the latency and shape of the response and, if the response is delayed, a majority of the fibers must be involved.

PSVEPs provide a sensitive extension of the clinical examination and commonly used clinical tests (visual acuity, clinical and formal visual fields, pupillary responses, fundoscopic examination, and red color desaturation). To demonstrate the relative sensitivity of the PSVEP, 198 patients with multiple sclerosis who had had PSVEP testing were studied retrospectively by extracting pertinent aspects of the neuroophthalmologic examination from their medical records [6]. When the PSVEP was normal, there was never an abnormality found on the clinical examination. Even when the PSVEP was abnormal, various clinical examinations were often normal. For example, in those patients with abnormal PSVEPs, the visual fields by usual clinical examination (confrontation) were normal in 96%, formal fields were normal in 55%, pupillary responses were normal in 74%, fundus appearance was normal in 39% and there was no red color desaturation in 27% (only 22 patients had this test reported). These figures convey the degree of sensitivity that the test can add to the routine clinical ophthalmological examination. However, if the formal visual field examination is done carefully, a greater incidence of clinical abnormalities can be found even in asymptomatic patients [48, 66, 70, 78, 105] although it never matches that of the PSVEP.

Despite the sensitivity of the PSVEP, the abnormalities produced by the demyelinating plaques of optic neuritis and MS are indistinguishable from abnormalities produced by many other retinal, compressive and degenerative diseases. Thus, abnormal findings demonstrated by the PSVEP must be carefully integrated into the clinical situation by a physician familiar with the clinical use of this test. He or she must decide if other procedures (e.g., electroretinography, formal visual fields, radiologic studies, subspecialty consultation) are indicated to differentiate the possible causes of the conduction delay. Blumhardt [3] has evaluated the role of PSVEPs in the early diagnosis of MS and has reiterated the point that the test provides a sensitive, objective extension of the clinical neurological examination but is etiologically nonspecific.

A large number of clinical studies attest to the sensitivity of the PSVEP in

revealing demyelinating lesions in the optic nerve, and, in our experience, more than 95% of patients who have a clear history of optic neuritis have abnormal PSVEPs. Of the more than 400 patients with optic neuritis presented in the literature, 89% had PSVEP abnormalities; in some studies, the percentage is closer to 100%. When there was no clinical evidence for optic nerve involvement, the incidence of PSVEP abnormalities was 51% (of 715 patients) [13].

When the diagnosis of MS is suspected because of typical symptoms and/or signs referable to other central nervous system locations, then the demonstration by an abnormal PSVEP of a clinically-silent conduction defect in the optic nerve can further delineate the anatomic distribution of the disease process and thus narrow the range of diagnostic possibilities. Optic nerve demyelination is a common finding in autopsy material of MS patients [54, 64], and this is paralleled by the incidence of PSVEP abnormalities, which ranges from a high of 96% [32] to a low of 47% [37]. In a large number of clinical studies encompassing almost 2000 patients with all MS classifications, the average abnormality rate found was 63% [13]. Of 464, 322 and 799 patients classified as possible, probable and definite MS, the average abnormality rates were 37%, 58% and 85%, respectively. These figures reflect the greater likelihood of optic nerve lesions with more definite clinical diagnosis. Of 744 patients reported as having no history or clinical findings of optic neuritis, 51% had PSVEP abnormalities (ranging from a high of 93% in Halliday et al. [32], to a low of 34% in Purves et al. [82]). The differences between studies are best explained by the different definitions of MS used, some studies being composed of a preponderance of one class of patients. Note also that screen and check sizes differed greatly between the studies mentioned above. Contrasts, when reported, were all above 74%. Luminance levels varied so much that the reliability of the measurements has to be doubted. Nuwer et al. [74] studied first-degree relatives of MS patients and found interocular latency difference abnormalities in 6 of 110, although absolute P100 latencies were normal. Shibasaki et al. [95] have found that Japanese patients with MS have a higher incidence of absent PSVEP responses than was seen in series reported from Western countries. Noseworthy et al. [73] found a greater number of PSVEP abnormalities in patients older than 50 years as compared with younger patients. For a more comprehensive index to the literature on ON and MS, see Halliday [34] and Chiappa [13].

P100 latency abnormalities are usually present whatever the time interval since the clinical episode of optic neuritis. Shahroohi et al. [94] reported PSVEP abnormalities five years after the clinical episode, and Halliday et al. [32] reported patients who had abnormal PSVEPs 15 years later. Only about 5% of patients with abnormal PSVEPs have the P100 latency return to normal even when followed for 10 or 15 years after visual acuity has returned to normal following an episode of optic neuritis. However, Matthews et al. [59] found a patient whose PSVEP, although still abnormal three years after an attack of optic neuritis, had returned to normal after another three and a half

years. They suggested that in some patients a very slow healing process might be at work. When the latency difference between the two eyes can be used for interpretation (sometimes patients will have binocular PSVEP abnormalities when first studied), then the percentage of patients in whom the PSVEP returns to normal drops further. Thus, if optic neuritis is suspected and the patient complains of moderate to severe visual difficulty but the PSVEP is normal, that diagnosis is highly unlikely, especially in the acute situation.

Serial PSVEPs have been recorded in MS patients relative to both disease progression and therapeutic trials. These studies must be interpreted in light of the normal variability seen over time; Oken et al. [76] found absolute P100 latency shifts up to 11 msec and interocular latency difference changes up to 9 msec in 20 normal subjects tested 2–13 months apart. Halliday et al. [33] have followed patients with serial recordings over several years, noting step-like increases in latency associated with relapses characterized by visual impairment; if there was no visual system involvement, PSVEPs tended to remain unchanged. Matthews and Small [58] reported that 61% of 39 eyes exhibited parallel latency and acuity improvements over an 18 month period; but they also found that of nine eyes which had latency increases into an abnormal range, six had concurrent improvements in acuity. Aminoff et al. [1] found no relationship between changes in nonvisual clinical status and PSVEPs. Smith et al. [97] found no PSVEPs changes in eight patients treated with three days of high dose methylprednisolone infusions (1 gram daily). Gilmore et al. [29] saw transient PSVEP improvement in some patients given infusions of the calcium antagonist verapamil.

There have been various attempts to increase the sensitivity of the test in this clinical area. Phillips et al. [80] found that hyperthermia increased the incidence of PSVEP abnormalities. Oishi et al. [75] tested three different check sizes and found abnormalities more common with smaller checks (25 minutes), occasionally only with larger checks (100 minutes) and less often with 50 minute checks. Spatial vision in MS has been further investigated in MS by Regan et al. [84], Neima and Regan [69], Coupland and Kirkham [16], Plant [81] and Kupersmith et al. [48] using sinusoidal gratings and psychophysical techniques. Cant et al. [9] and Camisa et al. [8] found that lower luminance levels revealed more abnormalities and suggested routine use of more than one intensity level. However, this effect was not observed by others [23, 36] except for restricted foveal stimulation [36]. Mitchell et al. [68] studied the recovery cycle of PSVEPs in MS patients and found that there was no good correlation between conditioning (first) responses with abnormal latencies and abnormally delayed test (second) responses. They interpreted this as indicating that the conduction defects are in different locations. Kaufman et al. [41] used combined pattern electroretinograms and PSVEPs to localize the conduction defect in acute optic neuritis and patients with MS, usually finding normal P-ERGs and delayed PSVEPs. Long-standing disease with optic atrophy, presumably with axonal involvement and retrograde degeneration of retinal ganglion cells, often had absent P-ERGs.

Patients with acute transverse myelitis show PSVEP abnormalities in only a small proportion of cases [90,110]. Blumhardt et al. [4] studied 31 patients in whom the spinal cord symptoms developed over hours to days (9 of these were classified as transverse myelitis) and found PSVEP abnormalities in 10%. Ropper et al. [90] found no PSVEP or BAEP abnormalities in 12 patients with acute transverse myelitis. The chronic, progressive myelopathies have a greater incidence of abnormal PSVEPs. The abnormality rates ranged from 76% in the series of Bynke et al. [7] to 35% in the 100 patients with disease of more than six months duration studied by Blumhardt et al. [4].

It has been suggested that PSVEP data can be used clinically in the setting of undiagnosed spinal cord disease to help decide whether or not myelography is necessary [56]. Bynke et al. [7] suggested that if the clinical neuroophthalmological examination and the PSVEP are abnormal, and the CSF shows oligoclonal IgG banding, then radiological investigations can be limited or avoided. However, the possibility of concurrent diseases dictates very careful assessment of the clinical situation before an abnormal PSVEP (with or without other tests) should be used as presumptive evidence of MS to delay myelography. In fact, Blumhardt et al. [4] found five patients with abnormal PSVEPs and abnormal myelograms. Three had only borderline narrowing of the cervical canals and spondylotic changes (two of these have subsequently developed further signs of MS), but two had cord compression caused by prolapsed intervertebral discs. After laminectomy, one of these patients had little clinical change, but the other had a marked improvement. Conduction defects in the optic nerve secondary to demyelinating disease most commonly produce latency delays without much change in waveform configuration.

With respect to considerations of the pathophysiology involved in PSVEP abnormalities, the effects of segmental demyelination have not been well studied in small myelinated axons such as those in the optic nerves. McDonald [65] measured the length of 20 optic nerve plaques in 14 patients who died from multiple sclerosis; the length of the individual plaques varied from 3 to 30 mm, with a mean of 10.5 mm. Extrapolating from animal studies, he estimated that a demyelinated plaque of 10 mm in man would correspond to 50 internodes. Using the conduction velocity of the fastest fibers in the monkey optic nerve (10 meters per sec) and factoring in a 25-fold slowing of conduction over the demyelinated segment, he arrived at an estimate of 25 msec for an average delay to be expected in MS patients. This is similar to the delays actually seen in the PSVEPs of these patients. McDonald was careful to point out the possible errors in this formulation, but it is an interesting series of speculation. Noel and Desmedt [71] have suggested that longer delays in the somatosensory system could be attributed to: 1) more than one plaque, 2) larger plaques, and 3) the necessity for the low amplitude and desynchronized afferent volley to rely on temporal summation of synaptic potentials for eliciting the response from the next element in the pathway.

Also, the PSVEP P100 waveform is not the primary cortical response,

and delays in conduction through the optic nerve could have more complex effects on the sequence of signal processing along the visual pathways, i.e., geniculate bodies, cortex and thalamus. In this regard, Jacobson et al. [40] studied diphtheria toxin optic nerve lesions in cats using square wave grating discrimination to follow the time course of recovery of spatial frequency perception. They found a hierarchical progression with medium spatial frequencies returning first (1–4 days), then low (1–2 months) and finally high (5–8 months). These findings suggest that small checks might produce abnormal PSVEPs for a longer time than larger checks. They also found that the recovery time of pupillary reactivity to bright light and the length of recovery to spatial vision testing were both directly related to the magnitude of fiber loss. Furthermore, the anatomical findings suggested that the cat can have a 77% loss of optic nerve fibers and still recover visual acuity and contrast sensitivity.

### **BRAINSTEM AUDITORY EVOKED POTENTIALS**

The brainstem auditory evoked potential (BAEP) is recorded in response to a 10 sec click stimulus, most often using a vertex to earlobe derivation, and shows five peaks in the first 10 msec after the stimulus, arising in brainstem auditory structures from VIIIth nerve to inferior colliculus. Its clinical utility stems from the close relationship between the EP waveforms and specific anatomic structures. This specificity allows localization of conduction defects in the brainstem to within a centimeter or so. In addition, BAEPs (and SEPs) are very resistant to alteration by anything other than structural pathology in the brainstem auditory tracts. For example, barbiturate doses sufficient to render the EEG flat (isoelectric) and general anesthesia do not significantly affect BAEPs or SEPs. These factors of anatomic specificity, and physiologic and metabolic immutability are the basis of the clinical utility of both BAEPs and SEPs.

Brainstem auditory evoked potentials offer a look at physiologic anatomy. They provide a sensitive tool for assessment of brainstem auditory tracts and nearby structures. As with PSVEPs and SEPs, abnormalities demonstrated by BAEPs are etiologically non-specific and must be carefully integrated into the clinical situation by a physician familiar with the clinical use of this test. He or she must decide if other procedures (e.g., conventional audiometric studies, electrocochleography, electronystagmography, radiologic studies, subspecialty consultation) are indicated to differentiate the possible causes of the conduction delay.

There has been a large number of studies of BAEPs in patients with MS (see Chiappa [13] for a review and references). Of 1,000 patients in the literature with varying classifications of MS, 46% had abnormal BAEPs. For patients classified as definite, probable and possible MS, the average abnormality rates were 67%, 41% and 30%, respectively. Of patients reported as having no history or brainstem findings, 38% had BAEP abnormalities; abnormality rates varied from 21% to 55%. Thus, in one-fifth to one-half of MS patients

without brainstem symptoms or signs, BAEP testing will reveal evidence of clinically unsuspected lesions. Differences in definitions of MS, patient populations and techniques account for the variations between studies. For example, Noseworthy et al. [73] have found a higher incidence of BAEP abnormalities in MS patients over 50 years of age as compared with younger patients.

In a large group of MS patients, the reliability of BAEP techniques was demonstrated by the fact that all parameters in the MS patients with BAEPs interpreted as normal (the BAEP-normal MS group) showed no group statistical differences from the normal values [11]. Those MS patients who had BAEPs with abnormal interwave separations had latency values which were a mean of 4.9 SDs above the normal mean, and those MS patients who were determined to have abnormal BAEPs on the basis of an abnormal I/V amplitude ratio (17% of the BAEP-abnormal MS group) had ratios which were a mean of 5.5 SDs above the normal mean. These facts, and the higher incidence of abnormalities in the definite MS group, suggest that the BAEP is a reliable test for clinical usage.

Although the normal mean plus 3 SDs was used in the above study [11] as the upper limit of normal, the BAEP-normal MS patients (including those in the definite MS group) had values for both interwave latency and amplitude parameters which were essentially identical to the normal values. The fact that the values for the MS patients had a bimodal distribution (also noted for absolute wave V latency by Robinson and Rudge [87], being either completely normal or markedly abnormal, suggests that the smallest MS plaques in this part of the auditory system are sufficient to produce a marked conduction abnormality.

A majority of the BAEP abnormalities in MS patients are wave V amplitude abnormalities (absence or abnormally low amplitude of wave V was seen in 87% of the BAEP-abnormal MS patients [11]. The next most frequent abnormality, increased III-V IPL, was seen in 28% of the BAEP-abnormal MS patients. The presumed generators of waves III and V are the superior olivary complex and inferior colliculus, respectively, and thus the majority of the conduction abnormalities were found to occur between them, as would be expected since this is the longest segment of white matter in the tracts being tested. However, in those patients who had recognizable waves V, there was no significant correlation between the III-V separation and the wave I/V amplitude ratio, contrary to our expectations. In fact, in 17% of the BAEP-abnormal MS patients, the III-V separation was normal and the I/V amplitude ratio was abnormal. In addition, 3 patients had the unusual combination of no wave III, a recognizable wave V of normal amplitude, and an abnormal I-V separation. The disparity between these different kinds of abnormalities is not easily resolved merely by consideration of the known conduction deficits in demyelinated axons, such as slow conduction across the demyelinated segment and increased refractory period. Multiplicity of lesions, possible contributions to the BAEP waveforms from conduction in separate but parallel

tracts, and possible synchronous activation of different auditory tract structures need to be considered.

The importance of monaural stimulation is evident since 45% of the BAEP abnormalities were seen with stimulation of one ear only [11]. The prevalence of monaural abnormalities suggests that, with respect to the BAEP waveform generators, there is relatively little bilateral conduction, although known anatomic features had suggested otherwise.

Faster rates of stimulation alter all BAEP parameters, including interwave separations. It has been noted previously [88, 100] that increased click repetition rate revealed a higher incidence of abnormalities in the BAEPs of MS patients. However, in our group of MS patients, more BAEP abnormalities were not seen with 70 clicks per second, although abnormalities seen at 10 sec were sometimes worse at 70 sec [11]. Elidan et al. [25] have reported similar findings. The relative difficulty of waveform recognition at 70 sec, with increased waveform duration and indistinct peaks, restricted the clinical utility of that stimulus rate. In a few patients with diseases other than MS we have noted the reverse situation, i.e., that I-V separation was abnormal at 10 sec and normal at 70 sec. This normalization may be due to complete failure of conduction in the abnormal fibers at the faster rate, possibly due to an increased refractory period. With their abnormal contribution removed from the resultant waveforms the activity manifest is only that from the normally conducting fibers, hence the normal appearance. Although this effect was sought in the MS patients, it was not found. Phillips et al. [80] used hyperthermia but increased the yield of BAEP abnormalities by only one patient.

Emerson et al. [26] and Maurer [63] have noted that some patients with MS show BAEP abnormalities with only one click polarity, usually rarefaction clicks. The abnormality usually consists of a complete absence of wave V with one click polarity, and a normal wave V with the other. Decreasing click intensity results in a reappearance of wave V, and this might suggest a peripheral origin of the phenomenon. However, some of these patients have completely normal hearing on conventional audiometric tests, and this effect is not seen in normal subjects or patients with peripheral hearing disorders, so that it is presumably due to central conduction abnormalities, although firm human clinico-pathologic evidence for this is lacking.

In spite of obvious abnormalities in the BAEP, none of the MS patients studied here had clinical complaints of hearing difficulties, and click thresholds were essentially normal (formal audiograms were rarely obtained, but those which were obtained were normal). This is consistent with the findings of routine audiological testing in MS patients [51], but detailed auditory and vestibular testing [72], and interaural time discrimination and auditory localization testing [35], may reveal functional abnormalities in MS patients. In the latter study almost all MS patients with abnormal BAEPs also had abnormal interaural time discrimination. Occasionally MS patients do have symptomatic hearing difficulties and abnormal BAEPs apparently related to



the disease [20, 38, 39, 50] but none was seen in our group. Presumably there are plaques of demyelination in the eighth nerve (its proximal portion contains central myelin) or close to the cochlear nuclei in the lower pons. The occurrence of grossly abnormal BAEPs in conjunction with subjectively normal hearing may reflect the production of BAEP abnormalities by temporal dispersion of the click-induced volley as it ascends the affected tracts. It may be that, although these asynchronous potentials do not sum to generate a discrete peak of activity discernable at the scalp, the integrity of conduction, albeit deranged, is sufficient to sustain functionally normal hearing. However, this does not explain those cases where the amplitude and waveform shape are essentially normal and there is an abnormally large interwave separation. Perhaps in these cases the demyelination involves a majority of the fibers equally. Also, of course, BAEP waveform generation might have little to do with functional hearing.

The consistency of the BAEP, when followed over time in normals, suggests that it could be used to follow the activity of lesions affecting these tracts and might possibly provide assistance in evaluating the effectiveness of therapeutic measures. One study has suggested that the main value of BAEPs in patients with MS was to indicate clinically silent lesions, and that its value in monitoring the clinical condition of the individual patient was less [46]. Matthews et al. [61] followed for 38 months, after BAEP testing, 84 patients in whom the diagnosis of MS was under consideration. In nine of these patients an abnormal BAEP, at initial presentation, subsequently proved to be of diagnostic value revealing a separate, clinically-silent lesion, indicating a multifocal disease (and the patient on follow-up proved to have MS). Aminoff et al. [1] noted a significant increase in variability in the BAEP between tests in patients with clinical exacerbations of brainstem or cerebellar disease, but they also occasionally found a marked discrepancy between clinical and BAEP changes. Smith et al. [97] found no BAEP changes in MS patients following high-dose methylprednisolone therapy, whereas Gilmore et al. [29] noted some shortening of interpeak latencies following infusion of the calcium antagonist verapamil.

It should be reiterated here that a large part of the clinical utility of the BAEP lies in its ability to not only reveal unsuspected, and thereby multiple, lesions, but also document clinically equivocal findings. For example, some of our patients with MS initially presented symptoms and/or signs which could have been produced by disease in the labyrinths. Other than absence of wave I in three of the patients with Meniere's Disease, no abnormalities of interwave separations or amplitude ratios in the BAEP were seen in those 21 patients with labyrinthine diseases [11]. 37% of the MS patients who presented with nystagmus at the time of testing had BAEP abnormalities. Similarly, van Buggenhout et al. [105] found BAEP abnormalities in half of their patients who had vestibular lesions. Thus the BAEP can be helpful in this setting: if abnormal, then the lesion is clearly centrally rather than peripherally located. Conversely, 56% of the patients with an internuclear ophthalmoplegia (INO)

at the time of testing had abnormal BAEPs [11] so that the BAEP does not help to distinguish MS from the other causes of an INO (infarction and tumor [14]), which might also affect both medial longitudinal fasciculus and auditory tracts.

The BAEP is abnormal in some patients with system disorders affecting cerebellar function, particularly those who have spasticity, and thus is not helpful in differentiating possible MS in that setting.

Amyotrophic Lateral Sclerosis (ALS) sometimes presents initially with symptoms and/or signs which might be suggestive of MS; in our 26 patients with ALS there were none with abnormal BAEPs [11, Cascino et al. (Neurology, in press)]. Optic Neuritis (ON) and cervical transverse myelitis may have etiologies closely related or identical to that of MS; all of the patients in those groups had normal BAEPs, and the ON patients tested also had normal SEPs (the cervical transverse myelitis patients all had abnormal SEPs). Also, in a different study, 12 consecutive patients with inflammatory acute transverse myelitis (virtually or completely transverse lesions) had normal BAEPs [90]. Trigeminal neuralgia has also been associated with MS; in our 15 patients with trigeminal neuralgia there was none with abnormal BAEPs. Thus, as is also the case clinically, at the time of onset of ON, cervical transverse myelitis and trigeminal neuralgia there may be no EP evidence of lesions elsewhere in the CNS.

### **SHORT-LATENCY SOMATOSENSORY EVOKED POTENTIALS**

Short-latency somatosensory EPs (SEPs) are usually evoked with a 2 sec to 5 sec brief electrical pulse delivered transcutaneously to median, tibial or other nerves, and recorded at several points along the sensory pathway (e.g., for upper limb testing, over the brachial plexus, dorsal column tracts and nuclei, and somatosensory cortex). The peak labeled EP is generated in the brachial plexus, P/N13 in the upper cervical cord and lower medulla, and N19-P22 in the thalamus-cortex. The clinical utility of SEPs is related to the same factors of anatomic specificity and physiologic and metabolic immutability as were discussed above for BAEPs. SEPs offer a look at physiologic anatomy, and thus provide a sensitive tool for assessment of spinal cord and brainstem posterior columns, and medial lemniscal tracts and nearby structures. Again, abnormalities demonstrated by SEPs are etiologically nonspecific and must be carefully integrated into the clinical situation by a physician familiar with the clinical use of this test, who can decide whether or not other procedures (e.g., electromyography, radiologic studies, subspecialty consultation) are indicated to differentiate the possible causes of the conduction delay.

There has been a large number of studies of SEPs in patients with MS [13]. Of 1,000 patients with varying classifications of MS reported in the literature, 58% had abnormal median/digital SEPs and 76% had abnormal peroneal/tibial SEPs. In patients classified as definite, probable or possible MS, the average abnormality rates were 77%, 67% and 49%, respectively.

Although the effect of stimulus rate has been studied in normals, there has been no study of rate effects in patients with MS. Smith et al. [97] saw no change in median and tibial SEPs with infusion of high-dose methylprednisolone. Nuwer et al. [74] studied first-degree relatives of MS patients and found some abnormal interarm Erb's Point to N18 latency differences, although all other SEP parameters were normal. In published studies on the relationship between clinical sensory findings and SEPs in patients with MS, 42% (249/598) of patients reported to have no symptoms or signs referable to the sensory system had abnormal SEPs, whereas 75% (250/335) of patients with sensory system symptoms and/or signs had abnormal SEPs (both upper and lower limbs included). Note that there is about a 10% higher incidence of clinically-silent SEP abnormalities found on testing the lower limbs (as compared with the upper limbs).

Data from a group of 114 MS patients seen in our laboratory exemplify the findings that can be expected when using SEPs to test patients with (or suspected of having) MS. 29% of the patients had completely normal tests (both upper and lower limb). Upper limb SEPs were abnormal in 54% of patients, lower limb SEPs in 64%. In 18% of the patients, upper limb SEPs were normal when lower limb SEPs were abnormal, whereas the converse was true in 7%. Only 2% of patients had bilaterally abnormal upper limb and bilaterally normal lower limb SEPs, but the reverse was found in 11% of the patients. 37% of normal upper limb SEPs were associated with abnormal lower limb SEPs on the same side, whereas only 12% of normal lower limb SEPs were associated with abnormal upper limb SEPs ipsilaterally. Some of the conclusions that may be drawn from these results are: 1) when lower limb testing is normal, upper limb testing will reveal abnormalities in an additional, although small, group of patients, 2) SEP abnormalities in one limb (upper or lower) are not necessarily associated with SEP abnormalities in the other limb on the same side, although lower limb abnormalities will be more commonly associated with upper limb abnormalities than vice versa. Others have had similar results, the yield of abnormalities being greater with lower limb stimulation [24, 44, 95, 104].

Patients with suspected MS have been tested and the finding of all EPs normal except for SEPs pointing to an upper cervical cord conduction defect has prompted a myelogram that revealed significant cervical cord compression from spondylotic bars; some of these patients have improved with surgical decompression. Conversely, of course, multiple EP abnormalities do not necessarily indicate MS (see figure 7-20 in Chiappa [13] for a patient who had multiple EP abnormalities caused by multiple meningiomas).

Although every conceivable abnormality is seen in the SEPs of the MS patients, the most interesting is the absence of P/N13 (lower medullary component) with preservation of N19-P23 (thalamus-cortex) and a normal brachial plexus to N19 separation. The pathophysiology of such a finding and how it relates to the generation of the SEP waveforms are matters of pure

speculation. In our group of patients, 30% of the abnormalities were unilateral and 70% were bilateral, an incidence quite similar to the average in the literature. Of the bilateral abnormalities, 79% were identical and 21% were different on the 2 sides [13]. Roberts et al. [86] have used the dispersion of the thalamocortical waveforms, as determined by Fourier analysis, as an additional analysis parameter. Rossini et al. [91] registered SEP short-latency wavelets using restricted band-pass digital filtering and thereby increased the yield of abnormalities. Yamada et al. [111] studied long-latency in addition to short-latency SEP components and found additional abnormalities; they also felt that the long-latency components helped to resolve interpretative difficulties encountered with short-latency testing, especially when bilateral stimulation was used. Delwaide et al. [22] studied lumbosacral spinal SEPs in MS patients, and noted a correlation between intensity of spasticity and some elements of the EP waveform.

Matthews et al. [61] followed for 38 months after SEP testing 84 patients in whom the diagnosis of MS was under consideration. In only three of these patients, an abnormal SEP at initial presentation subsequently proved to be of diagnostic value in that it revealed a separate, clinically-silent lesion, indicating multifocal disease (and the patient on follow-up proved to have MS). Davis et al. [21] found that clinical motor and sensory findings in MS patients in the corresponding limb frequently correlated with abnormalities of the median nerve SEP cervical response. When new clinical features appeared, the SEP deteriorated in some patients but improved in others, and overall disability sometimes increased despite improved SEPs. Most SEP changes were not accompanied by clinical changes.

Ropper et al. [90] studied EP abnormalities in 12 consecutive patients with inflammatory acute transverse myelopathy (ATM) as their first neurological illness. All nine patients tested with median SEPs had normal findings, the lesions being below cervical levels mediating that response. Five of six patients tested with peroneal SEPs had abnormal findings (the sixth was tested eight months after onset when there was no residual neurological deficit). All of these patients had normal PSVEPs and BAEPs, and none developed new neurological signs during 18 months mean follow-up. The authors felt that the lack of other lesions by EP testing, and the failure to develop new clinical lesions, indicates that ATM, when defined as a virtually or totally complete transverse inflammatory lesion of the cord, is a different process from MS.

Attempts have been made to use SEPs—and other EPs—to gauge the effectiveness of plasmapheresis therapy in MS, but only a few patients have been studied so far and it is not yet possible to draw conclusions [19, 109].

Effects on SEPs of raising body temperature in patients with MS have been studied by Matthews et al. [58] and Kazis et al. [43]. The latter authors used intercurrent extra-CNS infection (viral or bacterial) as the hyperthermic agents, and the effect of toxins cannot be discounted as the cause of the observed SEP changes. Matthews et al. [58] used external heat to raise the

body temperature of their subjects and found that P/N13 amplitude was markedly diminished by the temperature increase. Phillips et al. [80] found that hyperthermia increased the yield of peroneal SEP abnormalities in MS patients.

### COMBINED EVOKED POTENTIAL STUDIES

The comparative utility of PSVEPs, BAEPs and SEPs have been studied in several groups of patients [11, 31, 44, 47, 56, 61, 80, 82, 102, 104]. As might be postulated on the basis of length of white matter tracts involved, the order of relative utility of the tests in revealing evidence of clinically unsuspected lesions was SEP, PSVEP and BAEP. These data suggest that there is not a specific differential susceptibility to demyelination in the systems involved in the tests. Rather, it is the length and amount of white matter tracts being tested which determine the likelihood of detection of a lesion in a given system. Phillips et al. [80] found increased abnormality rates in all EPs during hyperthermia.

Bottcher et al. [5] followed patients for two to four years after PSVEP, SEP and CSF immunoglobulin G testing and found that 81% of those in whom both the EPs and the IgG index were abnormal initially had entered a higher MS diagnostic class at the later evaluation. Those patients in whom either the EPs or IgG index were normal initially remained in the same diagnostic class. Walsh et al. [106] followed 56 patients for two and a half years and found an increased number of abnormalities in multimodality EPs, which was paralleled by an increase in overall clinical disability. However, Aminoff et al. [1] have noted that the correlation between changes in specific clinical features and EPs may be poor.

Noseworthy et al. [73] have studied PSVEP, BAEP and blink reflexes in patients presenting after age 50 with suspected MS. They found both in EPs and CSF electrophoresis to have high diagnostic yield in this difficult diagnostic group.

### MOTOR EVOKED POTENTIALS

Transcranial stimulation (electrical and magnetic) of the motor cortex is a subject of much current interest (see Young et al. [112] for a recent review and discussion of safety issues). Mills et al. [67] stimulated electrically over the arm area of the motor cortex, over the C7 vertebral level, and in the axilla, and recorded the evoked muscle action potentials of forearm flexor muscles in healthy controls and patients with MS. In the patients the cord-to-axilla conduction times were normal, while central conduction times (cortex to cord) were either markedly prolonged or absent. Snooks and Swash [98] used a similar stimulation technique to study spinal cord conduction velocities and found slowed motor conduction velocities between C6 and L1 in four of five patients with MS, all of whom had corticospinal signs in the legs. Cauda equina conduction was normal. These motor evoked potentials may provide a

tool for studying motor system abnormalities in MS (and many other diseases) and may afford closer clinical-electrophysiologic correlations.

### MAGNETIC RESONANCE IMAGING AND EVOKED POTENTIALS

Magnetic resonance imaging (MRI) is proving to be an invaluable tool in the investigation of patients with suspected demyelinating disease, especially the T2-weighted images. Immediate post-mortem studies have shown that demyelinated lesions 3 mm in diameter are seen, and that the apparent lesion size on MRI is accurate [99]. Where signal intensity varied, so did the degree of inflammation, demyelination and gliosis, and it was thought that MRI could distinguish gliotic and nongliotic demyelinated lesions. Serial MRI scans show the appearance and evolution of asymptomatic lesions [79] and enhancement may afford a measure of activity [30]. MRI has been shown to be better than EPs and CT in revealing multiple lesions in the CNS [17, 27, 45, 77], including the spinal cord [55], but, of course, MRI is no more specific than EPs with respect to etiology. However, in the brainstem, EPs reveal a significant number of conduction defects not seen by MRI [2, 17, 28, 45]. Similarly, it can be expected that optic nerve lesions will be detected more reliably by EPs than MRI. Thus, although as a general statement it can be said that the overall neurologic workup of the patient suspected of having demyelinating disease is better served by MRI (and most patients with MS will eventually have an MRI scan), in selected cases specific questions are better answered by EPs, and some anatomic areas are better tested by EPs.

Portions of the text used with permission from Chiappa, 1983.

### REFERENCES

1. Aminoff MJ, Davis SL, Panitch HS: Serial evoked potential studies in patients with definite multiple sclerosis. *Arch Neurol* 41:1197-1202, 1984.
2. Baumhelfner RW, Tourtellotte WW, Ellison G, Myers L, Syndulko K, Cohen SN, Shapshak P, Osborne M, Waluch V: Multiple sclerosis: correlation of magnetic resonance imaging with clinical disability, quantitative evaluation of neurologic function, evoked potentials and intra-blood-brain-barrier IgG synthesis. *Neurology* 36(1):283, 1986.
3. Blumhardt LD: Do evoked potentials contribute to the early diagnosis of multiple sclerosis? In: Warlow Ch and Garfield J (eds), *Dilemmas in the Management of the Neurological Patient*. Edinburgh, Churchill Livingstone: 18-24, 1984.
4. Blumhardt, LD, Barrett G and Halliday AM: The pattern visual evoked potential in the clinical assessment of undiagnosed spinal cord disease. In: J Courjon, F Mauguière and M Revol (eds), *Clinical Applications of Evoked Potentials in Neurology*. New York, Raven Press 463-471, 1982.
5. Bottcher J and W Trojaborg: Follow-up of patients with suspected multiple sclerosis: a clinical and electrophysiological study. *Neurol Neurosurg Psychiat* 45:809-814, 1982.
6. Brooks EB and KH Chiappa: A comparison of clinical neuro-ophthalmological findings and pattern shift visual evoked potentials in multiple sclerosis. In: JJ Courjon, F Mauguière, M Revol (eds), *Clinical Applications of Evoked Potentials in Neurology*. New York, Raven Press 435-437, 1982.
7. Bynke H, Olsson JE and Rosen I: Diagnostic value of visual evoked response, clinical eye examination and CSF analysis in chronic myelopathy. *Acta Neurol Scand* 56:55-69, 1977.
8. Camisa J, Bodis-Wollner I and Mylin L: Luminance-dependent pattern VEP delay in human demyelinating disease. *Society for Neuroscience Abstracts* 6:596, 1980.

9. Cant BR, Hume AL and Shaw NA: Effects of luminance on the pattern visual evoked potential in multiple sclerosis. *Electroencephalogr Clin Neurophysiol* 45:496–504, 1978.
10. Chiappa KH: Pattern shift visual, brainstem auditory, and short-latency somatosensory evoked potentials in multiple sclerosis. *Neurology* 30:110–123, 1980.
11. Chiappa KH, Harrison JL, Brooks EB and Young RR: Brainstem auditory evoked responses in 200 patients with multiple sclerosis. *Ann Neurol*: 135–143, 1980.
12. Chiappa KH and Ropper AH: Evoked potentials in clinical medicine. *N Eng J Med* 306: 1140–1150 & 1205–1211, 1982.
13. Chiappa KH: *Evoked Potentials in Clinical Medicine*. New York, Raven Press, 1983.
14. Cogan DG and Wray SH: Internuclear ophthalmoplegia as an early sign of brainstem tumors. *Neurology* 20:629–633, 1970.
15. Collins DWK, Black JL, Mastaglia EL: Pattern reversal visual evoked potential. *J Neurol Sci* 36:83–95, 1978.
16. Coupland SG and Kirkham TH: Orientation-specific visual evoked potential deficits in multiple sclerosis. *Canad J Neurol Sci* 9:331–337, 1982.
17. Cutler JR, Aminoff MJ, Brant-Zawadzki M: Comparative value of MRI and evoked potential studies in multiple sclerosis. *Neurology* 36(1):156, 1986.
18. Drayer BP and Barrett L: Magnetic resonance imaging and CT scanning in multiple sclerosis. *Ann NY Acad Sci* 436:294–314, 1984.
19. Dau PC, Petajan JH, Johnson KP, Panitch HS and Bornstein MB: Plasmapheresis in multiple sclerosis: preliminary findings. *Neurology* 30:1023–1028, 1980.
20. Daugherty WT, Lederman RJ, Nodar RH, Conomy JP: Hearing loss in multiple sclerosis. *Arch Neurol* 40:33–35, 1983.
21. Davis SL, Aminoff MJ, Panitch HS: Clinical correlations of serial somatosensory evoked potentials in multiple sclerosis. *Neurology* 35:359–365, 1985.
22. Delwaide PJ, Schoenen J, DePasqua V: Lumbosacral spinal evoked potentials in patients with multiple sclerosis. *Neurology* 35:174–179, 1985.
23. Diener HC, Koch W and Dichgans J: The significance of luminance on visual evoked potentials in diagnosis of MS. *Archiv Psychiatric und Nervenkrankheiten* 231:149–154, 1982.
24. Eisen A, Oduste K: Central and peripheral conduction times in multiple sclerosis. *Electroencephalogr Clin Neurophysiol* 48:253–265, 1980.
25. Elidan J, Sohmer H, Gafni M and Kahana E: Contribution of changes in click rate and intensity on diagnosis of multiple sclerosis by brainstem auditory evoked potentials. *Acta Neurol Scand* 65:570–585, 1982.
26. Emerson RG, Brooks EB, Parker SW and Chiappa KH: Effects of click polarity on brainstem auditory evoked potentials in normal subjects and patients: unexpected sensitivity of wave V. *Ann NY Acad Sci* 388:710–721, 1982.
27. Gebarski SS, Gabrielsen TO, Gilman S, Knake JE, Latack JT, Aisen AM: The initial diagnosis of multiple sclerosis; clinical impact of magnetic resonance imaging. *Ann Neurol* 17: 469–474, 1985.
28. Geisser BS, Kurtzberg D, Arezzo JC, Vaughan HG, Aisen ML, Smith CR, Scheinberg LC: Trimodal evoked potentials compared with magnetic resonance imaging in the diagnosis of multiple sclerosis. *Neurology* 36(1):158, 1986.
29. Gilmore RL, Kasarskis EJ, McAllister RG: Verapamil-induced changes in central conduction in patients with multiple sclerosis. *J Neurol Neurosurg Psychiat* 48:1140–1146, 1985.
30. Gonzalez-Scarano F, Grossman RI, Galetta SL, Atlas S, Silberberg DH: Enhanced magnetic images in multiple sclerosis. *Neurology* 36(1):285, 1986.
31. Green JB, Price R and Woodbury SG: Short-latency somatosensory evoked potentials in multiple sclerosis. Comparison with auditory and visual evoked potentials. *Arch Neurol* 37:630–633, 1980.
32. Halliday AM, McDonald WI and Mushin J: Visual evoked responses in the diagnosis of multiple sclerosis. *Br Med J* 4:661–664, 1973.
33. Halliday AM and McDonald WI: Visual evoked potentials. In: E Stalberg and RR Young (eds), *Neurology I: Clinical Neurophysiology*. London, Butterworths 228–258, 1981.
34. Halliday AM: The visual evoked potential in the investigation of diseases of the optic nerve. In: *Evoked Potentials in Clinical Testing*, edited by Halliday AM Churchill Livingstone, New York, pp 187–234, 1982.

35. Hausler R and RA Levine: Brain stem auditory evoked potentials are related to interaural time discrimination in patients with multiple sclerosis. *Brain Res* 191:589–594, 1980.
36. Hennerici M and Wist ER: A modification of the visual evoked response method involving small luminance decrements for the diagnosis of demyelinating disease. In: J Courjon, F Manguiere and M Revol (eds), *Clinical Applications of Evoked Potentials in Neurology*. New York, Raven Press 433–441, 1982.
37. Hoepfner T and Lolos F: Visual evoked responses and visual symptoms in multiple sclerosis. *Neurol Neurosurg Psychiatry* 41:493–498, 1978.
38. Hopf HC and Maurer K: Wave I of early auditory evoked potentials in multiple sclerosis. *Electroencephalogr Clin Neurophysiol* 56:31–37, 1983.
39. Jabbari B Marsh EE and Gunderson CH: The site of the lesion in acute deafness of multiple sclerosis—contribution of the brain stem auditory evoked potential test. *Clin Electroencephalogr* 13:241–244, 1982.
40. Jacobson SG, Eames RA and McDonald WI: Optic nerve fiber lesions, in adult cats: Pattern of recovery of spatial vision. *Exp Brain Res* 36:491–508, 1979.
41. Kaufman D, Celesia GG: Simultaneous recording of pattern electroretinogram and visual evoked responses in neuro-ophthalmologic disorders. *Neurology* 35:644–651, 1985.
42. Kayamori R, Dickins S, Yamada T, Kimura J: Brainstem auditory evoked potential and blink reflex in multiple sclerosis. *Neurology* 34:1318–1323, 1984.
43. Kazis A, Vlaikidis N, Xafenios D, Papanastasiou J and Pappa P: Fever and evoked potentials in multiple sclerosis. *Neurol* 227:1–10, 1982.
44. Khoshbin S and Hallett M: Multimodality evoked potentials and blink reflex in multiple sclerosis. *Neurology* 31:138–144, 1981.
45. Kirshner HS, Tsai SI, Runge VM, Price AC: Magnetic resonance imaging and other techniques in the diagnosis of multiple sclerosis. *Arch Neurol* 42:859–863, 1985.
46. Kjaer M: Variations of brain stem auditory evoked potentials correlated to duration and severity of multiple sclerosis. *Acta Neurol Scand* 61:157–166, 1980a.
47. Kjaer M: The value of brainstem auditory, visual and somatosensory evoked potentials and blink reflexes in the diagnosis of multiple sclerosis. *Acta Neurol Scand* 62:220–236, 1980b.
48. Kupersmith MJ, Nelson JI, Seiple WH, Carr RE and Weiss: The 20/20 eye in multiple sclerosis. *Neurology* 33:1015–1020, 1983.
49. Lacquaniti F, Benna P, Gilli M, Troni W, Bergamasco B: Brainstem auditory evoked potentials and blink reflex in quiescent multiple sclerosis. *Electroencephalogr Clin Neurophysiol* 47:607–610, 1979.
50. Lederman RJ Nodar RH, Conomy JP and Daugherty WT: Hearing loss in multiple sclerosis. *Neurology* 28: 406, 1978.
51. LeZak RJ and Selhub B: On hearing in multiple sclerosis. *Ann Otol Rhinol Laryngol* 1102–1110, 1966.
52. Lowitzsch K, Kuhnt U, Sakmann Ch, Maurer, Hopf HC, Schott D and Thater K: Visual pattern evoked responses and blink reflexes in assessment of MS diagnosis. *J Neurol* 213: 17–32, 1976.
53. Ludwin SK: Pathology of demyelination and remyelination. In: *Demyelinating Disease: Basic and Clinical Electrophysiology*, edited SG Waxman and JM Ritchie. Raven Press, New York, pp 123–168, 1981.
54. Lumsden CE: The neuropathology of multiple sclerosis. In: *Handbook of Clinical Neurophysiology*. Volume 9. Amsterdam, North-Holland, 175–234, 1970.
55. Maravilla KR, Weinreb JC, Suss R, Nunnally RL: Magnetic resonance demonstration of multiple sclerosis plaques in the cervical cord. *Am J Rad* 144:381–385, 1985.
56. Mastaglia FL, Black JL and Collins DWK: Visual and spinal evoked potentials in the diagnosis of multiple sclerosis. *Br Med J* 2:732, 1976.
57. Matthews WB, Small DG, Small M, Pountney E: Pattern reversal evoked visual potentials in the diagnosis of multiple sclerosis. *J Neurol Neurosurg Psychiat* 40:1009–1014, 1977.
58. Matthews WB and Small DG: Serial recording of visual and somatosensory evoked potentials in multiple sclerosis. *J Neurol Sci* 40:11–21, 1979.
59. Matthews WB and Small M: Prolonged follow-up of abnormal visual evoked potentials in multiple sclerosis: Evidence for delayed recovery. *J Neurol Neurosurg Psychiat* 46:639–642, 1983.
60. Matthews WB, Read DJ and Pountney E: Effect of raising body temperature on visual and



- somatosensory evoked potentials in patients with multiple sclerosis. *J Neurol Neurosurg Psychiatr* 42:250–255, 1979.
61. Matthews WB, Wattam-Bell, JRB, Pountney E: Evoked potentials in the diagnosis of multiple sclerosis: a followup study. *J Neurol Neurosurg Psychiatr* 45:303–307, 1982.
  62. Matthews WB, Acheson ED, Batchelor JR, Weller RO: (eds): *McAlpine's Multiple Sclerosis*. Churchill Livingstone, London, 1985.
  63. Maurer K: Uncertainties of topodiagnosis of auditory nerve and brain-stem auditory evoked potentials due to rarefaction and condensation stimuli. *Electroencephalogr Clin Neurophysiol* 62:135–140, 1985.
  64. McAlpine D, Lumsden CE and Acheson Ed (eds): *Multiple Sclerosis: A Reappraisal*. Edinburgh, Churchill Livingstone, 1972.
  65. McDonald WI: Pathophysiology of conduction in central nerve fibers. In: *Visual Evoked Potentials in Man: New Developments*, edited by JE Desmedt. Oxford, Clarendon Press: 427–437, 1977.
  66. Meienberg O, Flammer J and Ludin HP: Subclinical visual field defects in multiple sclerosis. *Neurol* 227:125–133, 1982.
  67. Mills KR and Murray NMF: Corticospinal tract conduction time in multiple sclerosis. *Ann Neurol* 18:601–605, 1985.
  68. Mitchell JD, Hansen S, McInnes A, Campbell FW: The recovery cycle of the pattern visual evoked potential in normal subjects and patients with multiple sclerosis. *Electroencephalogr Clin Neurophysiol* 56:309–315, 1983.
  69. Neima D and Regan D: Pattern visual evoked potentials and spatial vision in retrobulbar neuritis and multiple sclerosis. *Arch Neurol* 41:198–201, 1984.
  70. Nikoskelainen E and B Flack: Do visual evoked potentials give relevant information to the neuro-ophthalmological examination in optic nerve lesions? *Acta Neurol Scand* 66:42–57, 1982.
  71. Noel P and Desmedt JE: Cerebral and far-field somatosensory evoked potentials in neurological disorders involving the cervical spinal cord, brainstem, thalamus and cortex. *Prog Clin Neurophysiol* 7:205–230, 1980.
  72. Noffsinger D, Olsen WO, Carhart R, Hart CW, Sahgal V: Auditory and vestibular aberrations in multiple sclerosis. *Acta Otolarygol, Suppl* 303:4–63, 1972.
  73. Noseworthy J, Paty D, Wonnacott T, Feasby T and Ebers G: Multiple sclerosis after age 50. *Neurology* 33:1537–1544, 1983.
  74. Nuwer MR, Visscher BR, Packwood JW, Namcrow NS: Evoked potential testing in relatives of multiple sclerosis patients. *Ann Neurol* 18:30–34, 1985.
  75. Oishi M, Yamada T, Dickins S, Kimura J: Visual evoked potentials by different check sizes in patients with multiple sclerosis. *Neurology* 35:1461–1465, 1985.
  76. Oken BS, Chiappa KH, Gill E: Normal temporal variability of P100 latency. *Electroencephalogr Clin Neurophysiol* (In press), 1986.
  77. Ormerod IEC, McDonald WI, du Boulay GH, Kendall BE, Moseley IF, Halliday AM, Kakigi R, Kriss A, Peringer E: Disseminated lesions at presentation in patients with optic neuritis. *J Neurol Neurosurg Psychiatr* 49:124–127, 1986.
  78. Patterson VH and Heron JR: Visual field abnormalities in multiple sclerosis. *Neurol Neurosurg Psychiatr* 43:205–208, 1980.
  79. Paty DW, Isaac CD, Grochowski E, Palmer MR, Oger J, Kastrukoff LF, Nord B, Genton M, Jardine C, Li DK: Magnetic resonance imaging in multiple sclerosis: a serial study in relapsing and remitting patients with quantitative measurements of lesion size. *Neurology* 36(1):177, 1986.
  80. Phillips KR, Potvin AR, Syndulko K, Cohen SN, Tourtellotte WW, Potvin JH: Multimodality evoked potentials and neurophysiological tests in multiple sclerosis. Effect of hyperthermia on test results. *Arch Neurol* 40:159–164, 1983.
  81. Plant GT: Transient visually evoked potentials to sinusoidal gratings in optic neuritis. *J Neurol Neurosurg Psychiatr* 46:1125–1133, 1983.
  82. Purves SJ, Low MD, Galloway J and Reeves B: A comparison of visual, brainstem auditory, and somatosensory evoked potentials in multiple sclerosis. *Can J Neurol Sci* 8:15–19, 1981.
  83. Rasminsky M: Hyperexcitability of pathologically myelinated axons and positive symptoms in multiple sclerosis. In: *Demyelinating Disease: Basic and Clinical Electrophysiology*, (ed) SG Waxman and JM Ritchie. Raven Press, New York, pp 289–298, 1981.

84. Regan D, Bartol S, Murray TJ, Beverley KI: Spatial frequency discrimination in normal vision and in patients with multiple sclerosis. *Brain* 105:735-754, 1982.
85. Riemsdag FCC, Spekrijse H, Van Wessem Th. N: Responses to paired onset stimuli: implications for the delayed evoked potentials in multiple sclerosis. *Electroencephalogr Clin Neurophys* 62:155-166, 1985.
86. Roberts KB, Lawrence PD and A Elisen: Dispersion of the somatosensory evoked potential in multiple sclerosis. *Institute of Electrical and Electronic Engineers Transactions in Biomedical Engineering* 30:360-364, 1983.
87. Robinson K and Rudge P: The use of the auditory evoked potential in the diagnosis of multiple sclerosis. *J Neurol Sci* 45:235-244, 1980.
88. Robinson K and Rudge P: Abnormalities of the auditory evoked potentials in patients with multiple sclerosis. *Brain* 100:19-40, 1977.
89. Rolak LA: The flight of colors test in multiple sclerosis. *Arch Neurol* 42:759-760, 1985.
90. Ropper AH, Mielt T and Chiappa KH: Absence of evoked potential abnormalities in acute transverse myelopathy. *Neurology* 32:80-82, 1982.
91. Rossini PM, Basciani M, DiStefano E, Febbo A, Mercuri N: Short-latency scalp somatosensory evoked potentials and central spine to scalp propagation characteristics during peroneal and median nerve stimulation in multiple sclerosis. *Electroencephalogr Clin Neurophysiol* 60:197-206, 1985.
92. Sears TA and Bostock H: Conduction failure in demyelination: Is it inevitable? In: *Demyelinating Disease: Basic and Clinical Electrophysiology*, (eds) SG Waxman and Ritchie JM: Raven Press, New York, pp 357-376, 1981.
93. Sedgwick EM: Pathophysiology and evoked potentials in multiple sclerosis. In: *Multiple Sclerosis: Pathology, Diagnosis and Management*, (ed) Hallpike JF et al. Williams and Wilkins, 1983.
94. Shahrokhi F, Chiappa KH and Young RR: Pattern shift visual evoked responses: two hundred patients with optic neuritis and/or multiple sclerosis. *Arch Neurol* 35:65-71, 1978.
95. Shibasaki H, Kakigi R, Tsuji S, Kimura S, Kuroiwa Y: Spinal and cortical somatosensory evoked potentials in Japanese patients with multiple sclerosis. *Neurol Sci* 57:441-453, 1982.
96. Shibasaki H and Kuroiwa Y: Pattern reversal visual evoked potentials in Japanese patients with multiple sclerosis. *Neurol Neurosurg Psychiatry* 45:1139-1143, 1982.
97. Smith T, Zeeberg I, Sjo O: Evoked potentials in multiple sclerosis before and after high-dose methylprednisolone infusion. *Eur Neurol* 25:67-73, 1986.
98. Snooks SJ and Swash M: Motor conduction velocity in the human spinal cord: slowed conduction in multiple sclerosis and radiation myelopathy. *J Neurol Neurosurg Psychiatr* 48:1135-1139, 1985.
99. Stewart WA, Hall LD, Berry K, Churg A, Oger J, Hashimoto SA, Paty DW: Magnetic resonance imaging (MRI) in multiple sclerosis (MS): pathological correlation studies in eight cases. *Neurology* 36(1):320, 1986.
100. Stockard JJ and Rossiter VS: Clinical and pathologic correlates of brain stem auditory response abnormalities. *Neurology* 27:316-325, 1977.
101. Swart S and Millac P: A comparison of flight of colours with visually evoked responses in patients with multiple sclerosis. *Neurol Neurosurg Psychiatry* 43: 550-551, 1980.
102. Tackmann W, Ettlin T and Strenge H: Multimodality evoked potentials and electrically elicited blink reflex in optic neuritis. *J Neurol* 227:157-163, 1982.
103. Tackmann W, Strenge H, Barth R, and Sojka-Raytscheff A: Evaluation of various brain structures in multiple sclerosis with multimodality evoked potentials, blink reflex and nystagmography. *J Neurol* 224:33-46, 1980.
104. Trojaborg W and Petersen E: Visual and somatosensory evoked cortical potentials in multiple sclerosis. *J Neurol Neurosurg Psychiatr* 42:323-330, 1979.
105. van Buggenhout E, Ketelaer P and Carton H: Success and failure of evoked potentials in detecting clinical and subclinical lesions in multiple sclerosis patients. *Clin Neurol Neurosurg* 84:3-14, 1982.
106. Walsh JC, Garrick R, Cameron J, McLeod JG: Evoked potential changes in clinically definite multiple sclerosis: a two year follow up study. *Neurol Neurosurg Psychiatr* 45:494-500, 1982.
107. Waxman SG: Clinicopathological correlations in multiple sclerosis and related diseases. In: *Demyelinating Disease: Basic and Clinical Electrophysiology*, (eds) SG Waxman and

- JM Ritchie. Raven Press, New York, pp 169–182, 1981.
108. Waxman SG and Ritchie JM: Electrophysiology of demyelinating diseases: Future directions and questions. In: *Demyelinating Disease: Basic and Clinical Electrophysiology*, (eds) SG Waxman and JM Ritchie. Raven Press, New York, pp 511–514, 1981.
  109. Weiner HL and Dawson DM: Plasmapheresis in multiple sclerosis: a preliminary study. *Neurology* 30:1029–1033, 1980.
  110. Wulff CH: Evoked potentials in acute transverse myelopathy. *Dan Med Bull* 32:282–287, 1985.
  111. Yamada T, Shivapour E, Wilkinson T and Kimura J: Short- and long-latency somatosensory evoked potentials in multiple sclerosis. *Arch Neurol* 39:88–94, 1982.
  112. Young RR and Cracco RQ: Clinical neurophysiology of conduction in central motor pathways. *Ann Neurol* 18:606–610, 1985.

---

## 8. EVOKED POTENTIALS IN NONDEMYELINATING DISEASES

FRANÇOIS MAUGUIÈRE

### INTRODUCTION

#### **Diagnostic utility of evoked potentials in nondemyelinating diseases**

Evoked potentials (EPs) represent the only noninvasive method available to assess in "real time" the processing of sensory information in the human central nervous system. Most of the successes of this low cost investigation in clinical practice is due to its ability to disclose silent lesions causing delayed response in demyelinating diseases. In nondemyelinating processes the clinical applications of EPs have not yet been clearly defined; however in such diseases, EPs may be helpful: 1) to test sensory functions when clinical examination is not reliable (young children, comatose patients, suspected conversion disorder); 2) to decide whether more sophisticated or more invasive morphological investigations should be entertained in patients with purely subjective symptoms; 3) to assess the causative mechanisms of the neurological deficit or of the functional recovery. There are two questions that should be discussed before looking at the diagnostic yield of EPs in nondemyelinating processes: what is the specificity and localizing value of abnormal EP patterns? Is it possible to give unequivocal pathophysiological interpretation of abnormal waveforms?

#### **Specificity of latency and amplitude EP abnormalities**

It is generally accepted that demyelination causes conduction slowing and EP latency delays, whereas traumatic, vascular or tumoral lesions are more

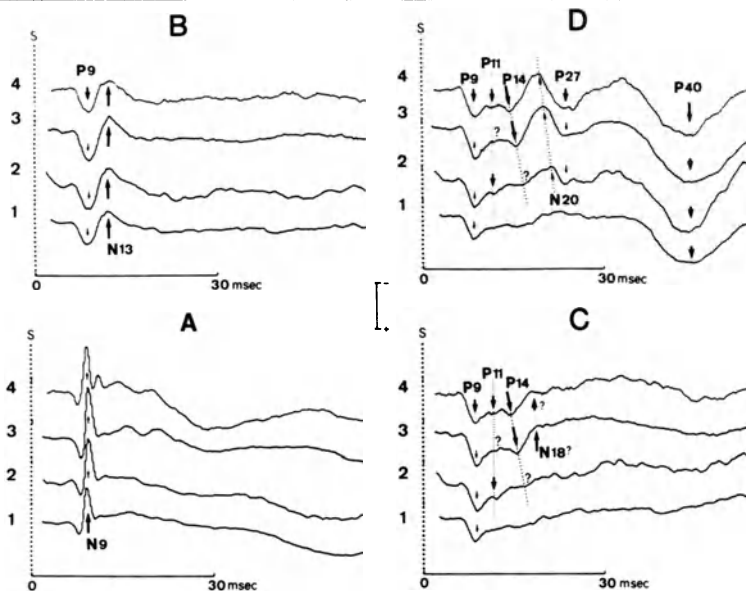
likely to result in amplitude abnormalities. This assumption is valid as a guideline but does not take into account the possible overlap between the respective effects of impaired axonal conduction, abnormal synaptic transmission, and cell loss which represent the three basic phenomena responsible for EP abnormalities.

For instance, in acute demyelination some EP components may be abolished or severely reduced because of conduction block [81]. Moreover, we have observed that in the early stages of MS temporal dispersion of afferent volleys may decrease the amplitude of some centrally generated axonal components, such as the scalp P14 far-field SEP to median nerve stimulation, without significant latency shift. Conversely, in the absence of any primary demyelinating process, compression of fiber tracts can slow down conduction velocity. Delayed EPs were shown to occur in compressive lesions of the optic nerve [29], acoustic nerve [10] and cervical spinal cord [51] (figure 8-1). It is commonly assumed that the latency shift due to fiber tract compression is smaller than in primary demyelinating disease [9, 29]. However, when the clinical context is equivocal, this observation is of little help in the interpretation of an individual EP study.

Abnormal synaptic transmission is another mechanism that could produce EP delays. It has been speculated that synaptic dysfunction at the retina for example, could produce delayed VEPs in Parkinson's disease [5]. This explanation is valid in particular for synaptic networks where one cell population modulates the efficiency of synaptic contacts between other cells. This seems to be the case for amacrine cells that serve as a trigger for the ganglion cells of the retina and that are dopamine-deficient in Parkinson's disease.

When the underlying pathology is an axonal degeneration or a neuronal loss, the amplitude of EPs should be reduced with no or negligible latency shift, except if axonal loss affects selectively the larger fibers. For instance, it was shown [6] that the visual responses to pattern shift stimulation were, as a group, significantly reduced in amplitude in patients with Friedreich's ataxia (now accepted to be a primary axonopathy). However, in spite of a highly significant inverse correlation between the amplitude and the latency of the P100 component, the amplitude of the response could not be defined as below the normal range in most individuals with Friedreich's disease owing to the large variability of response size in the healthy population. On the other hand P100 latency was delayed more than 2.5 standard deviations above the mean normal value in 55% of cases. Plotting of VEP latencies and amplitudes in normals, patients with Friedreich's ataxia, and patients with a history of optic neuritis clearly demonstrated an overlap of the Friedreich's ataxia population with the two others (figure 8-2).

Thus in a non-negligible percentage of patients with nondemyelinating diseases, amplitude decrement and latency shift of EP may co-exist, and the latter abnormality cannot be considered per se as indicating a primary demyelinating process. Amplitude abnormalities are often considered unreliable, and



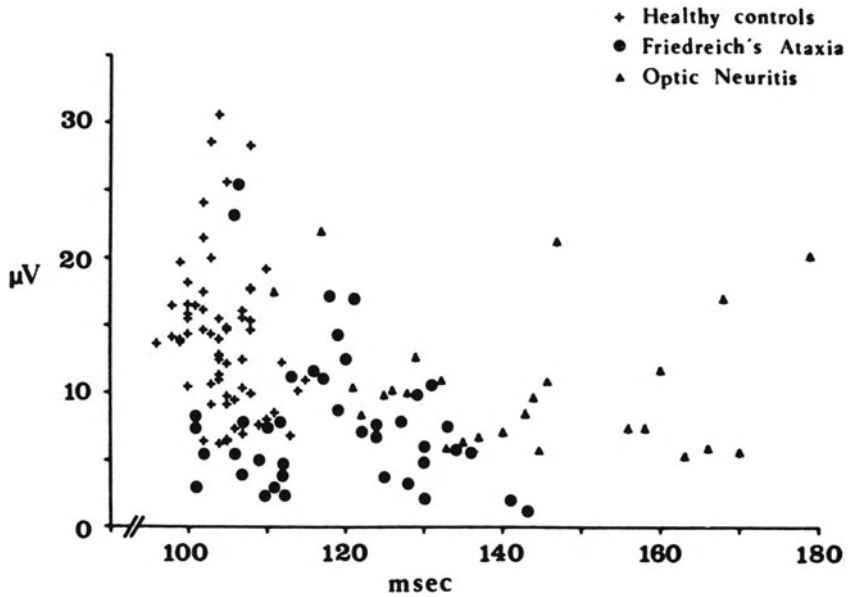
**Figure 8-1.** Post-operative evolution of SEPs—Neuroma of the 3rd cervical root

SEPs recorded at Erb's point are represented in A, those obtained at Cv6 spinal process are shown in B, ipsilateral and contralateral parietal responses are displayed respectively in C and D. Erb's point responses were obtained with a frontal Fz reference; all others with a noncephalic shoulder reference. Stimulation of the right median nerve at the wrist. Calibration 10  $\mu$ V in A and 5  $\mu$ V in B, C and D.

This 33-year-old female patient presented on admission a Brown-Sequard's syndrome under the 3rd cervical dermatoma with right side hemiparesis right tactile and joint position hypaesthesia and astereognosis of the right hand. Pain and temperature senses were impaired on the left side. No asymmetry of vibratory sense was noted. For each derivation the numbers indicate the order of successive post-operative records: 1: 9 days after surgery; 2: 2 months; 3: 6 months; 4: 1 year. In the four recording sessions normal responses were obtained at Erb's point (N9) and at the nucha (N13). On the scalp the far-field P9 and the P40 contralateral parietal components were constantly recorded. Immediately after surgery (traces 1C and 1D) the far-field P14, the diffuse N18 and the contralateral parietal P27 potentials were absent and the contralateral N20, if present, was considerably abnormal in amplitude and latency. The contralateral parietal P14, N20 and P27 components reappeared progressively with reduced amplitudes and delayed latencies (traces 2D, 3D and 4D).

This example of cervico-medullary SEP pattern illustrates 2 points: 1) Abnormal latencies can be observed in primary nondemyelinating diseases; 2) Late cortical components (in this case the P40 potential) may persist whereas earlier subcortical or cortical responses are absent or clearly abnormal [51].

so far attempts to develop EP amplitude indexes that permit identification of individuals with abnormally reduced EP components have been relatively unsuccessful. Side to side amplitude differences can be used in case of strictly unilateral hemispheric damage. They are particularly helpful for the interpretation of cortical auditory evoked potentials (AEPs) since monaural stimulation elicits evoked responses in both hemispheres through ascending and callosal



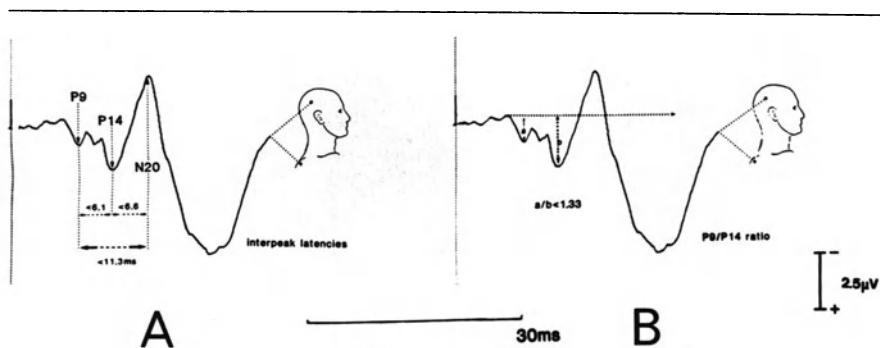
**Figure 8-2.** Latency and amplitude of the P100 VEP component in healthy controls, patients with Friedreich's ataxia and patients with a history of optic neuritis. VEPs obtained for each eye of 31 healthy controls, 21 patients with optic ataxia and from the affected eye of 24 patients who had recovered from a single typical episode of either monocular (22) or binocular (2) optic neuritis. In contrast to the patients with Friedreich's ataxia the cases of optic neuritis show a clear dissociation between the P100 latency increase and the amplitude changes. However there is a clear overlap between the two abnormal population [6].

fibers [65]. The amplitude ratio between a component known to be unaffected and a component likely to be abnormal in the suspected pathology can also be helpful. Figure 8-3 shows that the amplitude ratio between the far-field P9 (brachial plexus) and P14 (brainstem) potentials evoked by median nerve stimulation in normals has a gaussian distribution. When the afferent impulses in cervical spinal cord and brainstem are dispersed, this ratio can be significantly reduced while interpeak latencies remain normal.

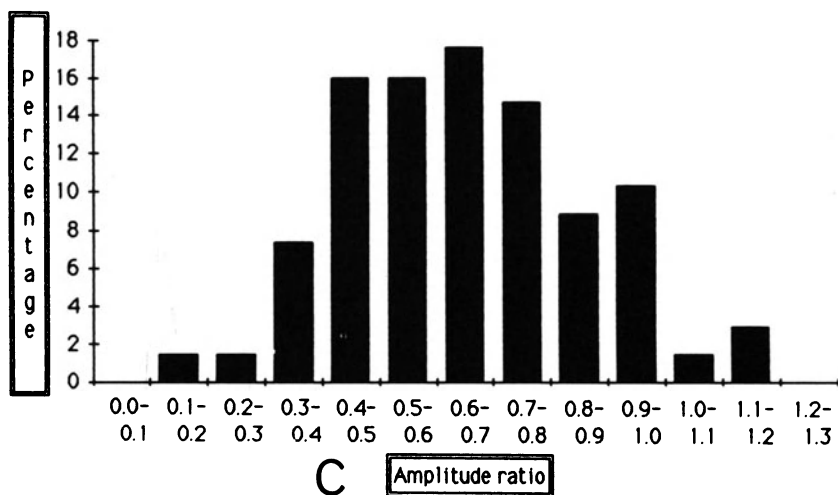
### Limits and pitfalls of the spatio-temporal analysis of EPs

#### *Spatial analysis*

The potential fields recorded on the surface of the scalp or at the neck may be generated either by deeply (far-field EPs) or superficially (near-field EPs) located sources. Recordings in normals support the view that a positive widespread scalp far-field response correspond to the front of action potential volleys traveling in the ascending sensory pathways [19, 37]. The near-field potentials may have an axonal or a post-synaptic origin, but their generators are generally modeled as dipoles. If the dipole is tangentially orientated and



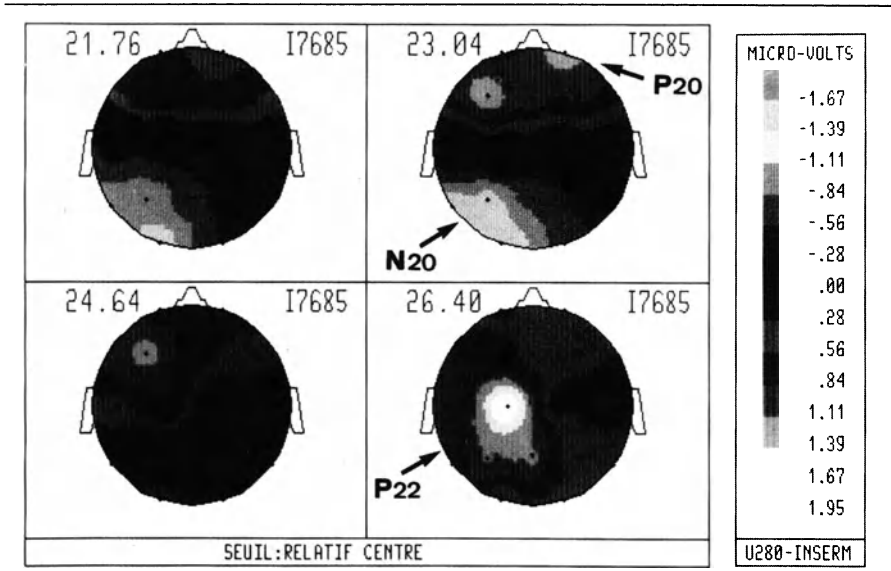
Distribution of P9/P14 amplitude ratio in normal controls



**Figure 8-3.** Latency and amplitude measurements of early P9, P14 and N20 SEPs. Noncephalic reference recordings of the contralateral parietal response to stimulation of the median nerve at the wrist. The transit times are evaluated by the P9-P14 and P14-N20 interpeak latencies (A). The amplitude ratio between the peripheral P9 and the brainstem P14 is measured from the onset of P9 (B). The distribution of the P9/P14 amplitude ratio calculated in 35 normal subjects is given in C. These data were obtained with filter band pass of 1.6–3200 Hz. Normative values for absolute and interpeak latencies are given in table 8-1.

close to the surface, both its positive and negative poles can be recorded with an appropriate electrode array. Consequently, the EP source would not be located at one of the maxima of the electric field, but between the two (at a depth that can be evaluated by recording of the magnetic field) and at equal distance from each maximum in the case of a theoretical tangent dipole [13, 83] (figure 8-4). The “paradoxical” lateralization of the P100 visual potential to



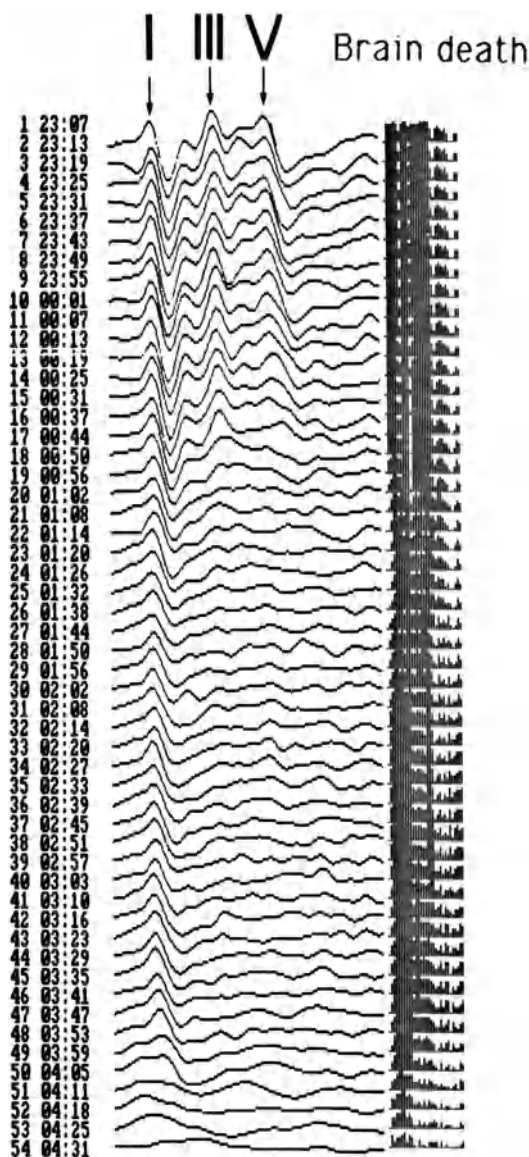


**Figure 8-4.** Sequential spatial maps of potential fields after finger stimulation. These maps were obtained 21.76, 23.04, 24.64 and 26.40 msec after stimulation of the right thumb of a normal subject. The mapping system is described with details in Deiber et al. [14]. This figure illustrates two different models of electric fields generated respectively by tangential (posterior parietal N20- frontal P20) and radial (frontal P22) dipoles. This spatial distribution accounts for some divergent views concerning the origins of early SEP components by showing that these potentials might be generated by the activities of two distinct generators that partially overlap in a very short period of time.

checkerboard half-field stimulation clearly illustrates this model [29]. If the dipole is radially orientated, the pole which is close to the surface will produce a field of concentric isopotential lines on a restricted area of the scalp (figure 8-4); then the EP source is assumed to be situated under the maximum of the electrical activity at a depth that cannot be actually measured by magnetic field recording which is blind to radial electrical sources. It is clear that all intermediates do exist between radially and tangentially orientated dipoles.

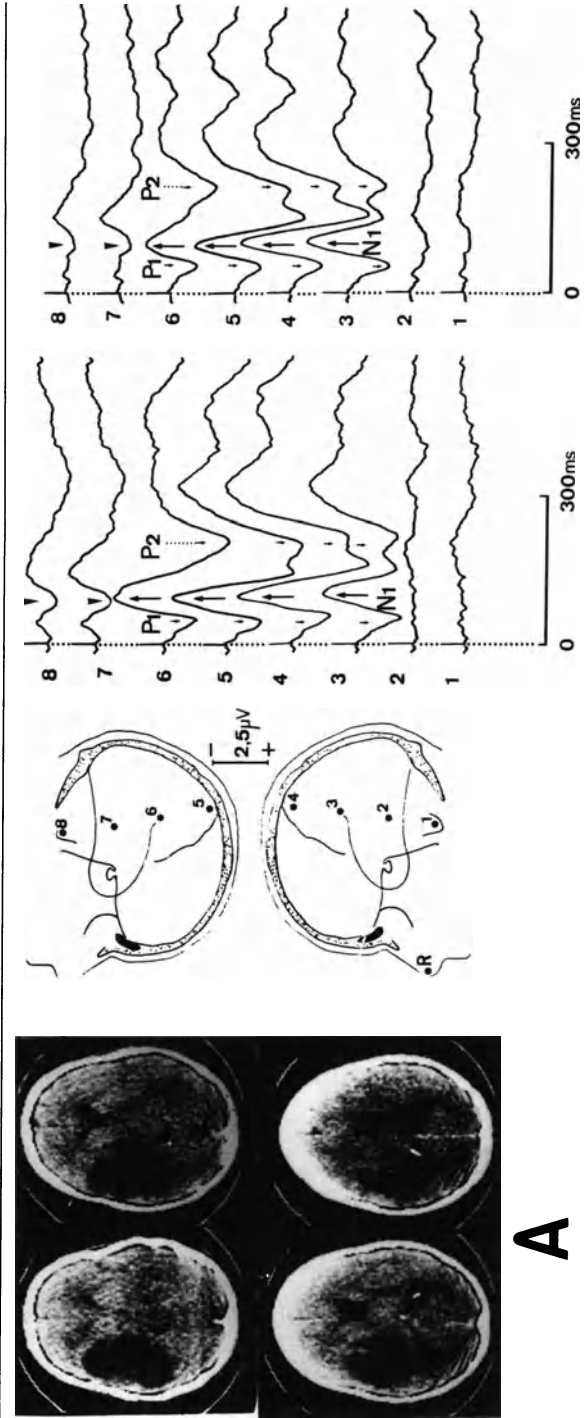
#### *Time analysis*

The averaging technique for EPs recording is based on the assumption that EP is a determinist signal reproducible on long sequences of iterative stimulations. It may be postulated that EP sources are sequentially activated during the processing of sensory informations. Thus, when all EPs components are missing after a given latency, the conduction is presumed to be interrupted beyond the level where the last present component is generated. This assumption is valid in most cases as illustrated in figure 8-5 that shows the progressive disappearance of waves V to 1 of the brainstem auditory evoked responses (BAEPs) during the rostro-caudal deterioration of brainstem functions in a

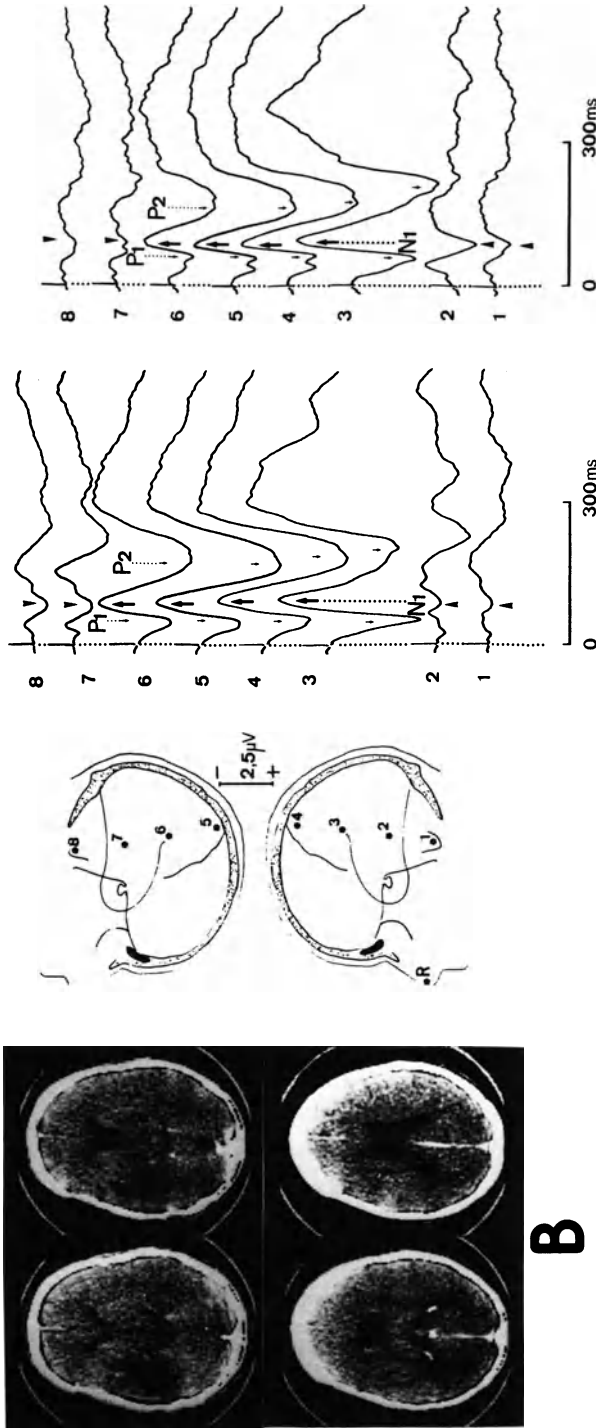


**Figure 8-5.** Rostro-caudal deterioration of BAEPs in brain death

The 54 BAEPs to 80 dB HL alternated clicks displayed in this figure were obtained in a head-injured comatose patient at a rate of one every 6 minutes between 23h. 07 and 4h. 31 with an analysis time of 12 msec. The histograms displayed on the right side correspond to the spectrum of the auto-adaptative Wiener digital filter used for the recording. At 23h.07 waves I to V are clearly identified; at 0h.31 the wave V has almost disappeared; from 1h.02 to 4h.05 only wave I persists. This evolution paralleled the rostro-caudal deterioration of the brainstem functions.



**A**



**Figure 8-6.** Late auditory evoked potentials (AEPs) in a case of left temporal glioma

In this 35-year-old ambidextrous female patient AEPs to tone bursts were recorded, with a coronal montage and a reference at the nose, before and after surgical removal of a left low-grade temporal astrocytoma with considerable mass effect. The patient presented partial auditory seizures, clinical examination was normal including dichotic listening test.

**A)** Before operation there was almost no positivity in the left temporal region after stimulation or right (right traces) or left (left traces) ear, the asymmetry index between right and left temporal responses clearly indicated a right hemispheric predominance (see section late AEPs for details). AEPs were otherwise normal.

**B)** Two weeks after operation there was no mass effect and a P100 positivity was now present also in the right temporal region

A possible explanation for this quick reversibility of the AEPs abnormalities could be that in the preoperative period the generator of the left temporal response was not destroyed but merely displaced by the tumoral mass. This view is in good correspondence with the finding that no extinction of the right ear was noticed in the dichotic listening test before operation. This example illustrates the fact that absence of EP components does not necessarily imply that the structure responsible for EP generation is destroyed; in such cases topographical studies using multichannel scalp montages could be helpful to differentiate between the two possible mechanisms of disappearance of EP components.

comatose patient. However, in some instances late events can persist even though earlier responses have disappeared. This most probably because sensory information is conveyed to the cortex by parallel pathways with independent processing time, synaptic relays and cortical targets (figure 8-1).

Thus, there are practical limitations to the use of spatio-temporal analysis of EPs to localize focal lesions in the central nervous system. The most important of these limitations is that both destruction and displacement of generators can make recording of EP components difficult, particularly when only using a limited number of electrodes (figure 8-6).

## SOMATOSENSORY EVOKED POTENTIALS

### Normal components

#### *Upper limb stimulation*

It is generally recognized that all the cervical and scalp events evoked by electrical stimulation of the median nerve at the wrist, with the exception of the supraclavicular N9 component and of its P9 far-field scalp homologue, are related to the activity of the dorsal column (DC) system. This was first pointed out more than twenty years ago by Halliday and Wakefield [30] who reported normal SEPs in patients with a dissociated loss of pain and temperature senses due to lesions of the spino-thalamic tract. However, the view of DC system spatially organized as to duplicate a single somatotopic map of the periphery, and made of neuronal channels with two synapses respectively in the DC and thalamic ventro-postero-lateral (VPL) nuclei, is an oversimplification that can lead to misinterpretation of SEP recordings. For instance there is anatomical evidence in cats that the cuneate nucleus has several brainstem targets apart from the the thalamic VPL [see ref 49 for details].

The centrally generated SEP components obtained with a noncephalic reference montage after stimulation of the median nerve at the wrist are the following (see figure 8-7 and chapter 3 for a more complete review of this topic):

1. The nuchal N11 component is recorded all along the posterior aspect of the neck with an onset latency that was found to increase from CV6 to CV1 spinal processes by  $0.95 \pm 0.15$  and  $0.89 \pm 0.12$  milliseconds respectively by Desmedt and Cheron [16] and Mauguière [47]. This shift of N11 onset latency is consistent with the hypothesis that it might be generated by the ascending volley of the action potentials in the dorsal columns of the cervical spinal cord (figure 8-8). As mentioned by Cracco [12] and illustrated in figure 8-8, it may be difficult in clinical practice to differentiate the N11 from the following N13 component; therefore the recording of the N11 scalp far-field homologue P11 has a practical utility.

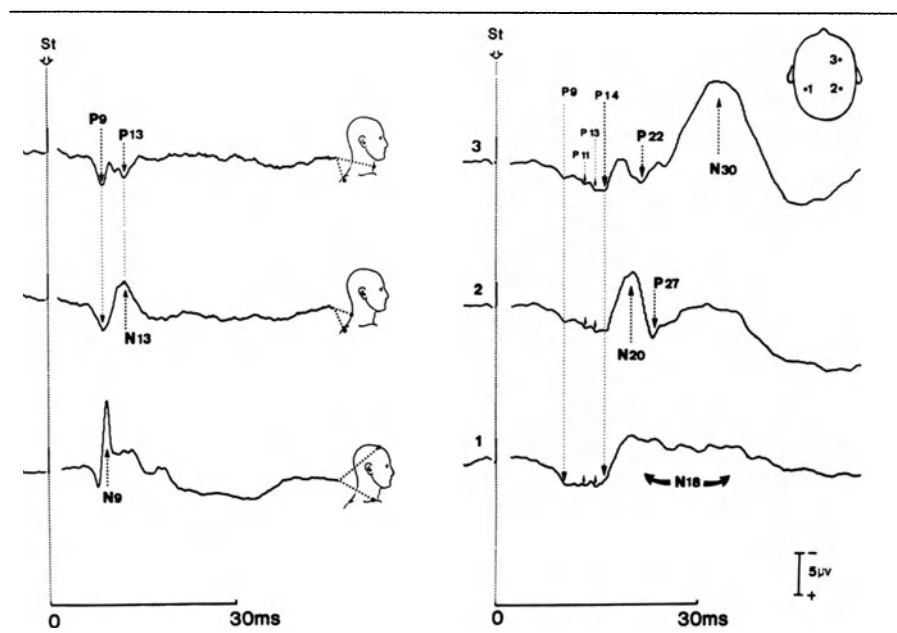
2. The N13 component is obtained at the nucha with a maximum amplitude at Cv5/Cv6 level and is recorded with a reversed polarity with an oesoph-

ageal or anterior cervical electrode [20] (figure 8-7). A fixed dipolar source in the dorsal horn perpendicular to the spinal cord axis could account for this spatial organization.

3. The scalp widespread P14 component is a far-field potential of brainstem origin. P14 is picked up at the ear lobe, but with a smaller amplitude than on the scalp. In our controls it peaks nearly one msec later than the cervical N13 [47].

4. The scalp N18 potential identified by Desmedt and Cheron [17] is a long-lasting diffuse negative shift which immediately follows P14 (figure 8-7). In normals, N18 can be fairly individualized only in the parietal region ipsilateral to the stimulation where there is minimal or no interference with later cortical components.

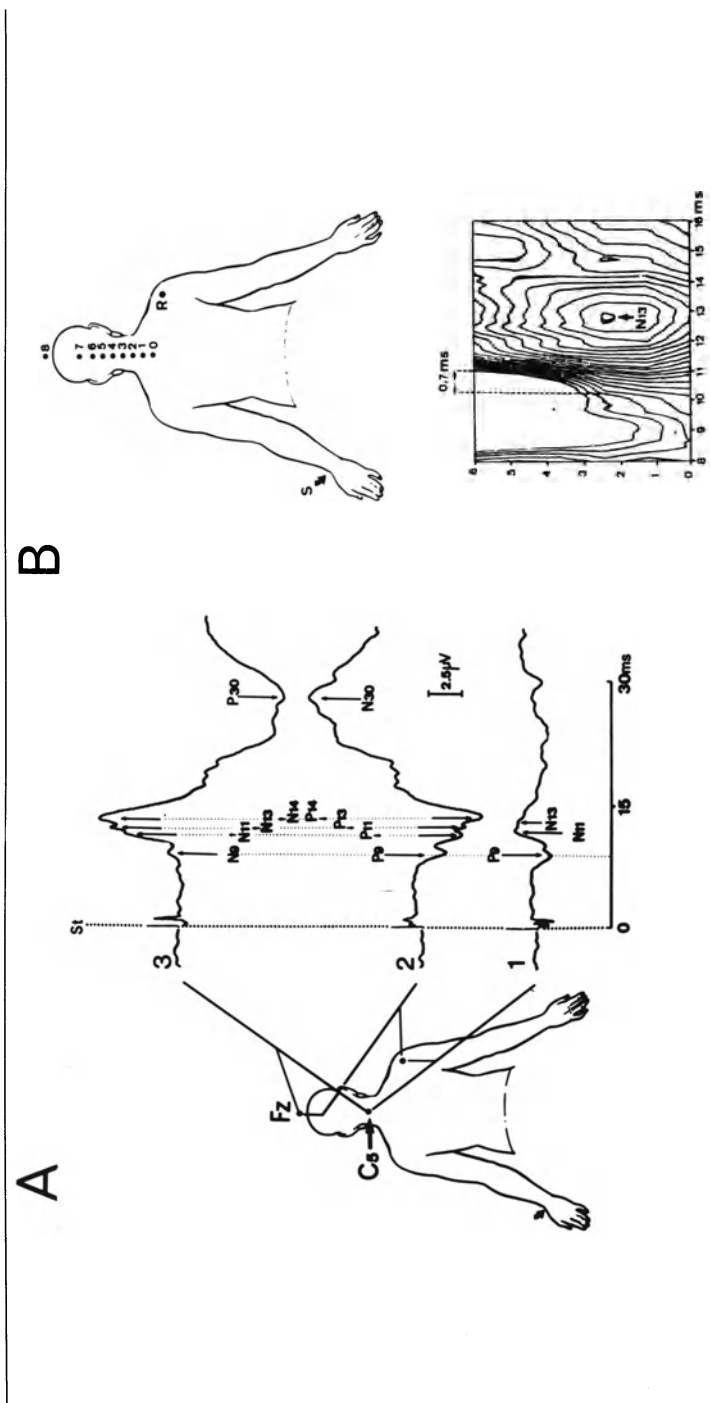
5. Two sets of cortical potentials, each made of two components, are super-



**Figure 8-7.** Normal SEPs to median nerve stimulation (noncephalic reference recordings, stimulation of the left median nerve at the wrist)

This figure illustrates the early SEPs that can be recorded with a shoulder reference. Note that in the ipsilateral parietal region (1) there is a long lasting negative shift that immediately follows the far-field positivites and corresponds to the widespread N18 potential. With 1.6–3200 Hz filter band-pass N18 is a long-lasting event. Filtering out of low frequencies changes the shape of N18 that can then be confused with an “ipsilateral” N20. Superimposition of ipsilateral and contralateral parietal responses is helpful to differentiate N18 from the contralateral parietal N20.

The nuchal N13 component is recorded as a positivity (P13) by an anterior cervical electrode. Contralateral parietal N20–P27 and frontal P22–N30 are consistently recorded in normal subjects. (see test for details).



**Figure 8-8.** Normal nuchal potentials (Stimulation of the median nerve at the wrist)

**A)** The responses obtained with shoulder (1) and frontal (3) references are illustrated. With frontal reference most of the cervical N9-N11-N13-N14 complex is due to the algebraic subtraction of the far-field positivities picked at the reference site (2). With the shoulder reference there is a P9 positivity corresponding to the activity of the brachial plexus followed by a small negativity in which the N11 and N13 subcomponents are not easy to identify.

**B)** Topographic study using spatio-temporal maps showing a 0.7 msec shift of N11 onset latency from lower to upper neck. The N13 potential is picked up only at the lower neck.

imposed on the widespread N18 (figure 8-7). The first one is the N20-P27 complex which is recorded in the parietal region contralateral to the stimulation; the second is composed of the P22 and N30 potentials which are located in the contralateral prerolandic region but often spread to the ipsilateral frontal region. These components are also present after finger stimulation, and their spatial distribution on the scalp is not distorted by ear lobe reference recordings that partially cancels N18 [14, 21] (figure 8-4).

All the centrally generated SEP components are preceded by the far-field P9 potential (homologue of the supraclavicular N9) which originates in brachial plexus roots and is present at the nucha and on the scalp.

In frontal (Fz) reference recordings the N18 and the far-field positive scalp components are cancelled and the cervical N9-N11-N13-N14 wave complex combines evoked activities picked up at the nucha and on the scalp (figure 8-8).

Conduction times in peripheral nerves, dorsal roots and central somatosensory pathways can be estimated by the recording of the Erb's point N9, spinal N13, far-field P14 and parietal N20. The conduction times (CTs) measured by interpeak latencies between Erb's point N9 (or far-field P9) and P14, and between P14 and N20 are of practical utility for studying diseases of central nervous system because they are fairly independent of arm-length. Central CTs can be evaluated in noncephalic or scalp reference montages [32]; in the latter condition, particularly when the waveform is abnormal, the distinction between the spinal N13 and the brainstem P14 positivity picked up at references site and injected as a N14 negativity in the cervical response may represent a real challenge. Control values obtained with both methods in our laboratory are given in table 8-1.

#### *Lower limb stimulation*

With a noncephalic reference electrode far-field positivities of spinal and brainstem origin are recorded on the scalp after stimulation of the tibial nerve [18, 41, 85]. In clinical routine, two early components are easy to obtain and used in most studies: 1) the lumbar negativity N21 (picked up at L1 spinal

**Table 8-1.** Normative data for absolute and interpeak latencies of early SEPs (35 normal adult subjects)

		Noncephalic reference			Frontal reference			
		Mean	SD	Mean + 3SD	Mean	SD	Mean + 3SD	
Absolute latencies (ms)	P9	10.34	0.89	13	N9	10.74	0.64	12.66
	P14	14.91	0.88	17.57	"N14"	14.33	0.83	16.82
	N20	19.81	1.17	23.31	N20	19.89	1.24	23.61
Interpeak latencies (ms)	P9-P14	4.56	0.52	6.12				
	P14-N20	4.87	0.58	6.61	"N14"-N20	5.7	0.61	7.53
	P9-N20	9.42	0.61	11.25	N9-N20	9.26	0.69	11.33



process with a dorsal, shoulder or knee reference) presumably generated in the dorsal horn of the spinal cord; 2) the vertex positivity P39 (present with a frontal, ear lobe or noncephalic reference) which has a “paradoxical” lateralization ipsilateral to the stimulation suggesting an origin in the interhemispheric aspect of the primary somatosensory cortex.

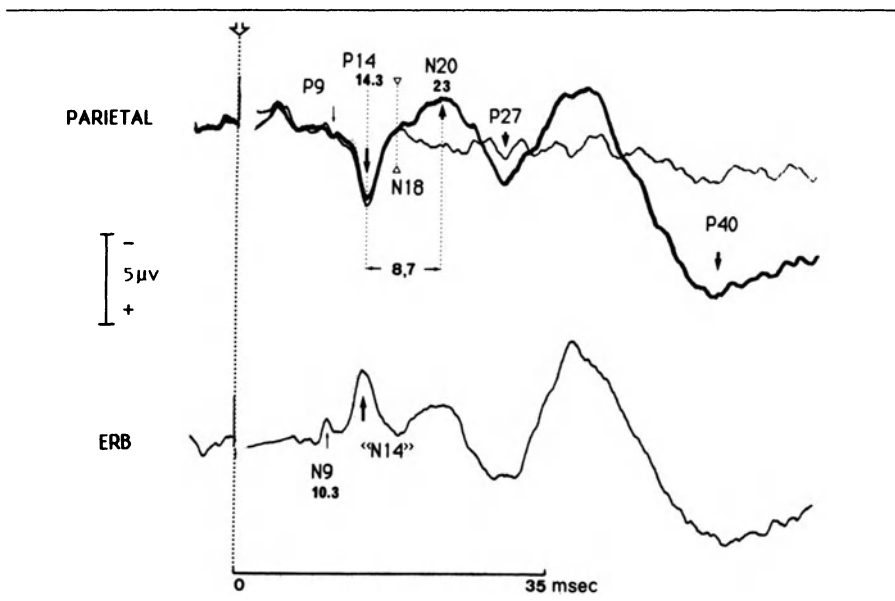
### **Abnormal SEP Patterns**

#### *Diseases of peripheral nerves and roots*

SEP MEASUREMENT OF CONDUCTION VELOCITIES IN PERIPHERAL NEUROPATHIES. The sensory conduction velocities in peripheral nerves (SCV) are usually measured by the recording of sensory nerve action potentials (SNAPs). In neuropathies when SNAPs are too small to be detected, the SCV can be indirectly estimated by the measurement of the onset latency of the contralateral parietal “N20” after stimulation of a cutaneous or mixed nerve at different levels; for instance wrist, elbow and axilla for the upper limb [15]. It was generally assumed that the cerebral response to non-noxious electrical stimulation of a mixed nerve was mainly due to myelinated cutaneous and joint afferents. However Gandevia et al. [25] demonstrated that stimulation of muscle afferents also elicits a cortical response with a latency very close to what is observed after stimulation of cutaneous afferents. Thus the SCVs indirectly measured by the recording of cortical SEPs to stimulation of a mixed nerve have a different signification than those obtained by the direct recording of SNAPs after selective stimulation of cutaneous afferents.

COMBINED INVOLVEMENT OF PERIPHERAL NERVE AND SPINAL CORD IN HEREDITARY ATAXIAS. In Friedreich’s ataxia it has been demonstrated that maximum SCV is only moderately decreased whereas the peak of the parietal N20 to finger stimulation, when obtainable, is delayed and desynchronized because of involvement of central somato-sensory pathways [60]. These abnormalities have been confirmed by others using mixed nerve stimulation [33, 35, 42, 61, 63, 68, 77]. When present, the N9 elicited by stimulation of the median nerve has a nearly normal latency but a reduced amplitude, however it contains antidromically conducted motor action potentials and its peak latency cannot be used to evaluate sensory conduction velocity. All studies agree that SEPs, including N9 and P9, are almost constantly abnormal in Friedreich’s ataxia. In a small proportion of cases, a desynchronized parietal N20 component persists, whereas the Erb’s point N9, cervical N13 and scalp P14 cannot be identified. Figure 8-9 illustrates a more exceptional SEP condition in Friedreich’s ataxia with abnormal P14-N20 interpeak latency co-existing with reduced N9/P9 and nearly normal brainstem P14. This aspect suggests an abnormal central conduction in the thalamocortical radiations.

In familial spastic paraplegia and hereditary cerebellar ataxia, SEPs differ from those observed in Friedreich’s disease in two main points: 1) the incidence of abnormal responses is smaller [63]; 2) peripheral N9/P9 components are normal in most cases [22, 63, 78].

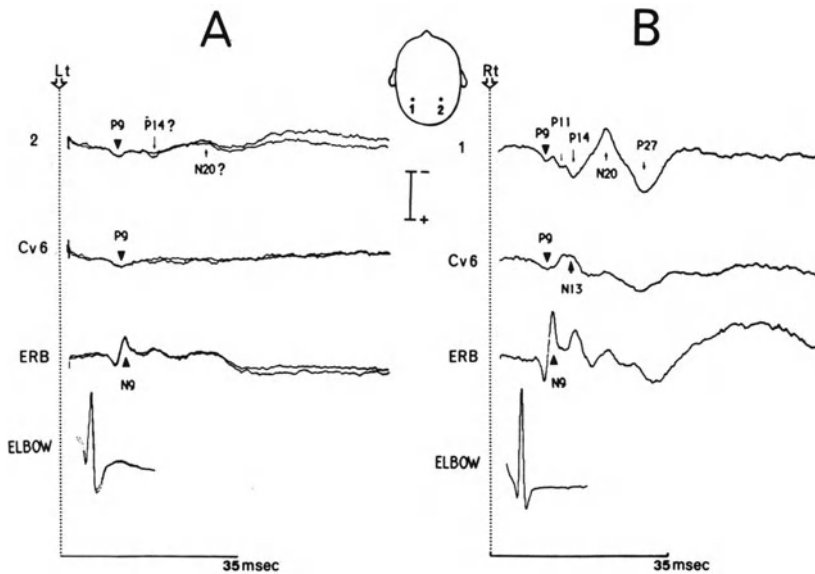


**Figure 8-9.** SEPs in Friedreich's ataxia (median nerve stimulation)

The lower trace was obtained at Erb's point with a frontal reference (Fz) and shows a reduced N9 potential followed by a "N14" which corresponds to the brainstem P14 which is picked at the front. The upper trace is a superimposition of the ipsilateral (thin trace) and contralateral (thick trace) parietal responses. It shows that, in spite of a very reduced peripheral N9/P9, brainstem P14 and contralateral parietal N20, P27 and P40 are present. In this case abnormal P14-N20 delay suggests central conduction slowing in the thalamo-parietal radiations.

A N9 component of normal latency with a delayed and/or reduced N13 would indicate conduction slowing in the dorsal root. Practically, such a pattern was observed only in a small percentage of patients with Guillain-Barré syndrome. Recently Yu and Jones [88], confirming the results of earlier investigations [26], reported a low incidence of this abnormal SEP pattern in patients with compressive radiculopathy but without myelopathy. The usefulness of SEPs to mixed nerve stimulation in addition to conventional EMG is not obvious in such patients.

The situation is different when the conduction is definitely interrupted by a traumatic rupture proximal to the dorsal ganglion; then, after stimulation of the median or ulnar nerves at the wrist, the Erb's point N9 and the far-field P9 potential persist (figure 8-10) when all later components are absent or reduced [34]. Such a pattern is useful to estimate the degree of involvement distal and proximal to the dorsal root ganglia in brachial plexus traction provided that the following limitations are taken into account: 1) N9 may be absent or significantly reduced at Erb's point in case of distal lesion associated to root avulsions or when the anatomical situation of brachial plexus roots in the supraclavicular fossa is modified because of the trauma (figure 8-10), 2) anti-



**Figure 8-10.** SEPs to median nerve stimulation in brachial plexus avulsion (A: left affected side, B: right normal side)

In proximal avulsion of the left brachial plexus roots nuchal N13 (Cv6), brainstem P14 and parietal N20 are absent or very reduced in amplitude while peripheral responses are present at elbow and Erb's point. In this case P14 and N20 were questionable after stimulation of the affected side, although definitely reduced. Amplitude reduction of N9 on the affected side was due, in this case, to displacement of torn roots in the supraclavicular fossa.

Calibration: 2.5  $\mu$ V for parietal and Cv6 leads; 5  $\mu$ V for elbow and supraclavicular derivations.

dromic volleys of action potentials in the motor axons participate in the genesis of N9 and attenuation of N9 may result from the anterograde degeneration of motor axons; 3) stimulation of median and ulnar nerves investigate mainly the C6-C7 and C8-T1 roots respectively, but not the C5 root which is the most frequently injured in these patients; 4) multiple root avulsions are necessary to cause unequivocal SEP abnormalities [76].

In practice SEP testing in patients with brachial plexus injury provides two informations: 1) when N9 is present and all later components absent multiple root avulsions are ascertained; 2) when N9 is present with reduced spinal and cortical components the lesion is proximal to the dorsal ganglion and either some of the tested roots are intact or all of them are damaged incompletely.

#### *Spinal cord lesions*

There has been a number of studies using SEPs in spinal cord trauma [10]. In most cases of complete functional transection of the spinal cord cortical SEPs to stimulation of nerves whose roots enter the spinal cord below the lesion are absent. However, in some cases recorded at the early stage the persistence of SEPs on the scalp may suggest some residual spinal cord function when

clinical examination would lead to more pessimistic conclusions and it is commonly assumed that normalization of SEPs may antedate clinical improvement. After a spinal injury, iterative SEPs can also detect clinically silent transient deterioration of conduction in the dorsal columns. This was found to occur between the third and sixth day after injury, and is presumably related to oedema of the spinal cord [66].

In a series of 20 spinal cord tumors (mainly ependymomas) we found that SEPs could be normal in spite of impaired sensations when the dorsal columns are infiltrated by the tumoral process, whereas the reverse situation (i.e., absent or clearly abnormal SEPs with clinically normal sensations) may be encountered in extrinsic compression of the cord [52]. As a rule, SEPs are very sensitive to spinal cord compression whatever the space-occupying lesion. A latency shift of SEPs can be observed in spinal cord compression or after surgical decompression in patients whose SEPs were absent preoperatively [51] (figure 8-1).

SEPs can be used to determine the upper level of dorsal column dysfunction in compressions or injuries of the spinal cord [36,40]. This, however, is a time consuming technique that does not add much complementary informations to the clinical examination.

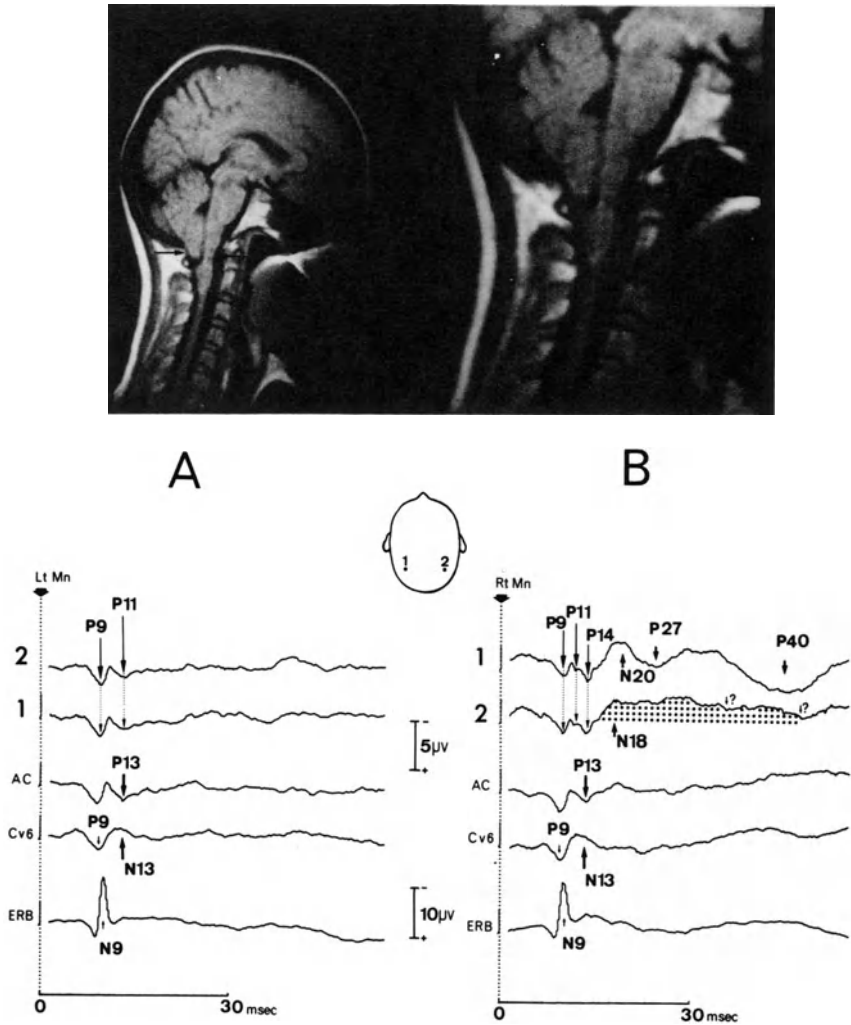
SEPs (particularly after stimulation of the lower limbs) can also help to assess the function of dorsal columns in various myelopathies with minimal or no clinical somatosensory signs, such as vitamin B12 deficiency [24], Strumpell's hereditary spastic paraplegia [22, 78] or amyotrophic lateral sclerosis [11]. As others [10] we have observed absent or reduced SEPs in the former two conditions but not in the latter one. Clinically unaffected members of families with hereditary spastic paraplegia and abnormal SEPs may represent asymptomatic heterozygotes.

#### *Lesions of brainstem thalamus and cortex*

Abnormal patterns of SEPs in these patients have been described in details elsewhere [53] and are illustrated in figures 8-11 to 8-15:

THE "CERVICO-MEDULLARY" PATTERN (FIGURE 8-11). In this pattern the far-field P9 and the spinal components N11 and N13 are present and normal when the far-field P14 and all later components are absent or abnormal [48, 51]. This pattern means that the volley of impulses ascending in the cervical dorsal columns is blocked or dispersed at the cervico-medullary junction; it can also be observed in brain dead patients [2, 3]. A persisting P11 scalp far-field positivity can be confused with a brainstem P14, particularly when it is delayed because of dorsal column compression at the cervico-medullary junction (figure 8-11). The recording of the cervical N13 helps in making the distinction between P9 and P14 since P11 peaks earlier and P14 later than N13. When not completely cancelled P14 is delayed and the P14 amplitude ratio is abnormally high in such patients (figure 8-1).

THE "THALAMO-CORTICAL" PATTERN (FIGURE 8-12). In thalamic, thalamo-

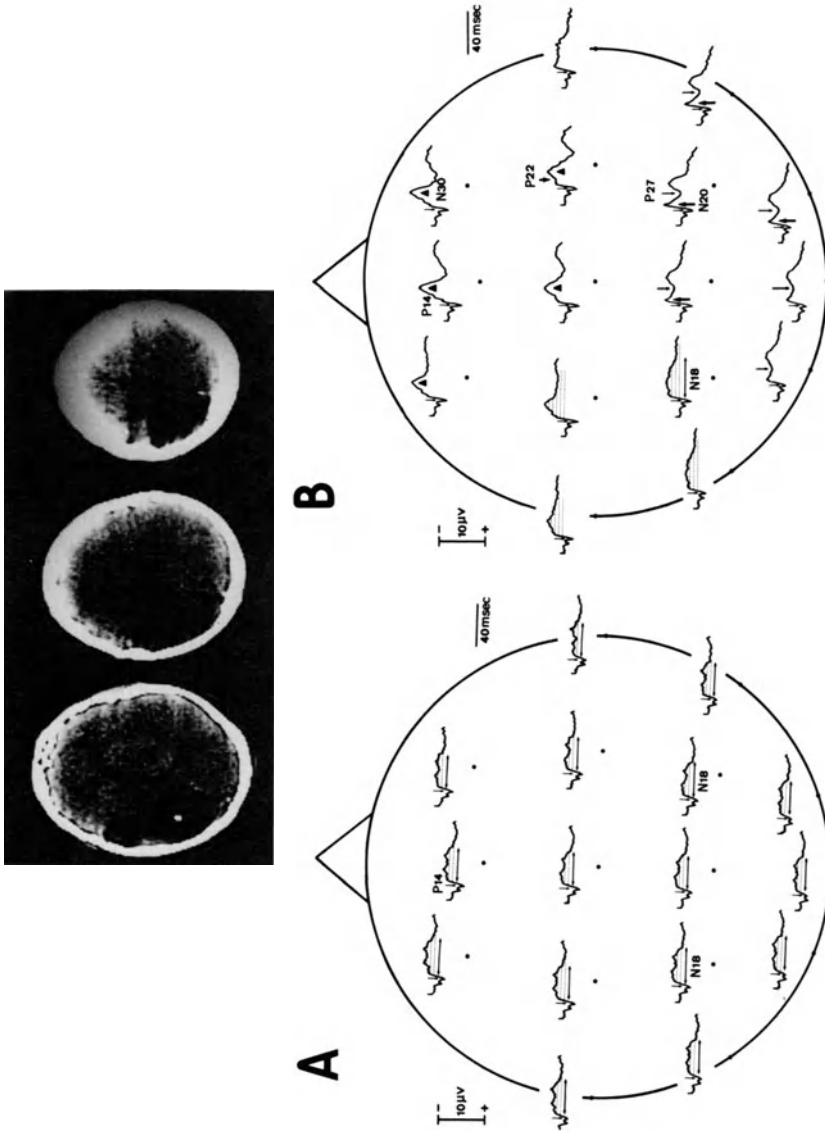


**Figure 8-11.** “Cervico-medullary” SEP pattern in a case of Arnold-Chiari malformation [51]. This female patient aged 42 had had a complete astereognosis of the left hand for more than 20 years when the SEP recordings were carried out.

A sagittal view of the cervico-medullary junction with NMR showed herniation of the tonsils into the foramen magnum (arrow). The IVth ventricle was not enlarged and communicated with the sub-arachnoid space.

**A)** Stimulation of the left median nerve: “Cervico-medullary” pattern; the positivity that immediately follows P9 can be interpreted as a delayed P11 and not as a reduced P14 since it peaked with a shorter latency than the normal P14 recorded after stimulation of the non-affected side (see text for details)

**B)** Stimulation of the right median nerve: Normal responses



**Figure 8-12.** "Thalamo-cortical" SEP pattern in a large cortical and subcortical parietal lesion  
**A)** After stimulation of the affected side all the cortical components were absent with normal far-field positivities and a persisting diffuse N18 negativity  
**B)** After stimulation of the normal side, parietal and frontal components were obtained showing a normal topography. The frontal N30 and, at a lesser degree, the parietal P27 were picked up near to the midline on the ipsilateral side. Consequently N18 could be isolated only in the ipsilateral parietal region

capsular or large pre-rolandic and post-rolandic cortical lesions associated with contralateral loss of tactile and joint position sensations, the cortical parietal and frontal components are absent on the damaged side with preserved scalp far-field positivities, including P14 [45, 49, 58, 75, 87]. The N18 diffuse negativity persists in this condition [49]. In 65 patients with recent thalamic or thalamo-cortical strokes and absent SEP cortical components we found that the P9/P14 amplitude ratio was within normal limits (mean value in normals + 3 SD).

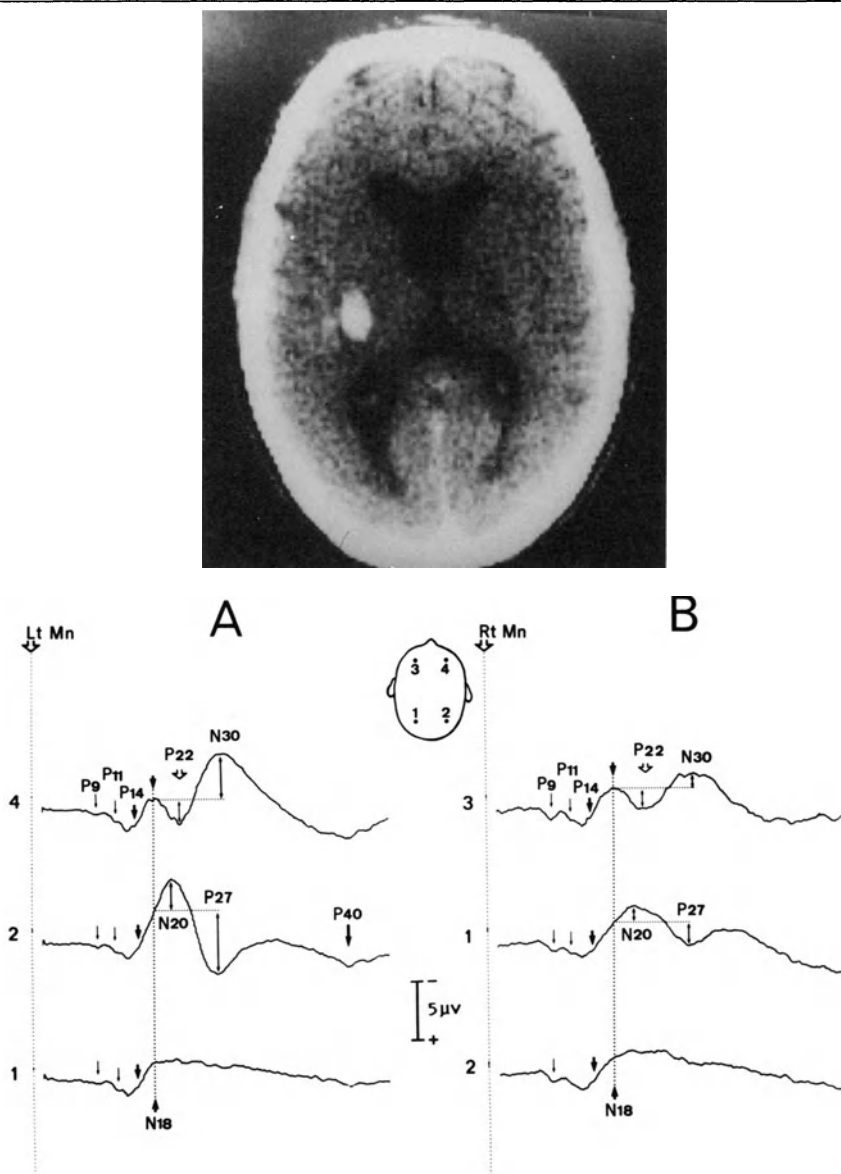
In patients with purely thalamic non-hemorrhagic stroke a fairly good correlation is found between SEP abnormalities, clinical status and CT scan data [27, 53]. In the postero-lateral infarctions of the geniculo-thalamic artery territory with absent SEPs, a loss of touch and position senses is constant, whereas early SEPs are normal in medial or antero-lateral infarctions that do not cause any somatosensory loss.

In capsular infarcts in the territory of the anterior choroid artery or in thalamo-capsular hematomas we observed no clear correlation between CT scan and SEP findings. In our series of 43 patients with this condition [53], 13 had normal SEPs and 22 had a thalamo-cortical SEP pattern with no cortical components and preserved N18; in the 8 remaining cases the cortical N20 and later components were only reduced in amplitude and delayed (figure 8-13). In these cases the degree of hemispheric somatosensory deafferentation cannot be accurately predicted from CT scan images, and somatosensory deficits that are not clinically obvious can be disclosed by SEP recordings particularly in patients with ataxic hemiparesis or thalamic neglect syndromes.

**THE "CORTICAL DISSOCIATED" PATTERN.** When the lesion is close to the cortex it may selectively damage selectively pre-rolandic or post-rolandic cortex or thalamo-cortical fibres in the corona radiata. Thus dissociated loss of pre-rolandic or post-rolandic components (figure 8-14) is more likely to occur in this condition than in thalamo-capsular lesions [48, 86]. Moreover, as illustrated in figure 8-15, after stimulation of the affected side cortical SEPs may be absent for one limb and normal for the other when the lesion is limited to a part of the somatotopic representation of the contralateral side of the body.

Our initial observation of persisting frontal P22 and N30 with absent parietal N20 and P27 in a large parietal lesion (figure 8-14) was recently confirmed by Slimp et al. [73] who reported a similar observation after excision of the SI area in man. Such a dissociated cortical SEP pattern suggests that frontal and parietal potentials might be triggered via independent thalamo-cortical pathways. This aspect was unequivocal in only 13 of our 66 patients with a lesion located in the cortex and in the subcortical white matter [53]. In the others, either the lesion spared the parietal and the prerolandic cortices and the responses were normal with no somatosensory loss, or it caused hemiplegia and hemianesthesia because of damage to the whole rolando-parietal region and SEPs were of the thalamo-cortical type with normal N18 and no cortical components.

**ENHANCED SOMATOSENSORY RESPONSES.** Since the earliest description by

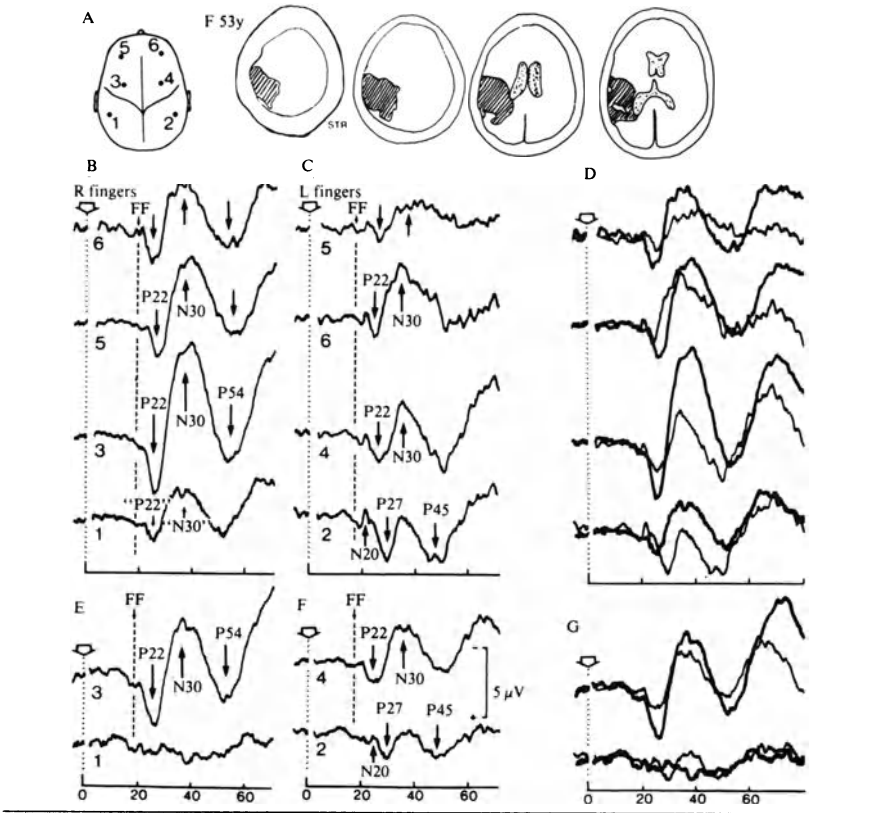


**Figure 8-13.** SEPs in a left posterior capsular hematoma

SEP recordings were obtained one month after the vascular accident; the right extremities were slightly ataxic and paretic but there was no clinical somatosensory deficit. Initially the patient had a complete astereognosis of the right hand with right joint and cutaneous hypesthesia and a "thalamo-cortical" SEP pattern (see figure 8-12).

One month after the vascular accident, the parietal and frontal cortical components were reduced and delayed after stimulation of the right affected side. (B) compared to those obtained on the normal side (A) in spite of normal sensations.

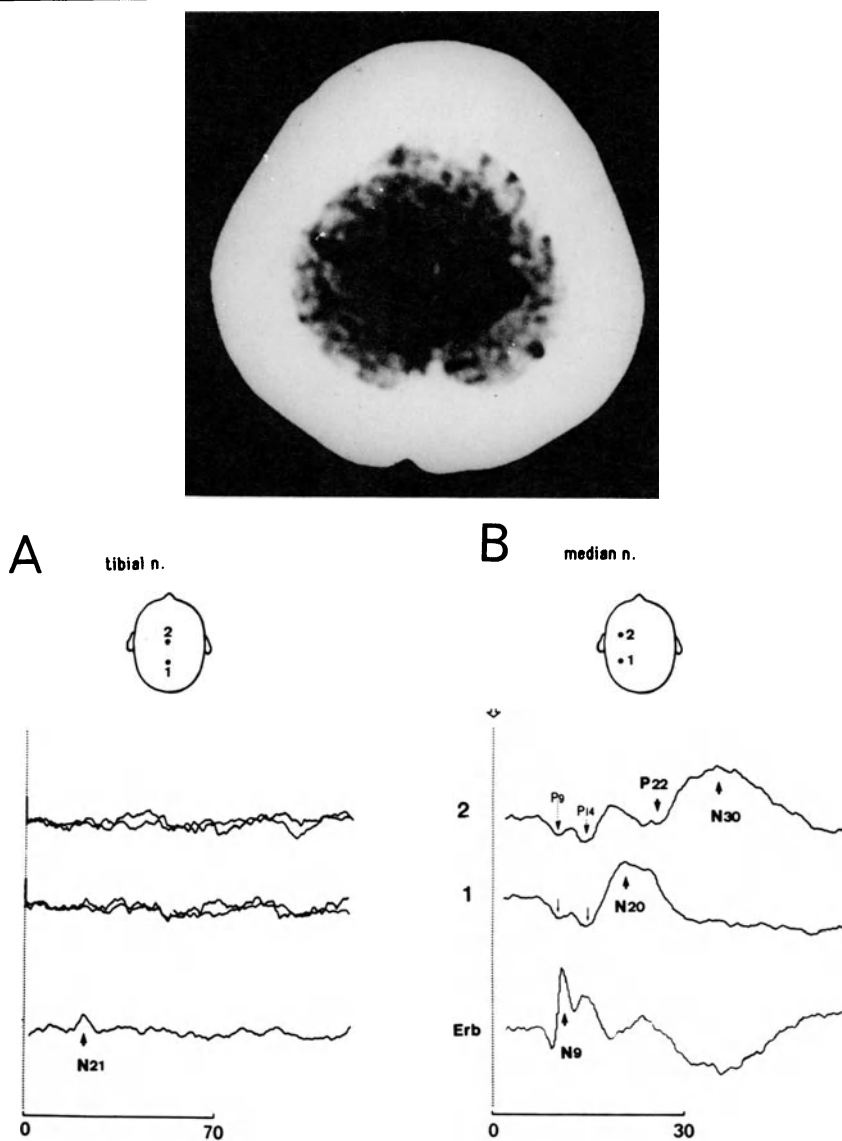




**Figure 8-14.** Dissociated loss of parietal cortical SEP components in a parietal lesion. Electrical stimulation of fingers II and III at intensities three times threshold (B, C) or near threshold (E, F). In D and G the responses of both hemispheres are superimposed the thicker trace corresponding to the SEPs to stimulation of the affected side.

This 53-year-old female patient had presented for five years a complete right anesthesia due to a left parietal infarct. After stimulation of the right fingers contralateral parietal responses were absent while prerolandic P22 and N30 were enhanced and volume-conducted backwards to the parietal recording site (B). This backward extension did not occur after stimulation at threshold intensity (E). [50]

Dawson in 1947 [13] the relation between myoclonus-related EEG spikes and giant SEPs in patients with dyssynergia cerebellaris myoclonica, progressive myoclonic epilepsy or focal reflex myoclonus has not been fully elucidated [62, 71, 72]. It is interesting to notice, however, that in patients with myoclonus giant SEPs can be recorded in the absence of myoclonus-related spikes and vice-versa; moreover both abnormalities may be absent. Thus patients who apparently have similar clinical symptoms can show different SEP abnormalities. Shibasaki and Kuroiwa [70] employed the technique of back averaging the EEG prior to the myoclonus (jerk-locked averaging) to establish that



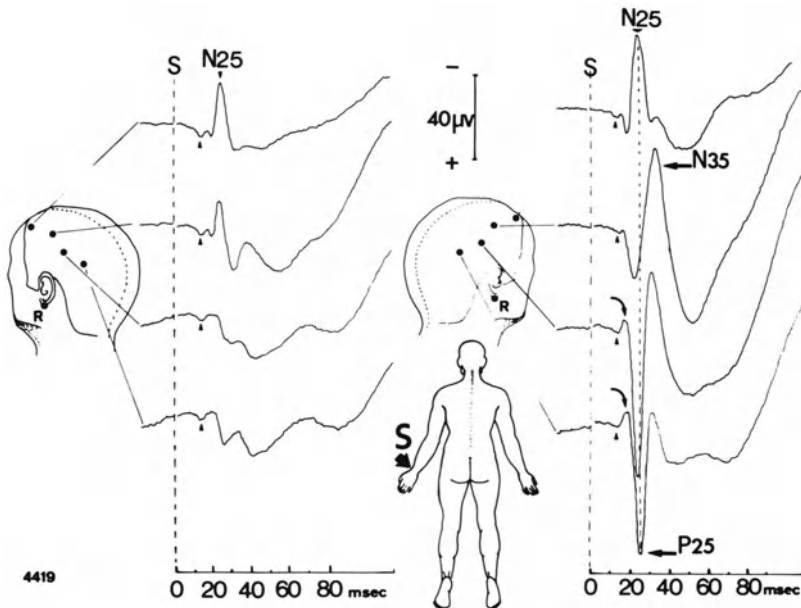
**Figure 8-15.** Selective loss of SEPs to lower limb stimulation due to a small parasagittal astrocytoma

This 42-year-old female patient presented somatosensory seizures that begun in the left foot with secondary extension to the whole left leg. On clinical examination there was only a hypesthesia for joint sensation in the left foot.

After stimulation of the left tibial nerve (A) the lumbar N21 negativity was obtained but the cortical responses were absent. After stimulation of the left median nerve responses were normal (B).

spontaneous myoclonus might be related to an abnormal cortical discharge even though the surface EEG showed no abnormality. The giant SEP is made of a P25-N30 complex [70] (figure 8-16). The interval between the peak of P25 or the back-averaged cortical spike and the onset of the myoclonus in the arm is approximately 20 msec, consistent with rapid conduction in the direct corticospinal pathway [54]. This observation supports the view that in patients with giant SEPs and myoclonus-related spikes the underlying pathophysiology is an abnormal cortical response to afferent impulses (pyramidal myoclonus) [28], whereas in patients with no giant SEPs or myoclonus related spikes the pathophysiology of myoclonic jerks is different. Thus the finding of giant SEPs is of diagnostic significance in the management of myoclonus patients.

The parietal N20 potential, when it can be identified, has normal latency and amplitude in most patients with myoclonus [44, 62, 67, 71]. Similarly the P14 is normal but difficult to identify because of its small size [44]. The normal size of the N20 component (figure 8-16) indicates that the sensory input into the cortex as well as the primary cortical response itself is not grossly abnormal.



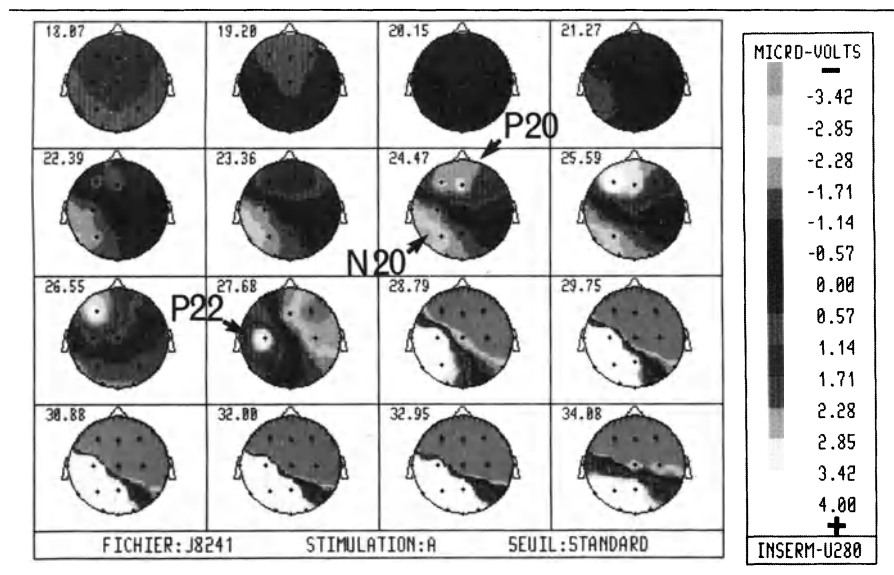
**Figure 8-16.** Giant SEPs in progressive dysynergia cerebellaris myoclonica (Median nerve stimulation)

These potentials were recorded with an earlobe reference and show that preceding the giant P25-N25 parieto-frontal dipolar complex (see also figure 8-17), far-field P14 (arrows) as well as contralateral parietal N20 (bent arrows) are obtained with normal amplitudes and topographies. Notice the calibration.

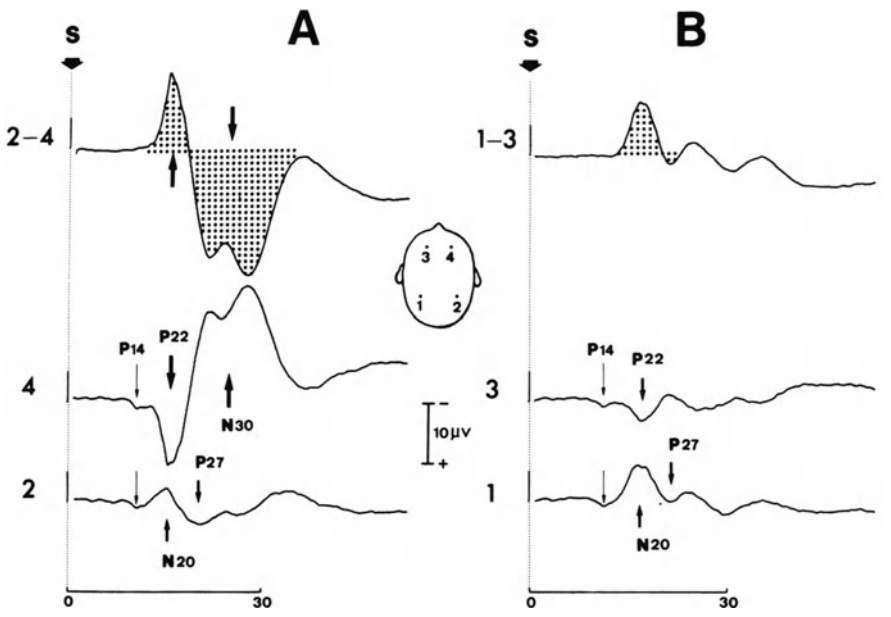
The question whether giant SEPs correspond to enlarged components of the normal response or to additional events not present in normal subjects has not been answered. Preliminary data from sequential spatial mapping studies illustrated in figure 8-17 show some similarity between the topographies of frontal P22-N30 components and abnormal giant responses.

Intravenously (IV) injected benzodiazepines reduce spontaneous myoclonus and reflex muscle jerking, but their effect on SEPs is a matter of controversy. In a group of five patients we found a significant 30% amplitude reduction of the giant SEP component 5 and 10 minutes after clonazepam 1 mg IV [43](i) Shibasaki et al. [71] observed similar effects after IV diazepam in one patient, but Rothwell et al. [67] noted an enhanced response after clonazepam in two patients.

Enhanced SEPs can also be observed on the damaged hemisphere in patients with supratentorial tumors, post-traumatic cortical atrophies, or long after an ischemic or hemorrhagic stroke. In these patients the enhancement of the response is moderate and myoclonus is exceptional. Loss of inhibitory control and post-lesional collateral sprouting of cortical afferents could be responsible for such SEP abnormalities. Frontal responses can be selectively enhanced in cortical atrophies and tumors (figure 8-18) even when there is no myoclonus triggered by somatosensory stimuli.



**Figure 8-17.** Sequential spatial maps of SEPs to right thumb and finger II stimulation in a case of progressive myoclonic epilepsy with distal action myoclonus. Amplitude, spatial distribution and timing of the parieto-frontal N20-P20 tangential dipolar field are normal (see 8-4). The equivalent of the prerolandic P22 is coupled to an ipsilateral negativity which is not observed in normals. Afterwards the giant P25-N25 dipolar field saturates the color scale.



**Figure 8-18.** Selective enhancement of the prerolandic P22 and N30 components in a patient with a right rolandic low-grade glioma

This figure shows that enhancement of SEP frontal components may be observed in other conditions than action myoclonus. This 57-year-old female patient had a progressive left hemiparesis but no seizure or myoclonus and no somatosensory loss.

After stimulation of the affected left side (A) only the frontal components are enhanced compared to those obtained on the normal side (B). With the parietal to frontal derivation (2-4 and 1-3) it is not possible to know which of the prerolandic or postrolandic components are enhanced on the damaged side.

### VISUAL EVOKED POTENTIALS (PATTERN SHIFT STIMULATION)

VEPs to pattern shift stimulation are certainly the most useful and most widely used electrophysiological method to detect silent lesions in multiple sclerosis. Methodology, data analysis, diagnostic yield of pattern shift VEPs in conditions other than primary demyelinating diseases have been extensively reviewed recently [29] and will be only briefly summed up in this chapter.

#### Normal components

The response to full-field stimulation obtained in the occipital region with a frontal Fz reference is the sum of a macular N75-P100-N145 complex and of a paramacular P75-N105-P135 complex. After half-field stimulation the former is recorded ipsilaterally to the stimulated half-field and the latter contralaterally. This clearly indicates that half-field stimulation and multichannel montages exploring both occipito-temporal regions are required for VEP investigations of visual field defects. Another consequence is that a persisting P135 para-

macular complex can be confused with a delayed macular P100 in case of central vision defect.

There are considerable variations among authors in literature concerning size of the stimulated field, spatial frequency, brightness, and contrast of the pattern, and methods to obtain pattern reversal (rotating mirror, TV screen, light emitting diodes, vertical gratings with a sinusoidal luminance profile). Most of the VEP finding that have been ascertained in non-demyelinating diseases have been obtained in conditions identical or very similar to those used by the Queen Square group. The VEP is elicited by the reversal in 10 msec of a circular checkerboard using a rotating mirror; the checkerboard is projected on a translucent screen which subtends a 16 degree radius at the eye and consists of 50' squares with brightness levels of 227 cd/m<sup>2</sup> and 8.2 cd/m<sup>2</sup> respectively for the white and black squares. These technical details are important because the normative values and the diagnostic yields are a function the recording procedures.

### **Abnormal VEP patterns**

#### *Diseases of the eyes*

An ophthalmologic disease should be suspected when unilateral or bilateral absence (or reduction) of pattern VEPs is associated with visual loss. However, delayed VEPs due to refractive errors can be misinterpreted and a careful ophthalmologic examination is an absolute prerequisite to VEP testing. Any refractive error that causes defocussing of the image should be corrected before testing. A shift of the P100 latency with amplitude reduction is more likely to occur with small stimulus field and small checks. Even with a checkerboard stimulus of low spatial frequency a large refractive error or opacities of the cornea, lens or vitreous can cause disappearance of the macular P100 potential and the persisting paramacular P135 can then be interpreted as a delayed response. The same limitation applies also to maculopathies causing central scotomata. In these conditions electroretinography may be a helpful complement to VEPs. Amblyopia may also be the source of a complicating problem in clinical EP testing when it manifests itself with a central scotomatous defect; however, in most cases tested with conventional checkerboard, P100 is reduced in amplitude without any significant shift of latency.

Glaucoma can be associated with delayed VEPs when there is a subjective visual impairment in the central six degrees of the visual field or when static perimetry shows a global decrease of retinal sensitivity. In practice before VEP testing with pattern reversal the measurement of retinal sensitivity in the central visual field using a Friedmann's analyser is quicker and more useful than the commonly used Goldmann's dynamic perimetry.

#### *Optic nerve, heredodegenerative and system diseases*

The pattern shift VEPs were reported as abnormal in various conditions such as toxic amblyopias due to alcohol tobacco abuse, vitamins B12 and E defici-

ency, ischemic optic neuropathy, neurosyphilis, sarcoidosis, Leber's optic atrophy, dominant hereditary optic atrophy, adrenoleucodystrophy, Charcot-Marie-Tooth disease, Friedreich's ataxia, hereditary spastic paraplegia, Huntington's chorea, pseudotumor cerebri, hypothyroidism, uremia and Parkinson's disease. In patients with Parkinson's disease there is no significant latency shift of P100 with a conventional TV checkerboard [23] whereas P100 is delayed after stimulation by a vertical sine-wave grating [5]. Follow-up studies indicated that VEP paralleled the clinical evolution in toxic and nutritional amblyopias, pseudotumor cerebri, and Parkinson's disease.

Neither amplitude reduction nor delayed latency of P100 can be viewed as specific of any of these aetiologies even though amplitude abnormalities are more likely to be caused by axonal damage and latency shifts by myelin loss; abnormal synaptic transmission could also account for delayed VEPs in Parkinson's disease.

The question whether VEPs could be helpful to detect heterozygotes in families with autosomic recessive diseases and subjects at risk for Huntington's disease is a very debated issue. In a recent study of Huntington's disease [31] a P100 of reduced amplitude but normal latency was found in 39% of clinically affected and in 7% of the subjects at risk; absence of the normal paradoxical lateralization of P100 after half-field stimulation was observed with a frequency of 69% and 16% in the same two groups of patients. Taking into account the technical difficulties of half-field stimulation and the need for long-term follow-up studies VEPs cannot be recommended at present time as a test for the detection of subjects at risk for Huntington's disease.

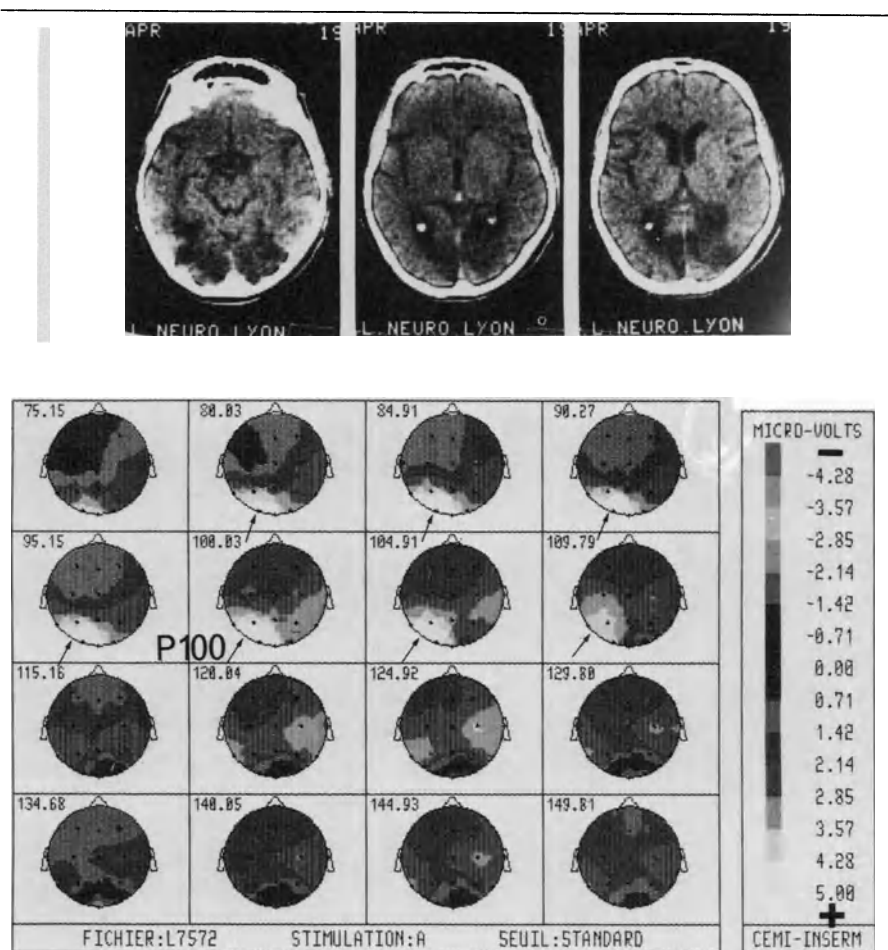
VEPs proved to be particularly sensitive to the effect of compression of the optic nerve. Amplitude reduction and, to a lesser degree, latency shift of P100 can be recorded even when clinical signs are minimal in patients with extrinsic compression of the optic nerve. Delayed VEPs in these patients can be misinterpreted as a symptom of primary demyelination.

#### *Visual field defects due to chiasmal and retrochiasmal lesions*

The scalp distribution of the VEPs to full-field stimulation in cases with bitemporal or lateral homonymous hemianopia can be deduced from what is known of the scalp distribution of macular and paramacular complexes. Blumhardt et al. [4] estimated at 65% the detection rate of VEP abnormalities to full-field stimulation in patients with homonymous visual field defects. This figure is low if one considers that the field defect was obvious on conventional perimetry in all of these cases. Half-field stimulation increased the percentage of abnormal VEPs to 84% in the series of Blumhardt, [1, 39] but cannot be carried out in uncooperative patients. Moreover the sparing of the macular field on the blind side is one of the reasons why VEPs may fail to detect hemianopia since both occipital lobes are activated by the stimulation [8]. Lastly VEPs cannot distinguish between total and scotomatous homonymous visual defects [1]. Thus present VEP techniques are definitely less sensitive than

campimetry as a means of detecting visual field defects or localizing the underlying lesion.

A persisting P100 can be observed in patients with cortical blindness due to bilateral occipital infarction provided that they are able to keep their eyes fixed in the direction of the stimulus [7] (figure 8-19). VEPs to flash stimulation were found to persist in a patient with cortical blindness in whom post-mortem examination showed infarctions in the white matter of both occipital



**Figure 8-19.** Spatial maps of VEPs to pattern shift stimulation in a case of cortical blindness (binocular stimulation)

This patient, as the few others reported in the literature, was able to keeping an unsteady fixation towards the screen where the pattern was displayed. He was otherwise behaving as a blind man but denied his visual deficit. There was a P100 slightly shifted to the left but with normal latency (see the text for a discussion).



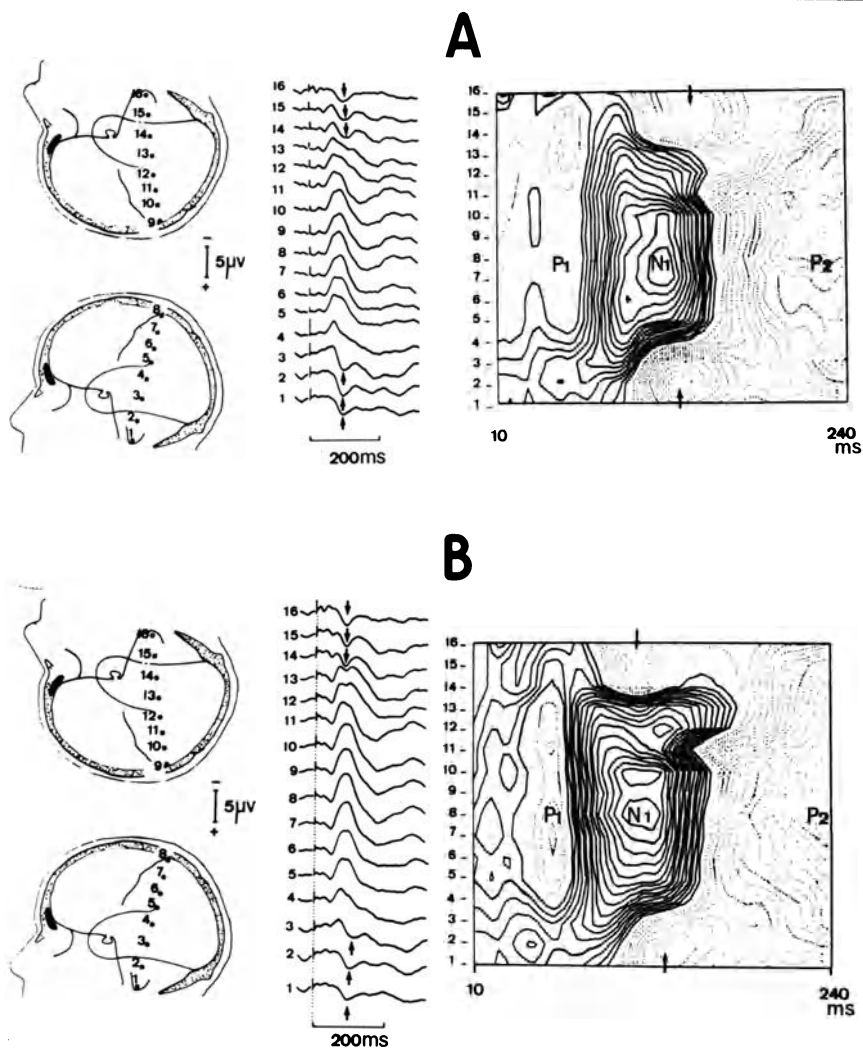
lobes [74]. It was hypothesized that this response was triggered by extrageniculo-calcarine connections between the optic nerve and the secondary occipital or temporal visual areas (retino-tecto-pulvinaro-cortical system). This hypothesis does not explain the persistence of P100 to checkerboard reversal since this component, at least for squares smaller than 1 degree, mainly reflects the activity of central retino-geniculate fibres projecting to the primary visual areas. Positron Emission Tomography (PET) studies of regional cerebral blood flow and glucose metabolic rate in one of these patients [7] demonstrated that an island of occipital cortex was metabolically active. This indirect argument supports the view that a surviving neuronal pool in area 17, disconnected from the associative visual cortex, is sufficient to generate a P100 potential but not for visual perception.

### AUDITORY EVOKED POTENTIALS

Scalp recorded EPs to auditory stimulation (AEPs) are usually classified into early (0–8 msec), middle (8–50 msec) and late (50–500 msec) responses. The early responses are known to originate in the eighth nerve and brainstem (BAEPs) while the origin of the middle latency components is still debated (acoustic radiations and/or primary auditory cortices). Late responses are of cortical origin and are modulated by attention, orientating reflex towards the stimulus, memory storage and decision making. The scope of neurological diseases where AEPs have been studied extends from acoustic neuroma to Alzheimer dementia and cannot be entirely covered here. Normal aspects and clinical applications of BAEPs have been reviewed recently by Chiappa [10], middle latency components have not been used routinely, and the modifications of attention-related late components (P300) in dementia are more useful for follow-up studies than for diagnosis in individual cases. In this chapter only the clinical utility and reliability of late AEPs in hemispheric lesions will be covered.

#### Normal late AEP components

Following monaural stimulation by a brief tone-burst in normals a large vertex response made of a N1 (N100) negativity and of a P2 (P200) positivity is constantly recorded with maximal amplitude in the fronto-central region [79]. Overlapping in time with the vertex response a P100 potential is recorded at the mastoid processes and in lower temporal regions when the nose is used as reference site (figure 8-20). Under these recording conditions part of the vertex N1 negativity is recorded at the nose reference site and, therefore, is injected in all leads as a positivity participating in the generation of the temporal P100 component [38, 82]. The scalp distribution in a coronal montage of the late AEPs obtained 60–250 msec following the stimulus [64, 79, 80] fits fairly well with a model assuming two sources situated in the temporal auditory cortex of each hemisphere [69].



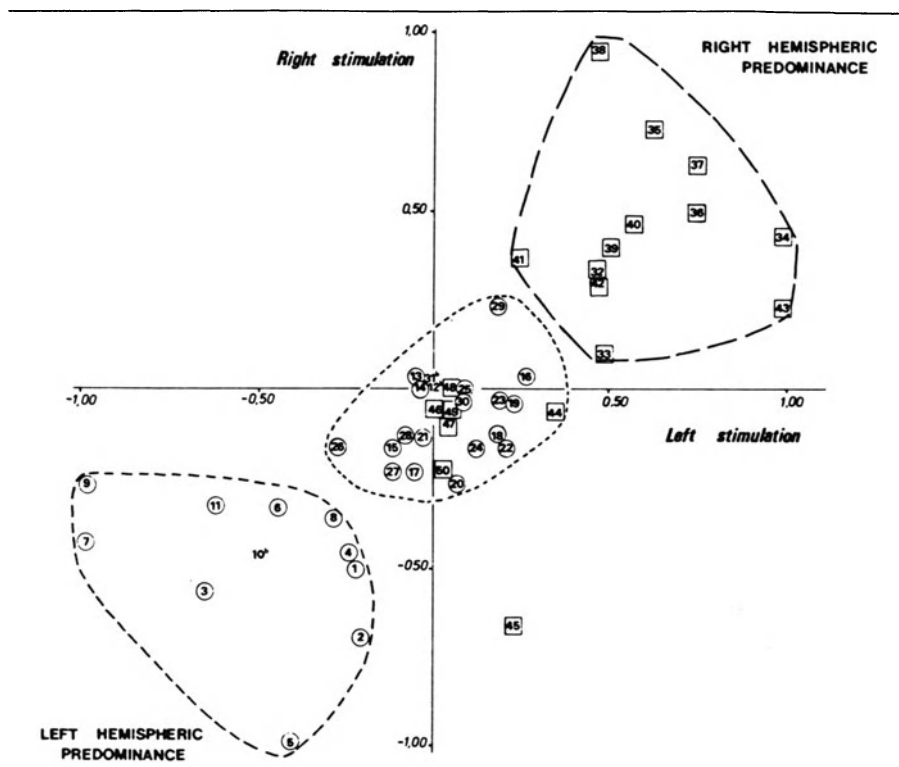
**Figure 8-20.** Normal late AEPs to right (A) and left ear stimulation. These traces and spatio-temporal maps illustrate the situation of the P1-N1-P2 complex at the vertex; they also illustrate the temporal P100 positivities (arrows, see text for details).

### Late AEP components in hemispheric lesions

Patients with unilateral damage to the auditory cortex are not deaf because the normal hemisphere still receives information from both ears. However, they have difficulty to repeat words delivered to the ear contralateral to the damaged hemisphere on dichotic listening testing (contralateral ear extinction). In a series of 52 patients with hemispheric lesions recorded with a nose reference,

**Table 8-2.** Late AEPs: Latencies and amplitudes of the temporal P100 in 50 patients with hemispheric lesions

Stimulated ear	Mean P100 latency ( $\pm$ SD) (msec)				Mean P100 amplitude ( $\pm$ SD) ( $\mu$ V)				
	Left ear		Right ear		Left ear		Right ear		
	Left	Right	Left	Right	left	Right	Left	Right	
Hemisphere									
Left hemispheric predominance n = 11	108.1 ( $\pm$ 15.8) n = 11	109.3 ( $\pm$ 24) n = 9	98.3 ( $\pm$ 17.5) n = 11	86.9 ( $\pm$ 32.7) n = 10	1.98 ( $\pm$ 0.60) n = 11	0.91 ( $\pm$ 0.36) n = 9	2.34 ( $\pm$ 0.42) n = 11	0.97 ( $\pm$ 0.38) n = 10	
No hemispheric predominance n = 27	105.8 ( $\pm$ 12.0) n = 26	98.1 ( $\pm$ 12.4) n = 26	101.3 ( $\pm$ 13.4) n = 26	98.6 ( $\pm$ 11.7) n = 26	2.39 ( $\pm$ 1.56) n = 26	2.66 ( $\pm$ 1.48) n = 26	3.00 ( $\pm$ 1.62) n = 26	2.51 ( $\pm$ 1.30) n = 26	
Right hemispheric predominance n = 12	91.2 ( $\pm$ 21.1) n = 11	92.7 ( $\pm$ 16.2) n = 12	103.0 ( $\pm$ 14.0) n = 11	104.0 ( $\pm$ 11.4) n = 12	0.76 ( $\pm$ 0.51) n = 11	2.55 ( $\pm$ 1.33) n = 12	0.86 ( $\pm$ 0.60) n = 11	2.15 ( $\pm$ 1.17) n = 12	



**Figure 8-21.** Values of the asymmetry index (I) in 50 patients with hemispheric lesions (see text for details)

Each case is numbered in a circle for right lesions, in a square for left lesions. In three patients the lesion was not strictly lateralized although they they were clearly predominant on one side. Principal component analysis showed that the main variable responsible for interindividual variability in the whole group was the amplitude of the temporal P100 potential. The three groups were individualized by using ascending hierarchic classification method.

**Table 8-3.** Results of dichotic listening test and AEPs in unilateral hemispheric lesions of the 50 patients tested (21 with left lesions, 29 with right lesions) only 38 were able to perform the test. Note that only one patient had no extinction in spite of absent AEPs. This case is illustrated in figure 8-6. The absence of the temporal component on the left side was probably due to a displacement and certainly not due to a destruction of AEPs generators.

	Abnormal temporal AEPs on the damaged side		Normal temporal AEPs on the damaged side	
	Left-sided lesions	Right-sided lesions	Left-sided lesions	Right-sided lesions
Dichotic test (total Nb)	9	8	6	15
Extinction of contralateral ear	8	8	4	11
Normal performances	1	0	2	4

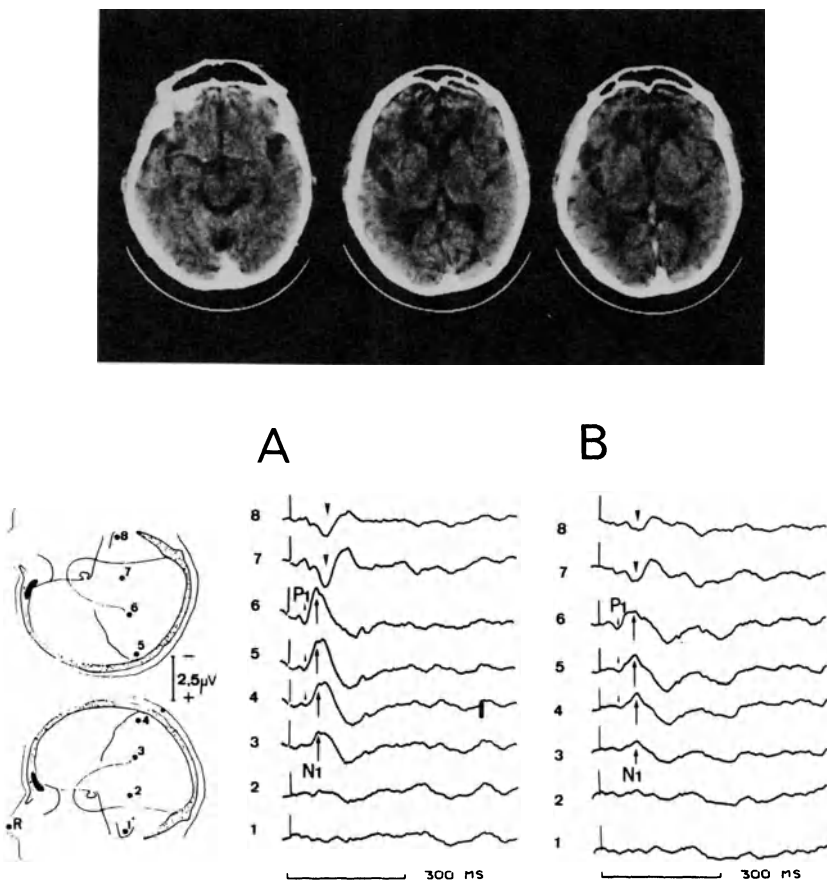
Peronnet and Michel [65] observed an abnormal right to left interhemispheric amplitude difference of the temporal component in several cases. All of the patients with asymmetrical AEPs presented extinction of the contralateral ear on dichotic listening testing but some of the patients with extinction of the contralateral ear had normal AEPs.

Extinction phenomenon can be encountered in split-brain patients and in patients with unilateral neglect and does not prove, per se, that the damaged hemisphere is deaf. The term hemianacusia was coined by Michel et al. [55] to individualize patients with abnormal late AEPs in the temporal region of the damaged hemisphere and contralateral ear extinction on dichotic listening test. These authors assumed that in such cases the recording of late temporal AEPs represented the only means to study central processing of auditory informations in the damaged hemisphere.

Using the same equipment and technique as Peronnet and Michel [65], i.e., randomly mixed monaural stimulations with 150 msec 1000 Hz tone bursts and coronal montage with a nose reference, we made similar observations in another series of 50 unpublished cases of hemispheric lesions (18 females, 32 males; mean age 54 years [max: 78, min: 20 years]; 41 strokes, 6 space occupying lesions, 3 post traumatic cortical atrophies; 42 right-handed, 6 left-handed and 2 ambidextrous).

In these patients interhemispheric amplitude differences of the P100 temporal AEPs were evaluated by calculating for each ear the following index:  $I = (A_{rh} - A_{lh}) / (A_{rh} + A_{lh})$  where  $A_{rh}$  and  $A_{lh}$  are the maximal amplitudes of the P100 recorded respectively at right and left temporal mastoids. When there is no right/left asymmetry of P100 the index 1 equals zero; it increases up to a maximal value of (+1) in case of reduced P100 in the left temporal region (right hemispheric predominance) and decreases down to a minimum of (-1) in the reverse situation (left hemispheric predominance). The 1 values calculated in our 50 patients are plotted in figure 8-21. The distribution of normal subjects using a similar two-dimensional representation is given in the paper by Peronnet and Michel [65]. Absolute latencies and amplitudes of the temporal P100 are given in table 8-2 and a demonstrative case of right hemispheric predominance is illustrated in figure 8-22.

Correlations between AEPs and dichotic listening are given in table 8-3. The main conclusion from this study was that 55% of our patients with extinction had normal AEPs, while all patients but one with asymmetrical AEPs had extinction. The only patient with normal performances in dichotic listening and absent AEPs on the damaged side had a temporal cystic astrocytoma with considerable mass effect; after surgery well defined temporal AEPs were present on both sides (figure 8-6). This observation illustrates our preliminary remark that the absence of an EP component can be due to spatial displacement of its generator (see paragraph "Spatial analysis"). There was a good correlation between abnormal temporal P100 and damage to the temporal lobe and the planum temporale. However, except for large temporal lesions, the degree of



**Figure 8-22.** Absent temporal P100 in the left temporal region in a patient with conduction aphasia

In this 76-year-old right-handed female patient AEPs were recorded one month after a vascular accident with transient right hemiparesis. CT scan disclosed a small temporal hypodensity near to the left sylvian fissure. When the AEPs were recorded the patient could understand fairly well written and oral material but was unable to repeat correctly words and sentences and to read aloud. There was a complete extinction of the right ear on dichotic listening test.

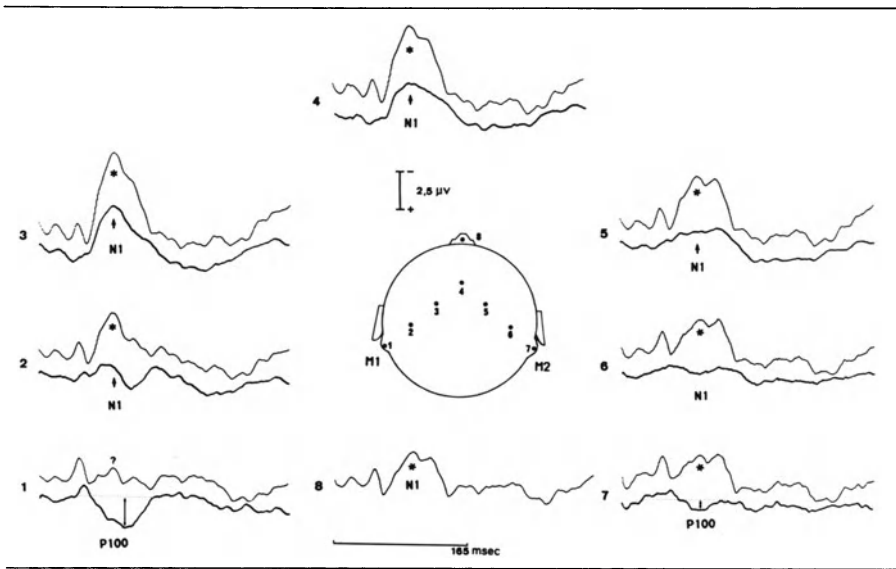
The temporal P100 response was absent in the left temporal region (leads 1 and 2) to left (A) and right (B) ear stimulation.

hemispheric auditory predominance could not be easily predicted from CT scans (see figure 8-22) and information provided by AEPs and CT was complementary and not redundant. The patient whose CT scan and AEPs are shown in figure 8-22 also illustrates the possibility of a hemianacusia without language deficit in right-handed patients with left hemispheric lesions [57]. In right-handed patients with left hemiplegia, transient verbal and behavioral anosognosia was found to be facilitated by the combined somatosensory and

auditory deprivations of the minor hemisphere assessed respectively by absent cortical SEPs and AEPs [46].

Another important finding was that abnormal AEPs, when present, were always recorded in the temporal region of the damaged hemisphere. This is not a trivial finding since the N1 activity picked at the nose could be logically responsible for an artefactual positivity in the temporal region of the affected side. Late AEP records obtained in one of our patients (figure 8-23) with both nose and noncephalic references show that the absence or reduction of the temporal P100 observed on the damaged side with a nose reference might be due to a cancellation between the vertex N1 that has an abnormal extension into the temporal region and the N1 which is recorded at the nose. Indeed in the noncephalic reference recording there is no extension of the vertex N1 and almost no temporal response on the normal side, whereas the vertex N1 is picked up in the temporal region on the damaged side. A possible explanation is that, in a noncephalic reference montage, the vertex N1 is normally balanced by a temporal positivity which is absent or reduced when the auditory areas are damaged.

Controversial data have been published in a few patients with clinical evidence of cortical deafness due to bilateral temporal lesions; AEPs were found to be absent by Michel and Peronnet [56] whereas they were present in one case recently reported by Woods et al. [84]. As for VEPs in cortical blindness, a dissociation between impaired auditory perception and persisting



**Figure 8-23.** Coronal distribution of cortical AEPs in a left hemiplegic right-handed patient with anosognosia and an infarction in the right middle cerebral artery territory (Thick traces: nose reference; thin traces noncephalic reference; see text for details)

AEPs is possible, and the combination of AEP recording and PET metabolic studies will be helpful to make a distinction between cortical deafness and auditory agnosia in patients with bilateral temporal lobe lesions.

## CONCLUSIONS

In most patients with nondemyelinating diseases, EPs cannot compete with morphological investigations to locate the lesion site, even when sophisticated mapping techniques are carried out. However EPs are the most simple complementary investigations to be performed when it is clinically relevant, for diagnosis or prognosis, to assess sensory functions or to determine where the transmission of sensory informations is interrupted or impaired.

Out of the clinical context almost none of the EP abnormalities has any specificity regarding the pathology of the lesion, but most of them can now be interpreted in pathophysiologic terms. Consequently EPs will probably be used in the near future in long-term follow-up studies of patients with stroke or degenerative diseases in order to better evaluate the natural history and to assess therapeutic trials. As a complement to anatomo-clinical correlations, EPs provide specific "real-time" informations on brain function to which metabolic studies are blind.

## REFERENCES

1. Aminoff MJ, Maitland CG, Kennard C, Hoyt WF: Visual evoked potentials and field defects. In: *Evoked Potentials II*. RH Nodar and C Barber (eds) Butterworth Publishers, Boston: 329–334, 1984.
2. Anziska BJ and Cracco RW: Short latency somatosensory evoked potentials: studies in patients with focal neurological disease. *Electroencephalogr Clin Neurophysiol*, 49:227–239, 1980.
3. Anziska BJ and Cracco RW: Short latency SEPs to median nerve stimulation: comparison of recording methods and origin of components. *Electroencephalogr Clin Neurophysiol* 52: 531–539, 1981.
4. Blumhardt LD, Barrett J, Kriss A, Halliday AM: The pattern evoked potential in lesions of the posterior visual pathways. *Ann NY Acad Sci* 338:264–289, 1982.
5. Bodis-Wollner I, Onofrijm: System diseases and visual evoked potential diagnosis in neurology: changes due to synaptic malfunction. *Ann NY Acad Sci* 338:327–348, 1982.
6. Carroll WM, Kriss A, Baraitser M, Barrett G, Halliday AM: The incidence and nature of visual pathway involvement in Friedreich's ataxia. *Brain* 103:413–434, 1980.
7. Celesia GG, Polcyn RD, Holden JE, Nickles RJ, Gatley JS, Koeppel RA: Visual evoked potentials and positron tomographic mapping of regional cerebral blood flow and cerebral metabolism; can the neuronal potential generators be visualized? *Electroencephalogr Clin Neurophysiol* 54:243–256, 1982.
8. Celesia GG, Todd Meredith J, Pluff K: Perimetry, visual evoked potentials and visual evoked spectral array in homonymous hemianopia. *Electroencephalogr Clin Neurophysiol* 56:16–30, 1983.
9. Chiappa KH and Ropper AH: Evoked potentials in clinical medicine. *New Engl J Med* 306: 1140–1150 and 1205–1211, 1982.
10. Chiappa KH: *Evoked potentials in clinical medicine*. Raven Press NY, 1983.
11. Cosi V, Poloni M, Mazzini L, Callieco R: Somatosensory evoked potentials in amyotrophic lateral sclerosis. *J Neuro Neurosurg Psychiat* 47:857–861, 1984.
12. Cracco RO: Spinal evoked response: peripheral nerve stimulation in man. *Electroencephalogr Clin Neurophysiol* 35:379–386, 1973.
13. Dawson GD: Investigations on a patient subject to myoclonic seizures after sensory



- stimulation. *J Neurol Neurosurg Psychiat* 10:141–162, 1947.
14. Deiber MP, Giard MH, Mauguiere F: Separate generators with distinct orientations for N20 and P22 somatosensory evoked potentials to finger stimulation? *Electroencephalogr Clin Neurophysiol* 65:321–334, 1986.
  15. Desmedt JE: Cerebral evoked potentials in: "Peripheral Neuropathy" PJ Dyck, PK Thomas, EH Lambert and R Bunge (eds): Saunders, Philadelphia. 1045–1066, 1984.
  16. Desmedt JE and Cheron G: Central somatosensory conduction in man: Neural generators and interpeak latencies of the far-field components recorded from neck and right or left scalp or earlobes. *Electroencephalogr Clin Neurophysiol* 50, 382–403, 1980.
  17. Desmedt JE and Cheron G: Noncephalic reference recording of early somatosensory potentials to finger stimulation in adult or aging man: differentiation of widespread N18 and contralateral N20 from the prerolandic P22 and N30 components. *Electroencephalogr Clin Neurophysiol* 52:553–570, 1981.
  18. Desmedt JE and Cheron G: Spinal and far-field components of human somatosensory evoked potentials to posterior tibial nerve stimulation analysed with oesophageal derivations and noncephalic reference recording. *Electroencephalogr Clin Neurophysiol* 56:635–651, 1983.
  19. Desmedt JE, Tran Huy N, Carmeliet J: Unexpected latency shifts of the stationary P9 somatosensory evoked potential far field with changes in shoulder position. *Electroencephalogr Clin Neurophysiol* 56:628–634, 1983.
  20. Desmedt JE and Nguyen TH: Bit-mapped colour imaging of the potential fields of propagated and segmental subcortical components of somatosensory evoked potential in man. *Electroencephalogr Clin Neurophysiol* 62:1–17, 1984.
  21. Desmedt JE and Bourguet M: Color imaging of parietal and frontal somatosensory potential fields evoked by stimulation of median or posterior tibial nerve in man. *Electroencephalogr Clin Neurophysiol* 62:1–17, 1985.
  22. Dimitrijevic MR, Lenman JAR, Prevec T, Wheatly K: A study of posterior column function in familial spastic paraplegia. *J Neurol Neurosurg Psychiat* 45:46–49, 1982.
  23. Ehle AL, Stewart RM, Lellelid NE, Leventhal A: normal checkerboard pattern reversal evoked potentials in Parkinsonism. *Electroencephalogr Clin Neurophysiol* 54:336–338, 1982.
  24. Fine EJ and Hallett M: Neurophysiological study of subacute combined degeneration. *J Neurol Sci* 45:331–336, 1980.
  25. Gandevia SC, Burke D, McKeon BB: The projection of muscle afferents from hand to cerebral cortex in man. *Brain* 107:1–13, 1984.
  26. Ganes T: Somatosensory conduction times and peripheral, cervical and cortical evoked potentials in patients with cervical spondylosis. *J Neurol Neurosurg Psychiat* 43:683–689, 1980.
  27. Graff-Radford NR, Damasio H, Yamada T, Eslinger PJ, Damasio AR: Nonhemorrhagic thalamic infarction: clinical, neuropsychological and electrophysiological findings in four anatomical groups defined by computerized tomography. *Brain* 108:485–516, 1985.
  28. Halliday AM: The electrophysiological study of myoclonus in man. *Brain* 90:241–284, 1967.
  29. Halliday AM: Evoked potentials in clinical testing. Churchill Livingstone, Edinburgh, 1982.
  30. Halliday AM, Wakefield GS: Cerebral evoked potentials in patients with dissociated sensory loss. *J Neurol Neurosurg Psychiat* 26:211–219, 1963.
  31. Hennerici M, Hömberg V, Lange HW: Evoked potentials in patients with Huntington's disease and their offspring. Visual evoked potentials. *Electroencephalogr Clin Neurophysiol* 62:167–176, 1985.
  32. Hume AL, Cant BR: Conduction time in central somatosensory pathways. *Electroencephalogr Clin Neurophysiol* 45:361–375, 1978.
  33. Jabbari B, Schwartz D, Chikarmane A, Fadden D: Somatosensory and brainstem auditory evoked response abnormalities in a family with Friedreich's ataxia. *Electroencephalogr Clin Neurophysiol* 53:24–25, 1982.
  34. Jones SJ: Investigation of brachial plexus traction lesions by peripheral and spinal somatosensory evoked potentials. *J Neurol Neurosurg Psychiat* 42:107–116, 1979.
  35. Jones SJ, Baraitser M, Halliday AM: Peripheral and central somatosensory nerve conduction defects in Friedreich's ataxia. *J Neurol Neurosurg Psychiat* 43:495–503, 1980.
  36. Jorg J, Dullberg W, Koeppen S: Diagnostic value of segmental somatosensory evoked potentials in cases with chronic para- or tetraspastic syndromes—in: "Clinical applications of evoked potentials in neurology" J Courjon, F Mauguière and M Revol. Eds *Adv Neurol*

- 32:347–358. Raven Press NY, 1982.
37. Kimura J, Mitsudome A, Beck DO, Yamada T, Dickins QS: Field distribution of antidromically activated digital nerve potential: model for far-field recording. *Neurology*. 33:1164–1169, 1983.
  38. Kooi KA, Tipton AC, Marshall R. Polarities and field configurations of the vertex components of the auditory evoked response: reinterpretation. *Electroencephalogr Clin Neurophysiol* 31:166–169, 1971.
  39. Kuruiwa Y and Celesia GG: Visual evoked potentials with hemifield pattern stimulation. Their use in the diagnosis of retrochiasmatic lesions. *Arch Neurol* 38:86–90, 1981.
  40. Louis AA, Gupta P, Perlash I: Localization of sensory levels in traumatic quadriplegia by segmental somatosensory evoked potentials. *Electroencephalogr Clin Neurophysiol* 62: 313–316, 1985.
  41. Lueders H, Andrish J, Gurd A, Wiecker G, George K: Origins of far-field subcortical potentials evoked by stimulation of the posterior tibial nerve. *Electroencephalogr Clin Neurophysiol* 52:336–344, 1981.
  42. Mastaglia FL, Black JL, Edis R, Collins DWK: Contribution of evoked potentials in the functional assessment of the somatosensory pathway. *Clin Exp Neurol* 15:279–298, 1978.
  43. Mauguiere F and Courjon J: Effects of intravenously injected clonazepam on the cortical somatosensory evoked response in dysynergia cerebellaris myoclonica. in “EEG and Clinical Neurophysiology” H Lechner and A Aranibar (eds) 433–444. Excerpta Medica Amsterdam, 1980.
  44. Mauguiere F, Bard J, Courjon J: Les potentiels évoqués somesthésiques précoces dans la dysynergie cerebelleuse myoclonique progressive. *Rev EEG Clin Neurophysiol* 11:174–182, 1981.
  45. Mauguiere F, Brunon AM, Echallier JF, Courjon J: Early somatosensory evoked potentials in thalamocortical lesions of the lemniscal pathways in humans. in: *Clinical Applications of Evoked Potentials in Neurology*. J Courjon, F Mauguière and M Revol (eds) *Advances in Neurology*. Vol 32. Raven Press, New York: 321–338, 1982a.
  46. Mauguiere F, Brechard S, Pernier J, Courjon J, Schott B: Anosognosia with hemiplegia: Auditory evoked potential studies. In: *Clinical Applications of Evoked Potentials in Neurology*. J Courjon, F Mauguière and M Revol (eds) *Advances in Neurology*. Vol 32. Raven Press, New York: 271–278, 1982b.
  47. Mauguiere F: Les potentiels évoqués somesthésiques cervicaux chez le sujet normal. Analyse des aspects obtenus selon le siège de l'électrode de référence. *Rev. EEG Clin Neurophysiol* 13: 259–272, 1983.
  48. Mauguiere F, Schott B, Courjon J: Dissociation of early SEP components in unilateral traumatic section of the lower medulla. *Ann Neurol* 13:309–313, 1983a.
  49. Mauguiere F, Desmedt JE, Courjon J: Neural generators of N18 and P14 far-field somatosensory evoked potentials studied in patients with lesions of thalamus or thalamo-cortical radiations. *Electroencephalogr Clin Neurophysiol* 56, 283–292, 1983b.
  50. Mauguiere F, Desmedt JE, Courjon J, Astereognosis and dissociated loss of frontal or parietal components of somatosensory evoked potentials in hemispheric lesions. *Brain* 106, 271–311, 1983c.
  51. Mauguiere F and Ibanez V. The dissociation of early SEP components in lesions of the cervico-medullary junction: a cue for routine interpretation of abnormal cervical responses to median nerve stimulation. *Electroencephalogr Clin Neurophysiol* 62:406–420, 1985.
  52. Mauguiere F, Ibanez V, Fischer C: Les potentiels évoqués somesthésiques dans les tumeurs intra-rachidiennes. *Rev EEG Clin Neurophysiol* 15:95–106, 1985.
  53. Mauguiere F: Short-latency somatosensory evoked potentials to upper limb stimulation in lesions of brainstem, thalamus and cortex. Suppl: 39 to *Electroencephalogr Clin Neurophysiol* “The London Symposia” XIth International Congress of EEG and Clinical Neurophysiology RJ, Ellingson, NMF Murray, AM Halliday (Eds) Elsevier. (Amsterdam) p 302–309, 1987.
  54. Merton PA, Morton HB: Stimulation of the cerebral cortex in the intact normal subject. *Nature*. 285:227, 1980.
  55. Michel F, Peronnet F, Schott B: A propos d'un cas de surdité de l'hémisphère gauche (hémianacousie droite). *Rev EEG Clin Neurophysiol* 6:175–178, 1976.
  56. Michel F and Peronnet F: A case of cortical deafness: Clinical and electrophysiological data. *Brain Lang* 10:367–377, 1980.
  57. Michel F, Peronnet F, Mauguiere F: Right hemiancousia without language deficit. In: *Clinical*

- Applications of Evoked Potentials in Neurology. J Courjon, F Mauguière and M Revol (eds) *Advances in Neurology*. Vol 32. Raven Press, New York: 257–261, 1982.
58. Nakanishi T, Shimada Y, Sakuta M, Toyokura Y: The initial positive component of the scalp recorded somatosensory evoked potential in normal subjects and in patients with neurological disorders. *Electroencephalogr Clin Neurophysiol* 45, 26–34, 1978.
  59. Noel P and Desmedt JE: Somatosensory pathway in Friedreich's ataxia. *Acta Neurol Belg* 76:271, 1976.
  60. Noel P and Desmedt JE: Cerebral and far-field somatosensory evoked potentials in neurological disorders involving the cervical spinal cord, brainstem, thalamus and cortex, in: "Clinical uses of cerebral, brainstem, and spinal somatosensory evoked potentials". Desmedt JE (ed) *Prog Clin Neurophysiol* 7; Karger. Basel. 205–230, 1980.
  61. Nuwer MR, Perlman SL, Packwood JW, Kark RAP: Evoked potential abnormalities in the various inherited ataxias. *Ann Neurol* 13:20–27, 1983.
  62. Obeso JA, Rothwell JC, Marsden CD: The spectrum of cortical myoclonus: from focal reflex jerks to spontaneous motor epilepsy. *Brain* 108:193–224, 1985.
  63. Pedersen L, Trojaborg W: Visual, auditory and somatosensory pathway involvement in hereditary cerebellar ataxia, Friedreich's ataxia and familial spastic paraplegia. *Electroencephalogr Clin Neurophysiol* 52:283–297, 1981.
  64. Peronnet F, Michel F, Echallier F, Girod J: Coronal topography of human auditory evoked responses. *Electroencephalogr Clin Neurophysiol* 37:225–230, 1974.
  65. Peronnet F and Michel F: The asymmetry of the auditory evoked potentials in normal man and in patients with brain lesions. in: "Auditory evoked potentials in man. Psychopharmacology correlates of EPs". JE Desmedt (ed) *Prog Clin Neurophysiol* 2:130–141. Karger Basel, 1977.
  66. Perot PL and Vera CL: Scalp-recorded somatosensory evoked potentials to stimulation of nerves in the lower extremities and evaluation of patients with spinal cord trauma. *Ann NY Acad Sci* 388:359–368, 1982.
  67. Rothwell JC, Obeso JA, Marsden CD: On the significance of giant somatosensory evoked potentials in cortical myoclonus. *J Neurol Neurosurg Psychiatr* 47:33–42, 1984.
  68. Sauer M: Somatosensible Leitungsmessungen bei neurologischen Systemerkrankungen: neurale Muskelatrophien und spinocerebelläre Ataxien. *Arch Psychiatr Nervenkr* 228:223–242, 1980.
  69. Scherg M and Von Cramon D: Two bilateral sources of the late AEPs as identified by a spatio-temporal dipole model. *Electroencephalogr Clin Neurophysiol* 62:32–44, 1985.
  70. Shibasaki H, Kuroiwa Y: Electroencephalographic correlates of myoclonus. *Electroencephalogr Clin Neurophysiol* 39:455–463, 1975.
  71. Shibasaki H, Yamashita Y, Neshige R, Tobimatsu S, Fukui P: Pathogenesis of giant somatosensory evoked potentials in progressive myoclonic epilepsy. *Brain* 108:225–240, 1985a.
  72. Shibasaki H, Neshige R, Hashiba Y. Cortical excitability after myoclonus. Jerk-locked somatosensory evoked potentials. *Neurology* 35:36–41, 1985b.
  73. Slimp JC, Tamas LB, Stolov WC, Wyler AR: Somatosensory evoked potentials after removal of somatosensory cortex in man. *Electroencephalogr Clin Neurophysiol* 65:111–117, 1986.
  74. Spehlmann R, Gross RA, HO SU, Leestma JE, Norcross KA. Visual evoked potentials and post-mortem findings in a case of cortical blindness. *Ann Neurol* 2:531–534, 1977.
  75. Stohr M, Dichgans J, Voigt K, Buettner UW: The significance of somatosensory evoked potentials for localization of unilateral lesions within the cerebral hemispheres. *J Neurol Sci* 61:49–63, 1983.
  76. Synek VM: Validity of median nerve somatosensory evoked potentials in the diagnosis of supraclavicular brachial plexus lesions. *Electroencephalogr Clin Neurophysiol* 65:27–35, 1986.
  77. Taylor MJ, Chan-Lui WY, Logan WJ: Longitudinal evoked potential studies in hereditary ataxias. *Can J Neurol Sci* 12:100–105, 1985.
  78. Thomas PK, Jefferys JGR, Smith IS, Loulakakis D: Spinal somatosensory evoked potentials in hereditary spastic paraplegia. *J Neurol Neurosurg Psychiatr* 44:243–246, 1981.
  79. Vaughan HG and Ritter W: The sources of auditory evoked responses recorded from the human scalp. *Electroencephalogr Clin Neurophysiol* 28:360–367, 1970.
  80. Vaughan HG, Ritter W, Simson P: Topographic analysis of auditory event-related potentials in: *Motivation, Motor, and Sensory Processes of the Brain*. Kornhuber HH and Deecke L (eds) *Prog in Brain Res* Vol 54, Elsevier Amsterdam: 279–285, 1980.

81. Waxman S: Membranes, myelin, and the pathophysiology of multiple sclerosis. *New Engl J Med* 306:1529–1533, 1982.
82. Wolpaw JR, Wood CC: Scalp distribution of human auditory evoked potentials. I: Evaluation of reference electrode sites. *Electroencephalogr Clin Neurophysiol* 54:15–24, 1982.
83. Wood CC, Cohen D, Cuffin BN, Yarita M, Allison T: Electrical sources in human somatosensory cortex: identification by combined magnetic and potential recordings. *Science* 227:1051–1053, 1985.
84. Woods DL, Knight RT, Neville HJ: Bitemporal lesions dissociate auditory evoked potentials and perception. *Electroencephalogr Clin Neurophysiol* 57:208–220, 1984.
85. Yamada T, Machida M, Kimura M: Far-field somatosensory evoked potentials after stimulation of the tibial nerve in man. *Neurology* 32:1151–1158, 1982.
86. Yamada T, Kayamori R, Kimura J, Beck DO: Topography of somatosensory evoked potentials after stimulation of the median nerve. *Electroencephalogr Clin Neurophysiol* 59, 29–43, 1984.
87. Yamada T, Graff-Radford NR, Kimura J, Dickins QS, Adams HP. Topographic analysis of somatosensory evoked potentials in patients with well-localized thalamic infarctions. *J Neurol Sci* 68, 31–46, 1985.
88. Yu YL and Jones SJ: Somatosensory evoked potentials in cervical spondylolysis. Correlation of median, ulnar and posterior tibial nerve responses with clinical and radiological findings. *Brain* 108:273–300, 1985.

---

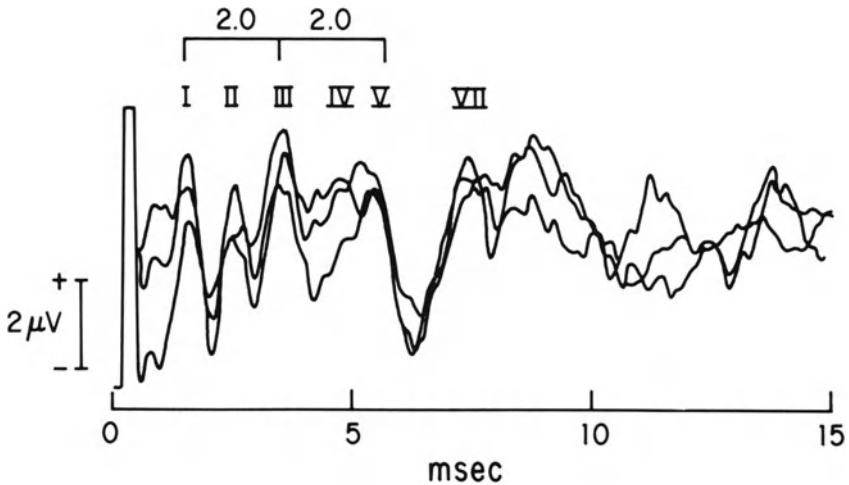
## 9. SENSORY EVOKED POTENTIALS IN COMA AND BRAIN DEATH

CARL ROSENBERG

ARNOLD STARR

Sensory evoked potentials recorded from scalp electrodes represent electrical events generated along the sensory pathways. Thus, they provide data about the functions of specific areas of the nervous system in a noninvasive manner to determine the locus of alterations in sensory pathways. For example, changes in auditory brainstem response can localize abnormalities in neural functioning to several different areas of the brainstem. This paper describes the current experience using evoked potentials as objective measures of the level of neural function in comatose patients and their prognostic value in predicting recovery. The common denominator of measurement of sensory evoked potentials is usually the latency and, in some instances, the amplitudes of the various subcomponents or waves comprising an evoked potential, and defining if these measures are within normal limits.

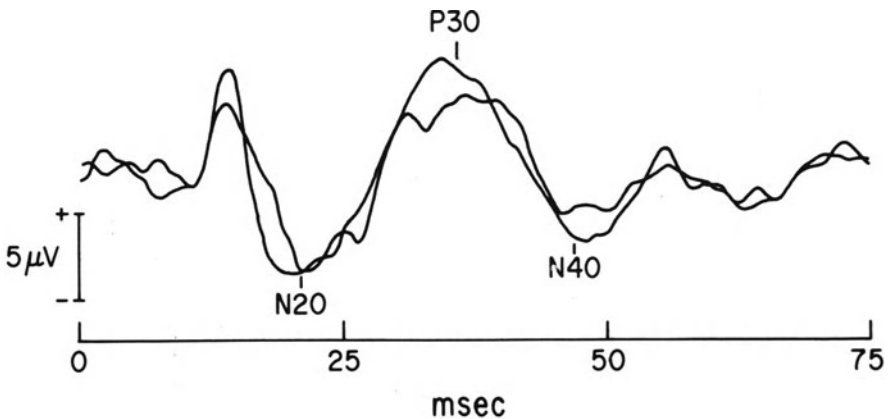
There are three different types of evoked potential measures of auditory pathway activity: 1) the auditory brainstem response (ABR), 2) the middle-latency auditory evoked potential (mAEP), and 3) the long-latency auditory evoked potentials (LAEP). The auditory brainstem response (figure 9-1) reflects activity arising in the auditory system from the cochlea through the brainstem. Seven waves can be identified in the initial 10 msec after click stimulation, though only waves I, III, and V, which are seen in all normal subjects, are used in clinical practise. Wave V of the ABR is generated in the region of the rostral pons; wave III from the region of the lower brainstem (cochlear nucleus or superior olive), and wave I from the VIII nerve. The middle-latency



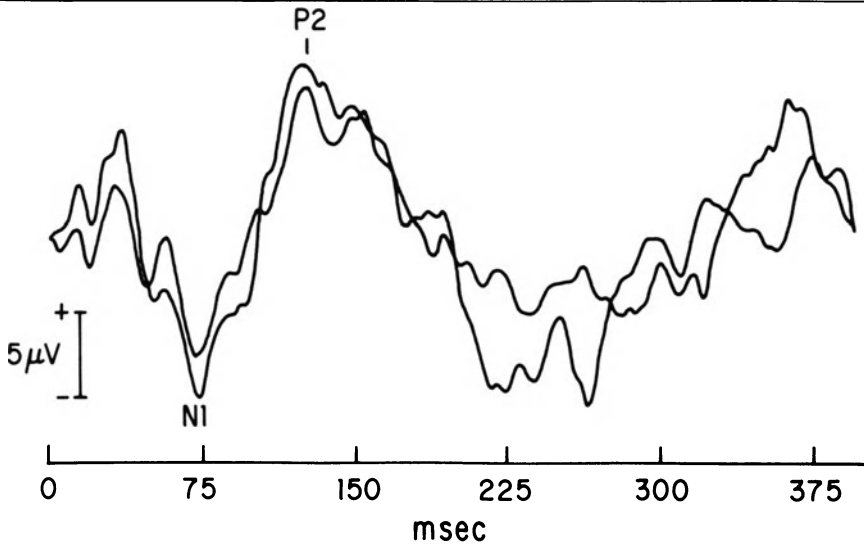
**Figure 9-1.** A normal ABR evoked by 11 clicks per second at 75 dB. Waves I, II, III, IV, V and VII are labeled.

auditory evoked potentials (mAEP) (figure 9-2) consist of N20, P30, and N40 waves reflecting activity in auditory structures in the temporal lobe [16, 22]. The long-latency auditory evoked potentials (1AEP) (figure 9-3), consisting of waves N100 and P200, reflect activity in widespread auditory associative cortical areas [32].

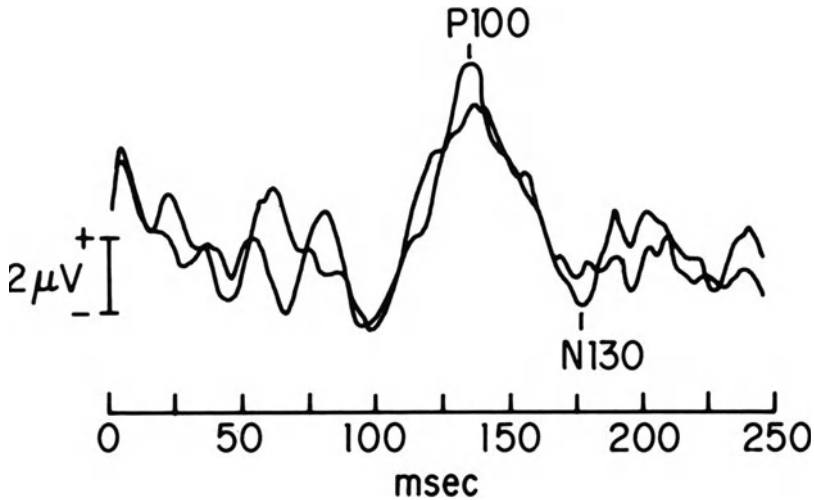
The visual evoked potential (VEP) (figure 9-4) to a checkerboard stimulus consists of at least the N70 and P100 waves derived primarily from the occipi-



**Figure 9-2.** A normal mAEP evoked by 11 tones per second at 75 dB. The components N20, P30, and N40 are labeled.



**Figure 9-3.** A normal 1AEP evoked by 1 tone per second at 75 dB. The N1 and P2 components are labeled.



**Figure 9-4.** A normal VEP evoked by a strong light flash. The P100 component is labeled.

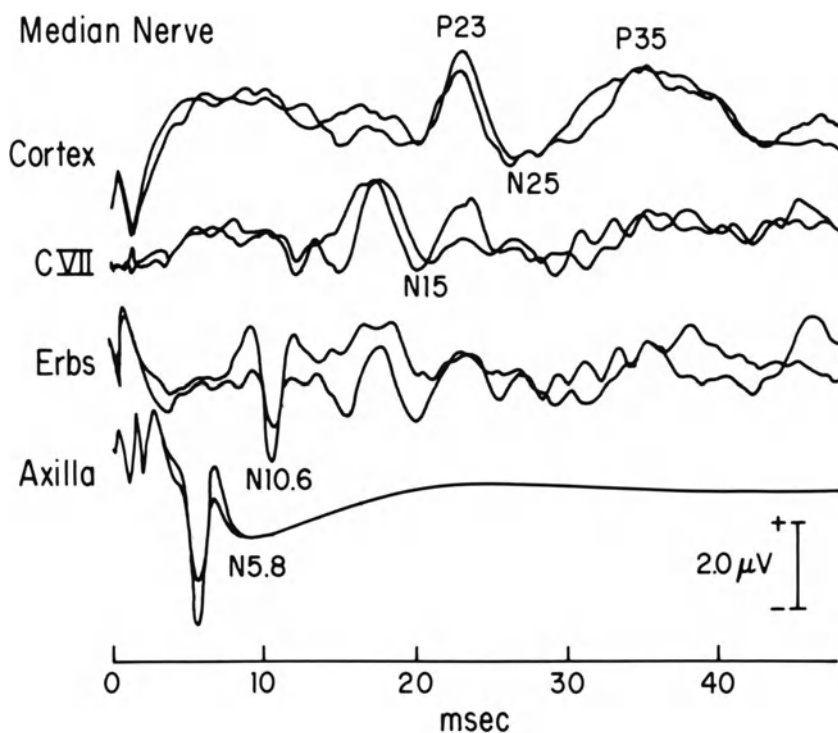
tal cortex and requires the integrity of function of the visual system from retina to occipital cortex. Any disturbance along this pathway will be reflected as an alteration of the VEP. In comatose patients, goggles or diffuse flash stimuli are used to test the visual system, and the resulting waveforms vary considerably

as a function of the luminance of the stimulus and individual variability. A P100 wave does dominate the potentials when low luminance levels are used.

The somatosensory evoked potentials (SEP) (figures 9-5 and 9-6) can be derived from local generator sites along the different somatosensory pathways by judicious placement of recording electrodes over nerve, spinal cord, brainstem and cortex. For stimulation of the upper extremity, these components occur at approximately 10, 13, and 19 msec, but the latency will vary with limb length.

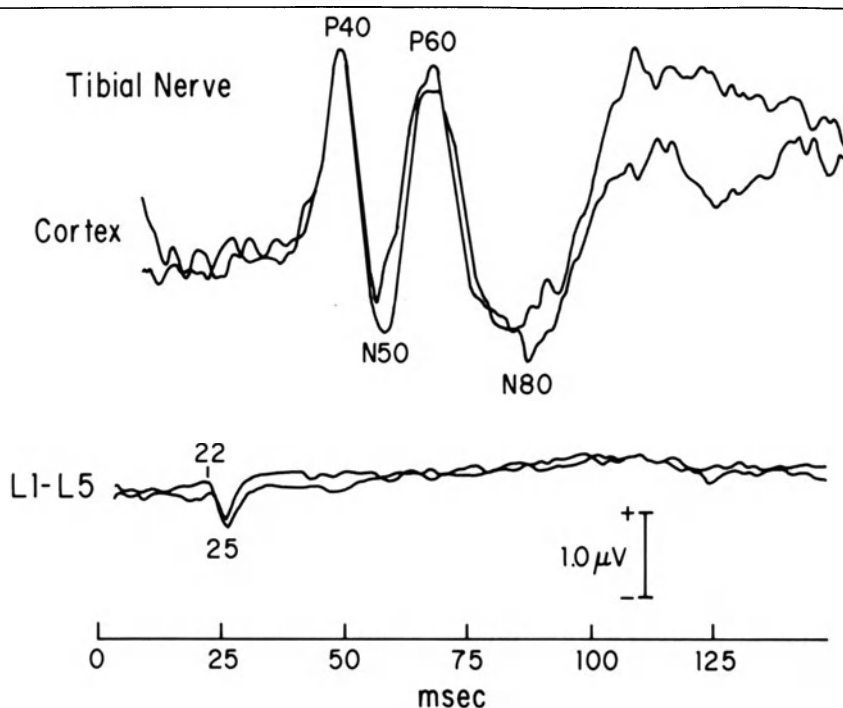
In comatose patients, sensory evoked potentials should be able to provide information as to the level of the lesion of the nervous system which is determining the comatose condition, i.e., cortical, subcortical, or brainstem. Abnormalities of evoked potentials can be correlated with the patient's clinically determined level of neural dysfunction and the patient's subsequent clinical outcome. These studies raise two issues with the clinical data and one with the evoked potential data.

The clinical issues are: 1) the standardization of the clinical definition of the



**Figure 9-5.** A normal SEP evoked by electrical stimulation of the median nerve at the wrist. The labeled responses are from the axilla, N6 from Erbs point, N10, Cervical vertebra VII, N15, and the contralateral cortex, P23, N25 and P35.





**Figure 9-6.** A normal SEP evoked by stimulation of the posterior tibial nerve at the ankle. The labeled responses are from the lumbar spine measured at L1-L5, and from the contralateral cortex.

level of coma, and 2) the standardization of the measurements of degree of recovery. The most common solution used by many in this field has been the Glasgow Coma scale (GCS) [28]. The Glasgow Coma Scale rates a patient's functioning in three different areas: 1) eye opening, 2) verbal response, and 3) motor response. The scoring is shown in table 9-1.

The standardizing of outcome is addressed by the scale developed by Jennett and Bond 1975 (Glasgow Outcome Scale, GOS), with five degrees of recovery: 1) *Good recovery (G)*: complete neurological recovery, or minor deficits that do not prevent the patients from returning to their former level of function, 2)

**Table 9-1.** Glasgow Coma Scale Ratings

Eye Opening		Verbal Response		Motor response	
Spontaneous	4	Oriented	5	Obeys	6
To speech	3	Confused	4	Localizes	5
To pain	2	Inappropriate	3	Withdraws	4
None	1	Incomprehensible	2	Flexion	3
		None	1	Extension	2
				None	1

*Moderate disability (MD)*: deficits present that prevent normal function, but allow self care, 3) *Severe disability (SD)*: marked deficits present that prevent self-care, 4) *Vegetative (V)*: no evidence of higher mental function, and 5) *Dead (D)*.

If sensory evoked potentials are to be evaluated in a consistent manner there is a need for consensus as to the manner of grading significant abnormalities. In our review of the literature it appears that each investigator utilizes his own system of grading for defining the degree of abnormality varying from the presence or absence of a potential to the degree of deviation from normal.

We will review the various studies correlating sensory evoked potentials in coma. First the investigations using a single test will be reviewed. These will be divided by modality, into auditory, visual and somatosensory. Next, the results of combinations of testing in two modalities will be reviewed. Finally, the results from testing with sensory evoked potentials from all three modalities will be considered. For each study, the clinical scales of coma and recovery, and the method of defining abnormalities on the sensory evoked potentials will be noted.

## AUDITORY EVOKED POTENTIALS

### ABRs and Head Trauma

Scales et al. [24] performed ABRs in seventeen comatose patients who had suffered blunt head trauma. They studied patients both at the time of admission, and three to six days later. The clinical criteria for localizing the level of neural dysfunction producing coma were defined as "specific signs of brainstem damage and/or generalized cephalic neurologic findings." Measures of outcome consisted of "death" or "recovery". Recovery was defined as "continuously appropriate cognitive behavior". The results of ABRs were divided into absent, abnormal (not normal for any reason), and normal. Three of their patients were clinically brain dead and without ABRs. Two had abnormal ABRs on initial and follow-up testing. Both these patients died. Three patients had abnormal ABRs initially but normal ABRs on follow-up testing. All three survived. Nine patients were normal on both initial and follow-up testing, and all survived.

The study by Scales et al. [24] shows that ABRs are useful in predicting the outcome from coma. Accuracy is improved with repeated testing. Unfortunately in this study oversimplified criteria were used to quantify coma and outcome. One cannot determine how compromised the patients were, and the accuracy of the ABRs in predicting outcome cannot be compared to other measures. The assessment of outcome is not specific. Outcomes from coma due to head trauma are far more varied than "dead" or "cognitively intact." One of the main questions in prognosis is the degree of cognitive recovery.

Tsubokawa et al. [30] reviewed the ABRs of 64 patients, 22 children and 42

adults who were comatose secondary to head trauma. All patients had GCS scores less than seven. The patients' outcomes were defined by the GOS. They divided the results of the ABRs into three categories: normal, mildly abnormal due to either an increase in the I-V interpeak latency or an absence of wave V, and abnormal with loss of additional ABR components.

Of the 18 adult patients with normal ABRs, 12 had good recoveries, five were moderately disabled, and one severely disabled. Of the six patients with only an increase of the I-V latency or a loss of wave V, four had a good recovery, one was in a vegetative state and one died. The 18 patients with further abnormalities of the ABRs had poor outcomes: with four remaining in a vegetative state and fourteen dying. Of the 10 children with normal ABRs, six had good recoveries, two moderate disabilities, and two severe disabilities. The six children with the milder type of abnormality, an increase of the I-V interval or loss of wave V, were evenly distributed between the first three categories of recovery. However, the five children with more severe abnormalities of the ABR had poor outcomes, with one in a vegetative state and four dying. These results suggest that a marked abnormality of the ABRs is an accurate predictor of a poor prognosis 18 of 18 in adults and 5 of 5 in children. However, the converse, that a normal or a mild abnormality of the ABR predicts a good prognosis is incorrect; only 16 of 24 adults and 8 of 16 children with normal ABRs recovered. The paper confirms the utility of ABR in coma and suggests that a division of abnormality based on a simple three-level system yields useful information. Further, the ABR's correlation with recovery in adults and children were quite similar.

Hall et al. [9] found similar results in 25 patients in coma due to head trauma. Both the GCS and the GOS were used to measure the clinical depth of coma and the recovery from coma. They used a different scale of grading abnormal ABRs: normal, mildly abnormal with an increase of the I-V interpeak latency or an abnormality of the V/I amplitude ratio, moderately abnormal with an absence of wave V, or markedly abnormal with loss of waves III and V. They found that patients with a normal or mildly abnormal ABRs had a good outcome while patients with a moderate or marked abnormality had poor outcomes. This study also shows that while some division of abnormality of ABRs may be useful, too fine a division may add little.

Uziel et al. [31] examined the ABRs of 53 patients with acute onset of coma, of whom 30 suffered head trauma, and compared these results with those from 23 patients in chronic coma. They divided the ABRs into two categories, normal and abnormal. Fourteen of 19 patients with acute coma due to head trauma and normal ABRs recovered, while 7 of 11 patients with abnormal ABRs died. However, in the 23 patients in chronic coma (persistent vegetative state), 12 had normal ABR's.

Uziel's study once again confirms that ABRs can be useful in predicting the outcome from acute coma but are of no use in predicting outcome once the comatose state becomes prolonged.

The general conclusion we draw from these three studies is that with acute coma from head trauma, abnormalities of the ABRs, especially severe abnormalities involving the loss of wave V and/or other components of the ABR, portend a poor outcome. Normal or mildly abnormal ABRs, while a good prognostic sign for survival, do not predict the degree of functional recovery.

#### **ABRs and non-traumatic causes of coma**

Lumenta [17] reviewed 19 patients with spontaneous intracerebral hemorrhage, 17 of whom were comatose (GCS < 7). Recovery was defined by the GOS. ABR results were divided into normal, unilaterally abnormal and bilaterally abnormal. Two patients with normal ABRs from stimulating either ear had a good outcome. Of the six with unilateral abnormalities of the ABR, only two had a good outcome. All 11 patients with bilateral abnormalities of the ABRs had poor outcomes. In contrast, Jain and Maseshwari [11] studying the ABRs in patients in coma secondary to meningoencephalitis found that the ABRs had little prognostic value.

Thus, the ABRs are better at predicting a poor outcome than recovery, when the etiology of the coma is head trauma. The ABR is a reflection of the integrity of activity in brainstem portions of the auditory system. Injuries due to head trauma that are sufficient to cause severe brainstem dysfunction will be evidenced by a loss of ABR components. The ABR is an index of the severity of the damage and the greater the damage, the worse the prognosis. However, coma from diffuse cerebral dysfunction accompanying strokes, anoxia, or mild head trauma usually occurs without intrinsic brainstem dysfunction. Furthermore, the brainstem auditory pathway may have special functional characteristics that can be selectively spared as in toxic-metabolic causes of coma (i.e., barbiturates, uremia, etc.) In these conditions the ABR is normal even though there may be other signs of compromised brainstem function (i.e., respiration, oculomotor-vestibular reflexes).

#### **ABRs, middle and long-latency auditory evoked potentials**

Karnaze et al. [13] reviewed both the ABRs and 1AEPs of patients who had sustained closed head trauma. The GCS was used to evaluate patients on presentation and the GOS was used to grade outcome. ABRs were defined as normal, mildly abnormal with an I-V interpeak latency of up to 0.4 msec above normal or a V/I ratio <0.5, moderately abnormal with a larger I-V interpeak latency or a smaller V/I amplitude ratio, and markedly abnormal with loss of wave V (or II and V). Their results with the ABRs confirmed the earlier experience, with a normal or mildly abnormal ABR being a positive sign for survival and a moderate or markedly abnormal ABR being a poor prognostic sign for recovery. The AEP results were divided into present or absent with the identifiable responses further divided into normal, mildly abnormal, moderately abnormal, and markedly abnormal based on the N1

latency. It was sufficient to divide the results of the 1AEP into present and absent to increase the accuracy of the ABR for predicting prognosis. The finding of a present 1AEP slightly increased prognostic accuracy when used in conjunction with the ABRs. The following combinations of results were noted: 1) a normal ABR and present mAEP predicted a good functional survival, 2) a present 1AEP and a normal ABR predicted survival, and 3) an absent 1AEP and abnormal ABR predicted a severe disability or death.

Rosenberg et al. [23] reviewed the ABRs, mAEPs and the 1AEPs of 25 patients in coma due to a variety of etiologies. Each patient had a GCS less than or equal to five. The evoked potential results were divided into three categories: normal, abnormal, and absent. Patient outcomes were divided into dead or survival. The ABRs alone were not a good predictor of patient survival. There was no difference in survival between patients with present but abnormal responses and normal responses with both the ABR and mAEP. Patients with evoked potentials present to all three tests had a better outcome than those lacking middle or long-latency AEPs. This study differs from that of Karnaze et al. [13, 14] in that the combination of the ABR and the 1AEP definitely improved upon the prediction of the quality of survival, possibly because only a few of the patients in Rosenberg's study were in coma due to head trauma, while all of the patients in Karnaze's study had sustained head trauma. As noted above, the ABR is useful in predicting the outcome from a coma due to head trauma, but of limited use if the etiology of coma is due to a diffuse metabolic process. Nevertheless, the accuracy of predicting recovery increases when tests of the cortical sensory pathways (1AEP) used.

## **VISUAL EVOKED POTENTIALS**

### **VEP alone**

Arfel et al. [2] reviewed the VEPs of 19 patients in coma, 18 of whom eventually died. In these 18 patients the morphology of the VEP deteriorated as the patients' condition worsened, while the VEP improved in the one patient who survived. Zeneroli et al. [34] studied 45 patients with hepatic cirrhosis with VEPs. With the onset of coma there was a delay in the latency of the components followed by degradation of waveform morphology. They noted that even prior to the appearance of altered sensorium there were changes in the VEP.

### **VEP and ABR**

Strickbine-Von Reet et al. [27] combined studies of ABRs and VEPs in evaluating 17 children in coma due to a variety of etiologies: six with hypoxia, three with trauma, three with a toxic encephalopathy, four with meningo-encephalitis, and one with a subarachnoid hemorrhage. The evoked potentials were rated as being present or absent. The VEPs in 10 patients were

absent. Five of these patients died and five were severely disabled. Of the remaining seven patients with preserved VEPs, six had good outcomes or were mildly disabled, and one was severely disabled. The six patients with the best outcome had both VEPs and ABRs present. This study exemplifies that combining evoked potential results from several modalities provides a more accurate prognostic statement about recovery from coma than can be made using any one test alone.

## **SOMATOSENSORY EVOKED POTENTIALS**

### **SEP alone**

Hume and Cant [10] measured the central conduction time from the spinal cord to the cortex (N13-N20) from median nerve stimulation in 18 patients within ten days of the onset of coma. There was no classification of the clinical stages of coma provided. The etiologies were equally divided between head trauma and other causes. The measure of central conduction time was classified as normal or abnormal, i.e., prolonged central conduction time from stimulating either median nerve. The patients' outcomes were classified as "good", the Good of the GOS, or "not good", the remaining four categories of the GOS. Ten patients had normal central conduction times with eight having "good" recoveries. Eight patients showed abnormal central conduction times with six having "not good" recoveries. Additionally, they tested 24 comatose patients within 35 days of the onset of coma (including the 18 studied above). Of the 13 with normal conduction times, 11 had "good" recoveries. Of the 11 patients with abnormal central conduction times, all were in the "not good" recovery category. Hume and Cant [10] extended these studies by measuring both the central conduction time and the amplitude ratio,  $N14/(N20-P25)$ , of 94 patients with coma secondary to head trauma. Nineteen patients were measured within six hours of the onset of coma, 22 within 7 to 16 days of coma onset, and 53 between 1 and 73 days of the onset of coma. The patients with normal conduction times and amplitude ratios within three and a half days of the onset of coma all had good recoveries. A consistent unilateral amplitude abnormality or prolonged conduction time predicted a persistent hemiparesis or hemiplegia. The more rapidly the patient's SEP measures improved, the better the degree of recovery. Bilaterally absent potentials were associated with the subsequent death of the patient. Hypothermia or high barbiturate levels could prolong the central conduction time and should be considered in evaluating the significance of the SEP results.

These are excellent studies showing that the SEP can provide a reasonable prediction of recovery from coma. The study reasserts the efficacy of follow-up studies. It shows that the more rapidly the test returns to normal, the better the outcome. The SEP can yield subtle information about the functional recovery, i.e., a persistent unilateral abnormality predicts a persistent hemiparesis. De la Torre et al. [3] reviewed the SEPs of 17 patients in coma from

head trauma who were unresponsive to verbal stimuli. The presence or absence of later components of the SEP (N44, P65, N82, P110, N130, and P150) were evaluated. A patient's prognosis worsened as the longer latency components were lost. The poorest prognosis was seen in patients having only the first two components, N11 and P21.

A similar result was found by Walser et al. [33] in reviewing the median nerve SEPs of 26 patients in coma due to anoxia. A good recovery was defined as being able to talk and follow verbal commands. They noted that patients with normal amplitude ratios of P15-N20/N20-P25 had a good prognosis.

These studies further illustrate that the SEPs can yield important prognostic information and that it may be possible to divide abnormal SEPs to provide additional prognostic information. The study by Walser et al. [33] demonstrates that, in contrast to the ABRs, the SEPs can be a useful predictor of outcome in nontraumatic etiologies of coma.

### **Somatosensory and visual evoked potentials**

In order to increase the sensitivity of the evoked potentials, the results from SEPs were combined with the results from other evoked potential studies. Pfurtscheller et al. [21] studied the long latency components of the median nerve SEPs (using vibration as the stimulus) with the VEPs in 27 patients with hypoxia or encephalitis. All the patients had a GCS measure between three and seven. The GOS was used for measuring recovery. Similar to de la Torre et al [3] they found that the better the definition of the later components of the SEP the better the prognosis. The VEPs added little information to predicting prognosis, probably reflecting that both the VEPs and late components of the SEPs require intact cortical functions. The etiologies of coma in this study (hypoxia and encephalitis) cause a diffuse dysfunction of the cerebral cortex that would be equally reflected in both the SEPs and the VEPs.

### **Somatosensory and auditory evoked potentials**

Lutschg et al. [18] reviewed the median nerve SEPs and ABRs from 43 children in coma, 26 from head trauma, and 17 from anoxia. All had a GCS less than seven. They divided the ABR results into normal, mildly abnormal with an increase of the I-V interpeak latency, and moderately abnormal showing a loss of components. They divided the SEP results into normal (central conduction times, N13-N20, defined by age dependent norms); mildly abnormal, showing a prolonged central conduction (N14 to N20) of less than five msec; moderately abnormal, showing a prolonged central conduction time of greater than five msec; and markedly abnormal, showing a loss of components. They divided the patient outcomes into normal, with deficits, and dead. The patients with head trauma were analyzed separately from those with anoxia. A normal ABR was a positive but not definite sign for recovery in patients in coma due to head trauma: six of nine patients with normal ABRs had normal

recoveries. A prolongation of the I-V interpeak interval (mild abnormality) provided no additional assistance for prognosis, 12 patients in this group were equally divided among the three outcomes. However, none of the five patients with absence of components of the ABR (moderate abnormality) had a good recovery. The prognostic accuracy of the ABRs in children in coma due to anoxia was similar to its accuracy with the children in coma due to head trauma, a result that differs from that previously reviewed in adults. There was little difference in the prognostic accuracy of the SEPs between the two patient populations. Of the 13 patients with normal SEPs, 11 had a normal outcome. None of the 19 patients with loss of components of the SEP had a good recovery. The measurement of central conduction time added little to the prognostic accuracy of the test. It is evident from this work that any loss of components from both the ABR (considering waves I, III, and V) and the SEP (in particular the N20 component) predicts a poor outcome. A normal ABR and SEP predict a good outcome.

There are situations when the results from the two evoked potential studies differ. Frank et al. [4] studied the ABRs and SEPs of five children in a chronic vegetative state secondary to anoxia. All had normal ABRs but abnormal SEPs with an absence of N19 and subsequent components of the SEP. Thus, in this circumstance the prognosis predicted by the two different sensory evoked potential tests differed. The ABR data suggested a good but incorrect outcome, while the SEP indicated a poor and correct outcome. Far from being a contradiction between the ABR and the SEP, these results show that the evoked potentials provide an accurate physiologic reflection of the patient's condition: a chronic vegetative state indicating preserved brainstem but altered cerebral functions. The ABR is most useful as a predictor of recovery in the initial period of coma, being best with head trauma and a useful adjunct in other etiologies. The ABR is not useful when the patient has been in coma for a prolonged period.

#### **ALL SENSORY MODALITIES: SOMATOSENSORY, VISUAL AND AUDITORY EVOKED POTENTIALS**

Lindsay et al. [15] investigated the use of ABRs, 1AEPs, SEPs (median nerve stimulation), and VEPs in 32 patients who had suffered acute head trauma. Coma was graded with the GCS and outcome with the GOS. The patients had GCS between three and fifteen. They classified the evoked potentials as present or absent, except in the case of the ABRs in which the number of components present was used. Each patient's evoked potential was rated by the poorer of the two potentials seen on testing either side. They found that abnormalities on the SEP were correlated with abnormalities of the 1AEP and the VEP. The presence or absence of abnormalities of the ABRs was not correlated with abnormalities of any of the other evoked potential studies. This study again illustrates that different evoked potentials test the integrity of different parts of the nervous system. The ABR is dependent on the integrity



of the brainstem, while the 1AEP, N20, and later components of the SEP and VEP are dependent on the integrity of cortical structures. The decision as to which evoked potential testing to perform is dependent on clinical factors; the duration of coma, the etiology of the coma, and the clinical question to be answered.

Anderson et al. [1] reviewed the SEPs, VEPs and ABRs from 39 patients who had suffered closed head trauma. All the patients had a GCS <7 with outcomes graded with the GOS. They used a four point scale of grading for each evoked potential, from one meaning normal to four meaning severely abnormal. They found that all three evoked potential studies were equally reliable at predicting a poor outcome, i.e., grades of three or four on any of the evoked potential studies predicted a poor outcome. However, only the SEP was useful in indicating a possibility of a good outcome, namely when there was a grade one or two result on the SEP. Grade one or two on the ABR or the VEP yielded little information about the quality of survival. These results confirm the trend noted above: The best prognostic information can be developed from evoked potential studies reflecting both brainstem and cortical function.

Many of the questions addressed in the studies reviewed above were addressed by Greenberg and his colleagues in papers published from 1977 to 1981. They evaluated the sensory evoked potentials of 51 comatose patients and developed a complex system of grading the resulting waveforms into four different injury patterns for each evoked potential test. The analysis period of the evoked potentials was longer than most investigators have employed, extending 200 msec for SEPs, 300 msec for VEPs, and 400 msec for AEPs, thereby encompassing many components not usually examined because of their variability of occurrence due to factors such as arousal, sleep stage, and attention. For instance, the SEP to median nerve stimulation was considered to consist of nine separate components in normal subjects: P15, N20, P29, N35, P50, N78, P98, N138, and P188. A grade I abnormality was a loss of the latter two components, P188 and N138; a grade II abnormality consisted of the loss of components after P35 (i.e., P98, N78, and P50); a grade III abnormality showed only components P15 and N20, while a grade IV abnormality consisted of only the P15 component. A similar type of grading system was used for the visual and auditory modality evoked potentials.

The outcome was correlated with the evoked potentials by using the most normal grade between the two sides. The presence of grade I or II evoked potentials, i.e., those having all but the longest latency components, predicted a good outcome or moderate disability with the SEPs being the most accurate of the sensory evoked potentials.

Greenberg and his associates [19] performed a retrospective study comparing the sensory evoked potentials, ABRs, 1AEPs, VEPs and SEPs, with outcome in 133 patients suffering from head trauma. They graded the sensory evoked potentials as described above, and combined them into two groups:

normal, consisting of grades I and II; and abnormal, consisting of grades III and IV. They added a further category, focal, used to describe the sensory evoked potentials when the potentials were abnormal to only one of stimulated sides. The clinical outcomes were placed into two categories: "good", meaning a good recovery or moderate disability; and "poor", meaning severely disabled, vegetative, or dead. They compared the prognostic accuracy of the evoked potentials, clinical features, including age, CT scan findings, intracranial pressure monitoring, GCS score, and pupillary responses. The results indicated that sensory evoked potentials were the best single indicator of prognosis. The best combination of indicators was the sensory evoked potentials and clinical features. Eighty percent of the patients with normal sensory evoked potentials had a "good" recovery, while 20 percent had "poor" recoveries ( $n = 82$ ). There were similar results if the evoked potentials showed only a focal abnormality, 72 versus 28 percent ( $n = 18$ ). When the evoked potential abnormality was confined to the long-latency components, thought to be generated in the cerebral cortex, only 10 percent had a "good" outcome, while 90 percent had a "poor" outcome ( $n = 10$ ). When the abnormality included the "brainstem", on the ABR or the early components of the SEP (before N20), all the patients had a "poor" outcome ( $n = 9$ ). When abnormalities were seen on both the "hemisphere" and "brainstem" evoked potentials, all the patients had a "poor" outcome ( $n = 14$ ).

Greenberg and his associates performed a prospective study of sensory evoked potentials in 100 patients in coma due to head trauma [7]. Sensory evoked potentials were performed within four days of injury. The outcomes were evaluated at one year after the injury. There were 31 patients in grade I: 71 percent had a good recovery, 16 percent were moderately disabled, three percent were severely disabled and 10 percent died. There were 31 patients in grade II: 61 percent had a good recovery, 13 percent were moderately disabled, three percent severely disabled and 23 percent died. Seventeen patients were in grade III: 35 percent had a good recovery, 18 percent were moderately disabled, six percent were in a vegetative state and 41 percent died. All of the 21 patients in grade IV had poor outcomes with 14 percent severely disabled, 10 percent vegetative, and 76 percent died. Although a grade of I or II predicted a good recovery, this recovery could take up to six months to occur. In addition, the prognostic accuracy of the sensory evoked potentials was altered by the presence of subsequent secondary complications, either cerebral or systemic. Not surprisingly, the worst complications were seen in the patients in grades III and IV. As the prognosis in a grade IV patient was so grim, the presence of complications did not alter the prognosis.

The results of Greenberg and his colleagues' studies stress two themes: first, sensory evoked potential testing can aid in the prediction of the outcome from acute coma, particularly when combined with clinical signs. Second, a combination of several modalities of evoked potentials in testing to define the activity of both the brainstem and the hemispheres was most helpful. Several

cautions must be exercised in accepting these conclusions. First and most obvious is that only patients with acute head trauma were tested. The articles previously reviewed indicate that the conclusions derived from patients in coma due to head trauma may not apply to patients with nontraumatic etiologies of coma. Second, the experience of other authors suggests that it may not be necessary to divide the results from each evoked potential test into so many subgroups.

Secondary medical complications can influence the accuracy of sensory evoked potentials in the assessment of prognosis. Newlon et al. [20] examined recovery and complications in 139 comatose patients using the prognostic accuracy of the initial evoked potential test as guidelines. Virtually all the patients with grade I potentials did well. Eighty percent of the patients in grade II had normalized their potentials to grade I within one year. Fifty percent of the patients in grade III improved to a grade II, while the other 50 percent either stayed at grade III or worsened. They made the following conclusions: Patients who went from grade II to grade I usually had a good outcome, while only 50 percent of those who stayed in grade II improved clinically. Those patients in grade III improving to grade II showed some clinical improvement, but if the grade of the sensory evoked potentials did not change then the outcome remained poor. All the patients who deteriorated from grade III to IV had a poor outcome. The changes in evoked potential testing could precede other clinical signs especially when secondary complications ensued.

Two important points are made by this study. First and paramount is that as a patient's condition changes, early prognoses become inaccurate. Therefore, repeat testing is advisable. Indeed, evoked potential testing can be the first indication of deterioration in some cases. Second, repeat testing can improve the accuracy of prognosis as the change in sensory evoked potentials can yield information of value.

## **BRAIN DEATH AND SENSORY EVOKED POTENTIALS**

Brain death is a special circumstance of coma. Evoked potentials can provide confirmatory evidence of brain death. Trojaborg and Jorgensen [29] reviewed the results of the SEP and VEP in 50 patients with isoelectric electroencephalograms and coma due to a variety of etiologies. Nineteen patients had evidence of preserved cranial nerve function. All showed wave forms to one of the two evoked potentials tests. Thirty-one patients had no evidence of cranial nerve function and only one showed a wave form to either somatosensory or visual stimulation. Starr [25] reviewed the ABRs of 27 patients meeting the clinical criteria of brain death. Sixteen patients showed no components, and in 11 only wave I was present. As Wave I is a reflection of VIII nerve function, the absence of all but wave I in the ABRs indicates complete disruption of the brainstem auditory pathways. Goldie et al. [8] reviewed ABRs and SEPs of 35 patients meeting the clinical criteria of brain death. They found that 21 patients

had no ABRs and six showed only wave I. However, they also found two patients showing both waves I and II. Twenty-nine of the brain dead patients were tested with SEPs to median nerve stimulation. All 29 had well defined peripheral nerve potentials measured over Erb's point. None of the 29 patients had any cortical responses. Steinhart and Weiss [26] studied the ABRs of ten children who met the criteria for brain death. All showed either wave I only or no components. Thus, sensory evoked potentials, especially those evaluating brainstem function (ABRs and SEPs), are useful adjuncts to determining the condition of brain death. Sensory evoked potential testing can only be used when: 1) the clinical picture supports a diagnosis of brain death, and 2) there is no disruption of the pathway between the peripheral sensory organs and the brainstem structures subserving them.

### CONCLUSION

We have reviewed the experience of using sensory evoked potentials in comatose patients to predict outcome, and offer these conclusions: first, it would be best to use those evoked potential procedures that test the functions of both brainstem and cerebral cortex. Optimally, this would include a battery of all of the sensory evoked potentials discussed above: ABRs, 1AEPs, VEPs, and SEPs. From a practical viewpoint the most useful tests are the ABR and the SEP; and of the two, the SEP should be performed if there is time for only one test. However, the utility of the evoked potential results in defining central nervous system functions will be curtailed if the peripheral receptors or peripheral nerves activated by the stimuli are damaged. For instance, auditory evoked potentials cannot be used in evaluating the brainstem and cortical auditory structures if the patient's cochlea or VIII nerve have been severely damaged. A lesion of the peripheral nerve, plexus, roots or spinal cord subserving the nerve can invalidate the SEP as regards central functions. A major limitation in evaluating the experience with sensory evoked potentials in coma is the lack of a consistent scale of defining the grade of abnormality. In contrast, the clinical scales of quantifying the level of coma and the degree of recovery from coma (Glasgow Coma and Recovery Scale), while imperfect instruments, still provide a uniform manner of communication for assessment.

Second, the etiology of the coma is an important variable in considering sensory evoked potentials results in the prognosis from coma. Abnormalities of sensory evoked potentials (particularly the ABRs) in a patient with head trauma have a different significance than the same set of abnormalities in a patient comatose due to anoxia.

Third, evoked potential studies should be repeated to provide updating of neural functions. While the initial test results can yield information of prognostic value, secondary complications can markedly change the initial prognosis. Sensory evoked potentials are sensitive to those secondary complications and provide a means for assessing their effects on the nervous system.

Finally, sensory evoked potentials are useful in determining central neural activity in patients suspected of brain death. The potentials dependent on brainstem function (ABRs, SEPs) are most relevant in this regard. However, these sensory evoked potentials can only be used when the peripheral nerve, spinal cord sensory pathways and the cochlea and its central connections are intact.

## REFERENCES

1. Anderson DC, Bundlie S, Rockswold GL: Multimodality evoked potentials in closed head trauma. *Arch Neurol* 41:369–374, 1984.
2. Arfel G, Albe-Fessard D, Walter St: Evoked potentials in coma (abstract). *Electroencephalogr Clin Neurophysiol* 25:93, 1968.
3. De la Torre JC, Trimble JL, Beard RT, Hanlon K, Surgeon JW: Somatosensory evoked potentials for the prognosis of coma in humans. *Experimental Neurol* 60:304–317, 1978.
4. Frank LM, Furgiele TL, Etheridge Jr JE: Prediction of chronic vegetative state in children using evoked potentials. *Neurology* 35:931–934, 1985.
5. Greenberg RP, Mayer DJ, Becker DP, Miller JD: Evaluation of brain function in severe human head trauma with multimodality evoked potentials Part I: Evoked brain injury potentials, methods, and analysis. *J Neurosurg* 47:150–162, 1977.
6. Greenberg RP, Mayer DJ, Becker DP, Miller JD: Evaluation of brain function in severe human head trauma with multimodality evoked potentials Part II: Localization of brain dysfunction and correlation with posttraumatic neurological conditions. *J Neurosurg* 47:163–177, 1977.
7. Greenberg RP, Newlon PG, Hyatt MS, Narayan RK, Becker DP: Prognostic implications of early multimodality evoked potentials in severely headinjured patients: A prospective study. *J Neurosurg* 55:227–236, 1981.
8. Goldie WD, Chiappa KH, Young RR, Brooks EB: Brainstem auditory and shortlatency somatosensory evoked responses in brain death. *Neurology* 31:248–256, 1981.
9. Hall JW, Huang-fu M, Gennarelli TA: Auditory function in acute severe head injury. *Laryngoscope* 92:883–890, 1982.
10. Hume AL, Cant BR: Central somatosensory conduction time after head injury. *Ann Neurol* 10:411–419, 1981.
11. Jain S, Maheshwari MC: Brainstem auditory evoked responses in coma due to meningencephalitis. *Acta Neurol Scand* 69:163–167, 1984.
12. Jennett G and Bond M: Assessment of outcome after severe brain damage: A practical scale. *Lancet* 1:480–484, 1975.
13. Karnaze DS, Marshall LF, McCarthy CS, Klauber MR, Bickford RG: Localizing and prognostic value of auditory evoked responses in coma after closed head trauma. *Neurology* 32:299–302, 1982.
14. Karnaze DS, Weiner JM, Marshall LF: Auditory evoked potentials in coma after closed head injury: A clinical-neurophysiologic coma scale for predicting outcome. *Neurology* 35:1122–1126, 1985.
15. Lindsay KW, Carlin J, Kennedy I, McInnes A, Teasdale GM: Evoked potentials in severe head injury analysis and relation to outcome. *J Neurol Neurosurg Psychiatry* 44:796–802, 1981.
16. Lott IT, McPherson DL, Starr A: Cerebral cortical contributions to sensory evoked potentials. *Electroencephalogr Clin Neurophysiol*, in Press.
17. Lumenta CB: Measurements of brain-stem auditory evoked potentials in patients with spontaneous intracerebral hemorrhage. *J Neurosurg* 60:548–302, 1984.
18. Lutschg J, Pfenninger J, Ludin HP, Vassella F: Brainstem auditory evoked potentials and early somatosensory evoked potentials in neurointensively treated comatose children. *Am J Dis Child* 137:421–426, 1983.
19. Narayan RK, Greenberg RP, Miller JD, Enas GG, Choi SC, Kishore PRS, Selhorst JB, Lutz HA, Becker DP: Improved confidence of outcome prediction in severe head injury: A comparative analysis of the clinical examination, multimodality evoked potentials, CT scanning, and intracranial pressure. *J Neurosurg* 54:751–762, 1981.

20. Newlon PG, Greenberg RP, Hyatt MS, Enas GG, Becker DP: The dynamics of neuronal dysfunction and recovery following severe head injury assessed with serial multimodality evoked potentials. *J Neurosurg* 57:168–177, 1982.
21. Pfurttscheller G, Schwarz G, Gravestein N: Clinical relevance of longlatency SEPs and VEPs during coma and emergence from coma. *Electroencephalogr Clin Neurophysiol* 62:88–98, 1985.
22. Picton T, Hillyard SA, Krausz HI, Galambos R: Human auditory evoked potentials: Evaluation of components, *Electroencephalogr Clin Neurophysiol* 36:179–190, 1974.
23. Rosenberg C, Wogenson K, Starr A: Auditory brainstem and middle- and long latency evoked potentials in coma. *Arch Neurology* 41:835–838, 1984.
24. Seales DM, Rossiter MA, Weinstein ME: Brainstem auditory evoked responses in patients comatose as a result of blunt head trauma. *J Trauma* 19:347–353, 1979.
25. Starr A: Auditory brainstem responses in brain death. *Brain* 99:543–554, 1976.
26. Steinhart CM, Weiss IP: Use of brainstem auditory evoked potentials in pediatric brain death. *Critical Care Med* 13:560–562, 1985.
27. Strickbine-Von Reet P, Glaze DG, Hrachovy RA: A preliminary prospective neurophysiological study of coma in children. *Am J Dis Child* 138:492–495, 1984.
28. Teasdale G and Jennett B: Assessment of coma and impaired consciousness: A practical scale. *Lancet* 2:81–84, 1974.
29. Trojaborg W, Jorgensen EO: Evoked cortical potentials in patients with “isoelectric” EEGs. *Electroencephalogr Clin Electrophysiol* 35:301–309, 1973.
30. Tsubokawa T, Nishimoto H, Yamamoto T, Kitamura M, Katayama Y, Moriyasu N: Assessment of brainstem damage by the auditory brainstem response in acute severe head injury. *J Neurol Neurosurg Psychiatry* 43:1005–1011, 1980.
31. Uziel A, Benezech J, Lorenzo S, Monstrey Y, Duboin MP, Roquefeuil B: Clinical applications of evoked auditory potentials in comatose patients. In: *Clinical Applications of Evoked Potentials in Neurology* (eds) J Courjon, F Manguiere and M Revol, Raven Press, New York, 195–202, 1982.
32. Vaughn HG, Ritter W: The sources of auditory evoked responses recorded from the human scalp, *Electroencephalogr Clin Neurophysiol* 28:360–367, 1970.
33. Walser H, Mattle H, Keller HM, Janzer R: Early cortical median nerve somatosensory evoked potentials: Prognostic value in anoxic coma. *Arch Neurol*, 42:32–38, 1985.
34. Zeneroli ML, Pinelli G, Gollini, Penne A, Messori E, Zani G, Ventura E: Visual evoked potential: a diagnostic tool for the assessment of hepatic encephalopathy. *Gut* 25:291–299, 1984.

---

## **10. ELECTROPHYSIOLOGIC MONITORING OF NEURAL FUNCTION DURING SURGERY**

JASPER R. DAUBE

Electrophysiologic monitoring has provided surgeons direct and immediate feedback about the function of neural structures that may be inadvertently damaged during surgery. The value of these techniques in many different types of surgery is just being realized, as the full range of electrophysiologic monitoring is applied. Many different electrical measures of neural function have been applied, and most have been found to be useful measures of neural function under anesthesia.

Cortical function can be monitored with electroencephalography (EEG) and surface recorded somatosensory evoked potentials (SEP). Thalamic nuclei can be localized with direct recording during stereotactic surgery. Eighth nerve and brainstem function can be monitored with auditory evoked potentials (AEP). Peripheral and central sensory pathways are monitored with SEP. Peripheral motor nerve function can be monitored with electromyography (EMG) and compound muscle action potentials (CMAP). Nerve action potentials (NAP) can be recorded directly from peripheral nerves and the eighth nerve. Visual evoked potentials have been limited by problems of adequate stimulus and appropriate applications. Motor evoked potentials have the capability for testing central motor pathways. Blink reflexes and F-waves become too variable under anesthesia to be used for monitoring.

The selection of a method from this variety of monitoring techniques is best done on clinical grounds for each individual patient, based on the structures most at risk. Often some combination of methods is needed. Patients undergoing posterior fossa surgery may need EMG, CMAP, AEP and SEP moni-

toring for large tumors, or only one or the other for smaller lesions. Patients undergoing peripheral nerve or plexus surgery may need SEP, NAP, or CMAP. SEP alone may provide adequate monitoring for stereotactic biopsy or depth surgery, for some types of spine surgery, for spinal cord AVM embolization, and for cortical resection. Carotid endarterectomies are best monitored with EEG recordings.

The selection of the monitoring method for an individual patient, and, in particular, the specific technical details, one must always keep in mind some general principles of surgical monitoring: early identification of reversible damage, recognition of all changes, rapid feedback to the surgeon, reliability, and minimal interference with the surgical procedure.

During the course of surgery, damage to neural structures may occur rapidly and irreversibly. Methods that can warn of the risk of such damage before it occurs are therefore desirable, even if they do not indicate the presence of damage that will produce clinical deficits. Such an approach carries with it the understanding that changes will be identified which are not serious in themselves.

The rates of change in neural function will vary with the type and severity of damage. Some will occur abruptly while others may develop gradually over 20–30 minutes. They can occur at a variety of times in relation to the surgical procedure. Some are seen immediately after an injury, others, particularly those with a mild compression, may be delayed for up to an hour. Surgical monitoring must therefore be carried on throughout the procedure, even after so-called critical periods in the surgery have been passed.

The surgeon is always working under pressure to complete the surgery smoothly and quickly. He must be able to proceed efficiently with his work. Surgical delays while waiting for monitoring results should be avoided in selecting methods. The surgeon must learn as quickly as possible after he has done something potentially damaging that damage has or has not occurred.

Equally important to the other concerns is the reliability of the changes in recording. This requires a well-defined set of baseline values during the initial low-risk portions of the surgery. The variation due to extraneous factors must be known so that the surgeon can be assured that if a change is reported to him, it is related to his surgical procedure and not to blood pressure, artifacts, technical problems or other factors.

Development of monitoring methods should always keep in mind the need to minimize interference with the surgical procedure. Monitoring techniques entirely outside the surgical field are preferred if adequate. They can reduce noise in the system from surgical manipulation as well as simplifying the surgical procedure.

The most commonly used applications are the monitoring of spinal cord integrity with SEP, and the monitoring of cranial nerve integrity with AEP, EMG and CMAP. Each of these will be described separately, followed by discussion of some of the less commonly used methods.



## **MONITORING OF POSTERIOR FOSSA SURGERY**

Many posterior fossa tumors are benign, with acoustic neurinomas most common among them [17, 19]. Their slow growth allows posterior fossa structures to accommodate to them as they grow to sizes of four centimeters or more. Their location and size make them difficult to operate on, but improved surgical techniques, especially microsurgery with an operating microscope, have markedly improved the outcome of this delicate surgery [16, 45].

Cranial nerve involvement is common with posterior fossa tumors, especially those over two centimeters in diameter. While acoustic nerve involvement with hearing loss is the most frequent, trigeminal involvement is also common, with facial sensory symptoms in 29% and sensory loss in 26% [17]. Facial weakness occurs in only 13% overall, but of patients with tumors over four cm, 56% have loss of facial sensation and 31% have facial weakness [15]. Electrophysiologic signs of facial nerve damage are present in an even higher proportion of patients, often without clinical symptoms or signs [22, 23, 42, 46]. In our experience, 6% of patients with acoustic neurinomas have abnormal facial nerve conduction studies, 44% have abnormal blink reflexes, and 78% have abnormal needle electromyography [14]. The extent of abnormality is proportional to the size of the tumor, and is an excellent predictor of the extent of post-operative deficit. While large tumors may impinge on the accessory and hypoglossal nerves, clinical symptoms or signs have not been reported.

### **Central sensory pathways**

Posterior fossa tumors may impinge on the brainstem, but it is rare for a patient to develop central deficit after surgery. If this possibility is a significant risk, median and/or tibial SEP can be monitored during posterior fossa surgery in addition to the other methods to be mentioned [41].

### **Acoustic nerve**

An increase in or complete loss of hearing is common after surgery for posterior fossa tumors, especially acoustic neurinomas [9]. It even occurs in up to 15% of patients undergoing microvascular decompression of cranial nerves V or VII [10]. Evoked potentials have been used to reduce the incidence of this complication. Standard surface recordings of AER are the easiest technically, requiring only the application of ear and vertex electrodes, and some type of small click stimulator in the ear canal [11, 43]. AER can be used effectively to monitor, but suffers from: 1) low amplitude responses, which may not be reliably recorded, especially with some preoperative deficit, and 2) the need to average large numbers of responses and the associated delay in feedback to the surgeon. The latter can be reduced by use of a running average [4] or two-dimensional digital filtering [47]. The loss or change in response that may be associated with only minimal change in hearing—a phenomenon incorrectly

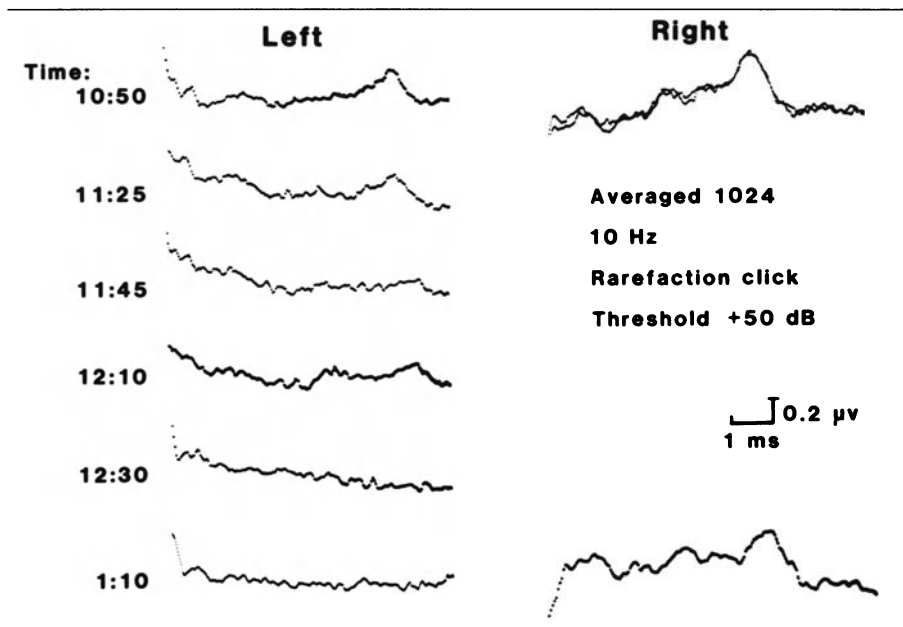
called a false positive—has been seen as a drawback, but only reflects the sensitivity of the monitoring. Injury to the eighth nerve during surgery may reduce the wave V evoked response amplitude, change its latency, or both, depending on the type of damage (figure 10-1). Amplitude reductions of more than 50% from baseline or latency increases of more than 0.5 msec are generally considered significant.

Direct recording of nerve action potentials from the VIIIth nerve with small wick electrodes offers a more rapid and direct monitor of damage, since the potential can be recorded without averaging (figure 10-2) [36]. Direct recordings can be most reliably used in microvascular decompression, but usually is not possible with tumors, especially if they are over 1 cm in diameter.

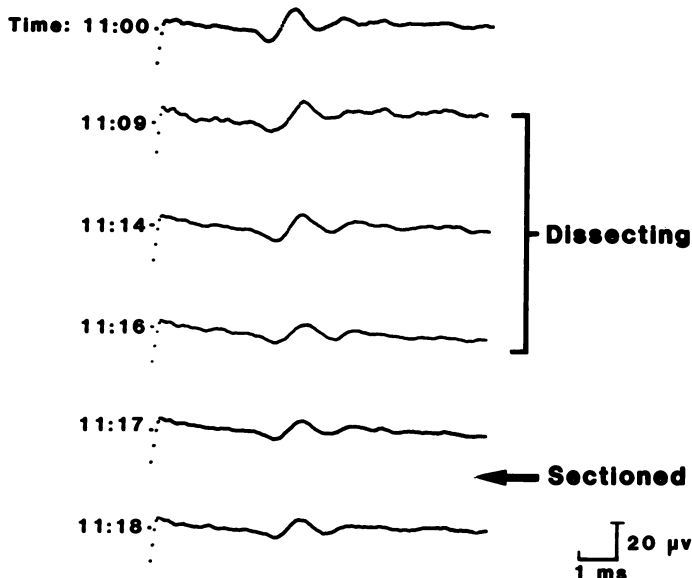
The third method of recording, with a needle electrode in the middle ear, monitors both the cochlear and VIIIth nerve response, and has improved the salvage rate of hearing [28, 40]. Peripheral loss detected with this method is likely to be due to ischemia. More central damage may not be recognized.

### Facial nerve

As the surgical techniques have improved there has been increasing emphasis on the preservation of facial nerve function after tumor removal. The outcome depends mainly on tumor size and location, and to a lesser extent on specific



**Figure 10-1.** Loss of scalp recorded auditory evoked potential (vertex—ear lobe) during left acoustic neurinoma surgery. Hearing was reduced preoperatively and further reduced postoperatively.



**Figure 10-2.** Direct eighth nerve action potential recording with click stimulation during vestibular nerve section for vertigo. Sixteen responses averaged.

surgical techniques. In patients with large tumors (over 4 cm), close to 100% have complete facial paralysis postoperatively, even though in 12% the nerve is intact after surgery. The nerve is intact after surgery in 85% of medium-sized tumors and in all small (less than 2 cm) tumors. Nonetheless, 95% of patients with medium-sized tumors have some post-operative weakness, and 50% have complete paralysis. Of patients with small tumors, 21% have complete paralysis and 68% have some weakness after surgery. Luckily, if the nerve is left anatomically intact, recovery of function occurs eventually in up to two-thirds of patients [9, 15]. The trigeminal nerve suffers less damage at surgery with only a very small percentage of patients suffering increased deficit. Lower cranial nerve damage occurs even less frequently during surgery. Clearly there is room for further improvement in preservation of motor nerve function in these very difficult surgical procedures.

In 1979, Sugita et al. [49] reported an enhancement of the preservation of facial nerve function with electrophysiologic monitoring during surgery for acoustic neurinoma. In their series of 22 cases, 20 were patients with tumors over 4 cm in diameter. Facial sensory loss was present preoperatively in 64%, and facial weakness in 55%. In addition to using the surgical microscope for identification and dissection of the nerves from the tumor, they applied direct electrical stimulation to the nerve using insulated bipolar coagulating forceps. Stimulation of 1–3 volts for 1 msec at rates of 2–4 Hz were applied by the surgeon while monitoring the movement of eyelid and lip muscles with a

mechanical monitor of movement. The response was amplified and listened to over a loudspeaker to give the surgeon immediate feedback when he was stimulating the nerve. With these techniques the authors preserved anatomical and physiologic function in 86% of their patients. Delgado has reported similar results [6].

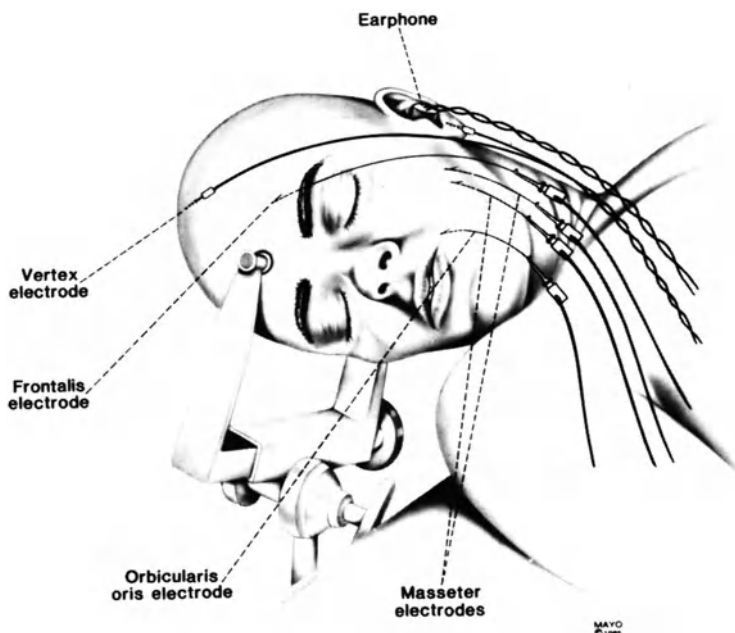
Three methods can be used to complement each other in providing different types of information for monitoring the facial nerve. 1) Preoperative EMG, blink reflexes and facial conduction studies define the amount of preoperative nerve damage and identify any spontaneous discharges. These reliably predict the likelihood of further loss of function during surgery. 2) Inadvertent mechanical stimulation of the motor nerves during the surgical procedure is monitored by visual and auditory monitoring of EMG activity in cranial muscles. 3) The location and function of the nerve in the operating field is monitored by recording the CMAP over cranial muscles in response to direct electrical stimulation of the nerve by the surgeon [18, 37].

### **EMG monitoring**

Recording electrodes are placed directly within cranial muscles of interest. For facial nerve monitoring this usually includes the orbicularis oculi and orbicularis oris muscles, and occasionally other facial muscles such as the frontalis and mentalis. The trigeminal nerve is monitored with electrodes in the masseter or the temporalis muscles. The spinal accessory and hypoglossal nerves are monitored with electrodes in the sternocleidomastoid or trapezius, and the genioglossus muscles respectively. To assure proper electrode placement and satisfactory recordings, the insertion is best performed before the patient is anesthetized, using standard electromyographic methods. Electrode location is confirmed by recording voluntary EMG activity.

A variety of EMG recording electrodes have been tested. Surface and subcutaneous electrodes cannot reliably record the discharges of a few motor units, and are noisier and less stable at the gains needed for the EMG recording. Standard concentric and monopolar EMG needle electrodes provide excellent quality EMG signals, but are somewhat uncomfortable and bulky. They also may get in the way of the anesthetist. The most satisfactory electrodes have proven to be fine wires with 2 mm bare tips inserted 5 mm apart through a 26 gauge needle, which is then removed. The wires are taped to the skin in loops and connected to the input of the preamplifier through a small hooked electronic probe (figure 10-3). The leads from the probes to the preamplifier must be kept as short as possible to reduce interference from external sources.

EMG recordings are made with standard gain, sweep and filter settings (gain: 200 or 500 microvolts; low filter: 32 Hz; high filter: 16 KHz; oscilloscope sweep speed: 10 msec/cm). Multiple muscle EMG recordings are monitored simultaneously over a loudspeaker as well as on an oscilloscope. EMG activity of interest is photographed and tape recorded.



**Figure 10-3.** Schematic diagram of recording electrodes used in monitoring posterior fossa surgery. Hooks represent intramuscular EMG wire electrodes. Vertex and ear needles are used to record BAER.

A number of different types of electrical activity are recorded from the EMG electrodes during surgery and must be distinguished from each other (figure 10-4). The discharges of interest, called neurotonic discharges, are those initiated by mechanical stimulation of the facial nerve. They must be distinguished from other activity arising in the muscle, and from electrical interference. The most common problem is that of irregular, triangular waves due to movement of the wires, which can be readily distinguished by their appearance. Equipment and fluorescent lights in the operating room also can contribute electrical artifact. Sixty cycle interference from gas humidifiers, lights and heating blankets can be eliminated by proper equipment isolation and grounding. The artifacts from nerve stimulators, Cavitron, and respirator can be easily recognized. Interference from cautery is best suppressed with a switch attached directly to the cautery control switch. EMG activity cannot be monitored during cautery.

The use of neuromuscular blocking agents is ended or reduced before EMG monitoring begins. While this increases the possibility of unwanted movement during surgery, the latter can be prevented with adequate levels of inhalation anesthesia. Muscle activity that must be distinguished from neurotonic discharges includes motor unit potentials if the patient is not deeply anesthetized,

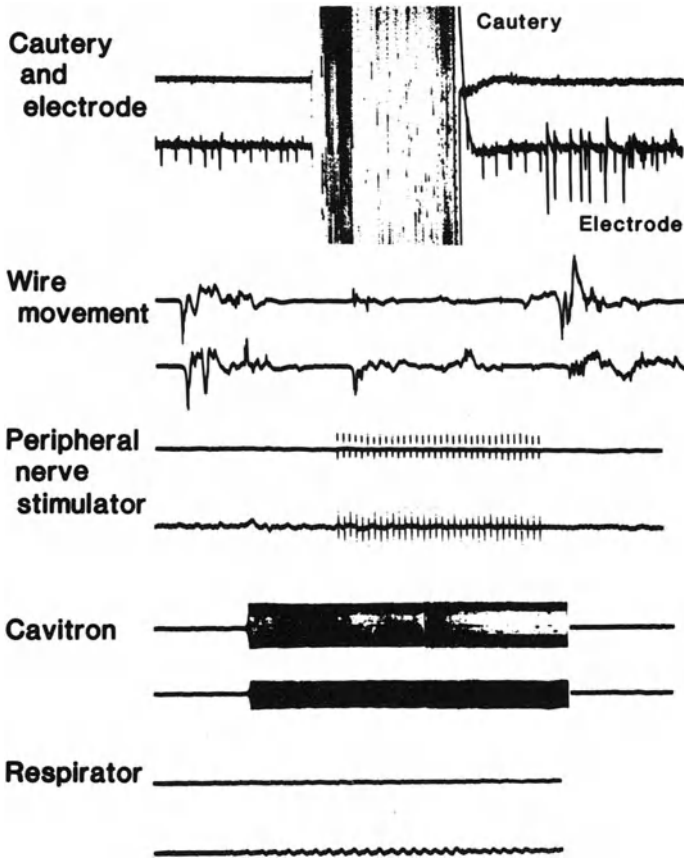
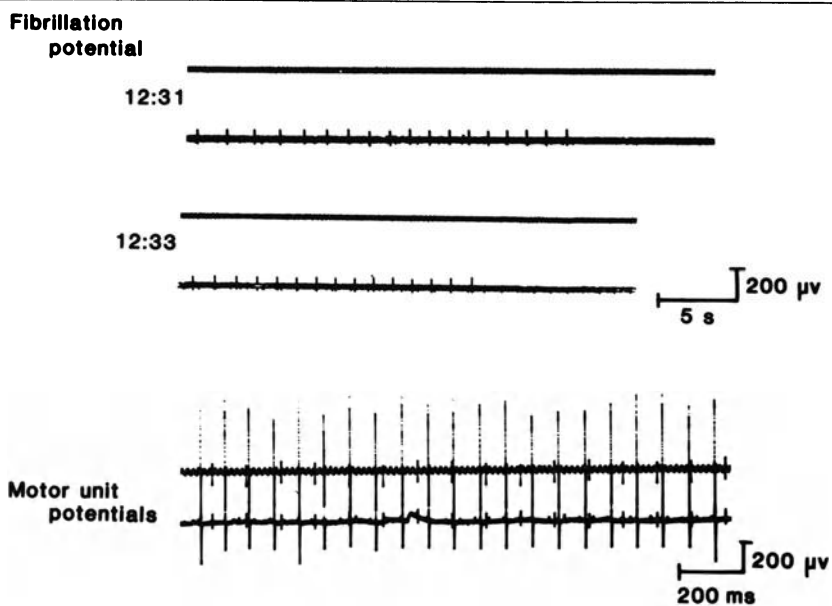
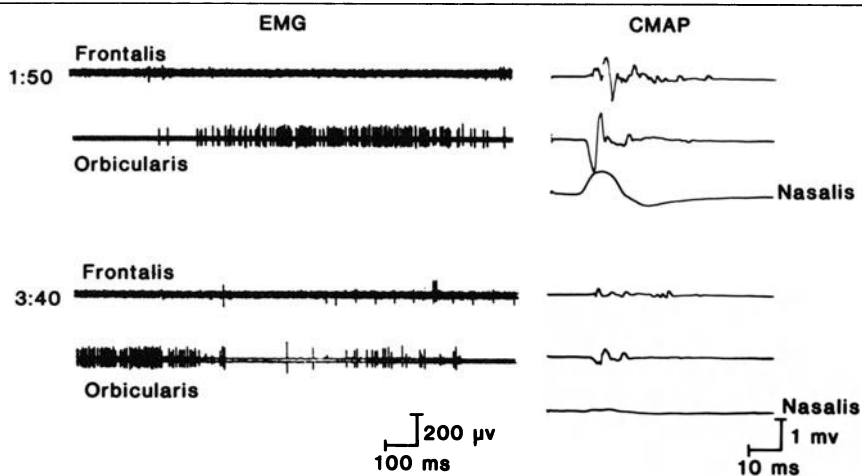


Figure 10-4. Artifacts recorded with EMG wire electrodes during surgical monitoring.

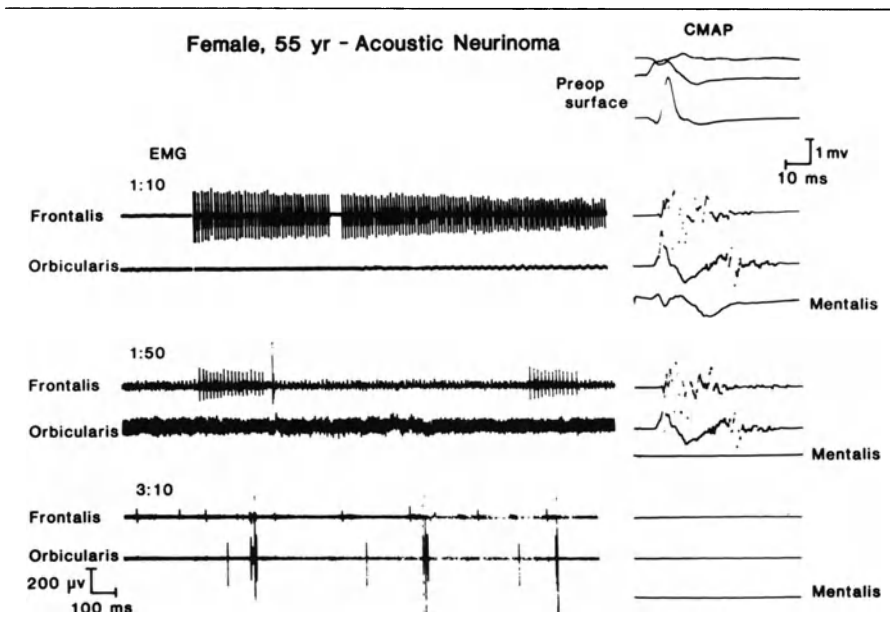
fibrillation potentials if the muscle has been partially denervated, myokymic discharges, end-plate noise and spikes, and complex repetitive discharges (figure 10-5). Each of these has been seen in these patients, but can be readily distinguished from neurotonic discharges by their typical firing patterns and action potential characteristics. The neurotonic discharges have a variety of forms but are all rapid bursts with an irregular recurrence (figures 10-6 and 10-7). They may last less than 100 msec or persist up to many seconds. The long bursts are more common after nerve stretching. Typically there are multiple neurotonic discharges occurring independently in each muscle. Often the different discharges occur at the same time in all the muscles innervated by one nerve, but not in muscles innervated by another nerve. Once familiar with them, the surgeon is able to readily recognize the sound of the neurotonic discharges as soon as he initiates them with surgical manipulation of the nerve. Seventh nerve section results in dense, long bursts of neurotonic discharges.



**Figure 10-5.** Spontaneous activity recorded from facial muscle during surgery for acoustic neurinoma.



**Figure 10-6.** Monitoring acoustic neuroma surgery with EMG and CMAP of facial muscles. Neurotonic discharges are shown at the left and loss of CMAP on the right. There was an incomplete facial palsy after surgery.



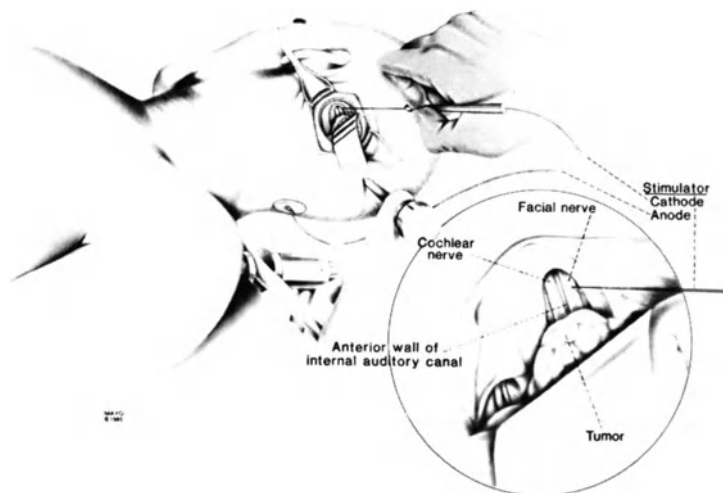
**Figure 10-7.** Monitoring acoustic neuroma surgery with EMG and CMAP. Dense neurotonic discharges occurred and the CMAP was lost. No residual facial function was present after surgery.

Neurotonic discharges are very sensitive indicators of nerve irritation and occur in virtually all patients who have been monitored. The discharges warn the surgeon when he is near the nerve and may not realize it, or assure him that he is not when he is concerned that he may be. The extent of postoperative loss of function is related to the density and frequency of the neurotonic discharges during surgery.

### Nerve stimulation

The other method used to monitor cranial nerve function is to record the compound muscle action potential evoked by direct stimulation of the nerve by the surgeon (figure 10-8). A hand-held bipolar stimulator is applied directly to the nerve, or to an area where the surgeon is looking for the nerve. Stimulation is applied at rates of 1–5 Hz with a stimulus duration of 0.05 msec and gradually increasing voltage. Full responses from the nerve are obtained at voltages of less than 25 volts. If there is intervening tumor tissue, fluid or a short between the stimulating poles, voltages up to 75 volts may be necessary. Stimuli at these higher voltages may result in current spread to nearby nerves and are best avoided. The stimulation may also be applied with a single prong, flush tip (cathode) stimulator with the anode placed elsewhere on the head. This eliminates the likelihood of local short circuit of the stimulating current, but increases the likelihood of current spread and the shock artifact.

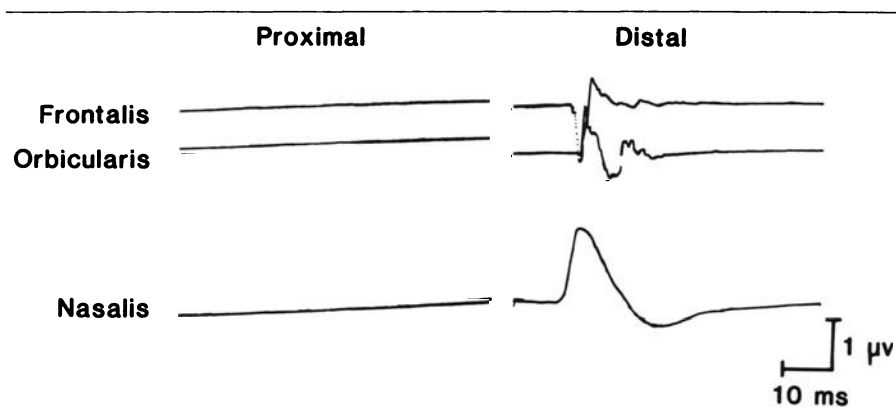




**Figure 10-8.** Schematic diagram of direct stimulation of cranial nerves during posterior fossa surgery. Monopolar stimulation is shown.

The response to the stimulus can be recorded from the wire electrodes used for EMG monitoring as complex, multispike waves whose amplitude and area cannot be readily measured. They therefore cannot be used to make reliable, quantitative measures of the amount of intact nerve. The latter is better accomplished with surface electrodes over the muscle of interest to record compound muscle action potentials. Surface electrodes applied before anesthesia with collodion assure firm adherence throughout the surgery. A baseline response to stimulation of the facial nerve at the mastoid bone is recorded for comparison with responses during surgery. The mentalis muscle has been found to give the most reliable, easily measurable responses in most patients, but the nasalis muscle is also occasionally used. Other facial muscles are less reliable.

If possible, the surgeon stimulates a distal segment of the nerve early in the procedure to determine the threshold for activation and voltage needed for a supramaximal response, and to compare with the baseline. Stimulation is then applied at intervals as the surgeon requests either to localize the nerve, or to determine if it is still intact (figure 10-6 and 10-7). In large tumors involving multiple nerves, the individual nerves can be identified and distinguished by electrical stimulation. If the nerve has been ruptured during dissection, it can still be activated distally, but no response is obtained from proximal portions (figure 10-9). There has been excellent correlation of the preservation of an evoked response during surgery and the preservation of facial function postoperatively. None of the patients with some residual evoked response had total facial paresis, and all of those who lost the response had complete paralysis [14].



**Figure 10-9.** Facial nerve stimulation at proximal and distal sites along the facial nerve after resection of an acoustic neurinoma shows total loss of function proximally. There was no residual facial nerve function postoperatively.

### Applications

Most of the monitoring has been for patients undergoing surgery for acoustic neurinoma. Some of the patients with large tumors have had preservation of function, a better outcome than without these procedures [14]. As well as improving outcome for single patients, the methods have also improved surgical techniques more generally by showing the surgeon what damages nerves. Patients with other tumors, mainly meningiomas, had similar results. Other surgical procedures involving cranial nerves can also be monitored with these techniques. Patients undergoing seventh nerve mobilization for hemifacial spasm can be monitored for both their spontaneous discharge (which usually subside with anesthesia), and for irritation of the seventh nerve during surgery. The discharges of hemifacial spasm can be evoked during surgery with peripheral facial nerve stimulation to test for adequate decompression [38]. Patients undergoing section of the trigeminal nerve for severe cluster headache can be monitored to be certain that the motor branch of the fifth nerve is not sectioned as well. Patients undergoing resection of chemodectoma can have monitoring of eleventh and twelfth nerves.

### MONITORING OF SPINE SURGERY

A small proportion, usually less than 0.5%, of patients undergoing corrective scoliosis surgery and other spine surgical procedures develop a persistent neurological deficit immediately postoperatively. Careful surgical techniques and stabilization of the spine during surgery have helped to hold this complication to a small number. However, the procedure is nonetheless devastating for those individuals who awaken paraplegic after spine surgery.

To further reduce this possibility, the wake up test was devised [13]. The

patient is awakened during the surgical procedure to assure continuity of spinal cord pathways after correction of a spinal deformity by having him voluntarily move his feet. While the wake up test provided help, it is difficult to perform and is associated with the problems of changing anesthetic levels. Also, it is not applicable to patients undergoing surgical procedures, such as spine tumors, in which there is no well-defined time of major hazard, and will not identify the slow or later development of spinal cord dysfunction that sometimes is seen.

Somatosensory potentials have therefore been applied by a number of workers as an additional method to monitor spinal cord function during surgery [1, 8, 12, 31, 39, 44, 53]. Animal studies have demonstrated the loss of somatosensory evoked potential with spinal cord damage. These studies have not all agreed on the relationship between type of damage or the site of damage and the loss of the SEP; compression and ischemia have differing effects, and descending pathway damage sufficient to produce motor paralysis has not always altered the SEP. Nonetheless, as Bennett [2] and others [7] have shown, experimental compressive lesions that compromise motor function do alter the SEP.

With the support of such animal research, SEP and MEP monitoring of patients during spine surgery has been developed by a number of workers using different methods. These can be divided into those in which SEP recordings are made within the operative field, those recording SEP outside the operative field, and those recording MEP [14].

### **Technical factors**

A number of technical factors must be considered with spine monitoring recordings [26]. Most of these have been best defined by Lueders et al., with confirmation by other groups. The rate of stimulation cannot be as fast as on an awake patient. Anesthetics make the sensory system more susceptible to fatigue. While SEPs can be recorded at 5 or even 10 Hertz in most awake patients, under anesthetic the scalp SEP will fatigue at rates over 3 Hz, and some patients will require stimulation as low as 0.5 or 1.0 Hz, especially at deeper levels of anesthesia.

The number of stimuli averaged can vary with background noise level. Since most patients are paralyzed, muscle activity is minimal. When nothing else is going on, responses can be clearly obtained with only 64 or 128 stimuli. However, most surgical recording situations have other sources of artifact than muscle, so 500 or sometimes even 1,000 stimuli are needed for reproducible traces.

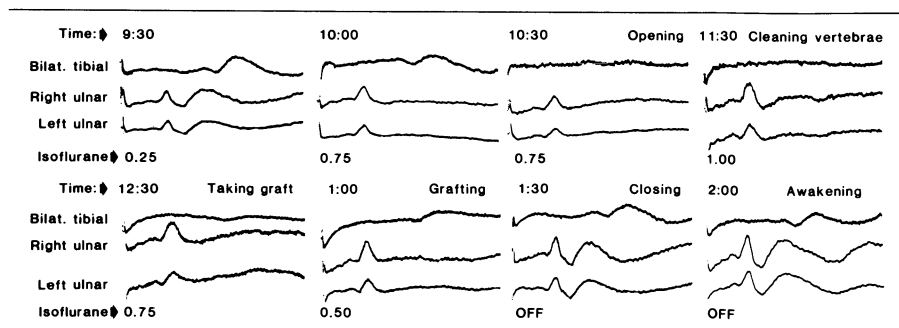
Technical problems are common in the operating room. Sixty Hz artifact occurs with gas warmer/humidifiers, blood warmers, and some electric drills, which should be moved away or removed. Recording wire movement must be eliminated. Wires can be disconnected, cut, dislodged, or damaged during the torso. The wires must be very firmly and multiply affixed, and shielded

wires are sometimes needed. Stimulating electrodes can also be displaced, requiring some type of peripheral monitor to assure their function. A constant current, isolated stimulator can prevent the risk of burns from the stimulator. Both level of anesthesia and blood pressure will change the latency and amplitude of responses (figure 10-10). Rare patients will show an enhancement of a scalp response after induction of anesthesia (figure 10-11), but most are reduced, with a small proportion lost at the scalp immediately after anesthesia induction. In a group of 140 patients undergoing thoracolumbar spine surgery at Mayo, there was a mean scalp amplitude reduction of 37% when anesthesia was inducted, with 5% of subjects entirely losing the response, even without underlying neurologic disease. Similarly there is a gradual reduction in amplitude and increase in latency with continued anesthesia (mean of 17%, with another 5% losing their responses). Latency was less variable, with only a 4–6% average increase during the course of anesthesia. Changes of the SEP at the neck with anesthesia are much less prominent.

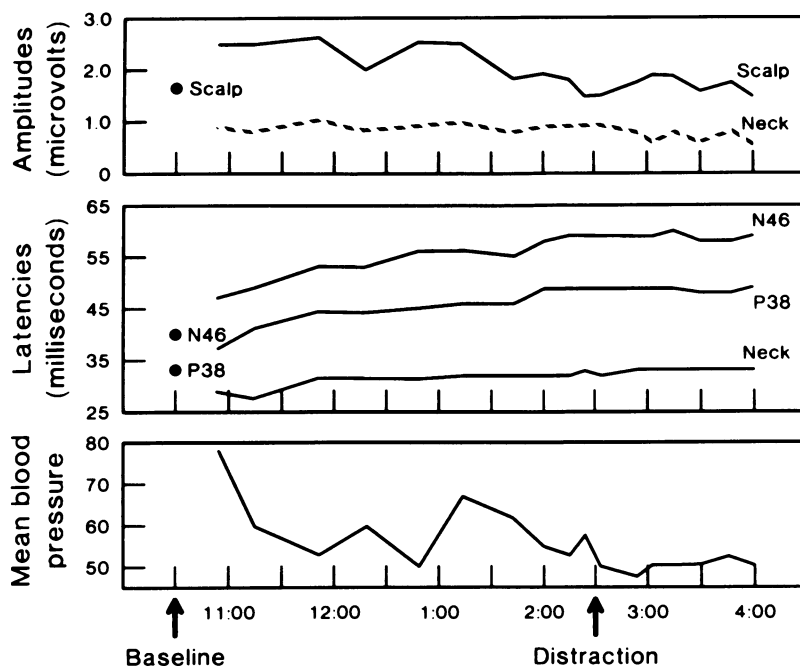
The response to different anesthetics is not consistent, but halothane most consistently reduces or abolishes the scalp recorded SEP. For both enflurane and isoflurane slightly more than half the patients have a reduction in evoked SEP, and a small number have an enhanced response immediately after anesthesia induction. Alterations in blood pressure can also reduce the amplitude of the evoked response, especially with mean blood pressures under 70 mm Hg.

### Extra-operative recordings

Recordings outside the operating field are by far the simplest to make, and can be performed without the direct assistance of the surgeon, leaving him free for the surgical procedure. Stimulation is applied to a peripheral nerve, usually either the peroneal or tibial in the leg, or the median or ulnar in the arm. Recordings are most commonly made from standard scalp derivations, usually CZ-FZ with leg stimulation, and C3' (C4')-FZ with arm stimulation. Other



**Figure 10-10.** Somatosensory evoked potentials monitored during cervical fusion for rheumatoid arthritis were reduced by anesthesia before surgical manipulation, and returned with reduction of the level of anesthesia.



**Figure 10-11.** Plot of the amplitudes and latencies of neck and scalp SEP during thoracic spine surgery for scoliosis. There is a gradual reduction in scalp amplitude and increase in latency before spine distraction. Note the increase in N20 amplitude immediately after induction of anesthesia.

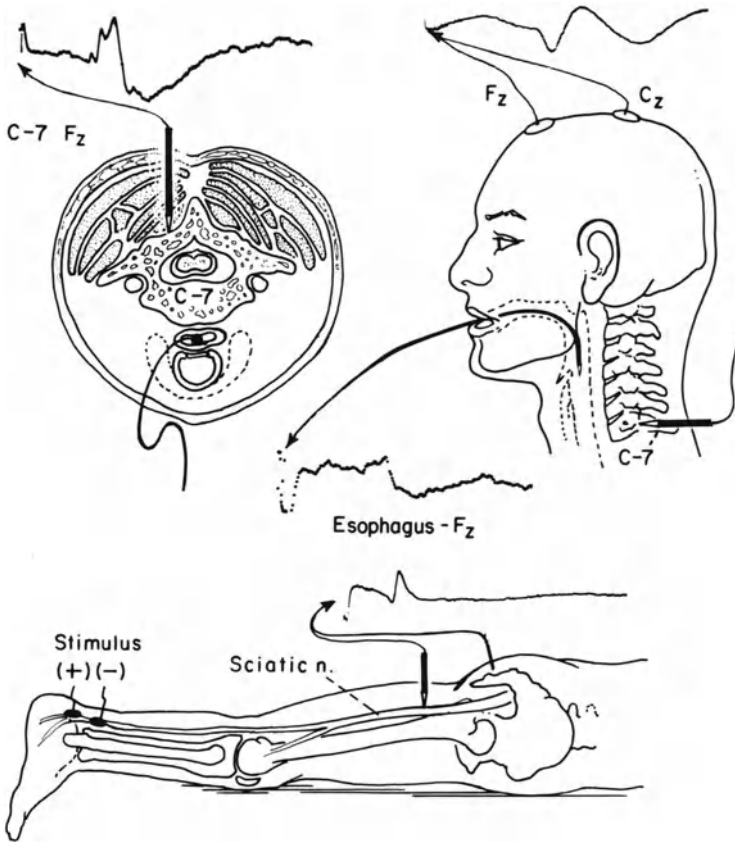
reference electrodes, such as the ears, are also used. Recordings can also be made over the spine and over peripheral nerves. Most of the early studies of surgical monitoring used peripheral stimulation with scalp recording, which generally gives a well-defined although unstable response. They may also be altered by blood pressure and anesthetic. Similar techniques can be used to monitor cord function during an embolectomy [3].

The following procedures have proven successful on over 400 patients with a variety of surgical problems, by a number of different surgeons. These simplified, reliable methods can be performed by technicians for either upper or lower spine surgery.

### Thoracic or lumbar surgery

Supramaximal surface stimulation is applied to each peroneal nerve at the knee and/or each tibial nerve at the ankle sequentially, continuously. Simultaneous bilateral stimulation of either peroneal or tibial nerves is applied if response to unilateral stimulation is too low to record reliably. Stimulation is begun at 3 Hz and reduced if response amplitude can be enhanced at lower rates.

Recordings are made at three levels (figure 10-12): 1) peripheral electrodes



**Figure 10-12.** Extraoperative recording of tibial SEP for monitoring thoraco-lumbar spine surgery. Simultaneous recording electrodes include:

- A) Needle near sciatic nerve at gluteal fold referenced to hip.
- B) Needle at C7 spine referenced to FZ or esophageal electrode at C3 referenced to FZ.
- C) Scalp discs, CZ-FZ.

record either over the cauda equina, near the sciatic nerve, or from peripheral muscles. These provide a peripheral monitor of the adequacy of stimulation. 2) A needle electrode in the cervical paraspinal muscles at C7 referenced to the shoulder or FZ on the scalp, records the cervical spinal cord potential. Both the leg and cervical recording electrodes are taped firmly in place with multiple wire loops to prevent dislodging. An electrode in the esophagus referenced to FZ can sometimes be used if surgery precludes a posterior recording. 3) A scalp recording from CZ to FZ utilizes collodion applied, surface electrodes that will remain firmly in place for many hours despite manipulation of the head and neck during anesthesia.

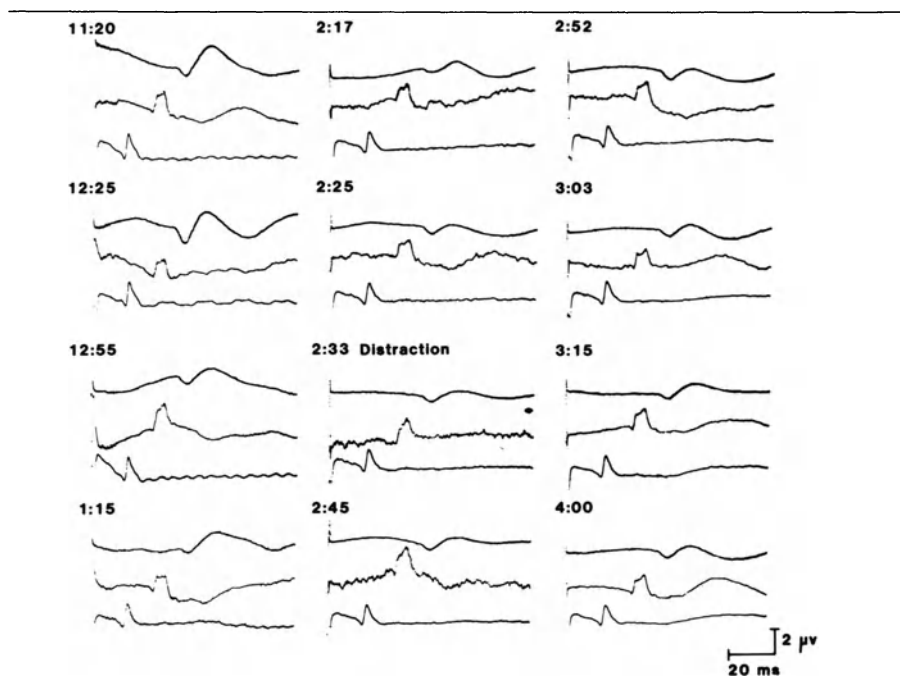
Filter settings are selected to enhance evoked response while reducing artifact. Low frequency settings of 32 (or 100) Hz and high frequency settings of 1600 Hz generally result in the most consistent recordings. Recordings are made sequentially before and during surgery (figure 10-13).

### Cervical surgery

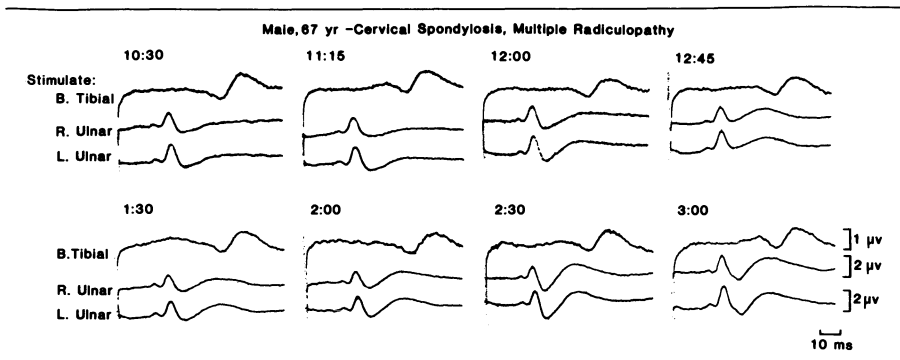
Stimulation is applied to the ulnar nerves on each side recording from an esophageal electrode referred to Fz, and from C3' (or C4') to FZ locations on the scalp. Stimulation is also applied serially to the tibial nerves at the ankles while recording from the esophageal and scalp electrodes (figure 10-14). Peripheral monitors of foot muscles or sciatic nerve, and ulnar hand muscles or ulnar nerve, are also recorded. Stimulation and recording parameters are similar to those for lower spine surgery.

### Applicants

Patients undergoing procedures are best selected for monitoring by surgeons on the basis of risk of neural damage. The ages range from 2 to 83 years and include many patients under age 15. The largest group of patients are teenagers



**Figure 10-13.** Sequential tibial SEP recorded at the sciatic nerve, cervical spine and scalp during scoliosis surgery in a 16-year-old girl. No SEP or clinical changes occurred after distraction.



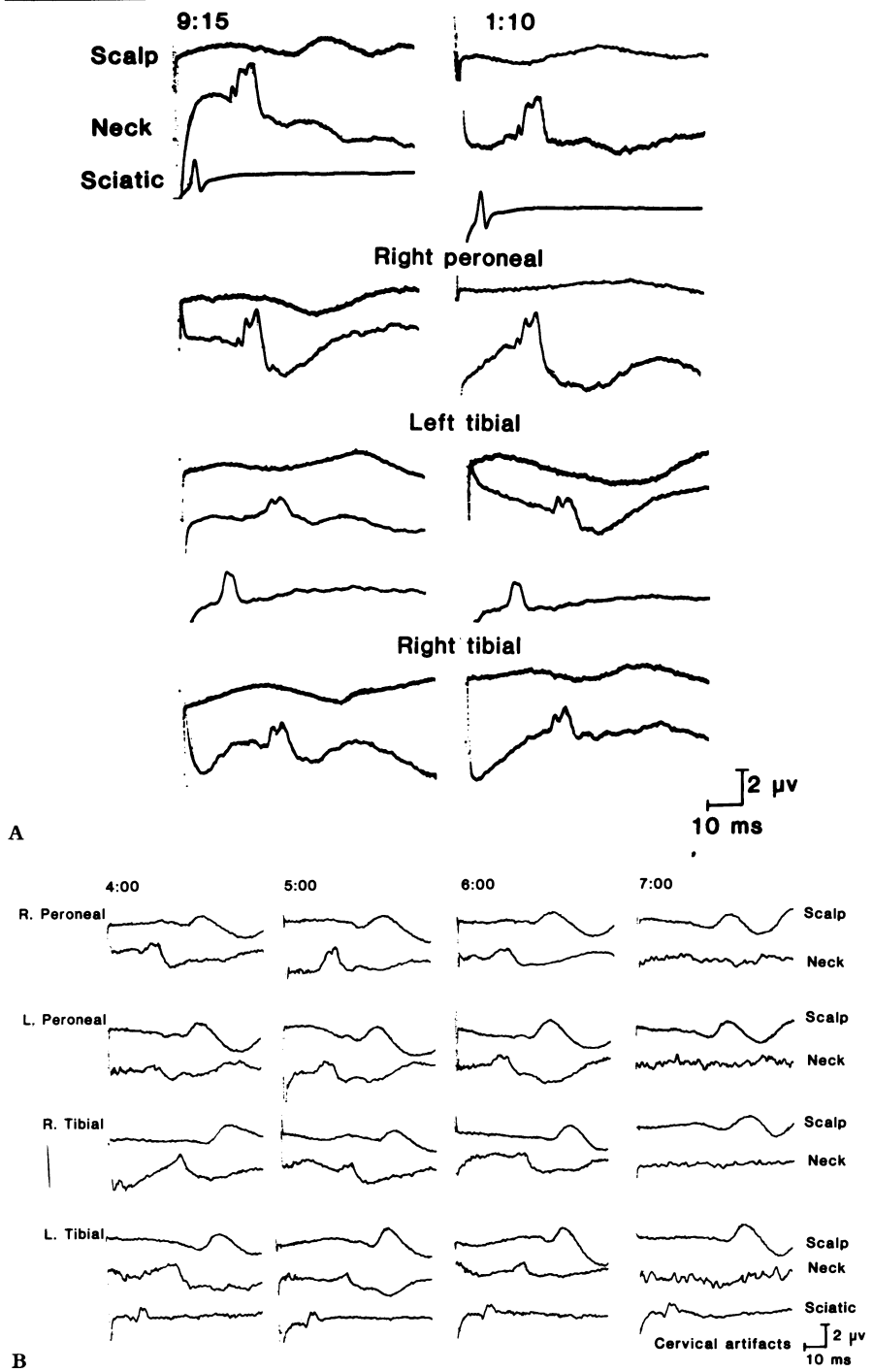
**Figure 10-14.** SEP monitoring at neck (esophageal to FZ) and scalp electrodes (CZ-FZ and C4-FZ) with tibial and ulnar stimulation during surgery for cervical spondylosis.

undergoing corrective surgery for scoliosis. Another large group are elderly individuals undergoing surgery for cervical spondylosis. Patients with bony spine tumors, thoracic aneurysm surgery [25, 35], traumatic spine damage, and spondylitis can also be monitored. Two-thirds of the surgical procedures are at the thoracic level.

A frequent problem during surgical monitoring is the variability of the evoked response from run to run because of artifact, blood pressure changes, anesthetic level, and other factors. Identification of a significant change in SEP therefore requires a consistent alteration in latency (2.0 msec more than baseline changes) and amplitude (50% less than baseline values) at both the neck and scalp sites with an intact peripheral response. This change must be shown not to be due to technical factors and greater than the baseline variation during the initial periods of the surgery. In a few patients recordings are only obtainable at one of the two cephalad sites, usually the neck (figure 10-15). In those cases changes need to be seen with stimulation of more than one nerve to be considered significant. No absolute change in amplitude can be considered evidence of spinal cord damage since in some cases without damage a scalp response appears to be lost transiently while other responses are intact. In other cases where damage was occurring, smaller but consistent alteration at two sites of stimulation showed evidence of compression before the major changes occurred.

SEP monitoring of spine surgery is sometimes frustrated by the inability to record reliable potentials over the scalp in patients both with the without preoperative neurological deficit. Intraoperative monitoring was requested on 379 patients undergoing spine surgery at Mayo over three years. Twenty-eight patients with neurological deficit could not be monitored because of inability to record responses over the spine or scalp. SEP monitoring was performed on 351 patients undergoing spine surgery using multichannel recording during individual stimulation of tibial and peroneal nerves.

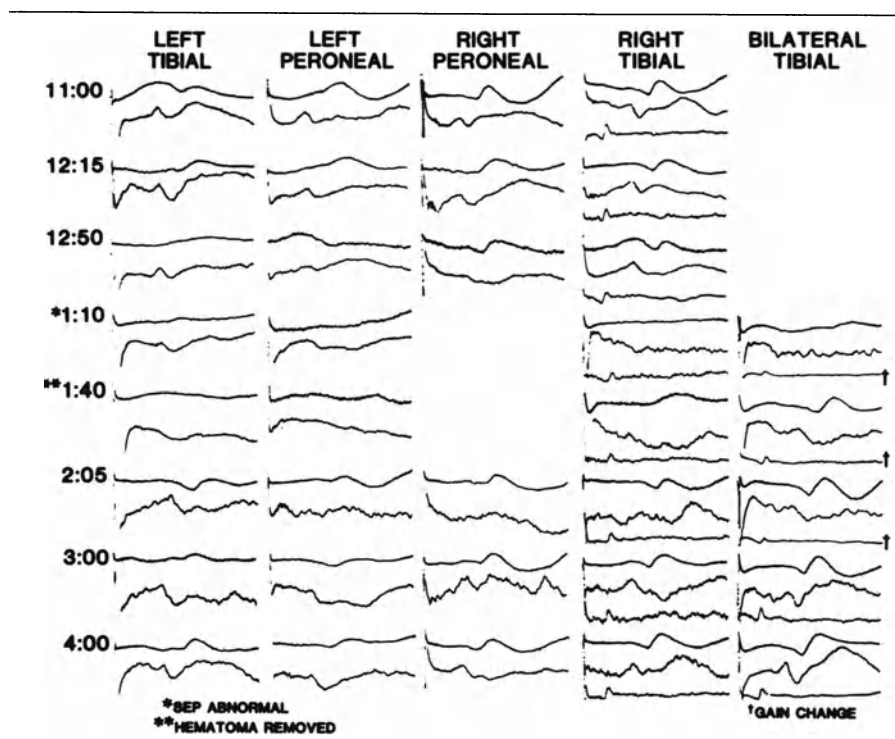




**Figure 10-15. A)** Excellent cervical potentials remain present when scalp responses are lost from anesthesia in a healthy 16-year-old girl undergoing fusion for idiopathic scoliosis. **B)** Cervical potentials become unrecordable at the neck because of excessive muscle activity as a 32-year-old man is awakening from fusion of a L2 spine fracture.

In 24 patients with intact preanesthetic SEPs, the scalp potential either could not be recorded immediately after anesthesia, or was lost within an hour of anesthesia, while well-defined neck potentials could still be recorded. In 17 patients neck potentials could not be recorded for technical reasons while scalp potentials were still obtained. In three patients scalp and neck potentials were lost in association with a loss of the sciatic potentials due to a peripheral stimulation failure. The addition of a cervical spine and peripheral recording location to the usual scalp recording enabled reliable monitoring to be performed on more patients.

SEP monitoring during spine surgery has proven of value in warning surgeons of potential damage to the spinal cord. Since such damage is an uncommon event, few patients are available to define the change in SEP with cord damage. In the surgical monitoring of spinal cord sensory pathways of the 351 patients undergoing spine surgery over three years, six had significant changes in SEP identified during surgery. Three were reversed surgically (removal of hematoma, removal of rods, and removal of spine wires) (figure 10-16 and

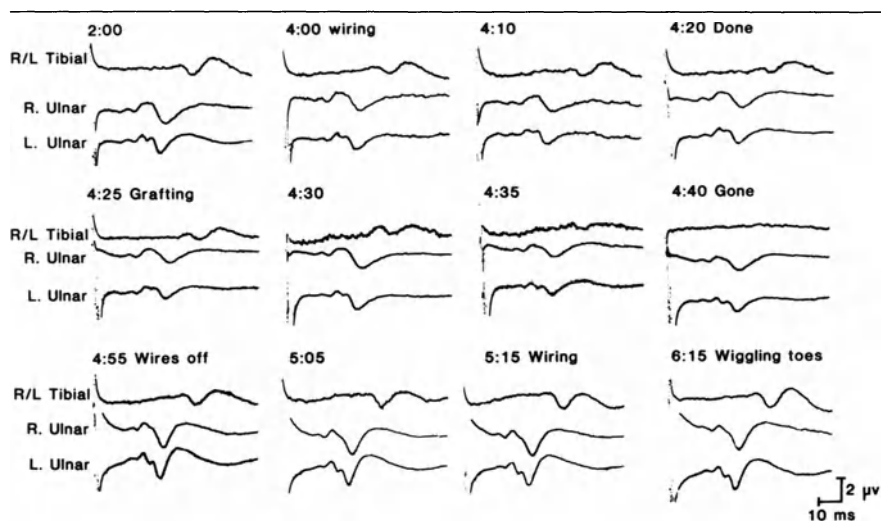


**Figure 10-16.** SEP monitoring during thoraco-lumbar spine surgery for severe spondylitis showed gradual loss of SEP, which returned shortly after laminectomy and removal of an intraspinal hematoma. No postoperative neurologic deficit.

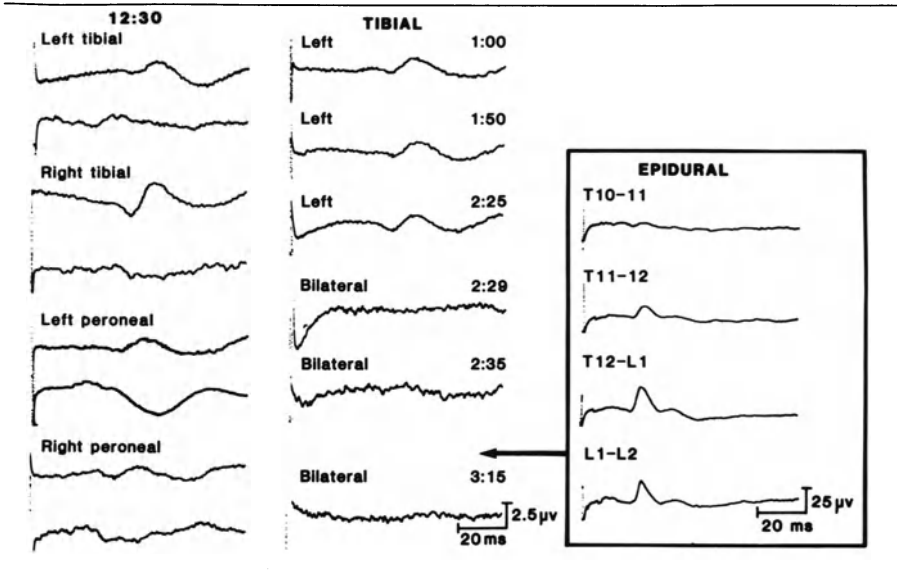
10-17) with no subsequent clinical deficit. One patient developed permanent postoperative deficit despite removal of rods. A tibial SEP that decreased after cord biopsy and a peroneal SEP that fell without apparent cause both recovered within 15 minutes during surgery. The former left no deficit, the latter an L5 radiculopathy. Two other patients had postoperative deficits of anterior spinal artery syndrome not manifest on SEP. Eight patients had evidence of new lumbar radiculopathy after surgery, only one of whom had the SEP change noted above. SEP changes were similar in most patients. The amplitude reduction began 10–30 minutes after cord injury. Amplitude decreased gradually over 10–15 minutes at neck and scalp with an increase in latency of up to three msec. In each of the three cases where surgical action corrected the SEP loss, the SEP recovered to baseline value within 5–10 minutes. While over 1,000 patients would need to be tested to show a statistically significant change in frequency of complication, these three out of over 300 cases illustrate the value and cost benefit. In one patient the SEP was lost abruptly with direct trauma to the cord and no recovery of function (figure 10-18). A few patients show an improvement in SEP during surgery (figure 10-19).

### Intra-operative recordings

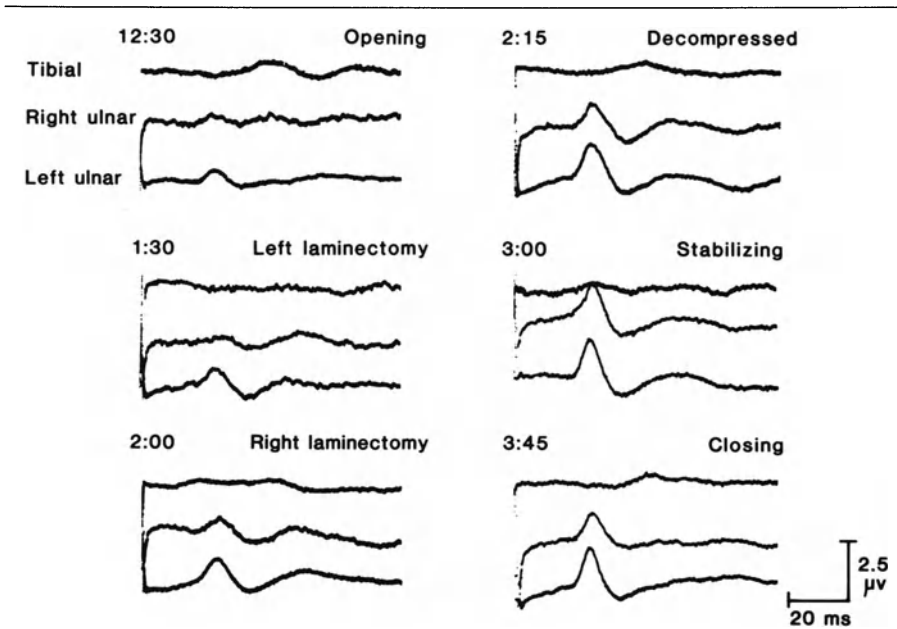
A number of methods of recording in the operating field have been developed to allow recording closer to the neural tissue. These methods include sub-



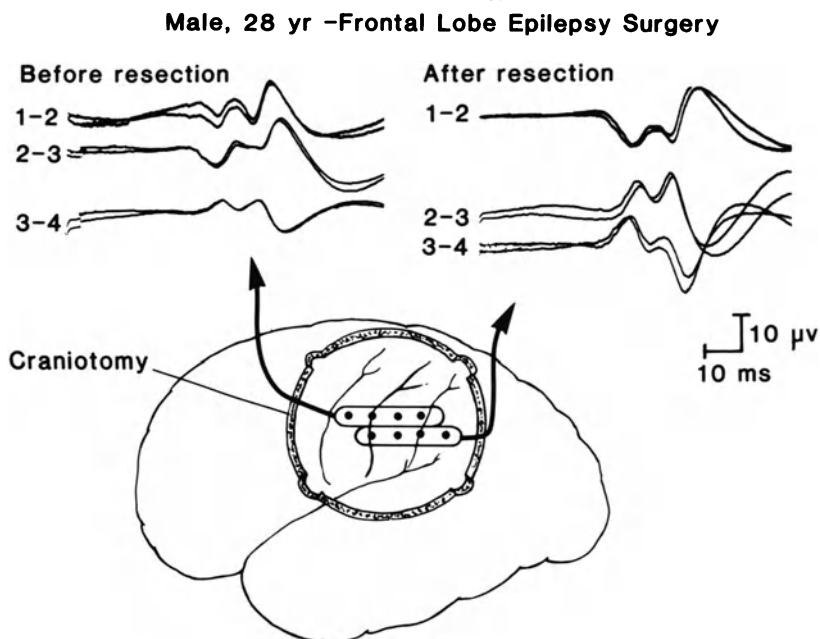
**Figure 10-17.** SEP monitoring during cervical spine surgery for an unstable C-6 fracture showed gradual loss of SEP which rapidly returned with removal of wires. There was no change in anesthetic level during this period. No postoperative neurologic deficit.



**Figure 10-18.** SEP monitoring of rod placement and fusion after resection of a spine tumor showed an abrupt loss of SEP with no return. Direct recording from the dura demonstrated a localized area of SEP loss. Postoperative paraplegia.



**Figure 10-19.** Gradual improvement of SEP during upper cervical cord decompression for rheumatoid arthritis. Postoperative clinical and SEP improvement as well.

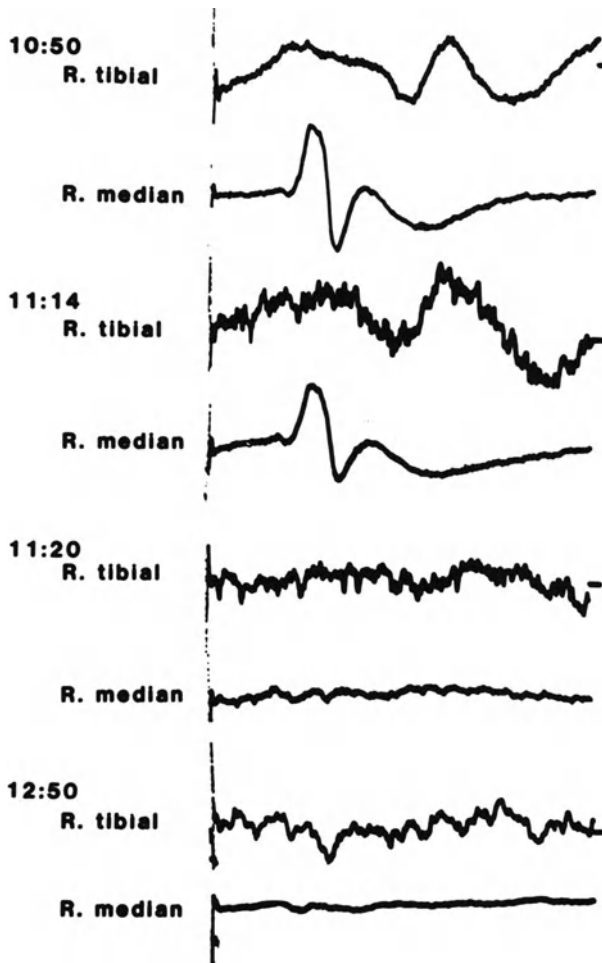


**Figure 10-20.** SEP recorded directly from the cortex before and after resection of a frontal cortex focus for epilepsy.

arachnoid, epidural, spinous process and intraspinal ligament recordings [7]. Lueders [30] used needle electrodes placed between the spinous processes just epidural to obtain much higher amplitude processes. Jones et al. [20, 21] have used epidural electrodes that are inserted between the spine and dural sac to give large, readily recorded potentials. Similar recordings have been made of descending activity with direct spinal cord stimulation and recording by Tamaka [51].

While recordings in the surgical field can give much larger responses, they are associated with the technical problems of the surgical procedure, adding to the surgical risk of infection, subjection to mechanical artifact, or by being limited to those surgical procedures in which the spine is opened to expose the dura. Such recordings also generally require much technical expertise for satisfactory recordings, and require that the surgeon be familiar and cooperative with the procedure. Recordings in the surgical field are most useful for spinal cord surgery, such as tumors or arteriovenous malformation where the directly recorded potential can localize the area of damage, or record responses too small to record with other methods. Small cotton wick electrodes work well.

SEP monitor only the sensory pathways, and have been applied with a variety of techniques. As such, patients can develop motor deficits without a

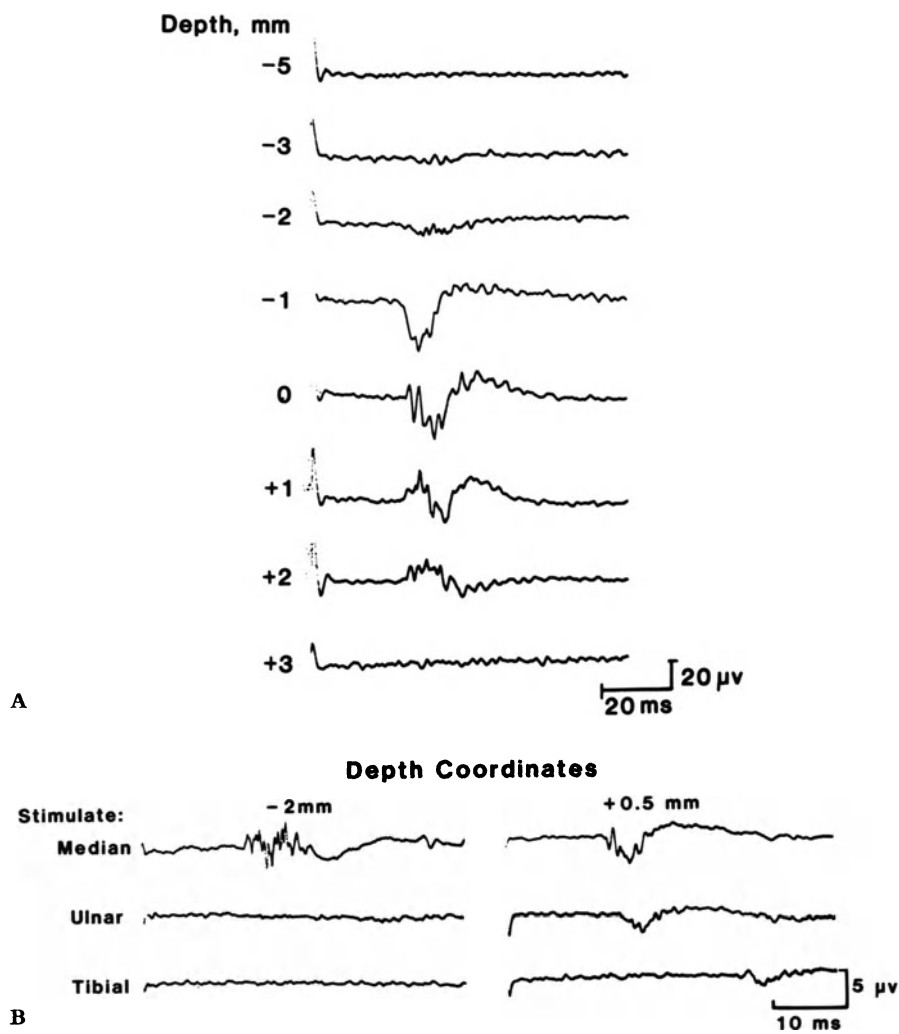


**Figure 10-21.** Abrupt, irreversible loss of tibial and median SEP at the scalp with coagulation of bleeding vessel during stereotaxic laser surgery for tumor. Patient awoke with hemiparesis and hemisensory loss.

change in SEP [27]. These are most likely due to ischemia of the anterior cord, and are often associated with lower motor neuron signs. In summary, spinal cord damage during surgery can result in either gradual loss of SEP some time after the surgical manipulation, which can still be reversed without deficit, or an abrupt irreversible loss.

#### **Motor evoked potentials (MEP)**

Recent studies have employed monitoring of descending activity by stimulation of the motor cortex through the skull while monitoring spinal cord



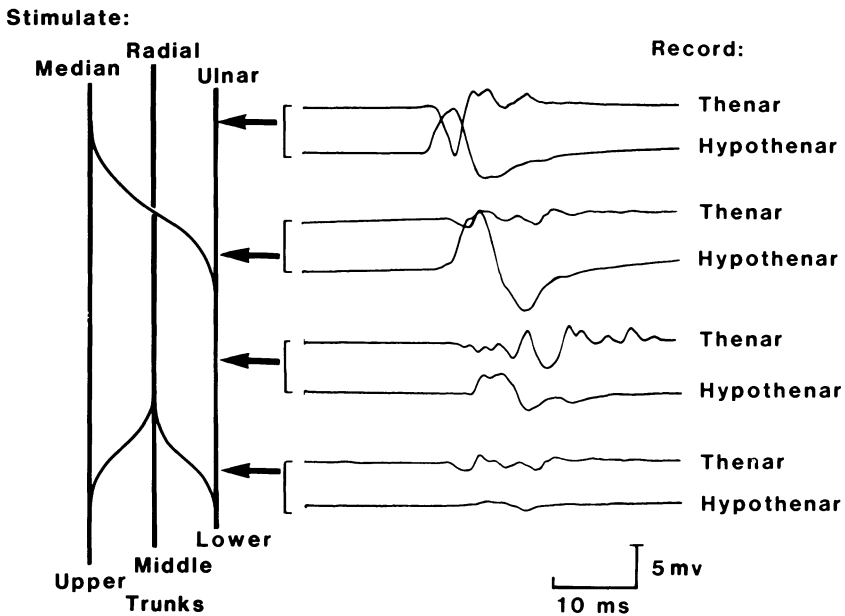
**Figure 10-22. A)** Median SEP recorded in one mm steps in the thalamus with a microelectrode prior to thalamotomy for Parkinson's disease. Note the phase reversal at +1. **B)** Responses are specific to stimulation of one nerve or digit within the thalamus (-2 mm), but can be recorded with stimulation of any nerve in the sensory pathway beneath the thalamus (+0.5 mm).

or peripheral motor responses [29, 34]. The method is too new to be fully assessed. Peripheral recording cannot be used reliably in a patient who has been paralyzed with neuromuscular blocking agents, since the motor activity in peripheral nerve may be below the resolution of standard recording methods. One recent report of motor evoked potentials (MEP) in 11 patients undergoing spine surgery suggests that MEP may become of major value in

monitoring motor pathways [5]. Responses could be recorded directly from the spinal cord with high voltage scalp stimulation throughout the procedures. Monitoring of either ascending or descending motor activity in the spinal cord results in relatively low amplitude evoked potentials that may be difficult to record, if the patient has pre-existent neurological damage.

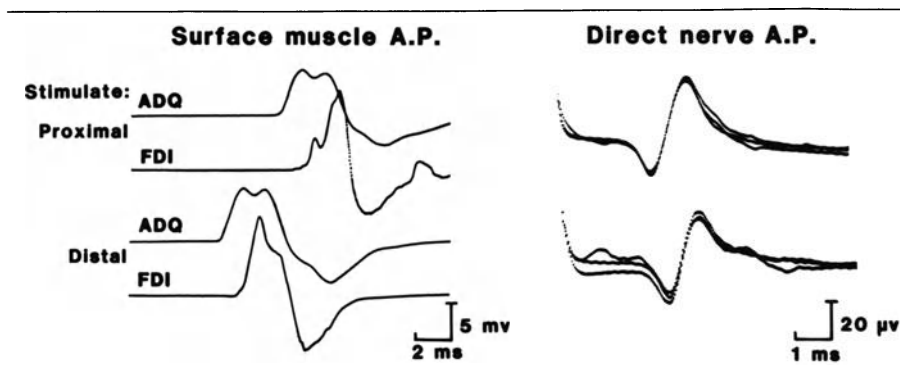
**CEREBRAL FUNCTION MONITORING**

Somatosensory evoked potentials have also proven useful in monitoring a variety of other cranial surgical procedures. Direct recording of SEP from the cortex prior to cortical resection for epilepsy can help the surgeon identify the sensory and motor strips with more certainty (figure 10-20). During deep, stereotatic surgery for tumors, or hippocampectomy for epilepsy, the scalp-recorded SEP can help identify both damage to sensory pathways (figure 10-21), and in a few cases, improvement in sensory pathway function (figure 10-19). While some reports have described value of SEP with carotid endarterectomy and aneurysm surgery [33, 50, 52], simultaneous recordings of SEP and EEG on a group of patients at Mayo showed no advantage for SEP. Currently only EEG monitoring is used. The methods of recording SEP to



**Figure 10-23** Localization of conduction block in brachial plexus along the medial cord with stimulation along its length. Note the progressive amplitude drop and dispersion with more proximal stimulation (lower traces).





**Figure 10-24.** Monitoring ulnar nerve during decompression and transposition with CMAP (left) and NAP (right) recording. Latency changes localized the abnormality at the medial epicondyle.

monitor cerebral function and the associated technical problems are similar to those described for monitoring SEP for spine surgery.

Direct recording of the SEP in deep structures has also proven of help in making deep, therapeutic lesions. Localization of the electrode for thalamotomy for Parkinsonism and other movement disorders has been facilitated by direct recordings from the thalamus (figure 10-22). Lesions in the dentate nucleus for spasticity have been guided successfully by SEP recordings in the dentate.

### PERIPHERAL MONITORING

Electrical monitoring during surgery on both the plexus and peripheral nerve has proven of help to surgeons [32]. When putting in grafts to permit regeneration of a severely damaged nerve, as in severe brachial plexopathy, SEP recorded at the neck and scalp can help to identify intact roots and trunks when all peripheral function has been lost [48].

When peripheral function is still intact, EMG and CMAP monitoring, as described for cranial nerve monitoring, can be used to identify the location of a nerve in a tumor (figure 10-23), to identify the site of a lesion along the length of nerve, and of most direct, immediate interest to the surgeon, to identify the occurrence of nerve irritation or damage (EMG neurotonic discharge) when attempting to remove local tumor.

Peripheral nerve action potentials can also be monitored directly from the nerve with hook electrodes along the length of the nerve, which can both stimulate and record to precisely locate an area of damage (figure 10-24) [24].

### SUMMARY

A multiplicity of electrophysiologic monitoring methods are available to assist the surgeon in operating on a patient in whom there is a risk of damage to

neural structures. The applications and problems of each method must be considered in selecting the monitoring technique for each individual patient.

## REFERENCES

1. Allen A, Starr A and Nudleman K: Assessment of sensory function in the operating room utilizing cerebral evoked potentials: A study of fifty-six surgically anesthetized patients. *Clin Neurosurg* 28:457-481, 1981.
2. Bennett M: Effects of compression and ischemia on spinal cord evoked potentials. *Exp Neurol* 80:508-519, 1983.
3. Berenstein Young W, Ransohoff J et al.: Somatosensory evoked potentials during spinal angiography and therapeutic transvascular embolization. *J Neurosurg* 60:777-785, 1984.
4. Boston JR: Algorithm for monitoring sensory evoked potentials. *J Clin Monitoring* 1:201-206, 1985.
5. Boyd SG et al.: Method of monitoring function in corticospinal pathways during scoliosis surgery. *J Neurol Neurosurg Psychiat* 49:251-257, 1986.
6. Delgado TE, Buchheit WA, Rosenholtz HR et al.: Intraoperative monitoring of facial muscle evoked responses obtained by intracranial stimulation of the facial nerve. *Neurosurg* 418-420, 1979.
7. Dinner D, Lueders H, Lesser R and Morris R: Invasive methods of somatosensory evoked potential monitoring. *J Clin Neurophysiol* 3:113-130, 1986.
8. Engler G et al.: SEP monitoring during Harrington instrumentation for scoliosis. *J Bone Joint Surg* 60-A:528-532, 1978.
9. Erickson DL, Ausman JI and Chou S: Prognosis of seventh nerve palsy following removal of large acoustic tumors. *J Neurosurg* 47:3134, 1977.
10. Friedman WA, Kaplan BJ, Gravenstein D and Rhoton Jr, AL: Intraoperative brain-stem auditory evoked potentials during posterior fossa microvascular decompression. *J Neurosurg* 62:552-557, 1985.
11. Grundy BL, Jannetta PJ, Lina A, Procopio P, Boston JR and Doyle E: Intraoperative monitoring of brainstem auditory evoked potentials. *J Neurosurg* 57:674-677, 1981.
12. Grundy B et al.: Intraoperative loss of somatosensory evoked potentials loss of spinal cord function. *Anesth* 57:321, 1982.
13. Hall J et al.: Intraoperative awakening to monitor spinal cord function. *J Bone Joint Surg* 60-A:533-536, 1978.
14. Harner S, Daube JR, Ebersold M: Electrophysiologic monitoring of neural function during acoustic neurinoma surgery. (submitted)
15. Harner S and Laws E: Posterior fossa approach for removal of acoustic neurinomas. *Arch Otolaryngol* 107:509-593, 1981.
16. Harner S and Laws E: Diagnosis of acoustic neurinoma. *Neurosurg* 9:373-379, 1981.
17. Harner S and Laws E: Clinical findings in patients with acoustic neurinoma. *Mayo Clin Proc* 58:721-728, 1983.
18. Harner S, Daube JR and Ebersold M: Electrophysiologic monitoring during temporal bone surgery. *Laryngoscope* 96:65-69, 1986.
19. House WF and Luetje CM (eds): *Acoustic Tumors*. Baltimore, University Park Press, 1979.
20. Jones et al.: Sensory nerve conduction in human spinal cord. *J Neurol Neurosurg Psychiat* 45:446-451, 1982.
21. Jones SJ, Carter L et al.: Experience of epidural spinal cord monitoring in 410 cases. In: J Schramm and S Jones (eds): *Spinal Cord Monitoring*. Springer, Berlin, 1985.
22. Kimura J: *Electrodiagnosis in Diseases of Nerve and Muscle*. FA Davis, 1983.
23. Kimura J and Lyon L: Alteration of orbicularis oculi reflex by posterior fossa tumors. *J Neurosurg* 38:10, 1973.
24. Kline DG, Hackett ER and Happel LH: Surgery for lesions of the brachial plexus. *Arch Neurol*, 43:170-181, 1986.
25. Laschinger JC, Cunningham Jr, JN, Isom W et al.: Definition of the safe lower limits of aortic resection during surgical procedures on the thoracoabdominal aorta: Use of somatosensory evoked potentials. *JACC* 2:959-965, 1983.
26. Lesser RP, Lueders H, Dinner DS et al.: Technical aspects of surgical monitoring using evoked potentials. In: A Struppler and A Weindel: *Electromyography and Evoked Potentials*.

- Springer-Verlag, 1985, 177–180.
27. Lesser RP et al.: Postoperative neurological deficits may occur despite unchanged intraoperative SEP. *Ann Neurol* 19:22–25, 1986.
  28. Levine RA, Ojemann RG, Montgomery WW and McGaffigan PM: Monitoring auditory evoked potentials during acoustic neuroma surgery: Insights into the mechanism of the hearing loss. *Ann Otol Rhinol Laryngol* 93:116–123, 1984.
  29. Levy WJ, York DH, McCaffrey M and Tanzer F: Motor evoked potentials from transcranial stimulation of the motor cortex in humans. *Neurosurg* 15:287–302, 1984.
  30. Lueders H et al.: New techniques for intraoperative monitoring of spinal cord function. *Spine* 7:110–115, 1982.
  31. Macon J and Poletti: Conducted SEP during surgery. *J Neurosurg*, 57:349–359, 1982.
  32. Mahla ME, Long DM, McKennett J et al.: Detection of brachial plexus dysfunction by somatosensory evoked potential monitoring—A report of two cases. *Anesthesiol* 60:248–252, 1984.
  33. McPherson RW, Niedermeyer EF, Otenasek RJ and Hanley DF: Correlation of transient neurological deficit and somatosensory evoked potentials after intracranial aneurysm surgery. *J Neurosurg* 59:146–149, 1983.
  34. Mills KR and Murray NM: Corticospinal tract conduction time in multiple sclerosis. *Ann Neurol* 18:601–605, 1985.
  35. Mizrahi EM and Crawford ES: Somatosensory evoked potentials during reversible spinal cord ischemia in man. *EEG Clin Neurophysiol* 58:120–126, 1984.
  36. Moller AR and Jannetta PJ: Monitoring auditory functions during cranial nerve microvascular decompression by direct recording from the eighth nerve. *J Neurosurg* 59:493–499, 1983.
  37. Moller AR and Jannetta PJ: Preservation of facial function during removal of acoustic neuromas. Use of monopolar constant-voltage stimulation and EMG. *J Neurosurg* 61:757–760, 1984.
  38. Moller AR and Jannetta PJ: Microvascular decompression in hemifacial spasm. *Neurosurg* 16:612–618, 1985.
  39. Nash et al.: Spinal cord monitoring during operative treatment of the spine. *Clin Orthoped* 126:100–105, 1977.
  40. Ojemann RG, Levine RA, Montgomery WM and McGaffigan BA: Use of intraoperative auditory evoked potentials to preserve hearing in unilateral acoustic neuroma removal. *J Neurosurg* 61:938–948, 1984.
  41. Piatt Jr JH, Radtke RA and Erwin CW: Limitations of brain stem auditory evoked potentials for intraoperative monitoring during a posterior fossa operation: Case report and technical note. *Neurosurg* 16:818–821, 1985.
  42. Raman RT, Reddy and Rao SV: Orbicularis oculi reflex and facial muscle electromyography. *J Neurosurg* 44:550–555, 1976.
  43. Raudzens PA and Shetter AG: Intraoperative monitoring of brain-stem auditory evoked potentials. *J Neurosurg* 57:341–348, 1982.
  44. Raudzens P: Intraoperative SEPs. *Anesth* 58:593–594, 1983.
  45. Rhoton Jr, AL: Microsurgical removal of acoustic neuromas. *Surg Neurol* 6:211–219, 1976.
  46. Rossi B, Buonaguidi A and Tusini G: Blink reflexes in posterior fossa lesions. *J Neurol Neurosurg Psychiatr* 42:465–469, 1979.
  47. Sgro JA, Emerson RG and pedley TA: Real-time reconstruction of evoked potentials using two-dimensional filter. *EEG Clin Neurophysiol* 62–372–380, 1985.
  48. Sugioka H: Evoked potentials in the investigation of traumatic lesions of the peripheral nerve and the brachial plexus. *Clin Orthoped Rel Res* 184:85–92, 1984.
  49. Sugita K, Kobayashi S, Matsuga N and Suzuki Y: Microsurgery for acoustic neurinoma—lateral position and preservation of facial and cochlear nerves. *Neurol Med Chir (Tokyo)* 19:637–641, 1979.
  50. Symon L, Wang AD, Costa e Silva IE and Gentili F: Perioperative use of somatosensory evoked responses in aneurysm surgery. *J Neurosurg* 60:269–275, 1984.
  51. Tamaka T et al.: Prevention of iatrogenic spinal cord injury utilizing evoked spinal cord potential. *Int Orthoped* 4:313–317, 1981.
  52. Wang AD, Cone J, Symon L and Costa e Silva IE: Somatosensory evoked potential monitoring during the management of aneurysmal SAH. *J Neurosurg* 60:264–268, 1984.
  53. Worth R et al.: Intraoperative SEP monitoring during spinal cord surgery. In: J Courgon (ed): *Clinical Applications of Evoked Potentials in Neurology*. Raven Press, 367–373, 1982.

---

## INDEX

- Acoustic nerve
  - conduction velocity of, 116
  - posterior fossa tumor surgery and, 243–244
- Acoustic neuroma
  - auditory evoked potentials (AEPs) of, 147–148, 212
  - posterior fossa tumor surgery and, 243–244
  - surgical monitoring of, 32
- Action potentials (APs), 105–106
- Adrenoleucodystrophy, 208
- AEPs, *see* Auditory evoked potentials (AEPs)
- Age, evoked potentials (EPs) effects of, 48
- Amblyopia exanopsia, 143
- Amplitude, far-field evoked potentials
  - latency comparisons, 17–21, 23
- Amyotrophic lateral sclerosis (ALS),
  - with brainstem auditory evoked potentials (BAEPs), 171
- Anoxia, evoked potentials (EPs) effects of, 48–50
- Anteroventral (AV) nucleus, 110
- Antidromic study
  - of median nerve, 10–12, 23
  - of radial nerve, 12–17
- Astrocytoma, somatosensory evoked potentials (SEPs) of, 51
- Auditory brainstem response (ABR), 223
  - brain death and, 237–238
  - comparison of other evoked potential (EP) measures in, 234–237
  - head trauma and, 228–230
  - non-traumatic causes of coma and, 230
  - somatosensory evoked potentials (SEPs) with, 233–234
  - surgical monitoring with, 241, 242
  - visual evoked potentials (VEPs) with, 231–232
- Auditory evoked potentials (AEPs), 210–217
  - acoustic nerve and, 243–244
  - amplitude differences in, 183–184
  - clinical use of, 145–146, 148–149
  - coma and, 156–157, 228–231, 233–234
  - comparison of other evoked potential (EP) measures in, 234–237

- hemipheric lesions with, 211–217
- normal late components of, 210
- surgical monitoring with, 154–156, 243–244
- see also* Short-latency auditory evoked potentials (SAEPs)
- Averaging
  - short-latency auditory evoked potentials (SAEPs) with, 126
  - somatosensory evoked potentials (SEPs) with, 70–71
- Benzodiazepines, with somatosensory evoked potentials (SEPs), 205
- Binaural interaction component (BIC), in short-latency auditory evoked potentials (SAEPs), 130–131
- Bipolar cells of retina, 88–89
- Blindness
  - auditory evoked potentials (AEPs) with, 216–217
  - pattern evoked potentials (PEPs) with, 146–147, 209–210
- Brachial plexus injury, 195–196
- Brain death, and somatosensory evoked potentials (SEPs), 237–238
- Brainstem
  - auditory evoked potentials (AEPs) of, 148, 154–157
  - posterior fossa tumor and, 243
  - short-latency auditory evoked potentials (SAEPs) and, 122, 132
  - somatosensory evoked potentials (SEPs) and, 80–82, 197–205
- Brainstem auditory evoked potentials (BAEPs), 210
  - multiple sclerosis (MS) and, 167–171, 174
  - time analysis with, 186–190
- Brainstem auditory responses, 68
- Bushy cells, 110
- Central auditory system, anatomy of, 109–115
- Central conduction time, estimation methods for, 82–84
- Cerebellar ataxia, hereditary, 194
- Cerebello-pontine angle (CPA) tumor, surgical monitoring of, 32
- Cervical surgical monitoring, 257
- Characteristic frequency (CF), 107–109
- Charcot-Marie-Tooth disease, 208
- Chiasma disorders, 143–144
- Cochlea, anatomy of, 106–107
- Cochlear microphonic potentials (CM), 107
- Cochlear nerve
  - action potentials (APs) of, 115
  - anatomy of, 107–109
  - conduction velocity of, 116
- Cochlear nucleus (CN)
  - anatomy of, 110–111
  - evoked potential (EP) recordings of, 117
  - frequency-following response (FFR) of, 133
- Coma, 223–239
  - auditory evoked potentials (AEPs) in, 156–157, 228–231, 233–234
  - clinical issues in, 226–227
  - comparison of evoked potential (EP) measures in, 234–237
  - non-traumatic causes of, 230
  - outcome scales in, 227–228
  - prediction of outcome from, 236–237
  - somatosensory evoked potentials (SEPs) in, 157, 226, 232–234
  - visual evoked potential (VEP) in, 224–226, 231–232, 233
- Complex partial seizures, 53–54
- Compound muscle action potentials (CMAP), 241, 242, 246, 267
- Computerized axial tomography (CAT, CT), 158
  - auditory evoked potentials (AEPs) and, 215
  - multiple sclerosis (MS) on, 175
  - posttraumatic epilepsy on, 53
- Conduction velocity (CV)
  - afferent volley measurement of, 32–34
  - cochlear nerve, 116
  - dorsal column propagated volley with, 72–79
  - subcortical somatosensory evoked potentials (SEPs) with, 73
- Constant current stimulation, 69
- Contrast, in visual evoked potentials (VEPs), 97
- Cortical blindness
  - auditory evoked potentials (AEPs)

- with, 216–217
- pattern evoked potentials (PEPs) with, 146–147, 20–210
- Corticospinal lesions, somatosensory evoked potentials (SEPs) of, 30–32
- Dementia, with auditory evoked potentials (AEPs), 210
- Demyelinating disease, and evoked potentials (EPs), 161–162, 181–184
- Diazepam, with somatosensory evoked potentials (SEPs), 205
- Dorsomedial (DM) nucleus, 113
- Drugs, evoked potentials (EPs) effects of, 50
- Electrocardiography (EKG), somatosensory evoked potentials (SEPs) interference from, 70, 71
- Electroencephalography (EEG), 68, 241, 242, 266
- Electromyography (EMG) somatosensory evoked potentials (SEPs) interference from, 70
- surgical monitoring with, 241, 242, 246–250, 267
- Electronic averaging
  - short-latency auditory evoked potentials (SAEPs) with, 126
  - somatosensory evoked potentials (SEPs) with, 70–71
- Encephalomalacia, left frontal, 53–54
- Epilepsy, somatosensory evoked potentials (SEPs) of, 53–54, 70, 156, 202–204, 205
- Ependymomas, spinal cord, 197
- Ethambutol, with pattern evoked potentials (PEPs), 147
- Facial nerve, and surgical monitoring, 244–246
- Familial spastic paraplegia, 194, 208
- Far-field evoked potentials
  - animal studies of, 2–5
  - basic concepts of, 37–41, 68–69
  - clinical applications of, 22–24
  - factors determining latency and amplitude of, 17–21, 23
  - mathematical models of, 24–25
  - origin of, 1–2
  - peripheral nerve, 73
  - spatial analysis with, 184–186
- Filters, in short-latency auditory evoked potentials (SAEPs), 125–126
- Flight of colors (FOC) testing, 162
- Fovea
  - extrafoveal processing and, 90–91
  - ganglion cells and, 88–89
  - spatial tuning in, 91–93
- Foveal magnification factor, 90
- Foveal visual evoked potentials (VEPs)
  - accommodation, acuity, and adaptation in, 100
  - flicker and contrast in, 100
  - stimulus in, 99–100
- Frequency-following response (FFR), 133–134
- Frequency of stimulus
  - generator source and, 42–44
  - short-latency auditory evoked potentials (SAEPs) and, 133–134
- Friedreich's ataxia, 144, 182, 194, 208
- Ganglion cells, in visual pathway, 88–89
- Generator source
  - anatomy of system being stimulated and, 29–30
  - animal experiments with, 59–60
  - distribution measurement and, 41–42
  - intrasurgical recordings and, 54–59
  - latency measurement and, 32–35
  - pathology effects on, 50–54
  - physiological parameters and, 48–50
  - recording parameters and, 45–48
  - recordings of analogous potentials in study of, 60–61
  - stimulus parameters and, 42–45
  - surgical monitoring and, 30–32
- Glasgow Coma Scale (GCS), 227
- Glasgow Outcome Scale (GOS), 227–228
- Glaucoma, 87
  - pattern evoked potentials (PEPs) in, 98–99, 143, 207
- Guillian-Barré syndrome, 151, 195

- Hair cells, auditory system, 106–107
- Hand models of far-field evoked potentials, 24–25
- Head trauma, and auditory brainstem responses (ABRs), 228–230
- Hemianacusia, 212
- Hereditary ataxias, 194–196, 208
- High-cut filters, in short-latency auditory evoked potentials (SAEPs), 125–126
- Hippocampal sharp waves, 60–61
- Horizontal cells, 88
- Huntington's chorea, 208
- Hypoglossal nerve, during surgical monitoring, 246
- Hypothyroidism, 208
  
- Inferior colliculus (IC)
  - anatomy of, 112–113
  - evoked potential (EP) recordings of, 119–120, 168
  - frequency-following response (FFR) of, 133
- Inner ear, 106–107
- Intensity of stimulus
  - generator source and, 44–45
  - short-latency auditory evoked potentials (SAEPs) and, 128
- Internuclear ophthalmoplegia (INO), with brainstem auditory evoked potentials (BAEPs), 171
  
- Kainic acid, with short-latency auditory evoked potentials (SAEPs), 135–136
  
- Latency
  - estimation of, 32–35
  - far-field evoked potentials amplitude comparisons with, 17–21, 23
  - somatosensory evoked potentials (SEPs) evaluation and, 72
  - visual evoked potentials (VEPs) and, 98
- Lateral lemniscus (LL) nuclei
  - anatomy of, 112
  - frequency-following response (FFR) of, 133
- Lateral superior olivary nucleus (LSO), 112
  
- Leber's optic atrophy, 144, 208
- Long-latency auditory evoked potentials (IAEPs), 223
  - coma and, 230–231
  - comparison of other evoked potential (EP) measures in, 234–237
- Low-cut filters, in short-latency auditory evoked potentials (SAEPs), 125–126
- Lumbar surgical monitoring, 255–257
  
- Maculopathies, with visual evoked potentials (VEPs), 87, 97, 207
- Magnetic resonance imaging (MRI), 158
  - multiple sclerosis (MS) with, 151–152, 154, 175
- Mapping, with somatosensory evoked potentials (SEPs), 71, 205
- Medial geniculate body (MGB), anatomy of, 113
- Medial superior olivary nucleus (MSO)
  - anatomy of, 111–112
  - binaural interaction component (BIC) and, 130–131
  - evoked potential (EP) recordings of, 118
- Median nerve stimulation
  - analogous potentials study with, 61
  - intrasurgical recordings with, 57
- Median somatosensory evoked potentials (SEPs), 1–2
  - animal studies of, 3–4
  - antidromic study with, 10–12, 23
  - orthodromic study with, 8–10, 23
  - short latency peaks of, 5
- Methylprednisolone, with brainstem auditory evoked potentials (BAEPs), 170
- Midbrain, evoked potential (EP) recordings of, 120
- Midbrain lesion, evoked potential (EP) recordings in, 119–120
- Middle-latency auditory evoked potentials (mAEPs), 223–224, 230–231
- Middle ear, 106
- Motor evoked potentials (MEP)
  - multiple sclerosis (MS) and, 175
  - surgical monitoring with, 253, 264–266

- Multiple sclerosis (MS), 161–175
  - auditory evoked potentials (AEPs) in, 145, 147, 148, 149
  - brainstem auditory evoked potentials (BAEPs) in, 167–171, 174
  - combined evoked potential studies in, 174
  - magnetic resonance imaging (MRI) in, 151–152, 154, 175
  - motor evoked potentials in, 175
  - pathogenesis of, 161
  - pattern-shift visual evoked potentials (PSVEPs) in, 162–167, 174
  - short-latency somatosensory EPs (SEPs) in, 171–174
  - somatosensory evoked potentials (SEPs) of, 153–154
  - utility of evoked potentials (EPs) in, 161–162, 182
  - visual evoked potentials (VEPs) in, 96–97
- Myelination, and evoked potentials (EPs), 161–162
- Myoclonic epilepsy, somatosensory evoked potentials (SEPs) of, 70, 202–204, 205
  
- Near-field evoked potentials
  - amplitude of far-field potentials compared with, 18–20
  - basic concepts of, 37–41, 68–69
  - intrasurgical recordings with, 54–59
  - latency of far-field potentials compared with, 17–18
  - spatial analysis with, 184–186
- Nerve action potentials (NAP), 241, 242
- Neurosyphilis, 208
- Neurotransmitter, and visual pathways, 87, 88
- Nuclear magnetic resonance (NMR), posttraumatic epilepsy on, 53–54
  
- Octopus cells, 110
- Optic nerve, 88
- Optic nerve disorders, 143–144, 208
- Optic neuritis, 143, 144–145, 149
  - brainstem auditory evoked potentials (BAEPs) and, 171
  - magnetic resonance imaging (MRI) in, 175
- pattern-shift visual evoked potentials (PSVEPs) in, 163, 164–165
- short-latency somatosensory EPs (SEPs) in, 172–173
- Orthodromic study of median nerve, 8–10, 23
- Outer ear, 106
  
- Parkinson's disease, 88, 182, 208, 267
- Pattern evoked potential recordings (PEPs; PERGs), 87–101, 206–210
  - accommodation, acuity, and adaptation in, 100
  - checkerboard patterns versus sinusoidal gratings in, 93–95
  - clinical use of, 143–147, 153–154
  - contrast in, 97, 100
  - extrafoveal processing in, 90–91
  - eye diseases with, 207
  - foveal visual evoked potential (VEP) and, 99–100
  - functional organization of visual pathway and, 88–95
  - future directions in, 100–101
  - glaucoma and, 98–99
  - multiple sclerosis (MS) and, 162–167, 174
  - normal components of, 206–207
  - optic nerve, heredodegenerative and system diseases on, 207–208
  - spatial frequency and check size in, 96–97
  - stimulus orientation in, 97
  - transient versus steady-state stimulation in, 98
  - visual disturbances on, 143–147, 208–210
- Pattern-shift visual evoked potentials (PSVEPs), and multiple sclerosis (MS), 162–167, 174
- Peripheral auditory system, anatomy of, 106–109
- Peripheral nerve surgical monitoring, 267
- Peripheral neuropathies, with somatosensory evoked potentials (SEPs), 194
- Planum temporale lesions, 212
- Positron emission tomography (PET), and cortical blindness, 210



- Posterior fossa surgery monitoring, 49–50, 241–242, 243–252
- Posteroventral (PV) nucleus, 110
- Postsynaptic potentials (PSPs)
- short-latency auditory evoked potentials (SAEPs) and, 105–106
  - widespread slow negative wave from midbrain and, 120
  - volume conduction and, 122
- Posttraumatic epilepsy, somatosensory evoked potentials (SEPs) of, 53–54
- Pseudotumor cerebri, 208
- Radial nerves
- antidromic potential of, 12–17
  - comparison of amplitude of far-field and near-field potentials with, 18–20
  - evoked potentials and, 1–2
- SAEPs, *see* Short-latency auditory evoked potentials (SAEPs)
- Sarcoidosis, 208
- Scoliosis surgery monitoring, 30–32
- Sensory conduction velocities (SCV) in peripheral nerves, 194
- SEPs, *see* Somatosensory evoked potentials (SEPs)
- Short-latency auditory evoked potentials (SAEPs)
- action potentials of cochlear nerve in, 115
  - averaging process in, 126
  - brainstem entry time of acoustic nerve volley in, 116
  - central auditory system anatomy and, 109–115
  - contralateral and ipsilateral inferior colliculi (IC) stimulation in, 119–120
  - contralateral masking in, 131
  - early brainstem component of, 117
  - filters used with, 125–126
  - frequency specificity in recording of, 132–134
  - future developments of, 134–136
  - general waveform in, 126–127
  - generator sources in, 115–122
  - horizontal dipole field in pontine region in, 118
  - isolation and identification of
    - different components in, 126–132
    - monaural versus binaural stimulation in, 130–131
  - multiple sclerosis (MS) with, 171–174
  - noise in amplification of signal in, 124–125
  - peripheral auditory system anatomy and, 106–109
  - potential field distribution in, 131–132
  - signal-to-noise ratio in recording of, 122–126
  - stages in recording of, 122–124
  - stimulus artifact in, 124
  - stimulus intensity in, 128
  - stimulus polarity in, 129
  - stimulus repetition rate in, 128–129
  - vertical dipole field in midbrain in, 118–119
  - volume conduction in, 120–122
  - widespread slow negative wave from midbrain in, 120
- Sleep, evoked potentials (EPs) effects of, 50
- Somatosensory evoked potentials (SEPs), 1
- anatomy of system being stimulated and, 29–30
  - auditory brainstem responses (ABRs) with, 233–234
  - benzodiazepines with, 205
  - brain death and, 237–238
  - brainstem and cortical components of, 80–82, 197–205
  - central somatosensory conduction with, 82–84
  - cerebral function monitoring with, 266–267
  - “cervico-medullary pattern” with, 197
  - color imaging of, 71
  - coma and, 157, 226, 232–234
  - comparison of other evoked potential (EP) measures in, 234–237
  - “cortical dissociated” pattern with, 200
  - corticospinal lesions with, 30–32
  - critical analysis of recording techniques in, 65–84
  - data acquisition and analysis in,

- 69–71
- display of response in, 71
- dorsal column propagated volley with, 72–79
- dorsal horn segmental generator with, 79
- electronic averaging in, 70–71
- enhanced responses with, 200–205
- evaluation of response in, 72
- hereditary ataxias with, 194–196
- interaction of component potentials of different latencies in, 65–66
- lemniscal generator and scalp far fields with, 79
- lower limb stimulation and, 193–194
- map creation with, 71
- nomenclature used in, 66
- non-demyelinating diseases with, 190–205
- peripheral nerve far field and, 73
- peripheral neuropathies with, 194
- principles underlying recording of, 66
- sleep and, 50
- spinal cord lesions with, 29–30, 196–197, 253
- spinal entry time of, 73
- stimulation techniques in, 69–70
- surgical monitoring with, 241, 242, 258–264
- “thalamo-cortical” pattern with, 197–200
- upper limb stimulation and, 190–193
- volume conduction of, 66–69
- Spastic paraplegia, 194, 197, 208
- Spinal cord
  - latency estimates and, 32–35
  - somatosensory evoked potentials (SEPs) and, 71, 73
- Spinal cord lesions, somatosensory evoked potentials (SEPs) of, 29–30, 51, 196–197
- Spinal surgery monitoring, 252–266
  - extra-operative recordings in, 254–255
  - intra-operative recordings in, 261–264
  - motor-evoked potentials (MEP) in, 253, 264–266
  - patient selection in, 257–261
  - technical factors in, 253–254
- Spino-cerebellar pathway lesion, 32
- Spinothalamic lesions, somatosensory evoked potentials (SEPs) of, 29–30
- Spondylitis, 258
- Status epilepticus, 156
- Strumpell’s hereditary spastic paraplegia, 197
- Summating potentials (SP), 107
- Superior olivary complex (SOC)
  - anatomy of, 111–112
  - evoked potential (EP) recordings of, 117, 118, 168
  - frequency-following response (FFR) of, 133
- Surgery monitoring, 241–268
  - acoustic nerve and, 243–244
  - applications of, 252
  - auditory evoked potentials (AEPs) in, 154–156
  - central sensory pathways and, 243
  - cerebello-pontine angle (CPA) tumor with, 32
  - cerebral function in, 266–267
  - cervical surgery in, 257
  - electromyography (EMG) in, 246–250
  - extra-operative recordings in, 254–255
  - facial nerve and, 244–246
  - intra-operative recordings in, 261–264
  - motor-evoked potentials (MEP) in, 264–266
  - near-field potentials in, 54–59
  - nerve stimulation in, 250–251
  - patient selection in, 257–261
  - peripheral nerves in, 267
  - posterior fossa surgery with, 241–242, 243–252
  - scoliosis surgery with, 30–32
  - selection of method for, 241–242
  - spine surgery with, 252–266
  - technical factors in, 253–254
  - thoracic and lumbar surgery in, 255–257
  - wake up test in, 252–253
- Temporal lobe lesions, 212
- Thalamic lesions, somatosensory evoked potentials (SEPs) in, 79, 197–205, 267
- Thoracic surgical monitoring, 255–257

- Tibial somatosensory evoked potentials (SEPs), 1, 23
  - conduction velocity (CV) of, 73
  - dorsal column propagated volley with, 72–79
  - dorsal horn segmental generator with, 79
  - short latency peaks of, 5
- Toxic amblyopias, 207
- Transverse myelitis, 166, 173
- Trigeminal nerve, during surgical monitoring, 246
- Tympanic membrane, 106
  
- Ulnar nerve monitoring, 267
- Uremia, 208
  
- Ventrolateral (VL) nucleus, 113
- Verapamil, with brainstem auditory evoked potentials (BAEPs), 170
- Visual evoked potential (VEP), 206–210
  - accommodation, acuity, and adaptation in, 100
  - auditory brainstem responses (ABRs) with, 231–232
  - causes of abnormalities of, 87
  - clinical use of, 143–147
  - coma and, 224–226, 231–232, 233
  - comparison of other evoked potential (EP) measures in, 234–237
  - contrast in, 97, 100
  - extrafoveal processing in, 90–91
  - eye diseases with, 207
  - foveal, 99–100
  - functional organization of visual pathway and, 88–95
  - future directions in, 100–101
  - glaucoma and, 98–99
  - normal components of, 206–207
  - optic nerve, hereditary degenerative and system diseases on, 207–208
  - Parkinson's disease and, 182
  - receptive field of individual neurons in, 89–90
  - spatial frequency and check size in, 96–97
  - stimulus orientation in, 97
  - transient versus steady-state stimulation in, 98
  - visual field defects with, 208–210
- Visual pathway, functional organization of, 88–95
- Vitamin B12 deficiency, 197, 207
- Vitamin E deficiency, 207
- von Hippel-Lindau syndrome, 152
  
- Wake up test, and spinal surgical monitoring, 252–253
  
- X ganglion cells, 89, 98–99
  
- Y ganglion cells, 89, 98–99